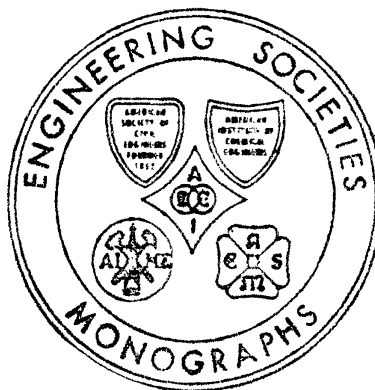


HYDRAULIC ENERGY DISSIPATORS

EDWARD A. ELEVATORSKI

Head, Hydraulics Laboratory and
Assistant Professor of Civil Engineering
University of Arizona



McGRAW-HILL BOOK COMPANY, INC.

NEW YORK TORONTO LONDON

1959

ENGINEERING SOCIETIES MONOGRAPHS

- Bakhmeteff: *Hydraulics of Open Channels*
Bleich: *Buckling Strength of Metal Structures*
Crandall: *Engineering Analysis*
Elevatorski: *Hydraulic Energy Dissipators*
Nadai: *Theory of Flow and Fracture of Solids*
Rich: *Hydraulic Transients*
Timoshenko: *Theory of Elastic Stability*
Timoshenko: *Theory of Plates and Shells*
Timoshenko and Goodier: *Theory of Elasticity*

HYDRAULIC ENERGY DISSIPATORS

Copyright © 1959, by the McGraw-Hill Book Company, Inc. Printed in the United States of America. All rights reserved. This book, or parts thereof, may not be reproduced in any form without permission of the publishers.

Library of Congress Catalog Card Number: 58-12996

The Maple Press Company, York, Pa.

P R E F A C E

Since 1819 there has been a great increase of knowledge pertaining to the hydraulic jump, stilling basins, and energy-dissipating devices. This fact, coupled with the evident interest of engineers and students, suggests the need for a publication of this type. It is hoped that this work will serve as a stimulus to further study of energy-dissipation devices, of which our knowledge is still somewhat fragmentary.

It is understandable that a book on this subject must, for the most part, be an adaptation of material drawn from many sources. Experimental as well as design data are included to serve both research and design engineers. A partial list of references to such literature is given at the end of each chapter. The reader will also find a considerable amount of material that either is new or has not been presented before.

A knowledge of the fundamental principles of fluid mechanics is presupposed, and derivations have been omitted except where they have appeared necessary in explaining new methods. However, a brief chapter is included to present the fundamentals of open-channel flow and to serve as a review of the subject.

In preparing the manuscript, the twofold purpose of securing an accuracy that is consistent with the best experimental data has been kept continually in mind. This has necessitated an examination of a vast amount of data and the preparation of a large number of illustrations and tables.

Many types of energy dissipators have been used throughout the world, and usually the design of each has varied quite radically to meet the problem at hand. The best type suited for protection against scour at a particular location depends largely upon the relationship between the existing tailwater depth and the depth required to form a hydraulic jump. Analyses are made of the formation of the hydraulic jump in various-shaped channels. As part of the analyses, a large number of empirical formulas have been developed, which can be used directly to

solve most practical problems. Criteria for the design of stilling basins and bucket-type dissipators are presented to serve as a guide in designing such structures. It is emphasized that the criteria presented herein provide only a general solution and that for large or unusual structures model studies are advisable.

Although the engineer responsible for the hydraulic design of a project receives indispensable help from model tests, particularly when no adequate means of analysis exists, the primary responsibility for the acceptance of a particular design must rest with the designer. He must determine what actual conditions may develop in the prototype which cannot be foreseen by model tests.

A chapter is included on the subject of erosion and channel retrogression below dams. In many cases erosion has led to the failure of structures and, as a result, the subject of energy dissipation has become one of increasing importance. As the better dam sites are used up, more and more structures must be built on permeable foundations, and scour control will become more important to the safety of the structure.

No claim is made for the originality of the methods of treatment enumerated herein, and sources are freely acknowledged throughout the text. I wish to acknowledge the many libraries, universities, hydraulic laboratories, and individuals that supplied material for this text. In particular, I should like to thank the libraries and offices of the Bureau of Reclamation and the Corps of Engineers, United States Army, for their splendid assistance and cooperation.

Edward A. Elevatorski

CONTENTS

Preface	v
Notation	xi
1 FUNCTIONS OF ENERGY DISSIPATORS	1
1-1. Spillway Structures	1
1-2. Outlet-works Structures	3
1-3. Diversion Structures	5
1-4. Drop Structures	5
2 BASIC CONCEPTS OF OPEN-CHANNEL FLOW	6
2-1. Flow Classification	6
2-2. Nomenclature	6
2-3. Bernoulli's Theorem Applied to Open-channel Flow	7
2-4. Conservation of Momentum	8
2-5. Velocity-head and Momentum Corrective Factors	9
2-6. Specific Energy	9
2-7. Critical Flow	10
2-8. Froude Number and Kinetic-flow Factors	13
2-9. Open-channel Slopes	13
2-10. Open-channel Formulas	14
3 ELEMENTS OF THE HYDRAULIC JUMP	16
3-1. Description	16
3-2. Basic Requirements	16
3-3. Forms of the Hydraulic Jump	17
3-4. Uses of the Hydraulic Jump	19
4 HYDRAULIC JUMP IN RECTANGULAR CHANNELS	22
4-1. Momentum Formula	22
4-2. Theoretical Investigations	24
4-3. Verification of the Momentum Formula	25

4-4.	Dimensionless Equations	27
4-5.	Kinetic-flow-factor Relationships	28
4-6.	Height and Length of the Hydraulic Jump	29
4-7.	Location of the Hydraulic Jump	32
4-8.	Effects of Viscosity and Surface Tension	35
4-9.	Formation of Jump at an Abrupt Drop	35
4-10.	Formation of Jump at an Abrupt Rise	36
5	HYDRAULIC JUMP IN NONRECTANGULAR CHANNELS	39
TRAPEZOIDAL CHANNELS		
5-1.	Pressure-Momentum Relationships	39
5-2.	Critical-depth Determination	41
5-3.	Momentum Formula	42
5-4.	Length of the Hydraulic Jump	43
5-5.	Trapezoidal Chutes	45
CIRCULAR CONDUITS		
5-6.	Critical-depth Determination	46
5-7.	Trial-and-error Solutions	47
5-8.	Experimental Results	48
5-9.	Practical Applications	49
5-10.	Air Entrainment	50
EXPONENTIAL CONDUITS		
5-11.	Exponential Conduits	50
5-12.	Graphical Solution	51
6	HYDRAULIC JUMP IN SLOPING CHANNELS	53
6-1.	Sloping Aprons	53
6-2.	Historical Résumé	55
6-3.	Basic Considerations	56
6-4.	Experimental Investigations	59
6-5.	Length of Hydraulic Jump on Sloping Aprons	60
6-6.	Stepped Sloping Aprons	60
6-7.	Practical Applications	62
7	ENERGY DISSIPATION BY THE HYDRAULIC JUMP	66
7-1.	Energy Dissipation	66
7-2.	Basic Energy Equations	69
7-3.	Energy Dissipation by Experimentation	70
7-4.	Friction Effects	72
8	HYDRAULIC-DESIGN CRITERIA	73
8-1.	Jump-height and Stage-discharge Relationships	73
8-2.	Preparation of Jump-height and Tailwater-rating curves	78
8-3.	Stilling-basin Design Discharge	79

8-4. Stilling-basin Width	79
8-5. Outlet Channels	80
9 HYDRAULIC-JUMP-TYPE STILLING BASINS	81
CANAL STILLING BASINS	
9-1. Design Procedure	81
9-2. Stilling-basin Length and Width	85
9-3. Stilling-basin Transitions	85
9-4. Diverging Channels	86
DIVERSION-STRUCTURE STILLING BASINS	
9-5. Design of Protective Works	87
SLUICEWAY STILLING BASINS	
9-6. Hydraulic Jump below a Sluice Gate	90
9-7. Constant-head Characteristics	90
9-8. Submerged Hydraulic Jump	93
10 STILLING-BASIN APPURTENANCES	94
10-1. Chute Blocks	94
10-2. Baffle Piers	95
10-3. End Sills	103
11 STILLING BASINS FOR SMALL OUTLET WORKS AND LOW AND MEDIUM-HIGH SPILLWAYS	107
11-1. Design Procedure	107
11-2. Uplift Forces	112
12 STILLING BASINS FOR LARGE OUTLET WORKS AND HIGH SPILLWAYS	114
12-1. Design Procedure	114
DIRECT SOLUTION FOR APRON ELEVATION STILLING-BASIN WALLS	
12-2. Stilling-basin Training Walls	123
12-3. Wing Walls	125
12-4. Splitter Walls	126
13 OUTLET-WORKS CONTROL MECHANISMS	123
GATES	
13-1. High-pressure Gates	130
13-2. Radial Gates	130
13-3. Jet-flow Gates	131
13-4. Vertical-leaf Gates	131
VALVES	
13-5. Needle Valves	132
13-6. Tube Valves	133

13-7. Hollow-jet Valves	133
13-8. Butterfly Valves	134
14 JET-DIFFUSION AND IMPACT STILLING BASINS	135
14-1. Jet-diffusion Basins	135
14-2. Free-jet Stilling Basins	137
14-3. Free-jet Chutes	140
14-4. Hump Stilling Basins	141
14-5. Impact Stilling Basins	144
15 SPECIAL STILLING BASINS	149
15-1. SAF Basin	149
15-2. Bhavani-type Stilling Basin	151
15-3. Roller-type Stilling Basins	152
15-4. Spillway Splitters	154
16 SKI-JUMP AND ARCH-DAM ENERGY DISSIPATORS	155
16-1. Ski-jump Energy Dissipators	155
16-2. Free-overfall Spillways of Arch Dams	160
17 DROP-STRUCTURE STILLING BASINS	164
17-1. Rectangular Drop Structures	164
17-2. Trapezoidal Drop Structures	167
18 BUCKET-TYPE ENERGY DISSIPATORS	169
18-1. Solid Roller Buckets	169
18-2. Slotted Roller Buckets	175
18-3. Trajectory Buckets	178
18-4. Tunnel Deflectors	183
19 MODEL TESTS AND HYDRAULIC SIMILITUDE	188
19-1. Hydraulic Model Studies	188
19-2. Hydraulic Similitude	189
19-3. Erosion Tests	193
19-4. Model-Prototype Conformances	193
20 EROSION BELOW DAMS	204
20-1. Prevention of Scour	204
20-2. Erosion below Existing Structures	206
Name Index	209
Subject Index	211

NOTATION

General Symbols Subscripts 1 and 2 denote sections before and after the hydraulic jump, respectively.

SYMBOL	DESCRIPTION
A	cross-sectional area
b	stilling-basin width
C_b	baffle-block coefficient
C_c	coefficient of contraction
C_d	coefficient of discharge
C_v	coefficient of velocity
D	conduit diameter
E	energy
E_w	energy (horsepower per foot of bucket width)
F	force
F	Froude number
f	function of
g	acceleration due to gravity
H	total head
h_f	friction lost
H_L	head lost
h_v	velocity head
K	constant
L	length
L_b	length of stilling basin
L_j	length of hydraulic jump
L_n	drop length
L_r	length of roller
L_x	distance from chute blocks to baffle piers
M	momentum

SYMBOL	DESCRIPTION
m	mass
n	coefficient of roughness (Manning)
P	total pressure
P	power
p	pressure per unit area
Q	total discharge
Q_c	total discharge (critical flow)
q	discharge per foot of width
q_c	critical discharge per foot of width
R	hydraulic radius
r	radius of conduit
S	average side slope
s	slope
s_c	critical slope
s_e	slope of energy gradient
s_f	friction slope
T	time
t	width of water surface
V	volume
v	mean velocity
v_a	actual velocity
v_c	critical velocity
v_o	initial velocity
v_t	theoretical velocity
w	weight
x	longitudinal distance
y	depth
\bar{y}	depth to center of gravity of cross section
y_c	critical depth
y_f	depth behind fall
y_j	height of hydraulic jump
y_m	mean depth
y_n	normal depth
y_s	depth of submergence
Z	elevation above datum
α	velocity-head corrective factor
β	momentum corrective factor
γ	specific weight
δ	dimensionless parameter
θ	angle of a flared section
λ	kinetic-flow factor

SYMBOL	DESCRIPTION
μ	dynamic viscosity
ν	kinematic viscosity
ξ	volumetric ratio of air to water
ρ	mass density
σ	surface tension
ϕ	angle between slope and horizontal

Special Symbols for Hydraulic Models *For magnitudes in both model and prototype, the following subscripts apply:*

p	prototype
m	model
r	ratio of m to p

Functions of Energy Dissipators

Modern dams and hydraulic structures are frequently of immense size, requiring the control of large volumes of water under high pressures. The energies at the base of the structures are often tremendous whether the discharge is through outlet conduits or over spillways. Some means of expending the energy of the high-velocity flow is required to prevent scour of the riverbed, minimize erosion, and prevent undermining of the dam itself. This may be accomplished by constructing an energy dissipator at the base of the structure designed to dissipate the excessive energy and establish safe flow conditions in the outlet channel.

Operation of any hydraulic-energy dissipator depends largely on expending a part of the energy of the high-velocity flow by some combination of the following methods: by external friction between the water and the channel, or between water and air, or by internal friction and turbulence. Frequently, a combination of these methods is utilized to expend the energy in almost every type of energy dissipator. Fundamentally, energy dissipators convert kinetic energy into turbulence and finally into heat.

The purpose of this chapter is to acquaint the reader with the functions and relationships that energy dissipators have with the elements of spillways and outlet-works structures. A brief discussion is presented regarding the functional elements of spillways, outlet works, diversion structures, and drop structures that employ energy dissipators as an integral part of their structure.

1-1. Spillway Structures. Spillways provide controlled releases of surplus water in excess of the reservoir capacity and convey it to the river channel below the dam in such a manner that the dam and foundation are protected from erosion and scour. The object of spillway design is to provide a safe and adequate structure for the least combined cost of spillway and dam.

Basic considerations affecting the design of spillways include capacity, crest control, control apparatus, structural stability, and adequate energy dissipation. The capacity of a spillway must be sufficient to accommodate the maximum discharge without allowing the reservoir surface to rise above a predetermined elevation. Determination of the maximum flood to be used as a basis for spillway design results from hydrological studies and available flood hydrographs.

A spillway crest may be uncontrolled, thereby permitting water to spill from the reservoir whenever the water surface is at a higher elevation than the crest, or it may be controlled by gates installed on the crest. The length of the spillway crest affects the elevation of the crest and also the required control apparatus. If no outside influence restricts the spillway length, the relation between the length and the crest elevation may be determined from a cost study of the various gate types and sizes.

Some of the most common types of spillway-control apparatus include roller, tainter, vertical-lift, and drum gates. Because of varying conditions, the most suitable gate is the one which satisfies, for the least cost, the conditions imposed by the head on the crest, the height of dam, and the hydraulic behavior of the gate. Piers may be located on the spillway crest for the purpose of supporting the control gates and the gate-operating mechanisms or a highway or gate-opened bridge. Their size and shape will vary in accordance with their function. Upstream and downstream sides of the piers should be streamlined in order to reduce contraction of the overflowing jet and provide a smooth water surface.

In general, spillways comprise five distinct elements: an entrance channel, a control structure, a discharge carrier, an energy dissipator, and an outlet channel. The entrance channel conveys water from the reservoir to the control structure, which regulates the discharge from the reservoir. Water is then conveyed from the high-level control structure to the low-level energy dissipator on the riverbed by the discharge carrier. An energy dissipator is required to reduce the high velocity of the flow to a nonerosive magnitude. Water from the energy dissipator is then returned to the riverbed by the outlet channel. In this text, concentration is given to the energy-dissipator element.

One of the most important considerations in the design of a spillway section is the method of controlling erosion of the riverbed at the downstream toe of the dam. An enormous amount of energy must be dissipated before the flow reaches the natural streambed. The structure which contains the energy-reducing action is commonly known as a "stilling basin." Of the several methods of dissipating the flow at the base of a spillway, the most common is the hydraulic jump. Other types of hydraulic-energy dissipators used in conjunction with spillways

are roller and trajectory buckets. Detailed discussions of each type of dissipator will be given in subsequent chapters.

The term "spillway outlets" is applied to the combination of structures and equipment required for the safe operation and control of the water released to serve the various purposes for which the dam was constructed. These structures may be river outlets, when they serve to regulate the river flow and reservoir surface; penstocks, when they serve to provide passage of water to a power plant; or canal outlets, when they discharge water into open channels. The relative importance and design of the outlets will vary in accordance with the size and primary function of the project. The size and number of river outlets must be such that they satisfy the discharge requirements at various elevations of the reservoir. If the outlets are located in the overflow portion, the ends of the conduits should be turned downward to improve the flow characteristics in the outlets and to deflect the jet along the spillway face, avoiding minimum interference with spillway releases. The discharge from an outlet, whether from gates, valves, or free-flow conduits, usually emerges at a relatively high velocity. Some means of expending the energy of flow is usually provided in order to prevent scour of the bed and banks of the river channel, which might result in possible damage to the outlet structure or the dam itself. This may be accomplished by constructing a stilling basin immediately downstream from the outlet.

Location of the outlets in the spillway is generally advantageous from an economic viewpoint, since the conduit is usually of minimum length and the necessity of a valve house and separate stilling basin is avoided. An example of this is the Anderson Ranch Dam stilling basin, located on the South Fork of the Boise River near Boise, Idaho, as shown in Fig. 1-1. As illustrated in the photograph, the valves under the lower end of the spillway chute discharge into a common stilling basin.

1-2. Outlet-works Structures. Outlet works in storage dams provide a controlled release of water from the reservoir in such quantities and at such times as may be required. Principal features of outlet works include structures required to carry the water flow and to house and protect the operating mechanisms, including trashracks and fish-screen structures, tunnels, conduits, control and emergency gates and valves, gate chambers, shafts, valve houses, and energy dissipators. Normally, regulation of the discharge through the outlets is made by some means of gates or valves which may be operated at any degree of opening. The outlet may be designed to increase the outflow capacity during flood flows, to meet downstream demands, or to drain the reservoir for various reasons.

The operating capacity of the outlet works will, of course, be dependent upon the requirements to release the stored water. Discharge from an

outlet varies with the hydrostatic head, and consequently some means for controlling the flow is necessary in order that the outlet may continue to give the required discharge as the reservoir pool fluctuates. Regulation of the outflow is accomplished by operating the control gates or valves in a partially open position. For controlling and regulating the outflow from the reservoir, low-pressure slide gates or commercial gate valves are commonly used for heads up to about 50 ft, high-pressure slide gates for heads to about 75 ft, and needle or hollow-jet valves for higher heads. To make it possible to dewater the control gates for repairs without draining the reservoir and to shut off the flow should the control

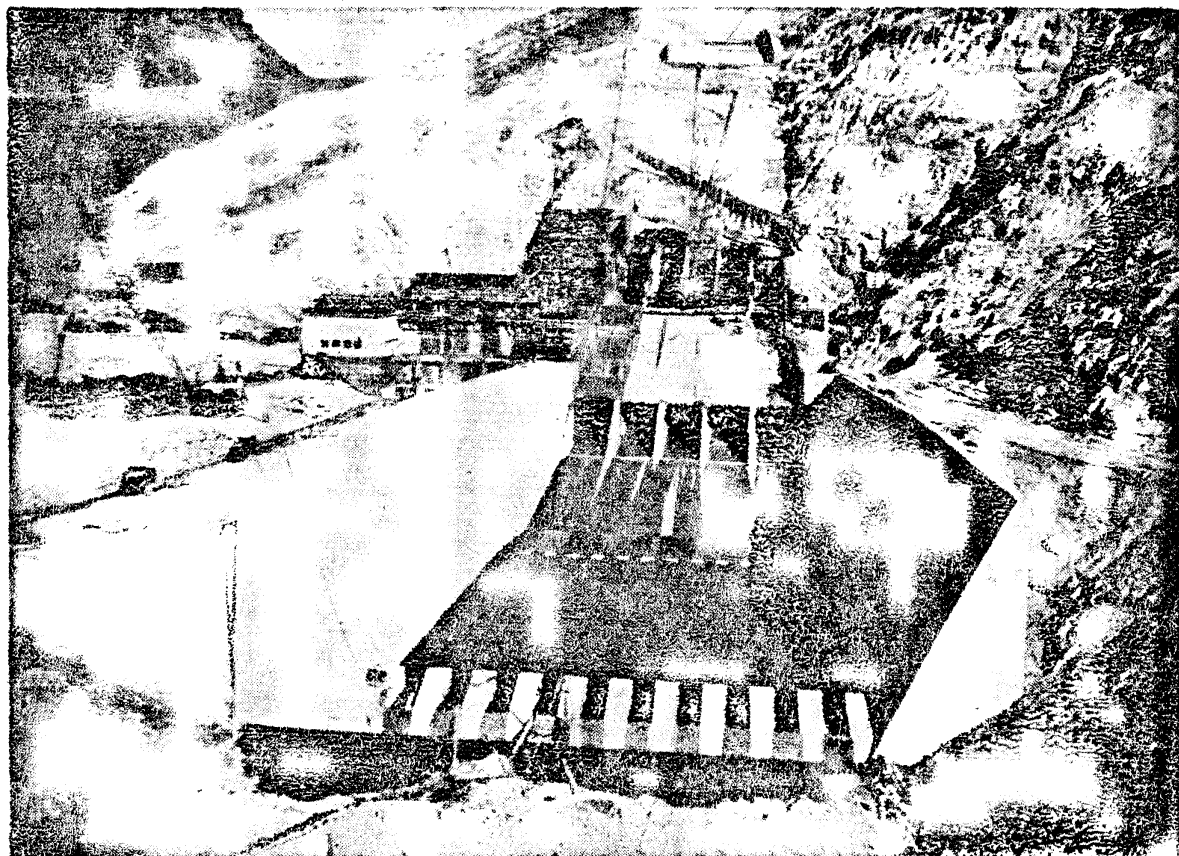


FIG. 1-1. Anderson Ranch Dam stilling basin. (*Courtesy of Bureau of Reclamation.*)

gates become inoperative, emergency gates should be installed farther upstream in the outlet.

In order to prevent or minimize scour resulting from high-velocity flows which discharge from gates, valves, free-flow tunnels or conduits, it will be necessary to construct an energy dissipator to reduce the velocity as quickly as possible upon emergence from the outlet. This may be accomplished by constructing, immediately downstream from the outlet, a water-stilling device into which the jets may be directed. Frequently, the designer utilizes the formation of the hydraulic jump to reduce the high-velocity flow and dissipate the excess energy. Other stilling devices which have been successfully employed for outlet works are deflector

buckets, jet, hump, and impact basins. Design principles are the same for one or more conduits, except for the problem of obtaining satisfactory operation when several conduits discharge into a single stilling basin. A detailed discussion of the merits of each dissipator will be given in subsequent chapters.

1-3. Diversion Structures. The term "diversion dam" applies to a dam whose sole purpose is to divert water. A typical diversion dam consists of an overflow section, a sluiceway, a headworks structure, upstream and downstream training walls, a nonoverflow section, and a stilling basin as required. The overflow section serves to pass the river flow and is usually designed to pass a flood of a 50- or 100-year frequency.

Protection against erosion and scour at the downstream toe of an overflow diversion dam is always necessary. For low diversion dams, sufficient protection against erosion can be secured by providing a wide downstream apron, with a cutoff wall to prevent undermining at the toe. Additional protection is secured by placing riprap in the channel below the apron.

For medium or high diversion dams, control of erosion can be made by allowing the hydraulic jump to form on the apron for a wide range of discharges and tailwater conditions. In some cases an upturned bucket may be employed where high-tailwater conditions exist and may be more economical because of the smaller volume of concrete needed for construction. A detailed discussion for energy dissipators required for diversion dams will be presented in a subsequent chapter.

1-4. Drop Structures. Drop structures or canal drops are needed to accomplish a lowering of grades and water surfaces in comparatively short distances. A drop structure usually includes an inlet section, a drop channel in which the lowering is made, a stilling pool in which the energies are dissipated, and an outlet section through which the water is discharged. The structure may be vertical or inclined, depending upon the discharge and height of the drop. Designs of stilling basins for inclined and vertical, rectangular- and trapezoidal-shaped drop structures are included in a later chapter.

2

Basic Concepts of Open-channel Flow

To understand the phenomenon of the hydraulic jump and energy-dissipation devices fully, it is essential that the reader have a clear conception of the many terms used in the study of open-channel-flow problems. This chapter will be devoted solely to a review of the basic principles of open-channel flow and present-day nomenclature.

2-1. Flow Classification. In general, flow can be classified as being steady or unsteady. During steady flow the velocity, pressure, and water surface at every section remain the same and do not change with respect to time. If at any one section these quantities continually change with respect to time, the flow is termed unsteady.

Open-channel flow may also be said to be uniform or varied. Uniform flow prevails when the water surface at every section remains constant; i.e., the water surface remains parallel to the bottom of the channel. The flow is said to be nonuniform, or varied, when the slope of the water surface changes from section to section and no longer parallels the channel bottom. The two types of flow are illustrated in Fig. 2-1.

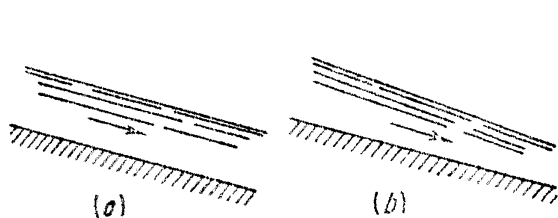


FIG. 2-1. Flow classification: (a) uniform flow, (b) varied flow.

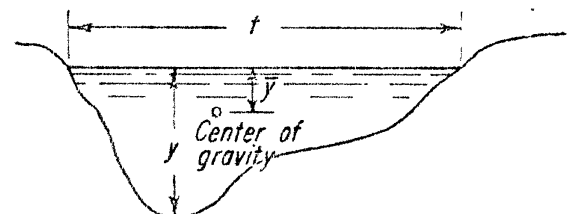


FIG. 2-2. Elements of an open-channel cross section.

In a natural channel, the flow may be uniform in one section and varied in another section. However, varied flow may be steady or unsteady, whereas uniform flow is necessarily steady.

2-2. Nomenclature. The elements that compose an open-channel cross section are shown in Fig. 2-2. The symbols shown in Fig. 2-2 are designated as follows:

y = maximum depth of water in the channel

\bar{y} = depth to center of gravity of the cross section

t = surface width

The hydraulic radius R is defined as being the quotient of the cross-sectional area divided by the wetted perimeter.

$$R = \frac{A}{\text{wetted perimeter}}$$

In a very wide channel, the mean depth approximates and becomes equal to the hydraulic radius. The mean depth y_m is defined as being the quotient of the cross-sectional area divided by the surface width. Or, in the form of an equation,

$$y_m = \frac{A}{t}$$

The discharge Q is defined as being the volume of water passing a section per unit time. The average velocity of the section can be found by dividing the discharge by the cross-sectional area. Frequently, formulas can be condensed by using the value of the discharge per foot of channel width, commonly designated by q (cubic feet per second per foot).

2-3. Bernoulli's Theorem Applied to Open-channel Flow. One of the well-known theories dealing with the energy of flowing water is the Bernoulli theorem. Bernoulli's theorem states that if water moves in a stream from one point to another at the same level, the sum of the static head and velocity head at the first point is equal to the sum of the same quantities at the second point, plus the intervening energy losses. The principle can be illustrated by Fig. 2-3.

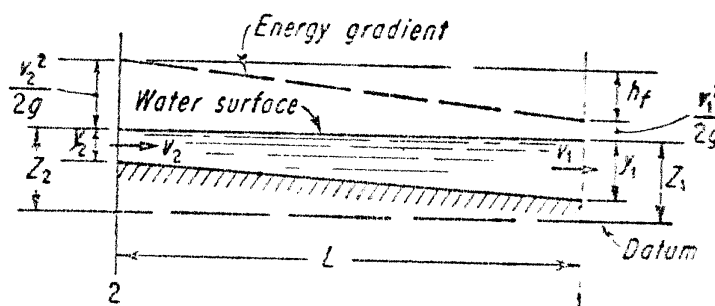


FIG. 2-3. Bernoulli's theorem applied to open-channel flow.

The following assumptions are made concerning the Bernoulli theorem:

1. From section 2 to section 1, there is no gain of energy and the only loss is due to friction.
2. The velocity over the cross section remains constant.
3. The energy per unit mass of fluid remains constant.
4. The fluid is considered to be incompressible.

At each section, three different types of energy prevail: potential, pressure, and kinetic. Each type can be explained as follows:

1. Potential energy is due to the elevation of the fluid. At a height Z above the datum plane, the potential energy is equal to mgZ , where m is the mass and g is the acceleration due to gravity.

2. Pressure energy will be equal to $mg(p/\gamma)$ where p/γ is the static head, p the pressure on the bottom of the channel, and γ the weight per unit volume.

3. Kinetic energy is due to the motion of the fluid and is equal to $\frac{1}{2}mv^2$, where v is the mean velocity of the section. Hence the total energy at a section will be

$$E = mgZ + mg \frac{p}{\gamma} + \frac{1}{2} mv^2 \quad (2-1)$$

A more convenient form can be had by dividing Eq. (2-1) by mg , thereby converting energy to head.

$$H = Z + \frac{p}{\gamma} + \frac{v^2}{2g} \quad (2-2)$$

Applying Bernoulli's theorem between sections 2 and 1, indicated in Fig. 2-3, we have

$$Z_2 + \frac{p_2}{\gamma} + \frac{v_2^2}{2g} = Z_1 + \frac{p_1}{\gamma} + \frac{v_1^2}{2g} + h_f \quad (2-3)$$

The term h_f represents the head loss due to the friction of the fluid on the sides and bottom of the channel, and will be equal to the product of the slope of the energy gradient and length of the section.

$$h_f = s_e L \quad (2-4)$$

The slope of the energy gradient indicates the loss of energy from one section to another.

In an open channel, the pressure is constant and atmospheric; therefore $p/\gamma = 0$. Accordingly, Eq. (2-3) may be reduced to the form of Eq. (2-5).

$$Z_2 + \frac{v_2^2}{2g} = Z_1 + \frac{v_1^2}{2g} + h_f \quad (2-5)$$

2-4. Conservation of Momentum. A fundamental principle involved in all cases of changes in velocities is that of the conservation of momentum. Since momentum cannot be changed by internal movements, it can then only be altered by an external force equal to the rate of change of momentum. As indicated in Fig. 2-3, the reduction of velocity from v_2 to v_1 results in a loss of momentum. The external force acting

to produce this change in momentum, in a time T , is

$$F = m \frac{v_2 - v_1}{T} \quad (2-6)$$

In Eq. (2-6), m is the mass of the volume of water flowing from section 2 to 1, since

$$m = \frac{Q\gamma T}{g}$$

Therefore Eq. (2-6) becomes

$$F = Q\gamma \frac{v_2 - v_1}{g} \quad (2-7)$$

Later the momentum principle will be employed to solve for the depth downstream of the hydraulic jump. It should be remembered that the reduction in velocity incurred by the jump must conform to both the laws of the conservation of energy and momentum.

2-5. Velocity-head and Momentum Corrective Factors. It can be readily seen that the velocity distribution throughout a channel cross section will rarely be uniform. As used in hydraulic computations, the velocity head is the average kinetic energy per unit width over a cross section perpendicular to the direction of flow. The square of the average velocity will always be less than the weighted average of the squares and consequently will yield a result which is too low by an amount depending upon the deviation from the average velocity.

A velocity-head correction factor α has been proposed by Johnson and O'Brien^{2*} which is dependent upon the ratio of the maximum velocity to the mean velocity and is approximately equivalent to Eq. (2-8).

$$\alpha = 1 + \left(\frac{v_{\max}}{v_{\text{mean}}} - 1 \right)^2 \quad (2-8)$$

To solve for α , it is necessary to know the velocity distribution in the channel. Experiments have shown that α may vary from 1.04 to 1.16.

Similarly, it is necessary to derive a momentum corrective factor β to compensate for the unequal distribution of velocities; thus

$$M = \beta \frac{Q\gamma v}{g} \quad (2-9)$$

For nonuniform velocities, β will vary from 1.01 to 1.06.

Obviously, when the velocities are uniform, both α and β will be equal to unity.

2-6. Specific Energy. In Sec. 2-3 we derived, by Bernoulli's principle, that for open channels

$$Z_2 + \frac{v_2^2}{2g} = Z_1 + \frac{v_1^2}{2g} + h_f \quad (2-5)$$

* Superscript numbers indicate works listed under References at the ends of the chapters.

If the friction term h_f is neglected and the datum is considered to be the bottom of the channel, Eq. (2-5) becomes

$$y_2 + \frac{v_2^2}{2g} = y_1 + \frac{v_1^2}{2g} \quad (2-10)$$

or

$$H_2 = y_2 + \frac{v_2^2}{2g}$$

and

$$H_1 = y_1 + \frac{v_1^2}{2g}$$

The terms H_1 and H_2 are known as the "specific energies" of the liquid flowing in a channel, referred to the datum of the channel bottom. Since

$$v = \frac{q}{y}$$

the specific energy for a rectangular channel of unit width becomes

$$H = y + \frac{q^2}{2gy^2} \quad (2-11)$$

An examination of Eq. (2-11) shows that for each value of H , two alternate depths of flow exist, each having the same amount of energy. The two stages of equal energy are depicted by Fig. 2-4.

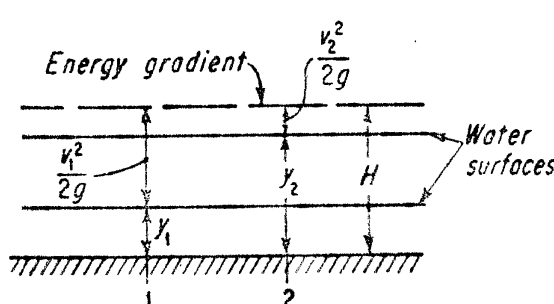


FIG. 2-4. Stages of equal energy.

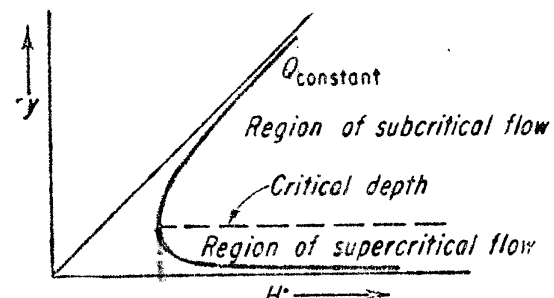


FIG. 2-5. Specific-energy diagram.

Since H is a function of the discharge, the specific-energy head can be plotted against the depth for a known discharge. A typical relationship between y and H for a constant discharge is shown in Fig. 2-5. At very small values of y , the specific energy curve is asymptotic to the horizontal axis, and at large values of y , the curve approaches a 45° line.

2-7. Critical Flow. An examination of the curve in Fig. 2-5 shows that the energy is minimum at one depth only. This depth, corresponding to the minimum energy, is known as the "critical depth." Depths less than and greater than the critical depth are known as supercritical and subcritical, respectively.

For any uniform channel, the specific energy becomes

$$H = y + \frac{v^2}{2g} \quad (2-12)$$

and, for steady flow,

$$v = \frac{Q}{A} \quad (2-13)$$

Differentiating Eq. (2-13), we have

$$\frac{dv}{dA} = \frac{Q}{A^2}$$

$$\text{or } \frac{dv}{dA} = -\frac{v}{A}$$

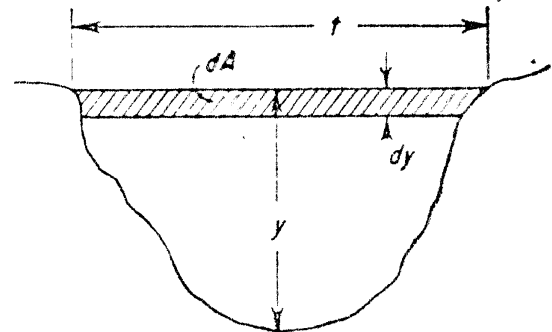


FIG. 2-6

Referring to Fig. 2-6,

$$\begin{aligned} dA &= t \, dy \\ \text{therefore } \frac{dv}{dy} &= -\frac{tv}{A} \end{aligned} \quad (2-14)$$

for critical flow,

$$v = \sqrt{gy} \quad (2-15)$$

Differentiating Eq. (2-15), we have

$$\frac{dv}{dy} = -\frac{g}{v} \quad (2-16)$$

Equating Eqs. (2-14) and (2-16); we have

$$-\frac{tv}{A} = -\frac{g}{v} \quad (2-17)$$

$$\begin{aligned} \text{or } \frac{v_c^2}{g} &= \frac{A}{t} \\ \text{and } \frac{Q_c^2}{g} &= \frac{A_c^3}{t} \end{aligned} \quad (2-18)$$

Equation (2-18) satisfies the criterion for critical flow for any open-channel cross section. For each specific channel shape, Eq. (2-18) can be solved to find the critical depth in terms of discharge and geometric properties.

For a rectangular channel, the critical depth will be a function of both the depth and the discharge. Equation (2-19) can be obtained by substituting the geometric properties of a rectangular channel into Eq. (2-18).

$$y_c = \sqrt[3]{\frac{q^2}{g}} \quad (2-19)$$

The critical depth for a typical triangular channel, shown in Fig. 2-7, will be a function of both the discharge and the geometric properties of the channel shape.

$$y_c = \sqrt[5]{\frac{2Q^2}{gZ^2}} \quad (2-20)$$

Similarly, by substitution in Eq. (2-18), the critical depth for a parabolic channel shown in Fig. 2-8 can be found in terms of the discharge and surface width.

$$y_c = \frac{3}{2} \sqrt[3]{\frac{Q^2}{gt^2}} \quad (2-21)$$

Although an equation for the critical depth in trapezoidal and circular channels can be found in terms of discharge and geometric properties, it is

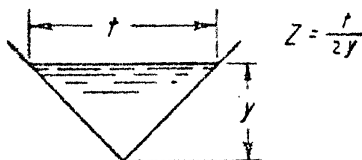


FIG. 2-7. Triangular channel.



FIG. 2-8. Parabolic channel.

rather complex, and it is suggested that Eq. (2-18) be solved by trial and error. If only a small number of solutions are required, the trial-and-error procedure will be the most expedient method.

At critical depth, the flow will have its minimum energy, but its discharge will be maximum. For a rectangular channel of unit width,

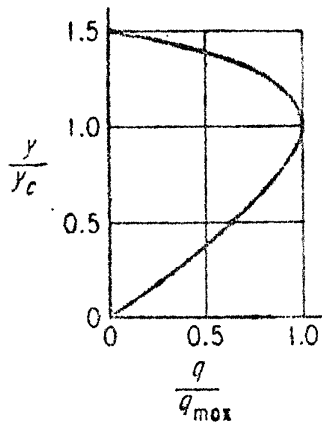


FIG. 2-9. Dimensionless-discharge diagram.

$$y_c = \sqrt[3]{\frac{q_{\max}^2}{g}} \quad (2-19)$$

$$\text{and} \quad H = y + \frac{q^2}{2gy^2} \quad (2-11)$$

Dividing Eqs. (2-19) and (2-11) by $y_c = \sqrt[3]{H}$, q/q_{\max} can be found in terms of y/y_c .

$$\frac{q}{q_{\max}} = \frac{y}{y_c} \sqrt{3 - 2 \frac{y}{y_c}} \quad (2-22)$$

When q/q_{\max} versus y/y_c is plotted, as shown in Fig. 2-9, we see that the maximum discharge occurs when $y/y_c = 1$.

Examination of the diagram shows that for a reduction in q , the depth will be increased for subcritical flow and decreased for supercritical flow.

Another analogy that is often used in open-channel-flow problems is the use of the "critical slope." By definition the critical slope is the one

grade which maintains uniform flow at the critical depth. For any slope flatter or steeper than the critical slope, the depth of flow will be respectively greater or less than the critical depth. The critical slope can be computed from the Manning formula

$$s_c = \frac{14.56 n^2 y_c}{R^{4/3}} \quad (2-23)$$

As noted in experiments and natural channels the conditions of flow at critical depth are very unstable and any slight disturbance may produce excessive wave action.

2-8. Froude Number and Kinetic-flow Factors. The value of F , the Froude number, expresses the ratio between the gravitational and inertial forces. For critical flow to occur,

$$\frac{v}{\sqrt{gy}} = 1 \quad (2-24)$$

or

$$F = 1$$

For subcritical or streaming flow, $F < 1$; at critical flow, $F = 1$; and for supercritical or shooting flow, $F > 1$.

It will later be seen that for model studies of hydraulic structures, the Froude number provides a criterion of similarity for the gravity and acceleration conditions of flow in both the prototype and model.

The Froude number serves as a flow indicator, since the velocity of the gravity wave is the same as the critical velocity of flow, or $v = \sqrt{gy}$. When $v > \sqrt{gy}$, the wave can only move downstream, and this fact is often utilized in the construction of water-stage regulators and gauges.

In some cases, the square of the Froude number, the "kinetic-flow factor," represented by λ , can be used to simplify empirical relationships. In the form of an equation,

$$\lambda = F^2$$

or

$$\lambda = \frac{v^2}{gy} \quad (2-25)$$

2-9. Open-channel Slopes. In general, there are five different types of slopes which may occur in any open channel: mild, steep, horizontal, critical, or adverse.

Previously, we have defined the critical depth y_c as being the depth at which, in a given channel, a given quantity of water flows with the minimum content of energy. It is now necessary to define the normal depth. For uniform flow, the depth from the water surface to the bottom grade line of the channel is the same at all sections, because of parallelism of the water surface and bottom grade line. This depth, known as the "normal depth," is commonly represented by y_n .

Channel slopes can be classified by the relationship between the normal and critical depths. The five types of slopes are illustrated in Fig. 2-10a to e. A mild slope is one so flat that it will sustain uniform flow only at a subcritical velocity, whereas the critical slope has just enough inclination to sustain uniform flow at critical velocity. Conversely, the steep slope will sustain uniform flow only at a supercritical velocity. In addition there are two cases in which the channel does not slope downward in the direction of flow—horizontal and adverse slopes, illustrated by Fig. 2-10d and e, respectively.

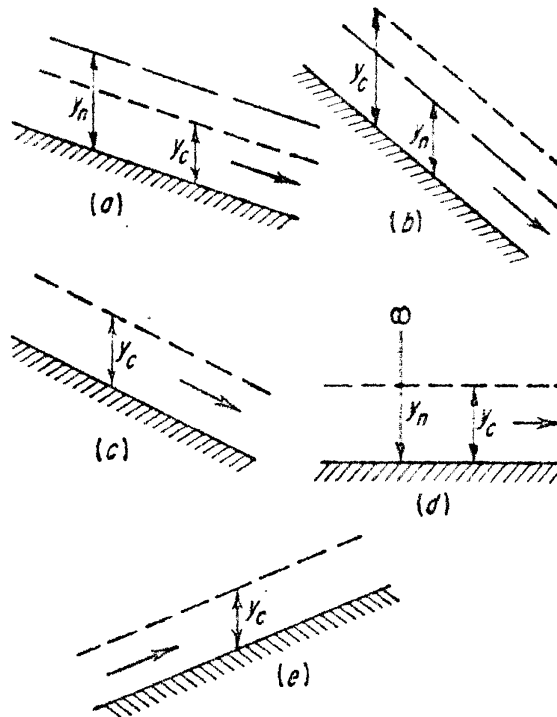


FIG. 2-10. Open-channel slopes: (a) mild, (b) steep, (c) critical, (d) horizontal, (e) adverse.

types of open-channel slopes will be discussed in a subsequent chapter.

2-10. Open-channel Formulas. In the past, many formulas have been employed to solve open-channel-flow problems. Frequently, the choice of a formula depended merely upon the designer's preference. Among the empirical formulas employed were those of Kutter, Ganguillet, Bazin, Chezy, and Manning. Today the Manning equation has been accepted and is used universally, since it is readily adaptable to computational procedures and graphical solutions. The Manning formula is usually written in the following form:

$$v = \frac{1.49}{n} R^{2/3} s_e^{1/2} \quad (2-26)$$

where v = mean velocity of the section

R = hydraulic radius

s_e = slope of the energy gradient

Surface profile, or backwater curves for gradually varied flow, can be found in numerous texts and will not be discussed here. For actual river channels or natural streams, flow at the normal depth is rare, and in many instances water-surface profiles are mistaken for being uniform. It is recommended that the flow profile be accurately analyzed to be sure that it is actually uniform within the limits of the required accuracy.

It should be noted that subcritical or streaming flow will prevail on a mild slope, whereas supercritical or shooting flow will occur only on a steep slope.

The uses of the five different

n = coefficient of roughness, dependent upon composition, condition, and alignment of channel

Values of n should be computed, if possible, from observed water-surface profiles. If stream-flow records are not available, the value of n corresponding to the approximate condition of the channel can be found in Table 2-1.

TABLE 2-1. VALUES OF MANNING'S n FOR NATURAL OPEN CHANNELS^{1,3}

n	<i>Channel condition</i>
0.016–0.017	Smoothest natural channels, free from growth, with straight alignment
0.020	Smoothest natural earth channels, free from growth, little curvature
0.0225	Well-constructed earth channels, in good condition
0.025	Small earth channels in good condition, and large earth channels with some growth on banks or scattered cobbles on the bottom
0.030	Earth channels with considerable growth, natural streams with good alignment, fairly constant sections, large floodway channels well maintained
0.035	Earth channels, considerably covered with small growth—cleared, but not continuously maintained floodways
0.040–0.050	Mountain streams with clean loose cobbles, rivers with variable sections and some vegetation growing on the banks, earth channels with thick aquatic growths
0.060–0.070	Rivers with fairly straight alignment and cross section, badly obstructed by small trees, with very little underbrush
0.100	Rivers with irregular alignment and cross section, moderately obstructed by small trees and underbrush—rivers with fairly regular alignment and cross section, heavily obstructed by small trees and underbrush
0.125	Rivers with irregular alignment and cross section, covered with growths of virgin timber and occasional dense patches of bushes and small trees, some logs and fallen trees
0.125–0.150	Rivers with irregular alignment and cross section, many roots, trees, bushes, large logs, and other drift on bottom, trees continually falling into the channel because of bank caving

It should be noted that the Manning formula applies only to steady uniform flow. For uniform flow, the slope of the water surface will parallel the bottom of the channel. Use of the Manning formula for varied flow may yield highly erroneous results.

REFERENCES

1. Houk, I. E.: Calculation of Flow in Open Channels, *Miami Conservancy District Tech. Rep.*, part IV, 1917.
2. Johnson, J. W., and M. P. O'Brien: Velocity-head Correction Factors for Hydraulic Flow, *Eng. News Record*, p. 214, Aug. 16, 1934.
3. Ramser, C. E.: Flow of Water in Drainage Channels, *Dept. Agr. Tech. Bull.* 129.

3

Elements of the Hydraulic Jump

Many types of energy dissipators or stilling basins have been used throughout the world and usually the design of each has varied quite radically to meet the problem at hand. Utilization of the hydraulic jump, whenever possible, to dissipate the energy has been the accepted practice. The purpose of this chapter is to acquaint the reader with the basic requirements, distinctive forms, and uses of the hydraulic jump.

3-1. Description. The hydraulic jump is defined as the sudden and turbulent passage of water from a low stage below critical depth to a high stage above critical depth, during which the velocity changes from supercritical to subcritical. The jump is accompanied by violent impact and consists of an abrupt rise of the water surface in the region of the impact between the rapidly moving stream and the slowly moving water. It will be observed that the water surface at the beginning of the abrupt rise is constantly falling against the oncoming stream, which is moving at a high velocity. Farther along in the jump, masses of water are continually boiling to the surface from greater depths, producing a large amount of foam and "white water." Figure 3-1 is a photograph showing the formation of the hydraulic jump at the St. Anthony Falls Dam.

3-2. Basic Requirements. A hydraulic jump will form when water moving at a supercritical velocity in a comparatively shallow stream strikes water having a substantial depth and subcritical velocity. It should be noted that it is impossible for the jump to form unless the upstream depth is less than the critical depth. For a jump to form, the pressure plus momentum after the jump must equal the pressure plus momentum before the jump. The pressure-plus-momentum requirement holds true regardless of the shape or slope of the channel.

The hydraulic jump may be expected to form under any of the following conditions:

1. At the base of a hydraulic structure where supercritical flow plunges into a pool.
2. At a constriction in a flume where supercritical velocities are reduced to subcritical velocities.
3. At the junction of a canal or channel where supercritical flow passes through critical to the subcritical stage.
4. Where the flow under a sluice gate is supercritical and impinges on a subcritical pool.
5. In a long flume where high velocities can no longer be sustained by a flat slope.



FIG. 3-1. Formation of the hydraulic jump below St. Anthony Falls Dam. (*Northern States Power Company*.)

6. The jump may occur in pipelines or conduits where the grade changes and cannot sustain supercritical flow.
7. In a uniform canal, a trashrack may cause so much loss of head that the stream below is at shooting stage and returns to normal flow through the hydraulic jump.

It should be remembered that the above conditions list only possible places where the jump may be expected to occur. In unusual circumstances, the jump may or may not form under these conditions. For all cases, the hydraulic jump must follow the basic requirements as outlined.

3-3. Forms of the Hydraulic Jump. There are essentially five different forms of the hydraulic jump which may occur on a horizontal apron and which may be encountered in the design of energy-dissipation devices. It is important to note that the energy-dissipation and internal charac-

teristics of the hydraulic jump vary considerably with each form. The following forms, illustrated by Fig. 3-2a to e, were made as a result of extensive experiments conducted by the Bureau of Reclamation. Each form has been classified in relation to the kinetic-flow factor of the entering stream.

When λ_1 varies from 1.5 to 2.5, surface undulations result as shown in Fig. 3-2a. These undulations are actually part of a standing wave and not a true hydraulic jump.

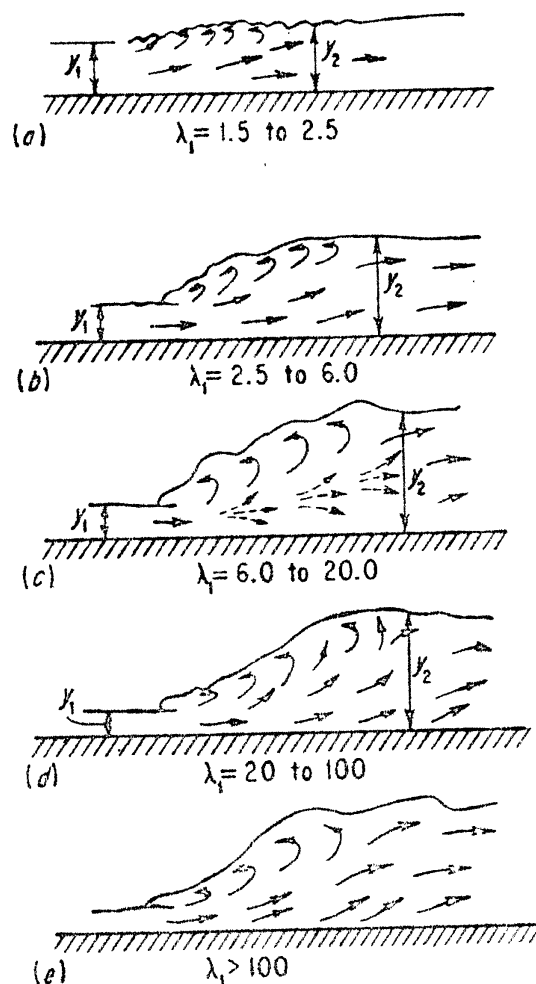


FIG. 3-2. Forms of the hydraulic jump: (a) surface undulations, (b) prejump, (c) transition, (d) range of good jumps, (e) choppy jump.

formed. In this range, the energy dissipated by the hydraulic jump will vary from 40 to 70 per cent.

Our fifth and last form is that of the choppy jump, which occurs when λ_1 exceeds 100, as illustrated in Fig. 3-2e. Here the high-velocity jet continues downstream for a long distance, with a considerable amount of spray and rough water resulting. Figure 3-3 is a photograph of a choppy jump formed below a tunnel of the Fort Randall Dam.

With values of λ_1 exceeding 100, long and deep stilling basins are

Our second form is that of the prejump, illustrated by Fig. 3-2b, occurring when λ_1 varies from 2.5 to 6. In this case the water surface is quite smooth and the velocity throughout is fairly uniform, but only a small amount of energy is dissipated.

The transition jump is form three, illustrated by Fig. 3-2c, which occurs when λ_1 varies from 6 to 20. This type of action is common in canal structures, where the entering jet oscillates back and forth from the bottom to the surface and back again. In some cases these oscillations have been known to travel for miles in canals, damaging earth banks and riprap. Although some success can be had with the use of wave suppressors, it is very difficult to design a stilling basin for this form of hydraulic jump.

When λ_1 varies from 20 to 100, well-stabilized jumps are formed as depicted by Fig. 3-2d. If possible, structures should be designed to ensure that a jump in this category will be

required, and because of the large value of y_2 needed, the employment of a bucket-type basin may offer a better solution than the conventional hydraulic-jump-type stilling basin.

The limits of the kinetic-flow factors indicated for various forms of the jump are not definite and may overlap.

3-4. Uses of the Hydraulic Jump. Although the most common use of the hydraulic jump is as an energy dissipator, the formation of the

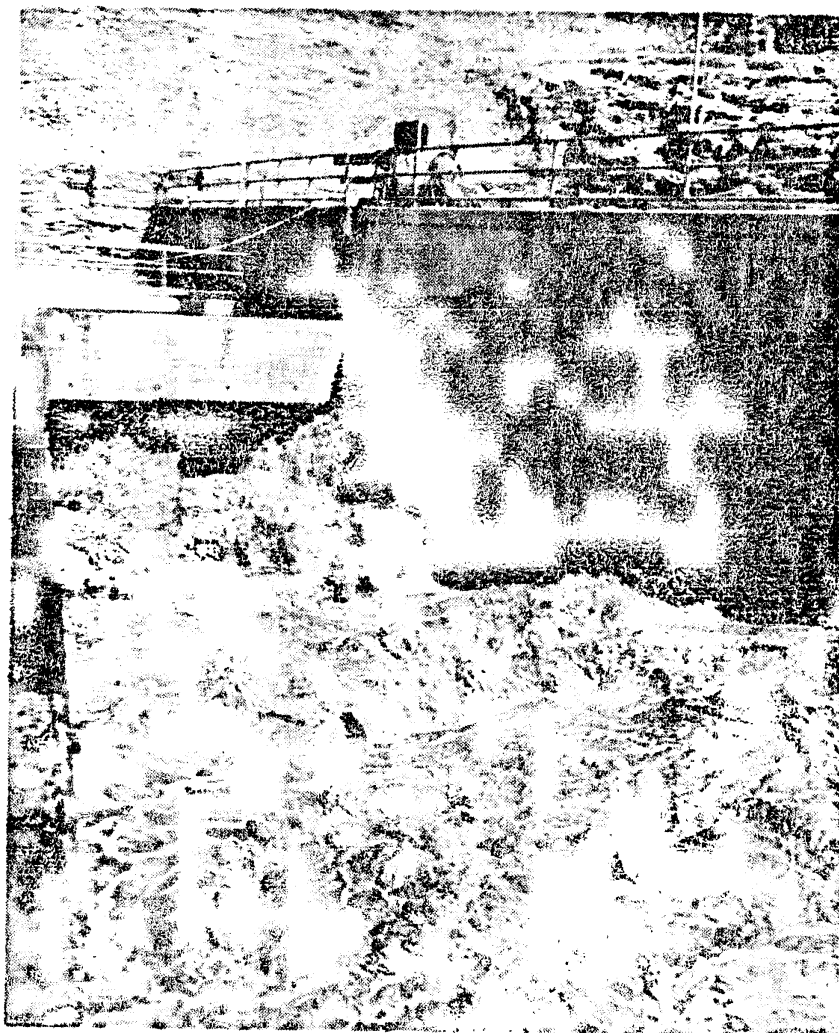


FIG. 3-3. Formation of a choppy jump below tunnel 12 of Fort Randall Dam, Pickstown, S.Dak., with sluice gates fully open. Approximate discharge is 59,000 cfs. (Courtesy of Corps of Engineers, Omaha District.)

hydraulic jump can also be used to increase the head in a canal, reduce uplift pressures, increase orifice discharges, indicate flow conditions, extract air from closed conduits, and mix chemicals for water purification.

The earliest use of a hydraulic jump was as a head increaser, which was first described by Da Vinci¹ in Bologna, Italy, during 1828. When a hydraulic structure is used for measuring purposes, it is desirable that the

head provided by the channel be maintained, in order to facilitate the supplies in the surrounding fields. The level to which the downstream water surface can be raised, under certain conditions, is called the "increased head." It is in this manner that the formation of the hydraulic jump helps to increase the head. This method is employed today in establishing the location of stream-gaging stations.

The most common use of the jump is as an energy dissipator and will be completely discussed in a later chapter. Frequently the hydraulic jump is used to prevent scouring action below hydraulic structures such as spillways, drop structures, outlet works, and sluice gates.

As previously explained, the hydraulic jump can be formed only when a stream flowing with supercritical velocity is transformed to one with a subcritical velocity. During the velocity reduction, the stream loses a considerable amount of energy, and in some cases, the percentage of energy dissipated may be as high as 80 per cent of the initial energy. Exhaustive tests made both with models and with prototypes have established that the hydraulic jump is the best means of dissipating energy below hydraulic structures.

The requirements for connecting sewers designed by the city of Chicago were that the flow be odorless, noiseless, vibrationless, and free from energy due to the high velocity. The problem was solved by permitting a hydraulic jump to form which dissipated a large percentage of the initial energy. Water below the hydraulic jump then flowed with a low velocity into the interceptor line.

Because of the seepage of water below a stilling-basin apron, a certain amount of pressure is formed, which tries to lift up the apron. If the masonry of the apron is not heavy enough to balance this uplift pressure, there is a possibility that the masonry structure will be lifted off its foundation. When the hydraulic jump is permitted to form on the apron, the weight of the water on the apron adds to the weight of the concrete and thereby helps to counterbalance the uplift pressure.

When the hydraulic jump is formed downstream from a sluice gate, it can prevent the tailwater from backing up against the gate and keep the discharge "free." If the outflow becomes submerged the discharge will be decreased as the water backs up against the gate. Utilization of the hydraulic jump may help to increase the discharge from a sluice gate.

The presence of the hydraulic jump does indicate that there is a definite break in the energy gradient. When the hydraulic jump forms, the flow upstream is necessarily supercritical. Since supercritical flow exceeds the velocity of the gravity wave, backwater cannot travel upstream. Consequently, the control for supercritical flow must be upstream.

The formation of the hydraulic jump is an important method by which air pockets from water-supply pipelines can be removed. A pipeline

summits the accumulation of air prevents the proper operation of pipelines and interferes with the carrying capacity of the lines. Turbulence produced by the formation of the hydraulic jump will make air available to the flowing water. As the air is gradually removed, the position of the hydraulic jump gradually moves downstream. Airflow measurements indicate that the rate of air entrained by the hydraulic jump depends to a large extent upon the discharge and the Froude number upstream of the hydraulic jump.

The churning action of the jump furnishes a cheap and efficient means for thoroughly mixing water being prepared for treatment with the addition of chemicals. This process was used at Cleveland's Baldwin Filtration Plant, which had a capacity at the time (1922) of 165 million gpd. In 1927, experiments were conducted by Ellms and Levy² related to the addition of solutions of alumina and suspensions of lime to the water just prior to its entrance into the throat of a flume. The time of passage through the hydraulic jump and pool immediately beyond was about 30 sec. It was observed that the mixing process takes place quickly, with the required thoroughness and uniformity.

The loss of head produced by the jump may be made low, if not lower than, that produced in any conventional baffle or mixing chamber. Structures in which the jump may be produced are simple, requiring only a small amount of material for their construction, and they cost far less than a conventional baffle mixing device.

REFERENCES

1. Da Vinci, L.: "Del Moto dell'Acqua," Bologna, Italy, 1828.
2. Ellms, E. W., and A. G. Levy: The Hydraulic Jump as a Mixing Device, *J. Am. Water Works Assoc.*, January, 1927.

4

Hydraulic Jump in Rectangular Channels

The formation of the hydraulic jump in a horizontal rectangular channel will be the case most frequently encountered by the designer. In this chapter the various formulas, previous investigations, and physical properties of the hydraulic jump in a rectangular channel are discussed.

4-1. Momentum Formula. In the past, various formulas have been employed to compute the depth of water downstream from a hydraulic jump. Some of the formulas commonly used will now be presented. It will be readily noted that, in some cases, the earlier formulas did not yield correct results because they were dimensionally incorrect. The momentum formula agrees very well with experimental data and is now universally accepted without doubt.

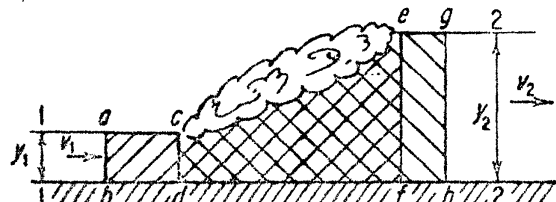


FIG. 4-1. Theory of the hydraulic jump.

to the position $cdhg$, and the following characteristics will be observed:

1. The water entering at ab is transparent and has a uniform high velocity.
2. The water leaving at gh is also transparent, but in comparison to ab has a relatively low velocity.
3. It will be observed that between c and e the surface rises rapidly and is greatly disturbed by spraying and spattering, a product of the turbulence. The entire mass $edef$ appears milky, and this suggests the presence of much internal impact. Since the density of the mixture is less than that of water, the surface stands correspondingly higher than it would if no air were present. The surface again becomes smooth and level as soon as all the air bubbles rise to the surface.

In passing from the position *abfe* to the position *cdhg*, the moving mass of water loses much of its momentum and consequently there is a reduction in velocity. The rate of momentum lost must be equal to the unbalanced force acting to retard the motion of the moving mass and must prevail in accordance with Newton's second law of motion.

It is apparent that the static pressure of the water against the vertical section *cd* acts toward the right (downstream). Opposed to this force is the hydrostatic pressure against the vertical section *cf* (upstream) and the surface friction along the bottom *df*. In practically all cases, the friction is small and may be neglected.

The following assumptions are made in the analysis:

1. The channel is rectangular in shape, having parallel side constraints.
2. A horizontal floor exists.
3. All friction losses are neglected.
4. The hydraulic jump is assumed to take place instantaneously.
5. Streamline flow exists immediately before and after the jump.

In Fig. 4-2, y_1 and v_1 represent the depth and velocity, respectively, upstream of the jump, and P_1 the total hydrostatic pressure over the vertical section *cd*. For simplicity, the channel width will be assumed to be unity.

The change in hydrostatic pressure ΔP from section 1 to section 2 is computed from the total depth at each section.

$$\Delta P = P_2 - P_1 \quad (4-1)$$

and, for a rectangular channel of unit width,

$$P_2 - P_1 = \frac{1}{2}\gamma(y_2^2 - y_1^2) \quad (4-2)$$

The change in momentum ΔM will be computed from the velocity of the main stream itself, since the roller has no downstream velocity effect. Thus

$$\Delta M = \frac{\gamma q(v_1 - v_2)}{g} \quad (4-3)$$

In accordance with Newton's second law of motion, the change in hydrostatic pressure must equal the change in momentum.

$$\Delta P = \Delta M$$

$$\text{or } \frac{\gamma q v_1}{g} + P_1 = \frac{\gamma q v_2}{g} + P_2 \quad (4-4)$$

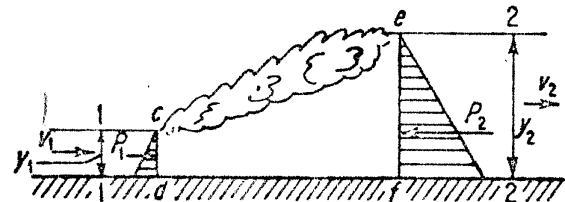


FIG. 4-2. Schematic diagram of the hydraulic jump.

For a rectangular channel, Eq. (4-4) becomes

$$y_2^2 - y_1^2 = \frac{2q}{g} (v_1 - v_2) \quad (4-5)$$

Substituting q/y for v and collecting terms, we have

$$y_1 y_2 (y_1 + y_2) = \frac{2v_1^2 y_1^2}{g} \quad (4-6)$$

and solving for y_2 in terms of y_1 and v_1 , Eq. (4-6) becomes

$$y_2 = -\frac{y_1}{2} + \sqrt{\frac{2v_1^2 y_1}{g} + \frac{1}{4} y_1^2} \quad (4-7)$$

or, in terms of q ,

$$y_2 = -\frac{y_1}{2} + \sqrt{\frac{2q^2}{y_1 g} + \frac{1}{4} y_1^2} \quad (4-8)$$

Similarly $y_1 = -\frac{y_2}{2} + \sqrt{\frac{2q^2}{y_2 g} + \frac{1}{4} y_2^2}$ (4-9)

4-2. Theoretical Investigations. In addition to the momentum formula, several investigators have developed formulas which, in general, are modifications or simplifications of the momentum formula. Depending upon the accuracy required, these formulas can be employed to render quick results.

Kennison,¹⁸ in 1916, simplified the momentum formula by dividing Eq. (4-6) by y_1^2 and, by collecting terms, obtained

$$\left(\frac{y_2}{y_1}\right)^2 + \frac{y_2}{y_1} = \frac{2v_1^2}{gy_1} \quad (4-10)$$

By plotting $v_1/\sqrt{gy_1}$ versus y_2/y_1 , Kennison obtained a straight-line relationship having the equation

$$y_2 = \frac{v_1 \sqrt{y_1}}{4} - 0.45y_1 \quad (4-11)$$

It should be noted that Eq. (4-11) is dimensionally incorrect. However, for low values of v_1 (less than or equal to 10 fps), values of y_2 within 1 per cent of the actual values can be obtained, and for high values of v_1 (greater than 10 fps) a better equation is

$$y_2 = \frac{v_1 \sqrt{y_1}}{4} - 0.50y_1 \quad (4-12)$$

Although the Kennison formula does not include a gravity term, the results of this formula agree remarkably well with the momentum formula.

In 1903, Merriman²² developed a simplified formula for the hydraulic jump. In developing his equation, Merriman assumed that the velocity head was lost in two ways: first by impact and second by the uplifting of the whole quantity of water through the height of the jump. Derivation of the Merriman formula will not be presented since this formula does not yield correct results. The results of the Merriman formula differ by approximately 15 per cent from those of the momentum formula. The Merriman simplified formula is usually written in the following form:

$$y_1 = \sqrt{\frac{2v_1^2 y_1}{g}} \quad (4-13)$$

In 1933, Inglis and Joglekar,¹⁶ engineers for the government of Bombay, India, modified the momentum formula by neglecting the $\frac{1}{4}y_1^2$ term of Eq. (4-7).

$$y_2 = -\frac{1}{2} y_1 + \sqrt{\frac{2v_1^2 y_1}{g}} \quad (4-14)$$

For some purposes, Eq. (4-14) can be used with advantage, since its simplicity renders it adaptable to rapid calculations.

It should be remembered that for the hydraulic jump to occur, the momentum and velocity must be lost at a rate sufficient to overcome both the friction and the adverse hydrostatic pressure. In most problems, the energy and momentum curves can be computed from the average velocity, but where local conditions cause a considerable deviation from the normal velocity distribution, a corrective factor should be applied to compensate for the fact that the average of the momentum and energy transported across elementary areas exceeds the momentum and energy based upon the average velocity.

4-3. Verification of the Momentum Formula. Since 1819, numerous experiments have been conducted to verify the momentum formula. Apparently, the first measurements to determine the height of the hydraulic jump preceded the development of the correct theory.

To the best of the author's knowledge, the first measurements and description of the hydraulic-jump phenomenon were made during October and November of 1818 by Bidone,⁵ at the Université Royale in France. Bidone's experiments were made in a small rectangular flume 1.066 ft wide, with a slope of 0.023. This early investigation perhaps served as an incentive to others to further investigate the phenomenon.

In 1828, Belanger⁴ suggested the application of the momentum principle to the hydraulic jump and was apparently the first to develop the correct mathematical theory. The momentum principle was later emphasized in 1860 by Bresse,⁶ and still later, in 1880, by Unwin.³⁰

Additional experiments to determine the depth after the jump were made in a rectangular flume 6.53 ft wide by Darcy and Bazin¹⁰ during 1856 and 1858. Results of the experiments appeared in *Recherches Hydrauliques*, published in Paris during 1865.

Still later, in 1913, Professor Gibson¹⁴ investigated the elements of the hydraulic jump. Of the early investigators, Gibson's results appear to give the best verification of the momentum principle. Gibson used a wider channel than his predecessors, and therefore his experiments, made in a flume 3 ft wide, were a better representation of an ideal frictionless channel.

The first investigations on the hydraulic jump made in the United States were during 1894 by Ferriday,¹³ at Lehigh University. Ferriday's experiments were made in a trough 0.66 ft wide, laid on different slopes to create a variety of velocities.

Additional experiments on the hydraulic jump were conducted in 1917 by Riegel and Beebe²⁵ of the Miami Conservancy District, Dayton, Ohio. The experiments of Riegel and Beebe were made in a rectangular flume 10 ft wide and agree very well with the momentum formula.

A series of experiments conducted by Safranez²⁶ on a two-dimensional physical study of the jump in a glass-walled flume 1.63 ft wide was made in 1929 at the Technische Hochschule, Berlin, Germany. Results of these experiments also verify the momentum theory.

A project was conducted by Bakhmeteff and Matzke² in the hydraulic laboratory of Columbia University to determine the general relationships that applied to hydraulic jumps of every size and nature. These experiments, made in a flume 0.5 ft wide, were therefore materially affected by friction.

During 1935, Kinney¹⁹ conducted a series of experiments on the hydraulic jump in the hydraulic laboratory of the State University of Iowa. All experiments were conducted in a horizontal, rectangular flume 2.185 ft wide.

More recently, in 1954, a large number of experiments on the hydraulic jump were performed in the hydraulic laboratory of the Bureau of Reclamation.⁷ A total of 125 tests were run in six rectangular flumes varying in width from 1 to 5 ft. The author has used the experimental data obtained by the Bureau of Reclamation in preparing Fig. 4-3. The relationship between y_2/y_1 and the kinetic-flow factor λ_1 shown in Fig. 4-3 verifies beyond doubt the applicability of the momentum formula to the hydraulic jump. In the experiments, the tailwater was varied until the hydraulic jump formed for the given kinetic-flow factor. It will be noted that the lower end of the curve does not fully agree with the experimental data. This seems to indicate the difficulty of making precise measurements in the vicinity of the critical depth.

4-4. Dimensionless Equations. Dimensionless equations can frequently be used to great advantage, since they often simplify and tend to generalize the relationships in question.

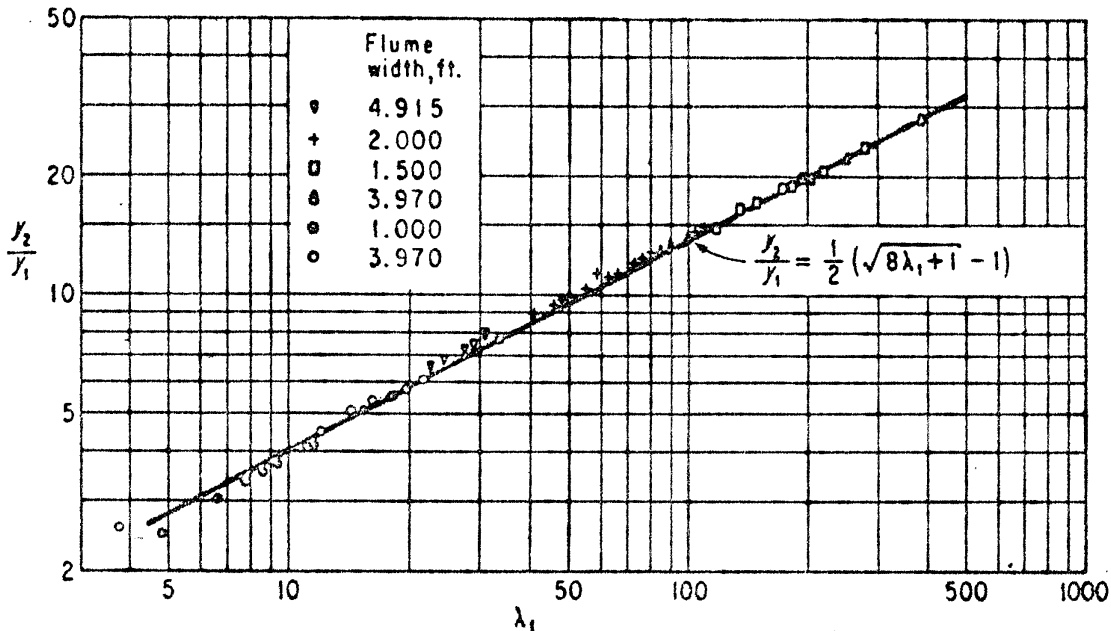


FIG. 4-3. Verification of the momentum formula.

The following analysis, originated by Crump,⁹ presents the relationship between y_1/y_c and y_2/y_c for a given discharge: if $v_1 = q/y_1$ is substituted in Eq. (4-6), we have

$$y_1 y_2 (y_1 + y_2) = \frac{2q^2}{g} \quad (4-15)$$

Since for a rectangular channel $y_c^3 = q^2/g$, Eq. (4-15) becomes

$$y_1 y_2 (y_1 + y_2) = 2y_c^3 \quad (4-16)$$

To obtain dimensionless ratios, divide each term of Eq. (4-16) by y_c^3 .

$$\frac{y_1}{y_c} \frac{y_2}{y_c} \left(\frac{y_1}{y_c} + \frac{y_2}{y_c} \right) = 2 \quad (4-17)$$

then let

$$x = \frac{y_1}{y_c} \quad \text{and} \quad y = \frac{y_2}{y_c}$$

Equation (4-17) becomes

$$xy(x + y) = 2 \quad (4-18)$$

which is a dimensionless equation, relating y_1/y_c and y_2/y_c for a rectangular channel.

Another dimensionless equation can be derived for a rectangular channel as follows:

$$H_1 = y_1 + \frac{1}{2} \frac{y_c^3}{y_1^2} \quad (4-19)$$

and similarly,

$$H_2 = y_2 + \frac{1}{2} \frac{y_c^3}{y_2^2} \quad (4-20)$$

Dividing by y_c , we have

$$\frac{H_1}{y_c} = \frac{y_1}{y_c} + \frac{1}{2} \left(\frac{y_c}{y_2} \right)^2$$

Let $s = \frac{H_1}{y_c}$ and $t = \frac{H_2}{y_c}$

If Eqs. (4-19) and (4-20) are divided by y_c , we have

$$s = x + \frac{1}{2x^2} \quad (4-21)$$

and $t = y + \frac{1}{2y^2}$ (4-22)

Both Eqs. (4-21) and (4-22) are also dimensionless and applicable only for rectangular channels.

4-5. Kinetic-flow-factor Relationships. Since gravity is an important factor in the formation of the hydraulic jump, the height of the jump will be a function of the kinetic-flow factor λ , which also serves as a flow indicator. As previously explained, λ is the square of the Froude number.

$$\lambda = \frac{v^2}{gy}$$

and, for a rectangular channel,

$$\lambda = \frac{q^2}{gy^3} \quad (4-23)$$

or, since $y_c^3 = q^2/g$, then

$$\lambda = \left(\frac{y_c}{y} \right)^3 \quad (4-24)$$

When $y = y_c$, $\lambda = 1$ and critical flow prevails.

If $\lambda_1 = v_1^2/gy_1$ is substituted into Eq. (4-7), the momentum formula becomes

$$\frac{y_2}{y_1} = \frac{1}{2} (\sqrt{1 + 8\lambda_1} - 1) \quad (4-25)$$

and similarly,

$$\frac{y_1}{y_2} = \frac{1}{2} (\sqrt{1 + 8\lambda_2} - 1) \quad (4-26)$$

From Eq. (4-24),

$$\frac{y}{y_c} = \frac{1}{\lambda^{3/2}} \quad (4-27)$$

and since $x = y_1/y_c$, then

$$x = \frac{1}{\lambda_1^{1/3}} \quad (4-28)$$

and

$$y = \frac{1}{\lambda_2^{1/3}} \quad (4-29)$$

When Eqs. (4-28) and (4-29) are combined, we have

$$\left(\frac{y_2}{y_1}\right)^3 = \frac{\lambda_1}{\lambda_2} \quad (4-30)$$

And since

$$\frac{y_2}{y_1} = \frac{1}{2} (\sqrt{1 + 8\lambda_1} - 1) \quad (4-31)$$

therefore

$$\frac{\lambda_1}{\lambda_2} = \left[\frac{1}{2} (\sqrt{1 + 8\lambda_1} - 1) \right]^3 \quad (4-32)$$

and

$$\lambda_2 = \frac{8\lambda_1}{(\sqrt{1 + 8\lambda_1} - 1)^3} \quad (4-33)$$

Similarly

$$\lambda_1 = \frac{8\lambda_2}{(\sqrt{1 + 8\lambda_2} - 1)^3} \quad (4-34)$$

The relationship between λ_1 and λ_2 is shown in Eqs. (4-33) and (4-34) and is applicable only for rectangular channels.

4-6. Height and Length of the Hydraulic Jump. The height of the jump can be defined as the difference between the depth of water upstream and downstream of the jump. Hereafter, it will be designated by y_j . Thus

$$y_j = y_2 - y_1 \quad (4-35)$$

It will be later shown that the length of the hydraulic jump bears a definite relationship to the height of the hydraulic jump.

The length of the hydraulic jump is of particular significance since it is the principal factor in determining the length of stilling basins. The longitudinal element of the jump is, without doubt, the most difficult element to measure. Certainly, this is partially because of differences in opinion as to exactly where the terminus of the jump lies. In addition, there is a lack of agreement among investigators as to the definition of the length of the jump.

In the past, there have been several definitions of the jump length. Two of the more commonly used definitions are depicted by Fig. 4-4a and b. In Fig. 4-4a, the length of the jump is from point A, where the jet with a supercritical velocity rises and meets the water with streaming flow, to point B, where there is a subcritical velocity.

In Fig. 4-4b, the length of the jump is taken to be that of the surface roller. The point B can be called the stagnation point, since at this

point some of the water moves downstream, while a portion of the flow rolls upstream and joins the jet having a supercritical velocity. It is therefore a matter of opinion as to the definition of the length of the jump.

The writer prefers the following definition: The origin of the jump is the point where the roller turbulence begins and the water becomes white and foamy because of the large amount of entrained air. Downstream, the terminus of the jump is defined as the point where no return flow is observable, and the point which would best represent the end of a stilling basin.

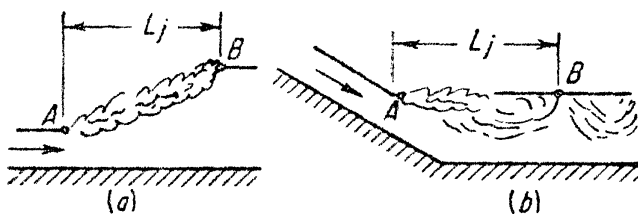


FIG. 4-4. Length of hydraulic jump.

In 1947, Behera and Qureshy,³ graduate students at the State University of Iowa, defined the length of the jump as follows:

The length of the jump is the distance between the toe of the jump and the section where a cylinder placed in the flow, on the floor of the channel, will just topple. At first the cylinder is placed far downstream and gradually moved upstream until it is toppled by the flow.

This method of finding the terminus of the hydraulic jump is to be commended, since it minimizes the personal factor accompanying other methods of determining the jump length. Forces exerted on the cylinder, however, are affected by the boundary layer near the channel floor.

Safranez,²⁶ while at the Technische Hochschule in Berlin, Germany, measured the length of the hydraulic jump in flumes having widths of 50 and 100 cm. It was observed that the length of the jump in the narrower flume was materially less than in the wider flume, indicating that friction does exert an influence on the length of the jump.

Bakhmeteff and Matzke² conducted extensive experiments at Columbia University during 1932 and 1933 in order to determine the longitudinal element of the hydraulic jump. These experiments were made in a flume 20 ft long, 22 in. high, and 6 in. wide. After examining the experimental results, the investigators proposed that the length of the hydraulic jump is a function of the kinetic-flow factor and of the height of the jump. Figure 4-5 shows the relationship of the kinetic-flow factor λ_1 to L_j/y_j and L_j/y_1 . The lengths of the hydraulic jump are probably affected by the friction of the narrow channel and therefore are somewhat less than the jump lengths produced in a wider channel.

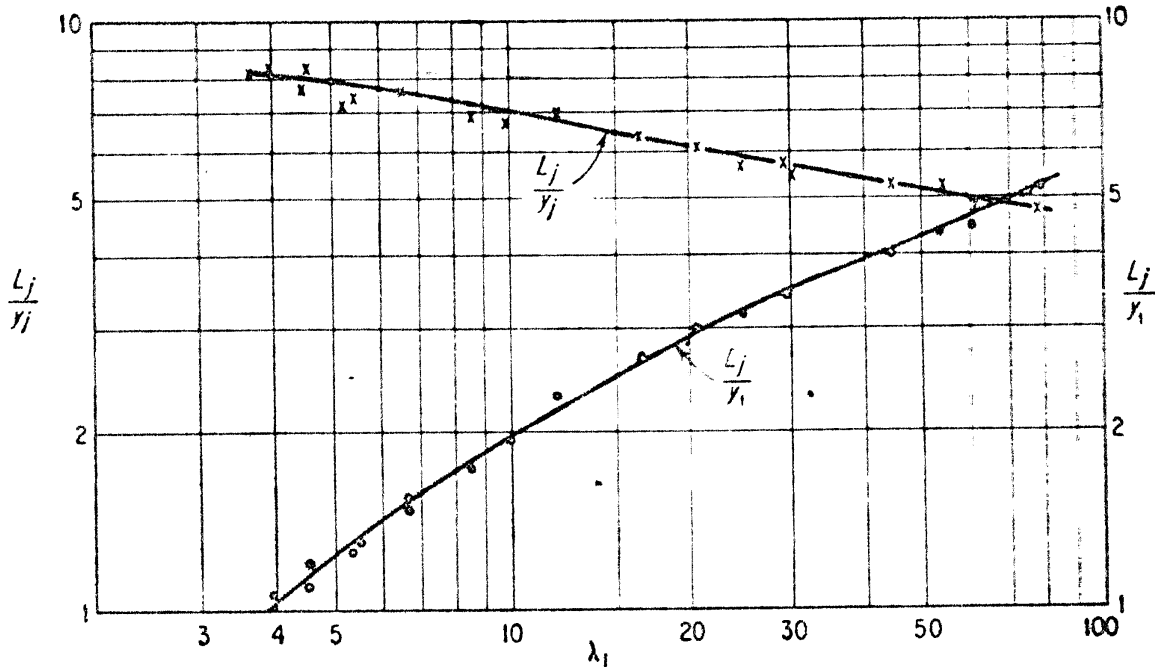


FIG. 4-5. Length versus height of hydraulic jump.

TABLE 4-1. LENGTH OF THE HYDRAULIC JUMP ON A HORIZONTAL FLOOR

Investigator	Date	Proposed formula
Ludin ²¹	$L_j = y_2 \left(4.5 - \frac{v_1}{v_c} \right)$
Safranez ²²	1927	$L_j = \text{approx } 5.2 y_2$
Bakhmeteff, Matzke ²³	1932-1933	$L_j = 5(y_2 - y_1)$
Knapp ²⁰	1932	$L_j = \left(62.5 \frac{y_1}{H_1} + 11.3 \right) \left[\frac{(v_1 - v_2)^2}{2g} - (H_1 - H_2) \right]$ $H = y + \frac{v^2}{2g}$
Smetana ²⁷	1934	$L_j = \text{approx } 6(y_2 - y_1)$
Kinney ¹⁹	1935	$L_j = 6.02(y_2 - y_1)$
Douma ¹¹	$L_j = 3y_2$
Posey ²⁴	1941	$L_j = \text{approx } 4.5-7(y_2 - y_1)$
Wu ²⁸	1949	$L_j = 10(y_2 - y_1)F_1^{-0.16}$
Woycicki ³²	1934	$L_j = (y_2 - y_1) \left(8 - 0.05 \frac{y_2}{y_1} \right)$
Ivanchenko ¹⁷	$L_j = 10.6\lambda_1^{-0.185}(y_2 - y_1)$
Einwachter ¹²	1933	$L_r = \left(15.2 - 0.241 \frac{y_2}{y_1} \right) \left[\left(\frac{y_2}{y_1} - 1 \right) - \frac{v_1^2(y_2/y_1 - 1)}{(y_2/y_1)^2 g} \right]$
Chertoussov ⁸	1935	$L_j = 10.3y_1(F_1 - 1)^{0.41}$
Page ²³	1935	$L_j = 5.6y_2$
Riegel, Beebe ²⁵ ..	1917	$L_j = \text{approx } 5(y_2 - y_1)$
Aravin ¹	1935	$L_j = \text{approx } 5.4(y_2 - y_1)$

NOTE: v_c = critical velocity, and L_r = length of roller.

Stevens²⁸ proposes that the length of the jump is a result of two motions: first, the translatory motion of the water prism downward and, secondly, the vertical motion due to the rate of conversion of kinetic to potential energy.

An interesting observation was made in 1937 by Willes³¹ regarding the effect of entrained air upon the length of the jump. Willes observed that for values of λ_1 less than 12, the admission of air into the jump decreased the comparative length of the jump, whereas for values of λ_1 greater than 12, the comparative length of the jump was increased. Table 4-1 summarizes the various proposed formulas for determining the length of the hydraulic jump.

In 1954, a series of measurements to determine the length of the hydraulic jump was made by the Bureau of Reclamation.⁷ In these experiments, the length of the jump was measured from the intersection of the chute and horizontal floor to a point downstream where the high-velocity jet began to leave the floor or to a point on the surface immediately downstream from the roller, whichever was longer. It was the intention of Bureau of Reclamation engineers to judge the length of the jump from a practical standpoint which would best represent the end of the concrete floor and side walls of a conventional stilling basin. In the experiments the Froude number was varied from 2 to 20.

An analysis of the experimental data indicated that a good relationship between the length and height of the hydraulic jump exists. Figure 4-6 shows this relationship, indicating that the length of the jump is 6.9 times the jump-height.

Contrary to the views of many investigators, the length of the hydraulic jump on a horizontal floor was found to be independent of the Froude number. It is possible, however, that when the Froude number exceeds 20, it may exert some influence upon the length of the hydraulic jump.

4-7. Location of the Hydraulic Jump. As previously explained in Chap. 3, the hydraulic jump will form only when the pressure plus momentum per unit time for both supercritical and subcritical stages of flow are equal.

It is important to determine just where the hydraulic jump will form. This can be predicted, within certain limits, depending upon the accuracy with which the friction losses can be estimated. The sections of equal pressure plus momentum between which the jump is included are not at the same location but are definitely separated along the longitudinal axis of the channel. The necessity of considering the length in determining the location of the hydraulic jump was first presented by Trahern,²⁹ who proposed that the hydraulic jump will form when the pressure plus momentum after the jump equals the pressure plus m-

tum before the jump, at a distance approximately equal to the length of the jump between the sections.

In considering the case of the hydraulic jump below a sluice gate, depicted by Fig. 4-7, the water surface curves for flow approaching the jump ab and leaving the jump ed can be computed by backwater-curve computations. The curve bc is a plot of the depths sequent to the depths of curve ab . Line fg is a horizontal line equal to the estimated length of the jump connecting curves bc and ed . Since the depth at g is sequent to depth y , the jump will form at location hg . If the tailwater depth is less than y_2 , the jump will move downstream until v_1 is sufficiently reduced, so that the y_2 depth required will be less.

The following rules will be useful in determining the pressure-plus-momentum relationships, and consequently in determining where the jump will form:

1. When the flow is supercritical, the pressure plus momentum increases as the depth decreases and decreases as the depth increases.
2. When the flow is subcritical, the pressure plus momentum increases as the depth increases and decreases as the depth decreases.

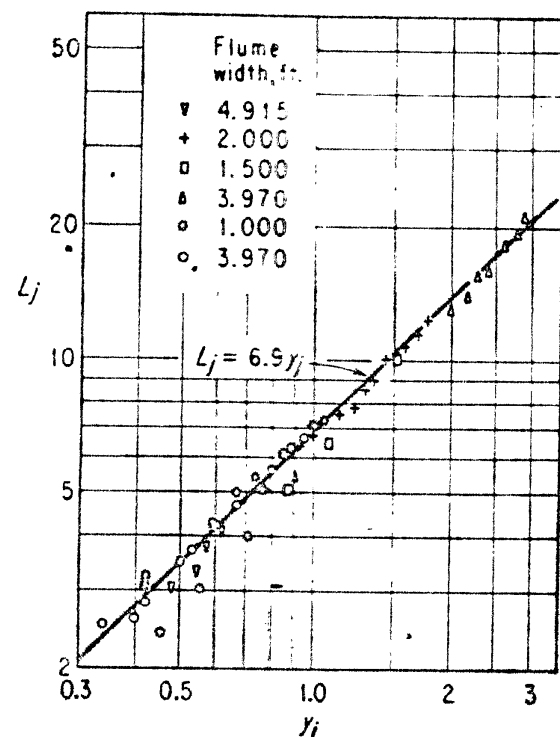


FIG. 4-6. Relation between length and height of hydraulic jump.

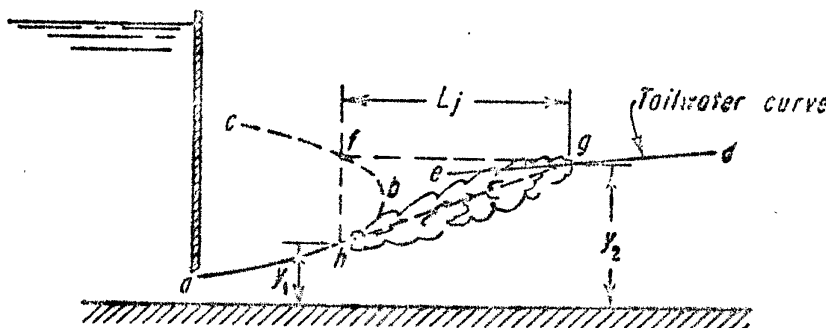


FIG. 4-7. Location of the hydraulic jump.

3. If the flow is accelerating when approaching the jump, the pressure-plus-momentum curve rises in the direction of the flow.
4. If the flow is decelerating when approaching the jump, the pressure-plus-momentum curve drops in the direction of the flow.

5. If the flow is uniform when approaching the jump, the pressure-plus-momentum curve will be horizontal.
6. If the flow is accelerating when leaving the jump, the pressure-plus-momentum curve drops in the direction of the flow.
7. If the flow is decelerating when leaving the jump, the pressure-plus-momentum curve rises in the direction of the flow.
8. If the flow is uniform when leaving the jump, the pressure-plus-momentum curve remains horizontal.

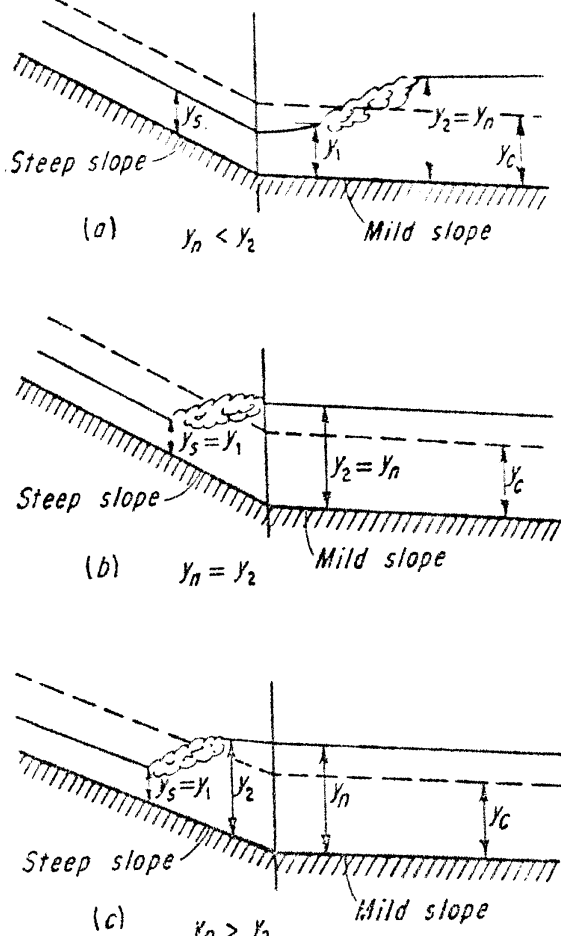


FIG. 4-8. Location of the hydraulic jump in steep and mild channels.

Case I. $y_n < y_2$. Figure 4-8a shows the case in which the normal depth on the mild slope is less than the conjugate depth y_2 corresponding to the normal depth in the steep portion y_s , and the jump will form when y_n is conjugate to y_s and the terminus of the jump at the junction of the slopes.

Case II. $y_n = y_2$. Figure 4-8b shows the case in which the normal depth on the mild slope is just equal to the conjugate depth y_2 corresponding to the normal depth in the steep portion y_s , and the jump will form when y_n is conjugate to y_s and the terminus of the jump at the junction of the slopes.

One of the problems that will be encountered by the designer is to find the location of the hydraulic jump at the junction of steep and mild slopes. This case is always present for a chute with a break in grade that changes from a steep to a mild slope. In the first case, shown in Fig. 4-8a, the jump may occur in either the steep or the mild portion of the channel.

Case I. $y_n < y_2$. If the normal depth in the mild portion is less than the upper conjugate depth y_2 corresponding to normal depth in the steep portion, supercritical flow will continue in the lower stage until extended to the mild portion, thereby increasing the depth on the mild slope. Downstream from the break in grade, the depth y_1 and the normal depth y_n are brought into conjugate positions, and the jump must occur under these conditions.

Case III. $y_n > y_2$. If the normal depth in the mild portion is greater than the conjugate depth y_2 corresponding to the normal depth y_n in the steep portion, shown in Fig. 4-8c, subcritical flow will extend upstream until y_1 and y_2 are brought into conjugate positions where the jump must occur.

4-8. Effects of Viscosity and Surface Tension. In 1941, Goodrum and Dubrow¹⁵ studied the effects of surface tension and viscosity upon the surface profile of the hydraulic jump. Results of the experiments indicated that surface tension had no effect upon the jump profile, whereas an increase in viscosity was accompanied by an increase in the slope of the face of the jump and a shorter jump length. Figure 4-9 is a

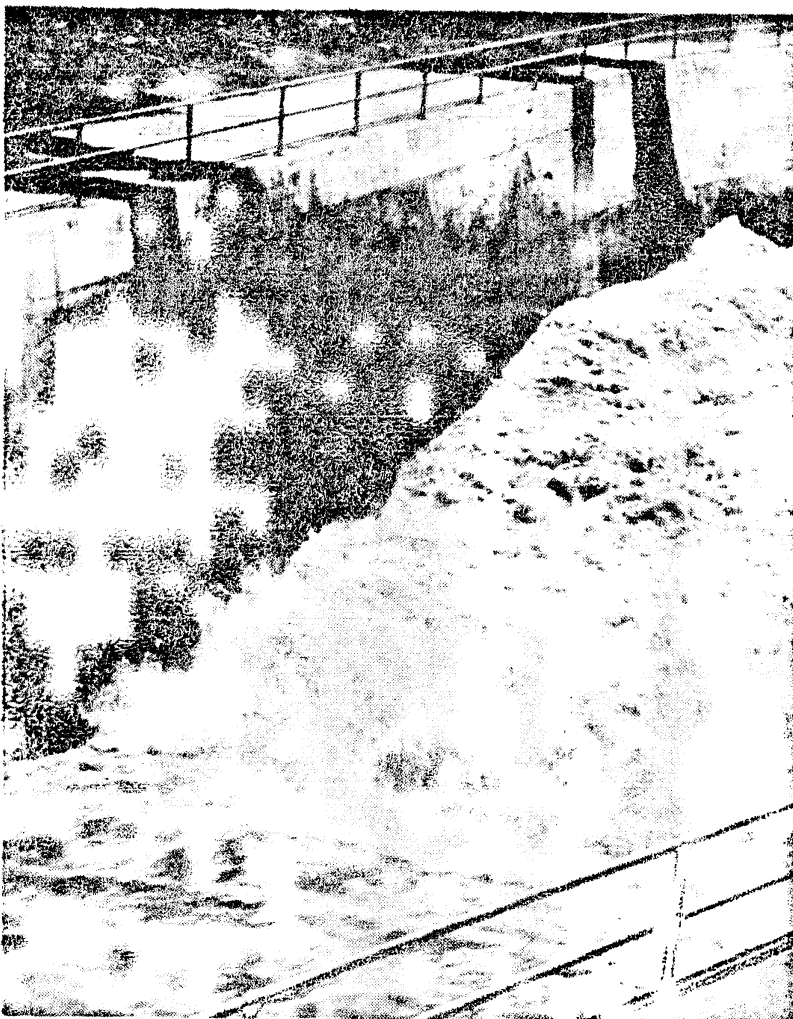


FIG. 4-9. Left side of the Mohawk Dam stilling basin, illustrating the profile of the hydraulic jump. Approximate discharge is 5,000 cfs. (*Courtesy of Corps of Engineers, Huntington District.*)

photograph of the stilling basin of the Mohawk Dam showing the profile of the hydraulic jump.

4-9. Formation of Jump at an Abrupt Drop. An abrupt drop in the bottom of a channel can be used effectively to provide the additional depth necessary for the hydraulic jump to form. The drop will stabilize the formation of the jump over a broad and continuous range of downstream depths and enable a shorter stilling basin to be employed. Moore and Morgan³⁴ investigated the characteristics of an abrupt drop in a channel bottom and found that two different forms of the jump may

occur. The transition between the two forms is characterized by an undular wave.

Figure 4-10a and b depicts the parameters at a rectangular abrupt drop. The relative height of the jump y_2/y_1 was found to be dependent upon the parameters $\Delta Z/y_1$, h/y_1 , and the entering Froude number. As the jump changes from one form to another, the value of the hydrostatic head h will change. When the jump forms upstream of the drop, the hydrostatic pressure has a maximum value of $\gamma h = \gamma y_2$, indicated in Fig. 4-10a. The hydrostatic pressure has a minimum value of $\gamma h < (\Delta Z + y_1)$ when the jump forms downstream from the drop.

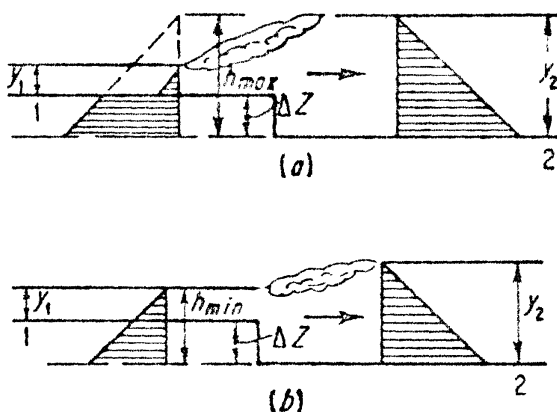


FIG. 4-10. Hydraulic jump at an abrupt drop.

By applying the momentum equations between sections 1 and 2, Moore obtained the following relationship between the parameters:

$$\lambda_1 = \frac{(y_2/y_1)^2 - (1 + \Delta Z/y_1)^2 - 2(\Delta Z/y_1)(h/y_1 - \Delta Z/y_1 - 1)}{2(1 - y_1/y_2)} \quad (4-36)$$

Equation (4-36) can be utilized to determine the effect of both the upstream and downstream geometry of the drop on the characteristics of the jump. A series of curves can be developed which will permit a direct reading of y_2/y_1 for values of $\Delta Z/y_1$ and λ_1 .

4-10. Formation of Jump at an Abrupt Rise. When excess tailwater exists, an abrupt rise, depicted by Fig. 4-11, can be constructed in the

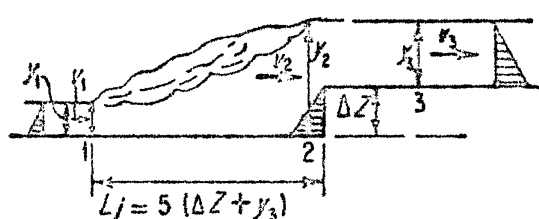


FIG. 4-11. Hydraulic jump at an abrupt rise.

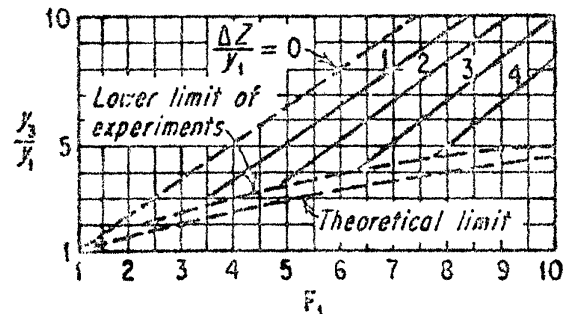


FIG. 4-12. Characteristics of hydraulic jump at an abrupt rise.

channel bottom to decrease the tailwater and permit the jump to form. Forster and Skrinde²⁵ investigated the effect of $\Delta Z/y_1$ at the end of the jump, $L_j = 5(\Delta Z + y_3)$, and found that it could best be related to y_3/y_1 and F_1 . A graphical summary of their results is shown in Fig. 4-12.

By applying the momentum equation between sections 2 and 3, for an abrupt rectangular rise with a width of unity, we have

$$\frac{\gamma y_2^2}{2} - \frac{\gamma y_3^2}{2} - \frac{\gamma h}{2} (2y_2 - h) = \rho q(v_3 - v_2) \quad (4-37)$$

Since, by the equation of continuity,

$$v_3 y_3 = v_2 y_2 = v_1 y_1$$

Then we can eliminate v_2 , v_3 , and y_2 from Eq. (4-37) and

$$\left(\frac{y_3}{y_1}\right)^2 = 1 + 2\lambda_1 \left(1 - \frac{y_1}{y_3}\right) + \frac{\Delta Z}{y_1} \left(\frac{\Delta Z}{y_1} - \sqrt{1 + 8\lambda_1} + 1\right) \quad (4-38)$$

For a fixed value of $\Delta Z/y_1$, Eq. (4-38) is implicit for y_3/y_1 in terms of λ_1 and may be solved by trial. The experimental curves presented in Fig. 4-12 conform closely to the theoretical curves.

For most tailwater-rating curves, the maximum value of ΔZ occurs for the maximum discharge condition. It is suggested that the F_1 and y_3/y_1 be determined for the maximum discharge, and the corresponding value of $\Delta Z/y_1$ be found by interpolating between the curves presented in Fig. 4-12. This procedure can be repeated for the anticipated range of discharges to find the minimum height ΔZ necessary to prevent the jump from being swept downstream.

REFERENCES

1. Aravin, W. I.: The Determination of the Length of the Hydraulic Jump, trans. by A. Luksch, *Trans. Sci. Research Inst. Hydrotechnics*, pp. 48-57, 1935.
2. Bakhmeteff, B. A., and A. E. Matzke: The Hydraulic Jump in Terms of Dynamic Similarity, *Trans. ASCE*, 1936.
3. Behera, B., and A. A. Qureshy: "Length Criterion for the Hydraulic Jump," unpublished M.S. thesis, State University of Iowa, June, 1947.
4. Belanger, J. M.: "Notes sur le cours d'hydraulique mémoires, École Nationale des Ponts et Chaussées," Paris, 1849-1850.
5. Bidone, G.: Observations on the Height of the Hydraulic Jump, *Trans. Roy. Soc. Turin*, pp. 21-80, 1819.
6. Bresse, J. A.: "Cours de mécanique appliquée," part 2, "Hydraulique," Mallet-Bachelier, Paris, 1860.
7. Bureau of Reclamation, Progress Report II, Research Study on Stilling Basins, Energy Dissipators, and Associated Appurtenances, *Hydraulic Lab. Rep. Hyd.-399*, June, 1955.
8. Chertoussov, M. D.: Some Characteristics Regarding the Length of the Hydraulic Jump, *Trans. Sci. Research Inst. Hydrotechnics*, pp. 67-76, 1935.
9. Crump, E. S.: "Note on an Approximate Method of Determining the Position of a Standing Wave," Government Printing Office, Punjab, Lahore, India, May, 1930.
10. Darcy, H. P. G., and H. E. Bazin: Observations of the Height of the Hydraulic Jump, *Recherches Hydrauliques*, pp. 284-292, 1865.

11. Douma, J. H.: Discussion of the Study of Stilling Basin Design, *Trans. ASCE*, pp. 490-523, 1934.
12. Einwachter, J.: Berechnung in der Wehrbreite gemessenen Langenausdehung von Deckwalzen, *Wasserwirtschaft u. Wasserwirtsch.*, Hefte 14 and 21, 1932.
13. Ferriday, R.: "The Hydraulic Jump," unpublished thesis, Lehigh University, 1894.
14. Gibson, A. H.: The Formation of Standing Waves in an Open Channel, *Proc. Inst. Civil Engrs. (London)*, paper 4081, part 3, 1913-1914.
15. Goodrum, J. C., and M. D. Dubrow: "Effects of Certain Fluid Properties upon the Profile of the Hydraulic Jump," unpublished M.S. thesis, State University of Iowa, February, 1941.
16. Inglis, C. C., and D. V. Joglekar: The Dissipation of Energy below Falls, Government of Bombay, *Public Works Dept. Tech. Paper* 44, p. 19, 1933.
17. Ivanchenko, A.: Discussion of the Hydraulic Jump in Terms of Dynamic Similarity, *Trans. ASCE*, 1936.
18. Kennison, K. R.: The Hydraulic Jump in Open Channels at High Velocity, *Trans. ASCE*, paper 1355, 1916.
19. Kinney, C. W.: "Stilling Pools for Spillways," unpublished M.S. thesis, State University of Iowa, p. 63, June, 1935.
20. Knapp, F.: Discussion of the Hydraulic Jump in Terms of Dynamic Similarity, *Trans. ASCE*, 1936.
21. Ludin, A., and D. P. Barnes: Investigation of the Length of the Hydraulic Jump at Berlin, *Civil Eng.*, p. 262, May, 1934.
22. Merriman, M.: "Treatise on Hydraulics," 10th ed., John Wiley & Sons, Inc., New York, 1916.
23. Page, N.: Discussion of the Hydraulic Jump in Terms of Dynamic Similarity, *Trans. ASCE*, 1936.
24. Posey, C. J., and S. M. Woodward: "Steady Flow in Open Channels," John Wiley & Sons, Inc., New York, 1941.
25. Riegel, R. M., and J. C. Beebe: The Hydraulic Jump as a Means of Dissipating Energy, *Miami Conservancy District Tech. Rep.*, part III, 1917.
26. Safranez, K.: Untersuchungen ueber der Wechselsprung, *Bauingenieur*, pp. 649-668, Sept. 13, 1929.
27. Smetana, J.: "Experimental Study of the Submerged or Expanded Hydraulic Jump," report translated from the Russian by A. D. Kalal, Bureau of Reclamation, 1934.
28. Stevens, J. C.: Discussion of the Hydraulic Jump in Terms of Dynamic Similarity, *Trans. ASCE*, 1936.
29. Trahern, J. W.: Location of the Hydraulic Jump, *Western Construction*, pp. 605-607, Oct. 25, 1932.
30. Unwin, W. E.: "Encyclopaedia Britannica," vol. 12, pp. 499-512, 1915.
31. Willes, W. H.: "A Photographic Study of the Effects of Entrained Air on the Hydraulic Jump," unpublished B.S. thesis, Utah State Agricultural College, 1937.
32. Woycicki, K.: The Hydraulic Jump and Its Top Roll and the Discharge of Sluice Gates, trans. by I. B. Hosig, Federal Institute of Technology, Zurich, Switzerland, chaps. 3 and 4, *Bur. Reclamation Tech. Memorandum* 435, 1935.
33. Wu, C. K.: "The Hydraulic Jump in Rectangular Channels," unpublished M.S. thesis, Texas A & M., January, 1949.
34. Moore, W. L., and C. W. Morgan: The Hydraulic Jump at an Abrupt Drop, *ASCE Hydraulics Division J.*, paper 1449, December, 1957.
35. Forster, J. W., and R. A. Skrindle: Control of the Hydraulic Jump by Sills, *Proc. ASCE*, April, 1949.

5

Hydraulic Jump in Nonrectangular Channels

At times, the designer may be confronted with the problem of determining the location and properties of the formation of the hydraulic jump in channel shapes other than rectangular. Formulas involving the formation of the hydraulic jump become quite complex for channels of non-rectangular shapes, and often a trial-and-error solution may be the most expedient method of solving the problem.

This chapter is devoted principally to determining the properties of the hydraulic jump in trapezoidal and circular channels. For large structures of nonrectangular shape, model studies are advisable to help predict operation of the prototype.

TRAPEZOIDAL CHANNELS

5-1. Pressure-Momentum Relationships. For trapezoidal channels, the momentum equation becomes complex, and if only a small number of solutions are required, the relationship between elements of the hydraulic jump can be found by trial and error or by plotting a series of pressure-plus-momentum curves. Unless a large number of solutions are required, the preparation of charts or nomographs is not justified.

The fundamental law of conservation of linear momentum can be applied to the hydraulic jump occurring in any prismatic channel. As previously discussed, the sum of the pressure plus momentum before the jump must equal the sum of the corresponding quantities after the jump. For a trapezoidal channel, the pressure and momentum relationship becomes

$$\gamma A_2 \bar{y}_2 - \gamma A_1 \bar{y}_1 = \frac{\gamma Q}{g} (v_1 - v_2) \quad (5-1)$$

In Eq. (5-1), $\gamma A_1 \bar{y}_1$ and $\gamma A_2 \bar{y}_2$ represent the total hydrostatic pressure before and after the jump, respectively, while $\gamma Q/g(v_1 - v_2)$ represents the rate of change of momentum per unit time.

By eliminating γ and applying the equation of continuity, Eq. (5-1) is reduced to the form

$$A_1\bar{y}_1 + \frac{Q^2}{A_1g} = A_2\bar{y}_2 + \frac{Q^2}{A_2g} \quad (5-2)$$

$$\text{Then } P + M = A\bar{y} + \frac{Q^2}{Ag} \quad (5-3)$$

or, for a constant discharge,

$$P + M = f(y) \quad (5-4)$$

Therefore, for a constant discharge, $P + M$ is a function of the depth only, as shown in Fig. 5-1, which is valid only for a channel of specific dimensions and constant discharge. Additional curves must be constructed when the discharge or dimensions of the channel are changed.

If a hydraulic jump forms in this channel, it must occur from a depth in the supercritical region to a depth in the subcritical region, as shown by the vertical dashed line in Fig. 5-1. Since $P + M$ is constant, y_2 can be found at the intersection of the vertical dashed line and the $P + M$ curve.

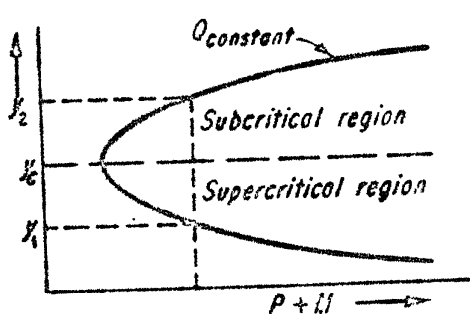


FIG. 5-1. Pressure-plus-momentum dia- gram.

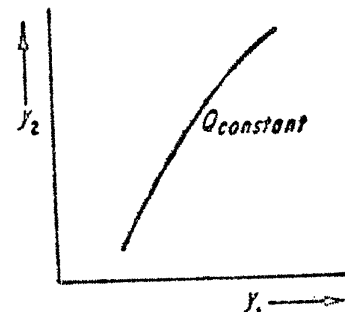


FIG. 5-2. Relation between y_2 and y_1 for a trapezoidal channel.

Figure 5-1 can readily be used if only a small number of solutions is required. If, however, a large number of solutions is required, it may be helpful to construct an additional diagram, as shown in Fig. 5-2, where the depths before and after the jump are plotted for a constant discharge. In this manner, values of y_2 corresponding to y_1 can be read directly from the curve.

Of the two quantities pressure and momentum, momentum is the more important. Since the momentum will be proportional to the square of the velocity, a coefficient β greater than unity should be applied to compensate for any unequal velocity distribution.

$$P_1 + \beta_1 M_1 = P_2 + \beta_2 M_2 \quad (5-5)$$

Theoretically, the hydrostatic pressure against a vertical section of a trapezoidal channel is $by^2/2 + Sy^3/3$, but because the triangular areas

are not in line with the momentum forces at the beginning of the jump, the hydrostatic pressure should be computed as

$$P = \frac{by^2}{2} + \frac{Sy^3}{6} \quad (5-6)$$

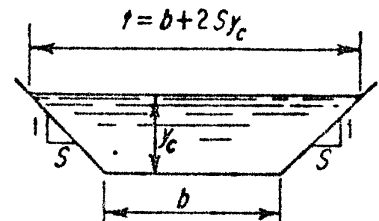


FIG. 5-3. Typical trapezoidal channel.

5-2. Critical-depth Determination. The problem of finding the critical depth in a trapezoidal channel has proven to be tedious and time-consuming. If only a small number of solutions are required, the critical depth should be found by a trial-and-error procedure.

By applying the critical-depth criterion to a trapezoidal channel, illustrated in Fig. 5-3, we have

$$\frac{Q_c^2}{g} = \frac{A_c^3}{t}$$

or, its reciprocal,

$$\frac{g}{Q_c^2} = \frac{t}{A_c^3} \quad (5-7)$$

In Eq. (5-7),

$$A_c = by_c + Sy_c^2$$

then

$$\frac{g}{Q_c^2} = \frac{b + 2Sy_c}{(by_c + Sy_c^2)^3} \quad (5-8)$$

By taking the square root of each side of Eq. (5-8), we have

$$\frac{\sqrt{g}}{Q_c} = \frac{1}{by_c + Sy_c^2} \sqrt{\frac{b + 2Sy_c}{by_c + Sy_c^2}} \quad (5-9)$$

Multiplying Eq. (5-9) by b^2 , we have

$$\frac{b^2 \sqrt{g}}{Q_c} = \frac{1}{y_c/b + Sy_c^2/b^2} \sqrt{\frac{1 + 2Sy_c/b}{y_c(1 + Sy_c/b)}} \quad (5-10)$$

letting

$$\psi = \frac{y_c}{b}$$

Then

$$\frac{b^2 \sqrt{g}}{Q_c} = \frac{1}{\psi + S\psi^2} \sqrt{\frac{1 + 2S\psi}{y_c(1 + S\psi)}} \quad (5-10)$$

Multiplying Eq. (5-10) by $b^{3/2}$, we have

$$\frac{b^{5/2} \sqrt{g}}{Q_c} = \frac{1}{\psi^{3/2}(\psi + S\psi^2)} \sqrt{\frac{1 + 2S\psi}{1 + S\psi}} \quad (5-11)$$

or

$$\frac{b^{5/2}}{Q_c} = \frac{(1 + 2S\psi)^{1/2}}{\psi^{3/2}(1 + S\psi)^{3/2} g^{1/2}}$$

Figure 5-4 shows the relationship between y_c/b and $b^{5/2}/Q_c$ for trapezoidal channels with various side slopes. With a known discharge and bottom width, $b^{5/2}/Q_c$ can be computed and y_c/b can easily be found from the appropriate curve. The product of the quantity y_c/b and the bottom width b will yield the desired critical depth. It should be noted that

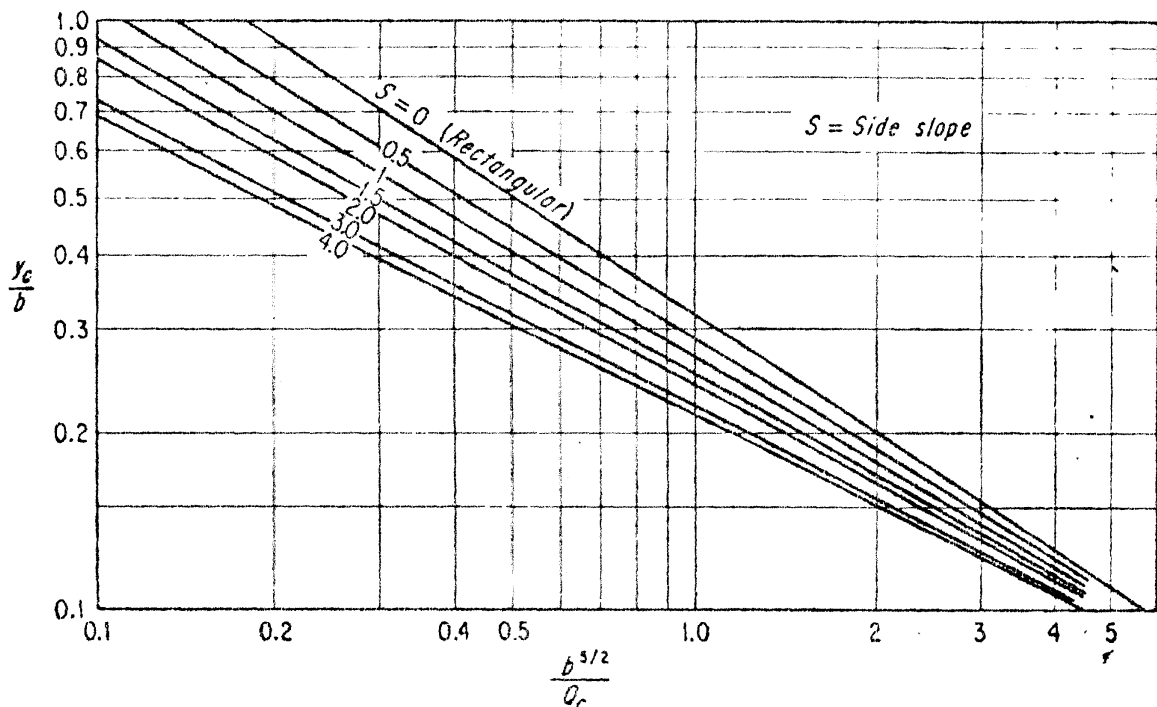


FIG. 5-4. Determination of the critical depth in trapezoidal channels.

Fig. 5-4 is not applicable to channels having metric units, since g in Eq. (5-11) was taken to be 32 ft per sec².

5-3. Momentum Formula. The general case of a trapezoidal channel which has different side slopes is shown in Fig. 5-5. As the velocity is reduced from v_1 to v_2 by the hydraulic jump, the reduction in momentum will be balanced by the difference in hydrostatic pressure.

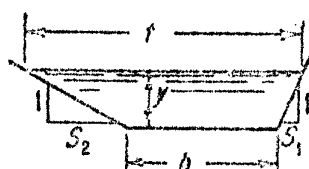


FIG. 5-5. Trapezoidal channel with varying side slopes.

For the trapezoidal channel, a single expression for the area can be found by using the average of the side slopes S (the horizontal distance per unit vertical distance), illustrated in Fig. 5-5. Let

$$S = \frac{S_1 + S_2}{2}$$

and

$$A = by + Sy^2$$

The hydrostatic pressure over a vertical section of a trapezoidal channel will then be

$$P = \frac{1}{2}by^2 + \frac{1}{3}Sy^3 \quad (5-12)$$

Since the triangular areas of the trapezoidal channel are not in line with the momentum forces at the beginning of the jump, the total hydrostatic pressure should be computed as

$$P = \frac{1}{2}by^2 + \frac{1}{6}Sy^3 \quad (5-13)$$

When Eq. (5-13) is substituted into the pressure-plus-momentum relationship, we have

$$\frac{y_2^2}{6}(3b + Sy_2) - \frac{y_1^2}{6}(3b + Sy_1) = \frac{Q}{g}(v_1 - v_2) \quad (5-14)$$

or $y_2^2(3b + Sy_2) - y_1^2(3b + Sy_1) = \frac{6Q}{g}(v_1 - v_2) \quad (5-15)$

Unless a large number of solutions are required, use of Eq. (5-15) is not recommended because of its complexity. Instead Eq. (5-2) should be solved by a trial-and-error procedure to find the depth y_2 in a trapezoidal channel.

5-4. Length of the Hydraulic Jump. In 1937, Hsing,⁴ a graduate student attending the State University of Iowa, conducted approximately 200 tests involving the formation of the hydraulic jump in trapezoidal channels. Hsing noted the following characteristics of the formation of the jump:

1. The observed jump-height agreed with the height computed by the momentum formula.

2. The most striking feature was the formation of two wings, one on each side of the jump, along the toe line. Two plan views of the jump are shown in Fig. 5-6a and b.

3. The water surface after the jump was not level, the wings being higher than the center portion.

4. The flow was unsymmetrical, and the dissymmetry often reversed itself from side to side. No logical explanation was found for the occurrence of the dissymmetry.

As in the case of a rectangular channel, the length of the hydraulic jump in a trapezoidal channel is also arbitrary. In his experiments, Hsing defined the length of the jump as follows:

The length of the jump in a trapezoidal channel is the distance from the intersection of the toe lines of the two wings, if they meet at the center; or to where a sudden change in slope is noticed, if the wings do not meet, to a horizontal tangent where the water surface has become level transversely.

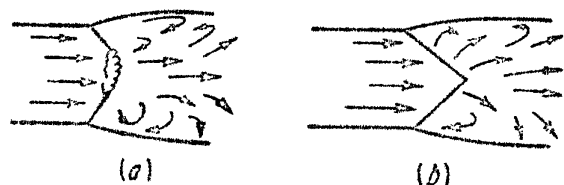


FIG. 5-6. Plan views of the hydraulic jump in a trapezoidal channel.

An explanation for the formation of the wings at the sides of the jump can be sought as follows. In a trapezoidal channel, the momentum per unit length is less at the sides, since less water is flowing there. Therefore, the upstream flow will be greater at the sides than at the center. With flatter side slopes, more water will gather at the sides, where the momentum per unit width is less. Consequently, the flow will go farther upstream, and the angle between the inner edge of the wing and axis of the channel will become smaller.

The inner edges of the wings are fairly straight and make equal angles with the axis of the channel. The average value of the angles determined by Hsing is shown in Table 5-1. Table 5-1 shows that the magnitude of

TABLE 5-1. ANGLES BETWEEN WINGS OF HYDRAULIC JUMP IN TRAPEZOIDAL CHANNELS⁴

Channel	Bottom width, ft	Side slope	Average value of angle, °
A	0.55	1 on 1	26
B	1.25	1 on 2	39
C	0.235	2 on 1	18

the wing angles depends principally upon the value of the side slopes. It is also concluded that the convergence of the wings depends upon the width above and below the jump and the condition of flow. A wider bottom, steeper side slopes, and lower jump-height will cause the wings to be shorter and separated from each other by a transverse toe line. Figure 5-7 is a photograph of the formation of a hydraulic jump in a trapezoidal channel located near Isleta, N.Mex.

Hsing proposed the following formula for the average length of the hydraulic jump in trapezoidal channels:

$$L_j = 5y_2 \left(1 + 4 \sqrt{\frac{t_2 - t_1}{t_1}} \right) \quad (5-16)$$

where t_1 = width of water surface before jump

t_2 = width of water surface after jump

TABLE 5-2. LENGTH OF THE HYDRAULIC JUMP IN TRAPEZOIDAL CHANNELS⁴

Channel	Side slope	Average value of L_j/y_j
A	1 on 1	33.5
B	1 on 2	22.9
C	2 on 1	44.2
Rectangular	6.9



FIG. 5-7. Formation of a hydraulic jump in a trapezoidal channel located near Isleta, N. Mex. Note formation of wings on the sides of the hydraulic jump.

The average ratio between the jump length and height of the jump determined by using the experimental data of Hsing is shown in Table 5-2. As shown in Table 5-2, the ratio L_j/y_j is much greater than the corresponding ratio for a rectangular channel. Also, it should be noted that L_j/y_j increases as the side slope decreases.

It is recommended that model studies be conducted to determine the length of the hydraulic jump for large trapezoidal channels or unusual flow conditions.

5-5. Trapezoidal Chutes. In the case of very short structures, trapezoidal chutes or stilling pools may be used to provide a saving in the excavation and consequently a more economical structure than a rectangular chute or basin. To avoid the concentration of flow in the center of a trapezoidal channel the water can be kept in two or more channels, as shown in Fig. 5-8.

In designing a trapezoidal chute, the velocity at the beginning of the pool should be determined by trial, and the downstream depth y_2 should be computed from the pressure-plus-momentum equation. The downstream hydrostatic pressure is computed by multiplying each individual area by the distance from the water surface to its vertical center of gravity. For discharges up to 200 cfs, two channels are usually sufficient, whereas above 200 cfs, three or more channels are required. Laboratory tests made by the Bureau of Reclamation indicate that a three-channel

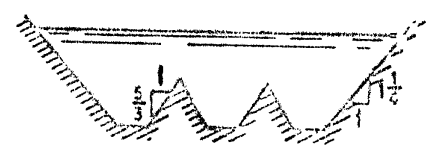


FIG. 5-8. Trapezoidal-chute side slopes.

structure will operate better when about 35 per cent of the water enters each outside channel, leaving 30 per cent of the flow for the center channel. Laboratory tests also indicated that better flow conditions prevailed when the side slopes were constructed to 1 horizontal and $\frac{5}{3}$ vertical for the inside channel.

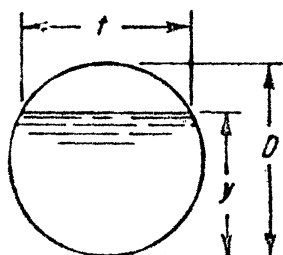


FIG. 5-9. Elements of a circular conduit.

of a partial circle can be found as a function of both the depth of flow and diameter of the conduit. The principal elements of a circular conduit are shown in Fig. 5-9.

In terms of an equation, the area can be expressed as a function of both the depth of flow and diameter of the conduit.

$$A = \frac{D^2}{4} \cos^{-1} \left(\frac{D - 2y}{D} \right) - \frac{1}{2} (D - 2y) \sqrt{Dy - y^2} \quad (5-17)$$

A graphical solution of Eq. (5-17) can be found by using the curve shown in Fig. 5-10. To find the area of a partial circle when y/D is known, determine the corresponding value of A/D^2 by using Fig. 5-10. The product of A/D^2 and D^2 will then yield the desired area.

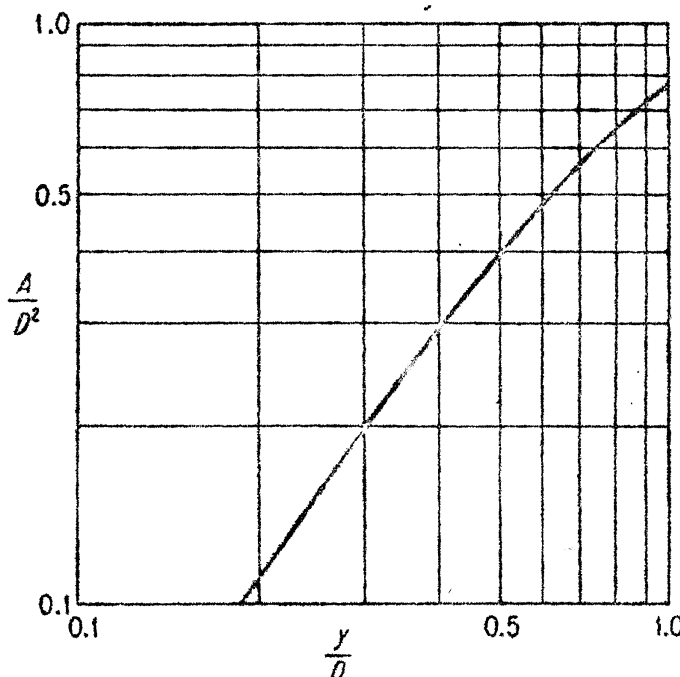


FIG. 5-10. Determination of the area of a circular conduit flowing partially full.

The critical depth is found by solving an equation in which the critical-velocity head is equal to one-half the mean depth of flow.

$$\frac{v_c^2}{2g} = \frac{y_m}{2}$$

$$\frac{v_c^2}{2g} = \frac{A_c}{2t}$$

or

Since the expression for the area A and the surface width t of circular channels when flowing partly full produces a complicated formula, it will be more convenient to use the diagram shown in Fig. 5-11. In Fig. 5-11

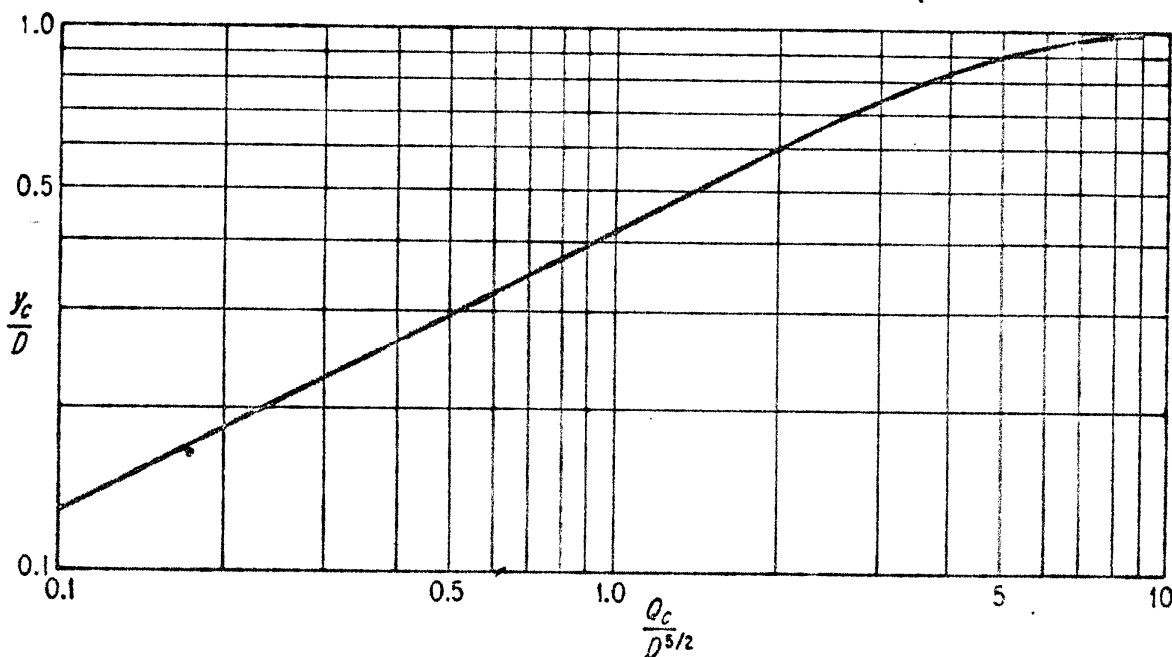


FIG. 5-11. Determination of the critical depth in circular conduits.

$Q_c/D^{3/2}$ is plotted against y_c/D . To determine the critical depth, compute $Q_c/D^{3/2}$, and find the corresponding value of y_c/D from Fig. 5-11. The product of y_c/D and D will yield the critical depth.

5-7. Trial-and-error Solutions. When supercritical flow in a conduit is retarded, it may be reduced to subcritical, thereby forming a hydraulic jump. A diagram showing the formation of a hydraulic jump in a closed conduit is shown in Fig. 5-12.

The first problem encountered in solving the momentum equation will be to find the hydrostatic pressure for conduits flowing partially full. Stevens⁹ derived the following expression for determining the hydrostatic pressure over a vertical section of a segment of a circle:

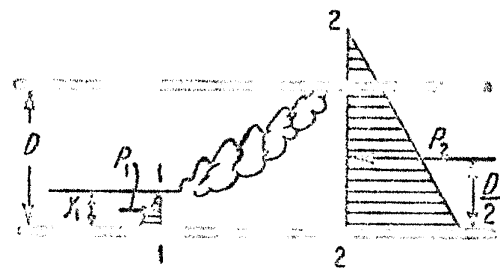


FIG. 5-12. Formation of the hydraulic jump in a closed conduit.

$$P = D^3 \left\{ \frac{(2Z + 1)^2 + 2\sqrt{Z(1 - Z)}}{12} + 0.00218(2Z - 1)[\sin^{-1}(2Z - 1) + 90^\circ] \right\} \quad (5-18)$$

In Eq. (5-18), $Z = y/D$, and P , the hydrostatic pressure, is expressed in cubic units of the liquid. A graphical solution of Eq. (5-18) is shown in Fig. 5-13. For any value of y/D , the corresponding value of P/D^3 can easily be found by referring to the curve shown in Fig. 5-13.

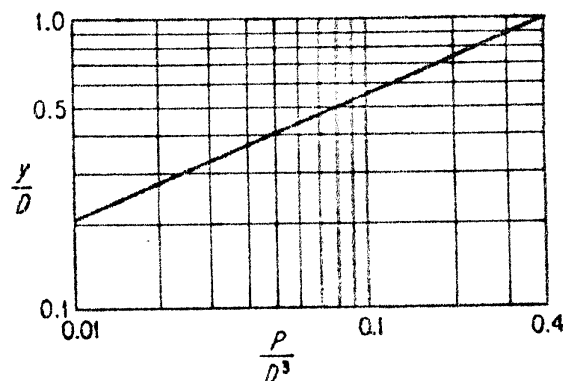


FIG. 5-13. Determination of the hydrostatic pressure over a circular segment.

After $(P + M)_1$ has been obtained, it is then a matter of trial and error to find the depth of flow corresponding to an equal value of $(P + M)_2$.

The pressure-plus-momentum relationship can be transformed into the following form:

$$P_2 A_2 - A_2 \left(P_1 + 2A_1 \frac{v_1^2}{2g} \right) + 2A_1^2 \frac{v_1^2}{2g} = 0 \quad (5-19)$$

By using the curves of both Figs. 5-10 and 5-13, A and P can both be found. After A_2 is found, the curve in Fig. 5-10 can again be used to find the downstream depth y_2 .

Up to this point, we have discussed the formation of the hydraulic jump in several types of sections, all of which were assumed to have a horizontal floor. For sloping channels, the pressure-plus-momentum equation must be modified to include the gravity component $w \sin \phi$.

$$P_1 + M_1 = P_2 + M_2 - w \sin \phi \quad (5-20)$$

where w = weight of hydraulic jump

ϕ = angle of channel floor with the horizontal

The term w can be computed from the length of the hydraulic jump, the area of the jump, and the unit weight of water, corrected for air entrainment, or it can be determined by experimentation.

Experiments made by Lane and Kindsvater³ with a 6-in. transparent-plastic conduit, for slopes ranging from 0° to 30° , approximate the relationship of Eq. (5-20). Figure 5-14 is a plot of $(P + M)_2 - w \sin \phi$ versus $(P + M)_1$.

5-8. Experimental Results. In 1936, Kindsvater⁴ investigated the characteristics of the formation of the hydraulic jump in a circular con-

duit. Kindsvater's principal aim in these tests was to confirm the momentum principle as applied to closed conduits. From his experiments, Kindsvater noted the following features:

1. For the lower discharges, the height of the hydraulic jump was not sufficient to fill the entire pipe, and the condition was that of free flow in an open conduit.

2. For higher discharges, the jump entirely filled the pipe, and pressures were exerted on the conduit.

3. In order to maintain a free jump, air must be supplied to the subcritical stream.

4. The formation of the hydraulic jump in an enclosed conduit agrees with the pressure-plus-momentum theory. However, $(P + M)_1$ was observed to be slightly greater than $(P + M)_2$. This was partially attributed to friction and the lack of uniformity of the velocity distribution below the jump. In addition, the computed momentum M_2 was less than the actual momentum based on the average velocity. This is partially attributed to the admixture of air with water at section 2.

M_2 can be computed from

$$M_2 = \frac{Qv_2(1 + \xi)\gamma}{g} \quad (5-21)$$

In Eq. (5-21), ξ is the volumetric ratio of air to water.

5-9. Practical Applications. During 1926, Ashley¹ investigated the use of the hydraulic jump in the design of high-velocity-flow sewer connections having a maximum design discharge of 32 cfs. Ashley's requirements were to find a structure which would be odorless, noiseless, vibrationless, and free from energy due to the high velocity of flow. Model studies indicated that the construction of either a drop manhole or a free fall into a pool would not satisfy the requirements. Experiments showed that sewage flowing smoothly down an incline approached a free-fall curve and, after its energy was taken out by the internal impact of the hydraulic jump, flowed at a low velocity into the interceptor. This method of designing sewer connections was used in subsequent years.

Jourdan and Reed⁷ utilized the hydraulic jump for dissipating the destructive energy of water flowing in pipelines and conduits with relatively small quantities of water discharging at medium or high velocities

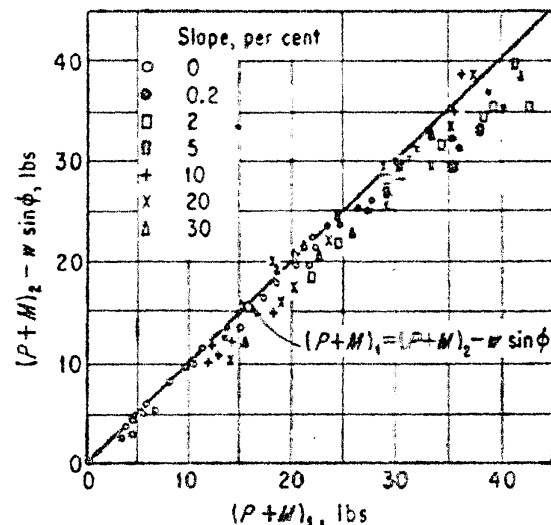


FIG. 5-14. Pressure-plus-momentum relationships for a circular conduit.

In this case, the jump was used successfully to reduce excessive erosion at the outlets of small conduits.

5-10. Air Entrainment. When the hydraulic jump completely fills the conduit, the access of air from downstream is shut off, and the air mixed with water by the turbulent action of the jump is carried away. Unless some source of air is admitted, a vacuum will tend to form in the space just downstream from the constriction. This will increase the effective pressure downstream and cause the water to move upstream in the conduit behind the constriction, thereby submerging the hydraulic jump.

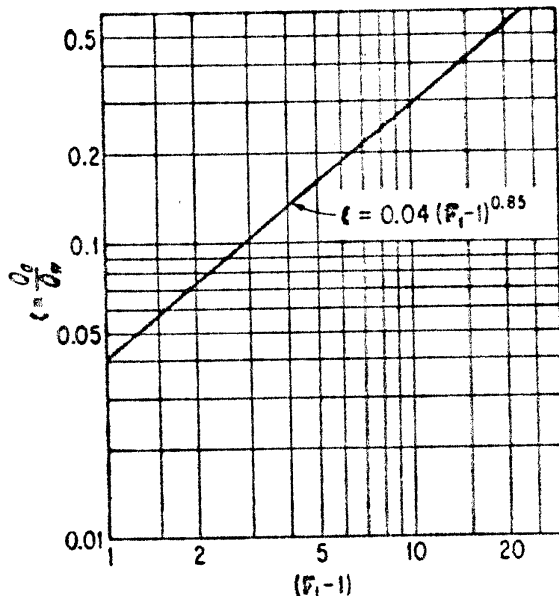


FIG. 5-15. Air demand for outlet conduits.

volume of air necessary to prevent a vacuum from being formed in the conduit. The volume of air required can also be computed from the equation

$$\xi = 0.04(F_1 - 1)^{0.85} \quad (5-22)$$

In Eq. (5-22), ξ is the volumetric ratio of air to water, and F_1 is the entering Froude number.

EXPONENTIAL CONDUITS

5-11. Exponential Conduits. The procedure for finding the height of the hydraulic jump in an irregular channel cross section is both complex and laborious. In most cases, if only a small number of solutions are required, the trial-and-error procedure is without doubt the best method. However, for exponential conduits, y_2/y_1 can be expressed in terms of the other variables.

The general equation required for the formation of the hydraulic jump in any channel is

$$P_2 - P_1 = \gamma \frac{Q}{g} (v_1 - v_2)$$

Since $Q = Av$ and $v_2 = A_1 v_1 / A_2$, we have

$$A_2(P_2 - P_1) = \frac{v_1^2}{g} A_1(A_2 - A_1) \quad (5-23)$$

Or, if the area can be expressed as a function of the depth y , then

$$A = f(y)$$

The hydrostatic pressure will be

$$P = \int A dy \quad (5-24)$$

and Eq. (5-24) becomes

$$A_2 \left[\int (A_2 - A_1) dy \right] = A_1(A_2 + A_1) \frac{v_1^2}{g} \quad (5-25)$$

For any exponential conduit, that is, any conduit in which the area can be expressed as equal to Ky^n and K is a determinable constant,

$$A = Ky^n$$

Equation (5-25) becomes

$$\begin{aligned} y_1^n \left(\frac{v_1^2}{g} \right) (y_1^n - y_2^n) &= \frac{y_2^n (y_1^{n+1} - y_2^{n+1})}{n+1} \\ \text{or } \frac{(y_2/y_1)^n [(y_2/y_1)^{n+1} - 1]}{(y_2/y_1)^n - 1} &= \lambda_1(n+1) \end{aligned} \quad (5-26)$$

For a rectangular channel, $n = 1$. Equation (5-26) becomes

$$\left(\frac{y_2}{y_1} \right)^2 + \frac{y_2}{y_1} - 2\lambda_1 = 0 \quad (5-27)$$

And similarly, for a parabolic channel, $n = \frac{3}{2}$. Equation (5-26) becomes

$$\left(\frac{y_2}{y_1} \right)^4 - \left(\frac{y_2}{y_1} \right)^{\frac{3}{2}} (2.5\lambda_1 + 1) + 2.5\lambda_1 = 0 \quad (5-28)$$

A theoretical and experimental analysis of the formation of the hydraulic jump in a parabolic flume has been presented by Argyropoulos.¹⁰ These investigations were conducted in the hydraulics laboratory of the National Technical University of Athens. The study included both horizontal and sloping parabolic flumes.

5-12. Graphical Solution. There are two distinct disadvantages in computing the height of the hydraulic jump for channels of irregular cross sections. First, for each cross section, a separate $P + M$ curve must be plotted. Secondly, every time the discharge changes, a new time-consuming curve must be plotted. Howell³ has developed a graphical solution which to some extent eliminates these two problems. Howell's graphical solution can be explained as follows:

1. For a particular cross section, plot two curves; first plot the pressure P versus $1/Ag$, where A is the cross-sectional area and g is the acceleration due to gravity. A typical diagram, obtained by plotting P on the abscissa and $1/Ag$ as the ordinate, is illustrated in Fig. 5-16.

2. Next draw a horizontal line from y_1 to the P versus y curve. At the intersection of this line and the P versus y curve, draw a vertical line up to the P versus $1/Ag$ curve.

3. The next step is to pass a line having a slope equal to $-Q^2$ through point A.

4. Finally, draw a vertical line from the point where the slope line intersects the P versus $1/Ag$ curve (B) to the P versus y curve. By drawing a horizontal line from this point to the y axis, the required solution for y_2 is obtained.

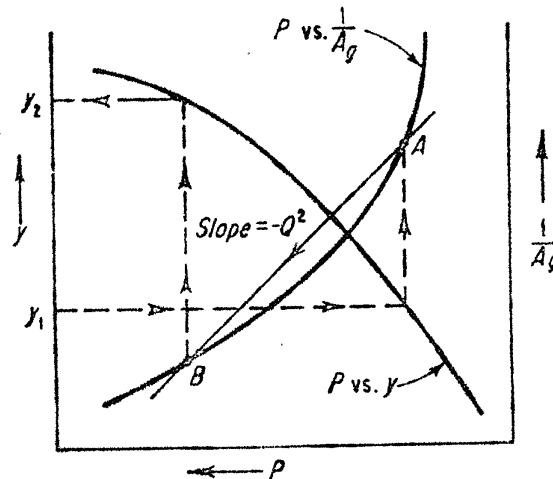


FIG. 5-16. Howell's graphical solution for determining the hydraulic jump in non-rectangular channels.

the pressures can be determined. The discharge will then be equal to the slope of the line drawn between the values of the two pressures.

REFERENCES

1. Ashley, W. H.: Experiments on the Hydraulic Jump in Sewer Connections: Drop Eliminates Odor, Noise, Vibration, and Energy Dissipation, *Eng. News-Record*, Sept. 20, 1926.
2. Corps of Engineers, Hydraulic Design—Reservoir Outlet Structures, *Eng. Manual, Civil Works Construction*, part CXVI, chap. 2, February, 1953.
3. Howell, D. D.: Hydraulic Jump in Irregular Cross-sections Computed by Time Saving Methods, *Civil Eng.*, pp. 64–65, November, 1953.
4. Hsing, P. S.: "The Hydraulic Jump in a Trapezoidal Channel," doctoral dissertation, State University of Iowa, August, 1937.
5. Kindsvater, C. E.: "Hydraulic Jump in Enclosed Conduits," unpublished M.S. thesis, State University of Iowa, 1936.
6. King, H.: "Handbook of Hydraulics," 3d ed., McGraw-Hill Book Company, Inc., New York, 1939.
7. Jourdan, J. W., and O. Reed: Hydraulic Design for a 100 Sec-ft. Conduit, *Eng. News-Record*, pp. 224–225, Aug. 8, 1929.
8. Lane, E. W., and C. E. Kindsvater: Hydraulic Jump in Enclosed Conduits, *Eng. News-Record*, pp. 815–819, Dec. 29, 1938.
9. Stevens, J. C.: The Hydraulic Jump in Standard Conduits, *Civil Eng.*, pp. 564–567, October, 1933.
10. Argyropoulos, P. A.: "Theoretical and Experimental Analysis of the Hydraulic Jump in a Parabolic Flume," paper presented before International Association for Hydraulic Research meeting, Lisbon, Portugal, July, 1957.

Howell emphasized that, since the intersections of the various lines may be flat, the accuracy may be increased by meticulously selecting the horizontal and vertical scales to avoid this condition.

Figure 5-16 can also be used to find the discharge once y_2 and y_1 are known. Once these values are known, the corresponding values of

6

Hydraulic Jump in Sloping Channels

In the past, considerable confusion has existed concerning the merits of sloping aprons and the proper way to design them. This has been, in part, due to the lack of definite and convincing design information.

The same physical laws as for the hydraulic jump on the horizontal apron apply to sloping aprons, except that the designer must include the extra force of gravity of the hydraulic-jump body on the sloping floor. Although it is not possible to standardize the design of a sloping apron nearly so much as for horizontal aprons, there nevertheless are certain rules that should be followed. The slope and over-all shape of the sloping apron must be determined from economic reasoning, while the length must be judged by the type and soundness of the riverbed downstream. For all cases, the apron arrangement desired should provide the greatest economy for the contemplated range of discharges and tailwater conditions.

6-1. Sloping Aprons. Relatively few stilling basins are constructed with horizontal aprons, because the formation of the hydraulic jump on a horizontal apron at high Froude numbers is very sensitive and may move with only slight changes in tailwater depth. Sloping floors or aprons are used to gain satisfactory operation over a wide range of tailwater conditions. In addition to this advantage, there is usually a large saving both in excavation and concrete construction.

There is a lack of agreement among engineers and designers as to the amount of energy that is dissipated on a sloping floor. When the slope is too steep, the high velocity of the water shoots out under the surface of the pool with little localized impact, making dangerous erosion likely. Relatively few experiments have been conducted in channels having steep slopes. Most designers have limited the slope of stilling-basin aprons to a maximum slope of 4 horizontal to 1 vertical. It should be remembered that the most desirable stilling basin is the one that can be constructed with the least cost and still operate properly under all conditions.

By increasing the tailwater depth, it is possible for the designer to move the front of the hydraulic jump up on the sloping apron. There are, in general, three types of jump formations that can occur on a sloping floor.

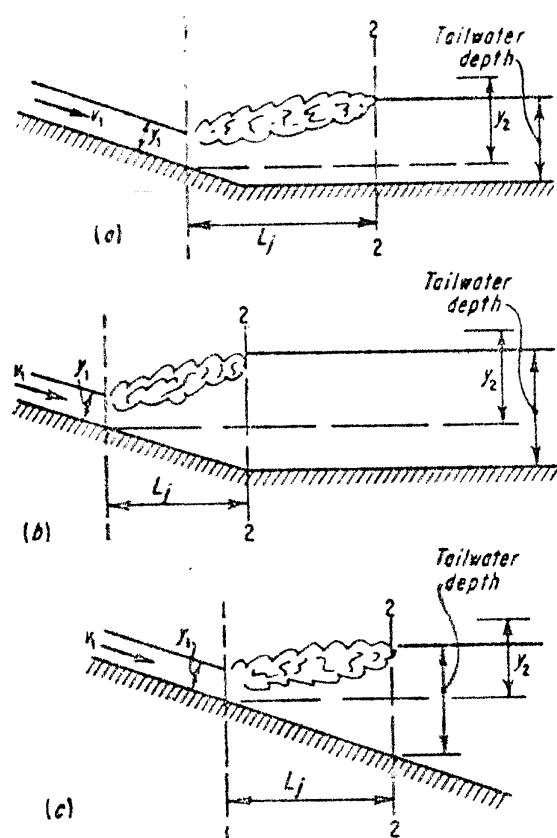


FIG. 6-1. Occurrence of the hydraulic jump on a sloping apron: (a) case I, (b) case II, (c) case III.

It will be noted that case II is virtually that of the hydraulic jump formed on a horizontal apron, operating with excessive tailwater. As the tailwater is further increased, the formation of the hydraulic jump can be changed progressively from case I to case II and finally to case III.

If the tailwater depth is increased by a vertical element Δy , the front of the hydraulic jump does not rise an equal amount vertically. Instead, the jump profile undergoes an immediate change as the slope becomes part of the stilling basin, as illustrated by Fig. 6-2.

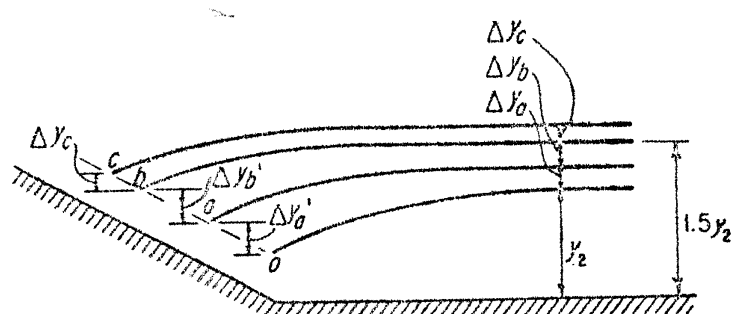


FIG. 6-2. Profile of the hydraulic jump on a sloping apron.

These are shown in Fig. 6-1a, b, and c.

The different formations of the hydraulic jump depend primarily upon where the terminus of the jump falls. As shown in Fig. 6-1a, case I prevails when the toe of the hydraulic jump forms on the slope, while the terminus, or end, of the jump occurs on the horizontal apron.

In case II, illustrated by Fig. 6-1b, the toe of the hydraulic jump occurs on the slope as in case I, but the end of the jump occurs at the junction of the slope and the horizontal apron.

As shown in Fig. 6-1c, case III prevails when the hydraulic jump forms entirely on the sloping apron. Cases II and III are practically the same, and further analysis will be made only of cases I and III.

For an increase in tailwater depth Δy_a , the front of the jump moves up on the slope to point *a*, or moves a vertical distance $\Delta y'_a$, which may be several times Δy_a . The same effect occurs to a lesser degree when the front of the hydraulic jump is moved to point *b*. Additional increments of tailwater depth produce the same effect, only to a lesser degree. This will continue until the tailwater approaches $1.5y_2$. For tailwater depths greater than this amount, the relation is geometric, and an increase in tailwater depth Δy_c moves the front of the hydraulic jump on the slope an equal vertical distance Δy_c .

6-2. Historical Résumé. The effect of a sloping floor upon the formation of the hydraulic jump was first studied in 1917 by Beebe and Riegel² of the Miami Conservancy District, located in Dayton, Ohio. Beebe and Riegel were principally interested in studying the effect of a stepped apron upon the design of the Germantown Dam outlet works.

In 1927, Ellms³ conducted several experiments in a rectangular flume 4 feet long, whose slope could be varied from approximately 9 to 17° . Several erroneous results were obtained by Ellms because the horizontal section of the flume he used was too small to contain the hydraulic jump. Also, Ellms neglected to compensate for the pressure force exerted on the bottom of the flume and to make allowances for the flaring sides of the flume.

An analysis was attempted by Yarnell, in 1934, to determine the apron-floor pressure under the hydraulic jump by assuming a straight-line profile from the beginning to the end of the jump. Over 600 tests were made in a glass-walled flume 2.5 ft wide, 3 ft deep, and 80 ft long. Investigations were made on slopes of 1 on 6, 1 on 3, 1 on 2, and 1 on 1. Unfortunately, Yarnell's work was interrupted by his death.

In 1935, Rindlaub⁴ conducted a series of experiments at the University of California hydraulic laboratory. Experiments were made in a glass-walled flume 3 ft deep and 0.5 ft wide. Investigations were made on four slopes of 8.2, 12.5, 24.2, and 30° , with most of the experiments being made on the slope of 12.5° . In his analysis, Rindlaub compensated for the pressure component on the sloping floor by including a dimensionless term, which can be determined experimentally, to account for any external forces.

Experiments in a rectangular channel having a maximum slope of 1 on 14 were performed in 1936 at Columbia University by Bakhmeteff and Matzke.¹ In order to compensate for the weight of the jump on a sloping floor, a dimensionless cubic equation was developed which was found to be dependent upon the shape of the jump. Unfortunately, the slopes investigated were very small, and consequently no generalization can be made from the results.

During 1941, Puls⁵ presented a method of routing stream flow through-

a hydraulic jump in open channels. Puls's analysis included several factors which previously were considered negligible. These forces included the friction of the channel boundaries, the shear applied to the top boundary of the stream, and the differential boundary reaction introduced by the weight of the jump body. Solution of the jump by the Puls step method is both long and laborious, and several trials must be made for each solution. It is doubtful that the added accuracy of this method is warranted.

Perhaps the most extensive work on the subject was completed in 1942 by Kindsvater,⁷ who evaluated a pressure coefficient by experimental measurements that were distinct for each channel slope and kinetic-flow factor. The majority of Kindsvater's work was made in a channel having a slope of 1 on 6, but general analyses of all slopes up to 1 on 3 were also made.

A laboratory investigation of the hydraulic jump on a slope of 1 on 3 was made in the hydraulic laboratory of the Tennessee Valley Authority, Knoxville, Tenn., by Hickox,⁶ who developed a useful relationship between the height of the jump and the kinetic-flow factor for each channel slope.

Further investigations were made during 1949 on slopes of 1 on 3, 1 on 4, and 1 on 6 by Dutta,⁴ at the University of Colorado. The intended purpose of Dutta's study was to find a useful relationship between the four variables of the jump— y_1 , v_1 , y_2 , and v_2 . Dutta constructed several useful diagrams where graphical solutions are made for each specific slope and all the four variables.

More recently, during 1954, extensive laboratory studies were conducted in the hydraulic laboratory of the Bureau of Reclamation. Experiments were made in channels whose slopes varied from 1 on 19 to 1 on 3.6. The results of these experiments are included in Sec. 6-4.

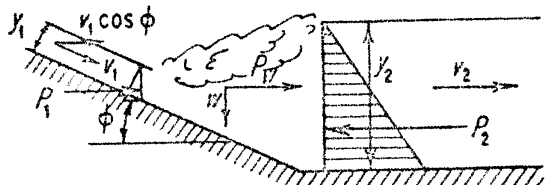


FIG. 6-3. Schematic diagram of the hydraulic jump on a sloping apron.

the dimensions and shape of the jump and can be evaluated by laboratory measurements.

The following derivation of a general formula for the formation of the hydraulic jump on a sloping floor is a modification of the original analysis made by Kindsvater.⁷ A general formula is developed for the occurrence of the jump on a sloping floor, as illustrated by Fig. 6-3. In the derivation of the formula, the following assumptions are made:

6-3. Basic Considerations. The momentum theory can also be applied to the formation of the hydraulic jump in sloping channels, if an additional force due to the force of gravity of the jump body on a sloping floor is included. This additional force is a function of both

1. No appreciable curvature of the streamlines exists.
2. Boundary friction is negligible.
3. Uniform velocities prevail at both the beginning and end of the jump.
4. There is no acceleration of the stream flow, which is obviously untrue for steep slopes.
5. Air entrainment is neglected.

By applying the pressure-momentum relationship for the case II shown in Fig. 6-3,

$$P_2 - P_1 - P_w = \gamma \frac{Q}{g} (v_1 \cos \phi - v_2) \quad (6-1)$$

For case II, the hydrostatic pressures before and after the jump become, for a channel width of unity,

$$P_1 = \frac{\gamma y_1^2}{2 \cos^2 \phi} \quad (6-2)$$

and

$$P_2 = \frac{\gamma y_2^2}{2} \quad (6-3)$$

P_w is a horizontal force due to the pressure of the weight of the jump on a sloping floor. It was found by experimentation that

$$P_w = \gamma \delta \left(y_2^2 - \frac{y_1^2}{\cos^2 \phi} \right) \tan \phi \quad (6-4)$$

In Eq. (6-4), δ is a dimensionless parameter that varies with both the Froude number and slope of the apron.

Substituting Eqs. (6-2), (6-3), and (6-4) in Eq. (6-1), we have

$$\frac{\gamma y_2^2}{2} - \frac{y_1^2 \gamma}{2 \cos^2 \phi} - \gamma \delta \left(y_2^2 - \frac{y_1^2}{\cos^2 \phi} \right) \tan \phi = \gamma \frac{Q}{g} (v_1 \cos \phi - v_2) \quad (6-5)$$

Since $v_2 = \frac{(v_1 \cos \phi)(y_1 \cos \phi)}{y_2}$

Eq. (6-5) becomes

$$\begin{aligned} \frac{\gamma y_2^2}{2} - \frac{\gamma y_1^2}{2 \cos^2 \phi} - \gamma \delta \left(y_2^2 - \frac{y_1^2}{\cos^2 \phi} \right) \tan \phi \\ = \gamma \left(\frac{v_1^2 y_1 \cos \phi}{g y_2} \right) \left(y_2 - \frac{y_1}{\cos \phi} \right) \end{aligned} \quad (6-7)$$

Dividing Eq. (6-7) by $(\gamma/2)[y_2 - (y_1 \cos \phi)]$, we have

$$\left(y_2 + \frac{y_1}{\cos \phi} \right) - 2\delta \left(y_2 + \frac{y_1}{\cos \phi} \right) \tan \phi = \frac{2v_1^2 y_1 \cos \phi}{g y_2} \quad (6-8)$$

Solving Eq. (6-8) for y_2 ,

$$y_2 = \frac{y_1}{2 \cos \phi} \left[\sqrt{\frac{8(v_1)^2 \cos^3 \phi}{gy_1(1 - 2\delta \tan \phi)}} + 1 - 1 \right] \quad (6-9)$$

or

$$\frac{y_2}{y_1} = \frac{1}{2 \cos \phi} \left(\sqrt{\frac{8\lambda_1 \cos^3 \phi}{1 - 2\delta \tan \phi}} + 1 - 1 \right) \quad (6-10)$$

The computed value of y_2 in Eq. (6-10) will be correct for cases II and III, but will not yield true results of y_2 for case I.

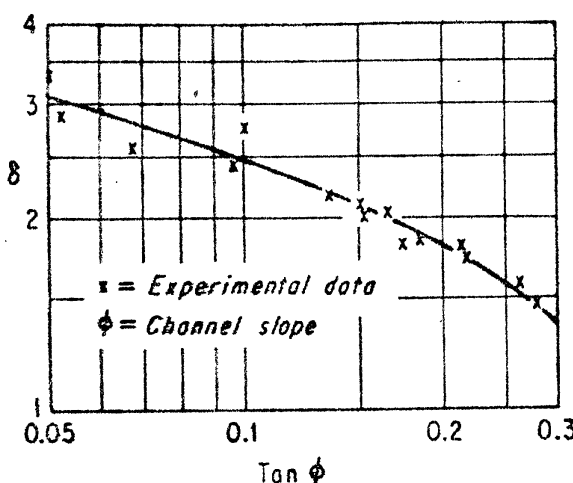


FIG. 6-4. Hydraulic jump in sloping channels.

As previously stated, δ is a dimensionless parameter that varies with both the Froude number and the slope of the apron. Experiments conducted by the Bureau of Reclamation indicate that the Froude number has little effect on δ and that it is principally dependent upon the slope of the apron. Assuming that δ is independent of the Froude number, a plot of $\tan \phi$ versus δ was made as shown in Fig. 6-4.

With a known slope, δ can be found from Fig. 6-4. Once the value of δ has been determined, y_2/y_1 can be computed directly by using Eq. (6-10).

As indicated in Fig. 6-4, for steep slopes the value of δ decreases, and consequently the height of the hydraulic jump becomes less important. It should be remembered that δ is dependent upon the method used to determine the length of the hydraulic jump. In the experiments performed by the Bureau of Reclamation, the length of the hydraulic jump was chosen to be equivalent to the length of the stilling basin.

The slope of the apron that is necessary to provide good jump action at the various discharges can be determined graphically. A relationship between the tailwater elevation and the distance from the pool entrance is shown in Fig. 6-5. In Fig. 6-5, the slope of the apron is determined graphically by striking off arcs having radii equal to depths $y_{2,\max}$, y'_2 , y''_2 , and y'''_2 for their respective discharges, Q_{\max} , Q' , Q'' , and Q''' . Each arc is struck off from a point equal to the elevation of the tailwater for the respective discharge. A line then drawn tangent to each arc will form the slope necessary for good jump action at the various discharges.

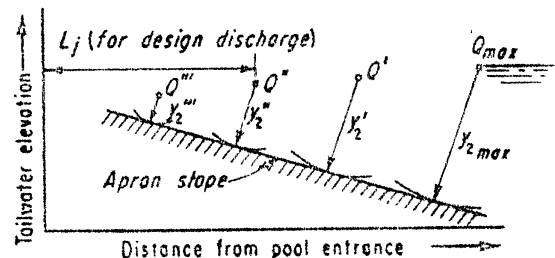


FIG. 6-5. Determination of apron slope.

the distance from the pool entrance

6-4. Experimental Investigations. Hickox⁶ developed a relationship between y_2/y_1 and various slopes which is shown in Fig. 6-6. Here the effect of the stream entering the stilling basin upon the depth of tailwater becomes negligible for the slope of 0.336.

In 1949, Dutta⁴ conducted a series of experiments at the University of Colorado for slopes of 1 on 3, 1 on 4, and 1 on 6. Experimental data compiled by Dutta are plotted in Fig. 6-6, so that we may compare them with the data presented by Hickox. As shown in the figure, Dutta's results agree very well with those developed by Hickox.

Experiments made by the Bureau of Reclamation³ indicate that y_2 will increase as the slope of the channel increases. Figure 6-7 shows the extra depth required for the hydraulic jump to form on a sloping apron compared to the depth required for the jump to form on a horizontal apron. The conjugate depth y_2 used in connection with a sloping apron is merely a convenient reference term and has no physical meaning. As an example, by using Fig. 6-7, it will be observed that for a slope of 1 on 8 the tailwater depth should be made equal to $1.5y_2$.

It has been found that when the Froude number varies between 4.5 and

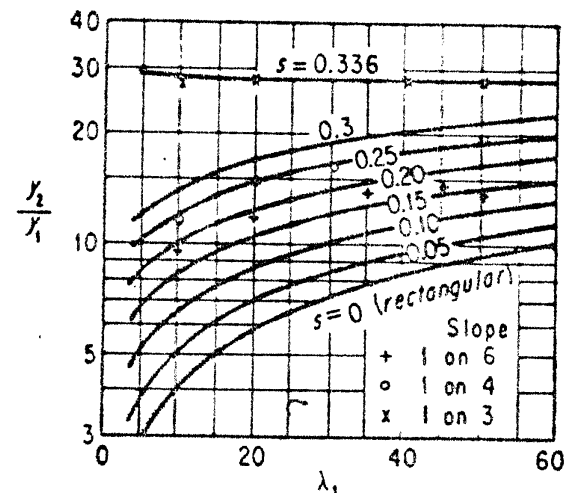


FIG. 6-6. Relative depth below jump in a sloping channel as a function of λ_1 and slope.

9, the formation of the hydraulic jump is least sensitive to tailwater fluctuations and that the tailwater depth can probably be lowered by 5 per cent. For values of the Froude number between 9 and 18, a 2 per cent reduction in tailwater depth may be possible. Caution should be exercised in permitting these reductions, since an additional reduction may cause the hydraulic

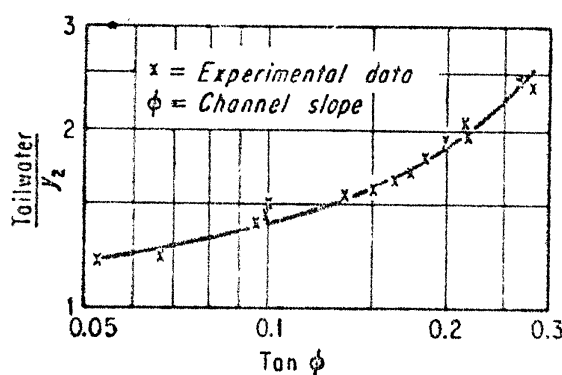


FIG. 6-7. Extra depth required by the hydraulic jump in sloping channels.

jump to sweep completely out of the basin. An attempt should be made to design a sloping-apron basin in which the Froude number varies between 4.5 and 9. For values of the Froude number exceeding 15, it is recommended that the tailwater depth be increased by 10 per cent. This will not only stabilize the hydraulic jump but will increase the performance of the stilling basin.

6-5. Length of Hydraulic Jump on Sloping Aprons. The longitudinal element of the hydraulic jump is difficult to ascertain. A portion of this difficulty is due to the lack of agreement among investigators as to the definition of the length of the hydraulic jump. In each analysis, it is important that the reported jump length be defined by the investigator.

Investigations of the length of the hydraulic jump were made by the Bureau of Reclamation.³ Figure 6-8 was constructed with the use of the data compiled by the Bureau of Reclamation. In the laboratory, the end, or terminus, of the jump was chosen as the point where the high-velocity jet began to leave the floor or as a point on the level tail-water surface immediately downstream from the surface roller, whichever was longer.

As shown in Fig. 6-8, the length of the hydraulic jump for case III is dependent upon the jump-height and apron slope. Apparently, the Froude number does not materially influence the length of the hydraulic jump. The Froude number, for the data used in preparing Fig. 6-8, varied from 2.9 to 17.9.

Figure 6-8 indicates that there is a good relationship between the height and length of the hydraulic jump. The formulas obtained

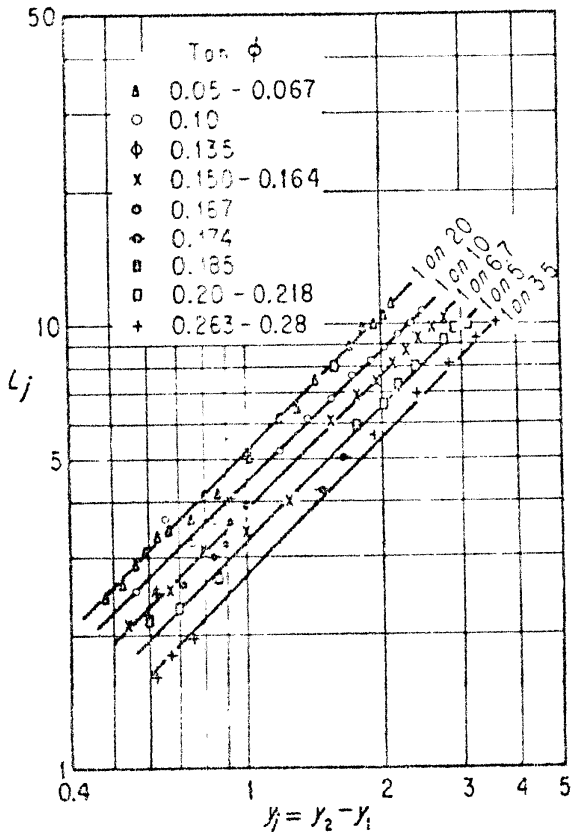
FIG. 6-8. Length of the hydraulic jump in sloping channels.

from the curves of Fig. 6-8 and listed in Table 6-1 can be used to determine the length of the hydraulic jump in sloping channels.

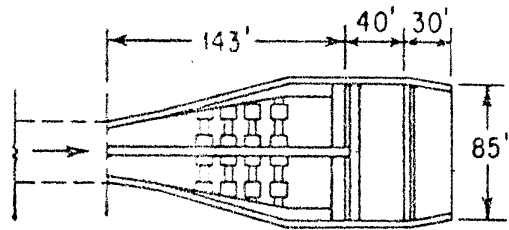
TABLE 6-1. FORMULAS FOR DETERMINING THE LENGTH OF THE HYDRAULIC JUMP IN SLOPING CHANNELS

Slope	Length of hydraulic jump
Horizontal	$L_j = 6.9(y_2 - y_1)$
1 on 20	$L_j = 5.2(y_2 - y_1)$
1 on 10	$L_j = 4.4(y_2 - y_1)$
1 on 6.7	$L_j = 3.8(y_2 - y_1)$
1 on 5	$L_j = 3.25(y_2 - y_1)$
1 on 3.6	$L_j = 2.75(y_2 - y_1)$

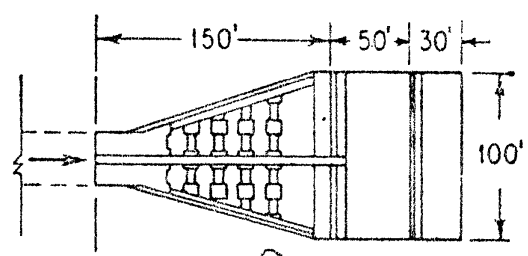
6-6. Stepped Sloping Aprons. Stepped sloping aprons were used at the outlet works of the Germantown and Englewood Dams, which were designed and constructed by the Miami Conservancy District.² The



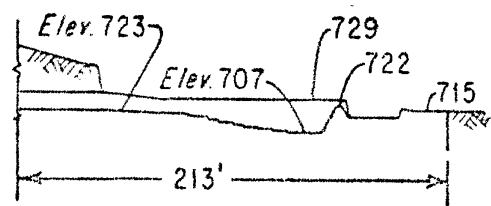
purpose of roughening the floor by a series of steps was to diminish the velocity above the jump materially and to permit the hydraulic jump to form over a wide range of tailwater conditions. Profiles of the outlet works of the Germantown and Englewood Dams are depicted in Figs. 6-9 and 6-10, respectively. Figure 6-11 is a photograph of the Germantown Dam outlet works, discharging approximately 5,000 cfs.



Plan



Plan



Center-line Profile

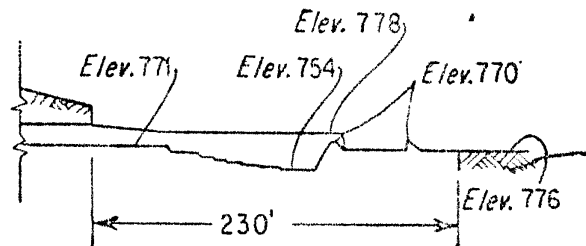


FIG. 6-9. Outlet works of the Germantown Dam, Ohio.

FIG. 6-10. Englewood Dam outlet works.



FIG. 6-11. Hydraulic-jump formation in the outlet works of the Germantown Dam. Approximate discharge is 5,000 cfs. (Courtesy of Miami Conservancy District.)

For the Arkabutla Dam¹⁰ constructed on the Coldwater River in Mississippi, a trajectory chute was used, followed by steps perpendicular to the diverging side walls which lead into a horizontal basin with two rows of floor blocks and an end sill. The curved chute is used in spreading the jet, and the steps are employed to increase the floor resistance and diminish the energy content of the flow. In order to distribute the flow evenly across the basin, the steps are placed perpendicular to the basin side walls. Figure 6-12 depicts the center-line profile and plan of the Arkabutla Dam apron.

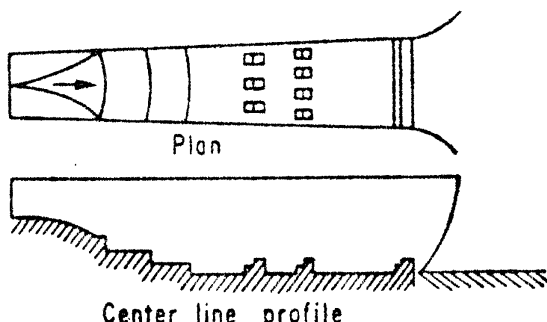


FIG. 6-12. Arkabutla Dam stilling basin.

Parallel steps preceded by a curved hump on the upper apron were employed in the outlet works of the Tappan Dam¹¹ to prevent the jump from being drowned. A profile of the outlet works of the Tappan Dam is shown in Fig. 6-13. In the Mohawk Dam,¹¹ steps were made perpendicular to the diverging side walls and the dividing wall shown in Fig. 6-14.

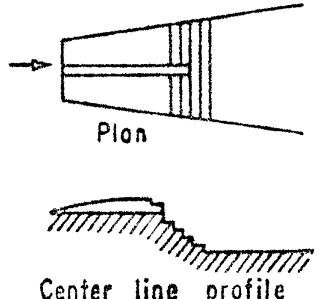


FIG. 6-13. Tappan Dam stilling basin.

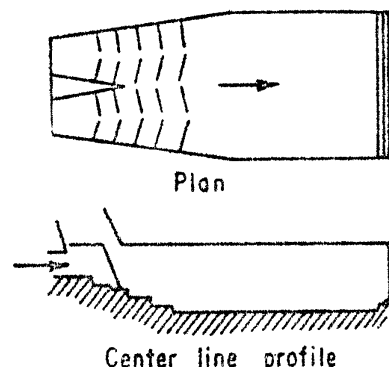


FIG. 6-14. Mohawk Dam stilling basin.

In this case, the steps were also employed to roughen the floor and thereby reduce the velocity.

6-7. Practical Applications. The Madden Dam¹² is an outstanding example of the use of a sloping apron. This structure, constructed during 1932 on the Chagres River in Panama, was designed for a flood discharge of 280,000 cfs. With a flood discharge of 280,000 cfs, a drop of 124 ft from headwater to tailwater occurred. During model tests, many slopes were tried, but a slope of 1 vertical to 4 horizontal was as steep as could be used to retain a good jump formation. For steeper slopes, it was observed that an overflowing jet cut under the tailwater, with little surface disturbance or energy loss. The sloped apron was adopted mainly for the economy of concrete costs and also to permit the jump to be formed under a variety of tailwater conditions. There is little to be

gained by using a sloping apron unless the entire length of the sloping portion is utilized. A deflector sill was placed at the end of the apron to deflect the flow away from the riverbed. Predictions of the location of the jump by model tests were later verified by operation of the prototype. The loss of energy has been almost instantaneous, and resultant erosion has been negligible beyond the concrete apron.

A tabulation of the basic data of 12 stilling basins that employ sloping aprons is given in Table 6-2.

TABLE 6-2.³ STILLING BASINS WITH SLOPING APRONS

Dam	Location	Apron slope	Maximum discharge, cfs	Actual velocity, fps	F_1	y_1/y_1	L_j	L_b
Bhakra.....	India	1 on 10	290,000	158	10.3	14.2	646	389.5
Canyon Ferry..	Montana	Varies	200,000	96	6.1	8.2	413	194
Capilano.....	British Columbia	1 on 4.5	43,000	117	9.6	13.2	384	234
Dickinson.....	S. Dakota	1 on 8	33,000	48	4.4	5.7	120	71
Folsom.....	California	1 on 8	250,000	133	8.4	11.5	578	324
Friant.....	California	1 on 7	90,000	108	12.0	16.5	266	222
Keswick.....	California	Varies	250,000	69	3.1	4.0	330	128
Madden.....	Canal Zone	1 on 4	280,000	87	5.7	7.7	382	150
Norris.....	Tennessee	1 on 4	197,000	106	7.9	10.7	422	224
Olympus.....	Colorado	Varies	20,000	54	5.4	7.3	155	92
Rihand.....	India	1 on 14	415,000	108	7.6	10.3	413	335
Shasta.....	California	1 on 12	250,000	141	11.4	15.8	469	309

NOTE: F_1 = entering Froude number for maximum discharge condition; L_j = length of hydraulic jump for maximum discharge condition, ft; L_b = length of stilling basin, ft.

The following rules are recommended to be used in designing sloping aprons.

1. Determine the apron arrangement which will give the greatest economy and still function properly for all conditions. These are the governing factors and the only justification for using a sloping apron.
2. Locate the apron so that the front of the jump will form at the upstream end of the apron for the maximum tailwater depth and discharge. Be sure that the tailwater depth and length of the basin available for energy dissipation are also sufficient for one-fourth, one-half, and three-fourths the basin capacity. There is a possibility that the worst condition might occur at a basin capacity of one-fourth, one-half, or three-fourths, instead of at the full capacity. If the tailwater depth is insufficient, it may be necessary to try a flatter slope or to reposition the sloping portion of the apron. The slope of the apron may vary, but the velocity distribution of the jet entering the hydraulic jump must be uniform.
3. In some cases, it is not economically possible to confine the hydraulic

jump within the stilling basin. An analysis of the data presented in Table 6-2 shows that the average over-all length of the listed sloping aprons is 60 per cent of the jump length for the maximum discharge condition. The length of the basin can be increased or decreased, depending upon the condition of the riverbed below the apron. If the apron is founded on loose material and riverbed conditions are poor, it will be advisable to make the total length of the apron the same as the hydraulic-jump length.

4. A solid, triangular sill placed at the end of the apron is the only appurtenance needed in conjunction with the sloping apron. It serves to lift the flow as it leaves the apron and thus acts to reduce scour. The dimensions of the end sill are variable, but the most effective sill height will be between $0.05y_2$ and $0.10y_2$, with an upstream slope of 1 on 3 or 1 on 2.

5. Where the discharge per foot of spillway width exceeds 500 cfs per ft or where asymmetry is involved, model studies are advisable.

6. For entering Froude numbers varying between the ranges 2 and 4.5, and 9 and 15, it is recommended that the tailwater depth be made equal to y_2 . Since the jump is least sensitive for Froude numbers varying between 4.5 and 9, the tailwater depth can probably be lowered by 5 per cent and made equal to $0.95y_2$. When the entering Froude number exceeds 15, it is recommended that the tailwater depth be increased by 10 per cent and made equal to $1.1y_2$ to stabilize the hydraulic jump. The additional tailwater depth will also improve the performance of the stilling basin.

REFERENCES

1. Bakhmeteff, B. A., and A. E. Matzke: The Hydraulic Jump in Sloped Channels, *Trans. ASME*, pp. 111-118, 1938.
2. Beebe, J. C., and R. M. Riegel: The Hydraulic Jump as a Means of Dissipating Energy, *Miami Conservancy District Tech. Rep.*, part III, 1917.
3. Bureau of Reclamation, Progress Report II, Research Study on Stilling Basins, Energy Dissipators, and Associated Appurtenances, *Hydraulic Lab. Rep. Hyd.-399*, June 1, 1955.
4. Dutta, D. N.: "Curves for the Determination of the Variables of the Hydraulic Jump in Sloping Channels," unpublished M.S. thesis, University of Colorado, 1952.
5. Ellms, R. W.: The Hydraulic Jump in Sloping and Horizontal Flumes, *Trans. ASME*, vol. 54, pp. 113-14, Nov. 30, 1932.
6. Hickox, G. H.: Discussion of the Hydraulic Jump in Sloping Channels, *Trans. ASCE*, vol. 109, paper 222S, 1944.
7. Kindsvater, C. E.: The Hydraulic Jump in Sloping Channels, *Trans. ASCE*, vol. 109, paper 222S, 1944.
8. Puls, L. G.: Mechanics of the Hydraulic Jump, *Bur. Reclamation Tech. Memorandum* 623, 1941.

9. Rindlaub, B. D.: "The Hydraulic Jump in Sloping Channels," published M.S. thesis, University of California, 1935.
10. Waterways Experiment Station, Corps of Engineers, Model Study of the Outlet Structures, for Arkabutla Dam, Coldwater River, Mississippi, *Tech. Memorandum* 167-1, 1940.
11. Waterways Experiment Station, Corps of Engineers, Spillways and Outlet Structures, Model Studies, *Exp. Sta. Bull. (Hydraulics)*, vol. 2, no. 4, 1939.
12. Model Tests Verify Design of Madden Dam Spillway, *Eng. News-Record* p. 42 July 14, 1932.

7

Energy Dissipation by the Hydraulic Jump

As previously explained in Chap. 3, the hydraulic jump produces a reduction in velocity from the supercritical to the subcritical range. During the velocity reduction, a considerable portion of the initial energy is dissipated into heat. The purpose of this chapter will be to discuss the energy dissipation accomplished by the hydraulic jump and to indicate methods for its determination.

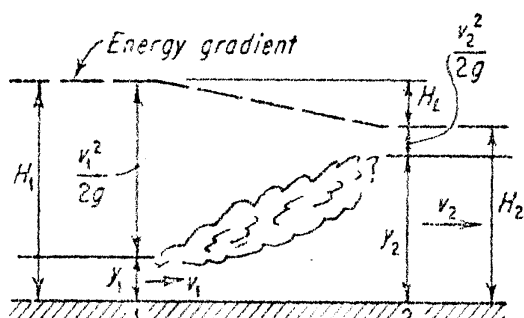


FIG. 7-1. Head lost by the hydraulic jump.

7-1. Energy Dissipation. For open channels, the energy head at all sections remains constant for uniform flow, but varies for nonuniform flow. Difficulties may arise when a very steep slope is encountered, since velocities at different elevations contain varying amounts of energy.

In Fig. 7-1, H_L represents the "head lost" through energy dissipation provided by the hydraulic jump. Analytically, the head lost can be found as follows:

$$\begin{aligned}
 H_L &= H_1 - H_2 \\
 &= \left(y_1 + \frac{v_1^2}{2g} \right) - \left(y_2 + \frac{v_2^2}{2g} \right) \\
 \text{or} \quad &= (y_1 - y_2) + \left(\frac{v_1^2}{2g} - \frac{v_2^2}{2g} \right) \tag{7-1}
 \end{aligned}$$

For a rectangular channel with a width of unity,

$$\begin{aligned}
 H_L &= (y_1 - y_2) + \frac{Q^2}{2g} \left(\frac{1}{y_1^2} - \frac{1}{y_2^2} \right) \\
 \text{or} \quad &= (y_1 - y_2) + \frac{Q^2}{2g} \left(\frac{y_2^2 - y_1^2}{y_1^2 y_2^2} \right) \tag{7-2}
 \end{aligned}$$

The pressure plus momentum after the jump must equal the pressure plus momentum before the jump.

$$(P + M)_1 = (P + M)_2$$

Therefore

$$P_2 - P_1 = \gamma \frac{Q}{g} (v_1 - v_2)$$

and

$$\frac{y_2^2 - y_1^2}{2} = \frac{Q^2}{g} \frac{(y_2 - y_1)}{y_2 y_1} \quad (7-3)$$

Solving Eqs. (7-2) and (7-3) simultaneously and eliminating Q^2/g , we find that

$$H_L = \frac{(y_2 - y_1)^3}{4y_2 y_1} \quad (7-4)$$

or, by dividing Eq. (7-4) by y_1 , we can derive the dimensionless equation

$$\frac{H_L}{y_1} = \frac{[(y_2/y_1) - 1]^3}{4(y_2/y_1)} \quad (7-5)$$

The relationship between H_L/y_1 and y_2/y_1 is shown in Fig. 7-2, which can be used to find the head lost as a result of the formation of the hydraulic jump.

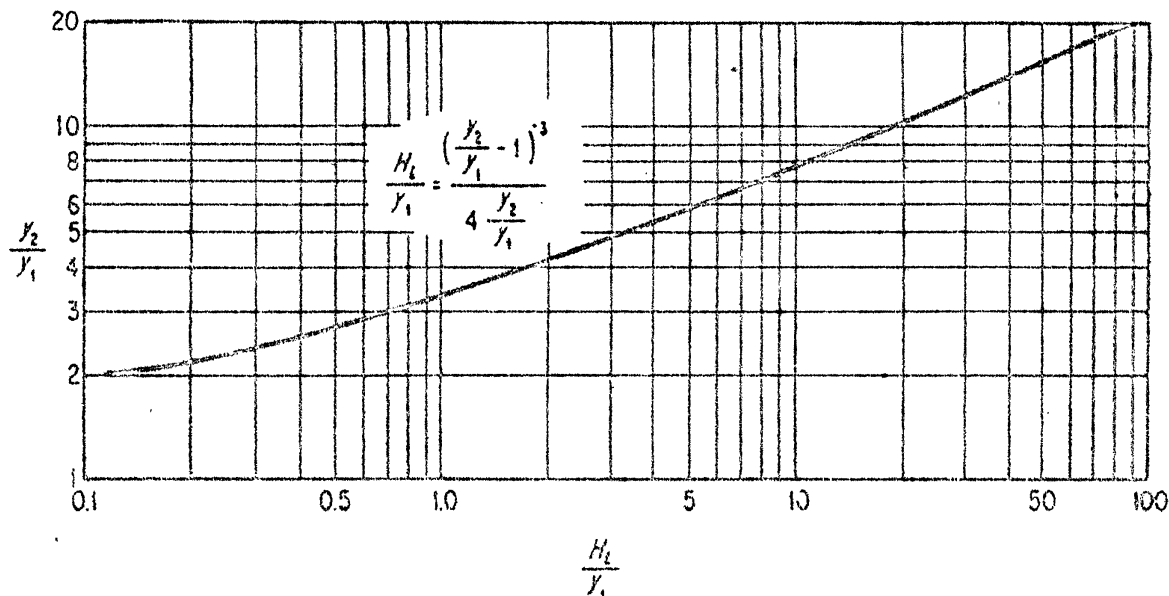


FIG. 7-2. Head lost by the hydraulic jump in rectangular channels.

Equation (7-5) is applicable only for rectangular channels. For non-rectangular channels the head lost produced by the hydraulic jump can be found by substituting the appropriate values into Eq. (7-1).

The head lost can also be found in terms of the depths before and after the jump and the kinetic-flow factor. For a rectangular channel having a width of unity,

$$\frac{y_2}{y_1} = \frac{1}{2} (\sqrt{1 + 8\lambda_1} - 1) \quad (7-6)$$

By substituting Eq. (7-6) in Eq. (7-5),

$$H_L = \frac{y_1(\sqrt{1 + 8\lambda_1} - 3)^3}{16(\sqrt{1 + 8\lambda_1} - 1)} \quad (7-7)$$

To find the actual percentage of energy dissipated, it is necessary to divide the head lost H_L by the initial energy head H_1 . The following method was originated by Stevens⁶:

$$\text{Per cent of initial energy dissipated} = \frac{100H_L}{H_1} = 100 \left[\frac{H_L}{y_1 + (v_1^2/2g)} \right]$$

or

$$\text{Per cent of initial energy dissipated} = \frac{12.5(\sqrt{1 + 8\lambda_1} - 3)^3}{(2 + \lambda_1)(\sqrt{1 + 8\lambda_1} - 1)} \quad (7-8)$$

At critical flow, when $\lambda_1 = 1$, Eq. (7-8) reduces to zero. In Fig. 7-3 a relationship between the percentage of energy dissipated by the jump and

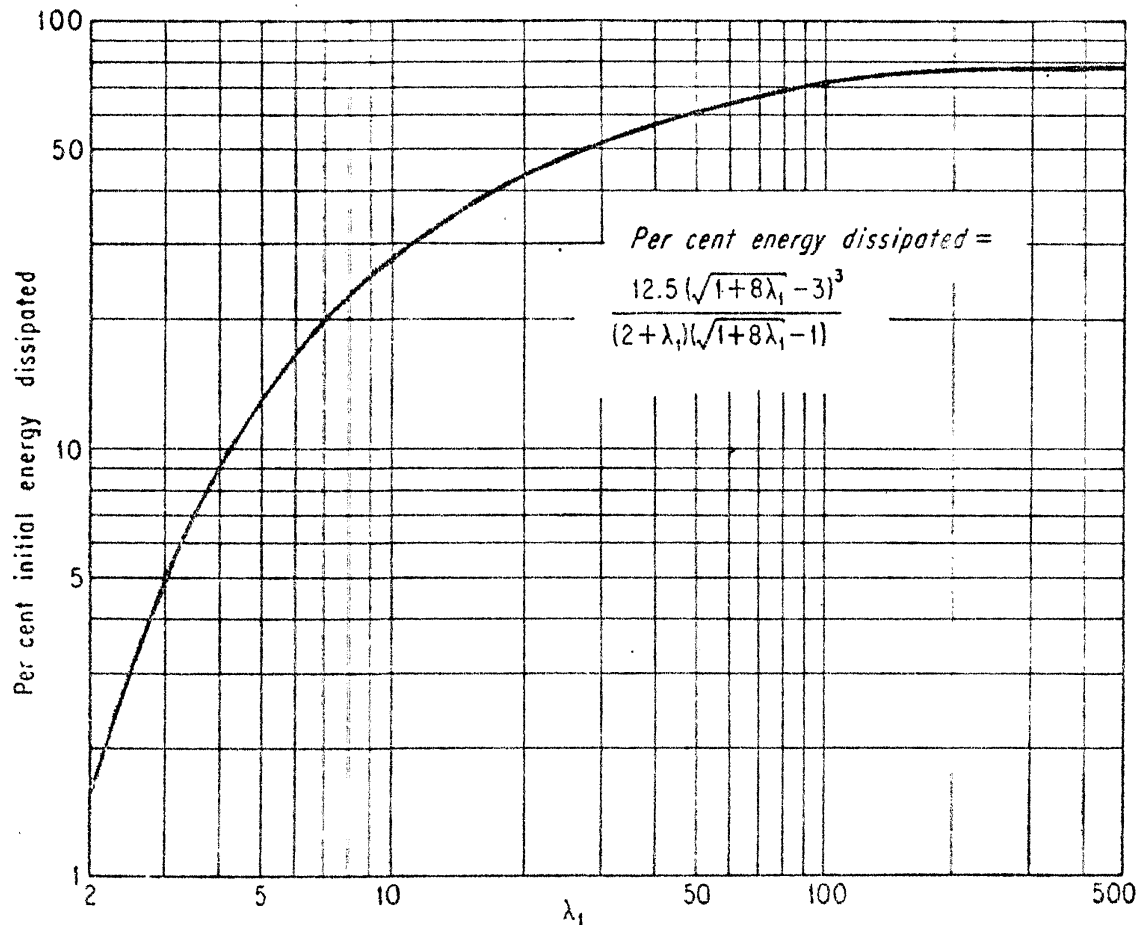


FIG. 7-3. Per cent of energy dissipated by the hydraulic jump in rectangular channels. The kinetic-flow factor is shown. As indicated in Fig. 7-3, the loss becomes greater as the height of the jump increases, and approaches zero as the height of the jump decreases. It should be noted that Fig. 7-3 is valid only for rectangular channels.

As an example, in order for water flowing in a rectangular channel to dissipate 50 per cent of its initial energy, the kinetic-flow factor must be equal to 27.5, as obtained from the curve in Fig. 7-3. If $y_1 = 1.0$ ft, v_1 must be equal to nearly 30 fps in order for 50 per cent of the initial energy to be dissipated by the hydraulic jump.

The specific energy for a rectangular channel is equal to

$$H_1 = y_1 + \frac{q^2}{2gy_1^2}$$

or

$$q^2 = 2gy_1^2(H_1 - y_1)$$

Dividing by H_1^3 ,

$$\frac{q^2}{H_1^3} = 2g \frac{y_1^2}{H_1^2} \left(1 - \frac{y_1}{H_1}\right)$$

then

$$\frac{q}{H_1^{3/2}} = 8.02 \frac{y_1}{H_1} \sqrt{1 - \frac{y_1}{H_1}} \quad (7-9)$$

7-2. Basic Energy Equations. An interesting analysis was made by Crump² regarding the use of dimensionless parameters in solving for the amount of energy dissipated by the hydraulic jump.

The upstream and downstream specific energies are as follows:

$$H_1 = y_1 + \frac{v_1^2}{2g}$$

and

$$H_2 = y_2 + \frac{v_2^2}{2g}$$

Applying the critical-flow criterion $v^2 = y_c^3 g / y^2$ to the above equations,

$$H_1 = y_1 + \frac{1}{2} \frac{y_c^3}{y_1^2} \quad (7-10)$$

and similarly

$$H_2 = y_2 + \frac{1}{2} \frac{y_c^3}{y_2^2} \quad (7-11)$$

Dividing Eqs. (7-10) and (7-11) by y_c , we have

$$\frac{H_1}{y_c} = \frac{y_1}{y_c} + \frac{1}{2} \left(\frac{y_c}{y_1}\right)^2 \quad (7-12)$$

and

$$\frac{H_2}{y_c} = \frac{y_2}{y_c} + \frac{1}{2} \left(\frac{y_c}{y_2}\right)^2 \quad (7-13)$$

If we let

$$x = \frac{y_1}{y_c} \quad y = \frac{y_2}{y_c} \quad m = \frac{H_1}{y_c} \quad n = \frac{H_2}{y_c}$$

then

$$m = x + \frac{1}{2x^2} \quad \text{and} \quad n = y + \frac{1}{2y^2}$$

and therefore

$$\frac{H_L}{y_c} = \frac{H_1}{y_c} - \frac{H_2}{y_c}$$

or

$$\frac{H_L}{y_c} = m - n \quad (7-14)$$

A general equation for H/y_c in terms of y/y_c is

$$\frac{H}{y_c} = \frac{1}{2} \left(\frac{y_c}{y} \right)^2 + \left(\frac{y}{y_c} \right) \quad (7-15)$$

A dimensionless specific-head diagram, shown in Fig. 7-4, can be constructed from Eq. (7-15). An inspection of Fig. 7-4 shows that two

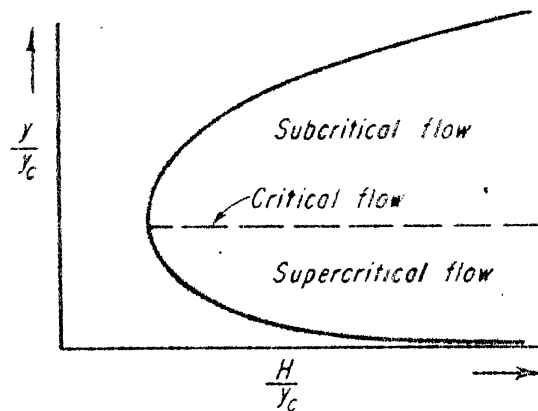


FIG. 7-4. Dimensionless specific-head diagram.

alternate depths are possible with the same energy content. A reduction in the specific head will lead to a reduction in depth if the flow is subcritical, whereas if the flow is supercritical, a reduction in the specific head will result in an increase in the depth of flow.

7-3. Energy Dissipation by Experimentation. Experiments were conducted in 1955 by the Bureau of Reclamation¹ to determine the

amount of energy dissipated by the hydraulic jump. In these experiments, the energy loss was determined by computing the difference between the upstream and downstream specific energies. By using the data compiled by the Bureau of Reclamation, a good relationship between the per cent of energy dissipated and the kinetic-flow factor was found. This relationship is shown in Fig. 7-5 and agrees remarkably well with the computed curve shown in Fig. 7-3.

The hydraulic jump can be separated into two portions, the principal stream and the roller. Translatory movement of the water particles is confined chiefly to the principal stream, while in the roller, the movement is essentially rotational. Another difference between the principal stream and the roller is that the principal stream is composed of clear water, whereas the roller is composed of a mixture of air and water.

The total energy loss in the jump is divided between the top roll and principal stream. It seems probable that the principal stream imparts part of its energy to the top roll and this is ultimately converted into heat by internal friction and turbulence of the roll.

Extensive investigations were made in 1942 by Oosterholt,⁴ at the Technische Hogeschool, Delft, Netherlands, concerning the dissipation

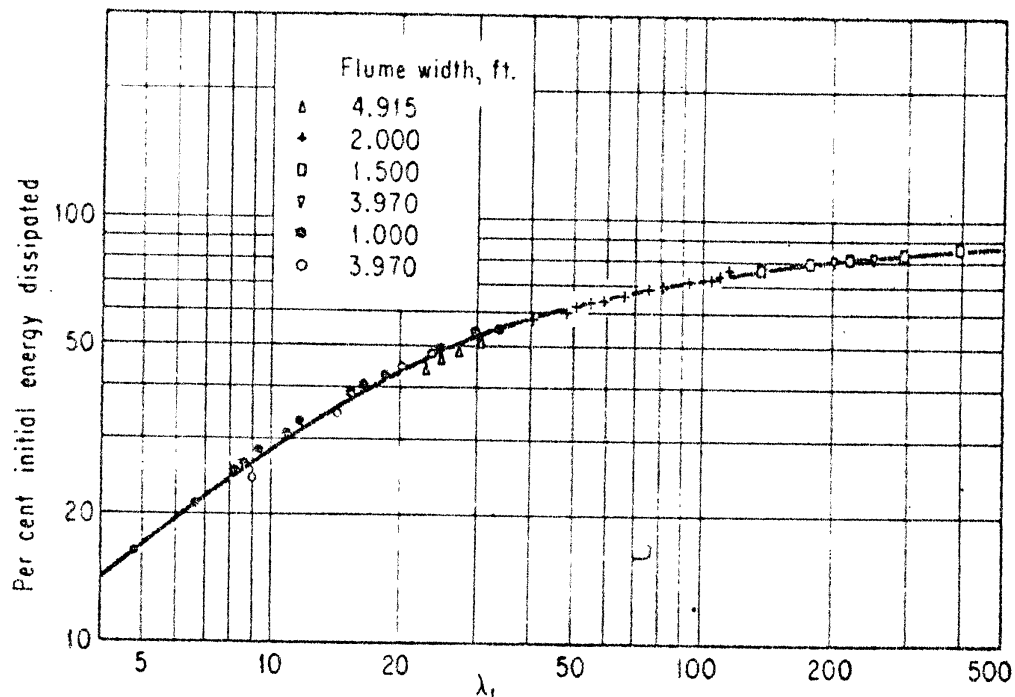


FIG. 7-5. Per cent of energy dissipation by the hydraulic jump in rectangular channels determined by experimentation.

of energy by the hydraulic jump. As a result of these experiments, it was found that most of the energy is dissipated mainly in the transition region between the roller and principal stream. The contribution given to energy dissipation by bottom friction is relatively small. At the junction between the oncoming stream and roller, there is a pronounced velocity gradient as the resulting shear gives rise to the rapid generation of turbulence.

Nagaratnam⁷ has shown that the effect of the turbulence is twofold. First, the mixing process diffuses all characteristics of flow-momentum, energy, and even turbulence itself—both laterally and longitudinally. Secondly, the increased viscous shear produces a rapid conversion of mechanical energy to heat. The roller is an indispensable part of the phenomenon, since without it the formation of turbulence, and hence energy dissipation, would be minimal.

In calculating the amount of energy dissipated by the hydraulic jump, it has been assumed that the velocity distribution is uniform before and after the jump. Experiments by the Miami Conservancy District⁸ clearly show that the velocity of the water gradually diminishes through

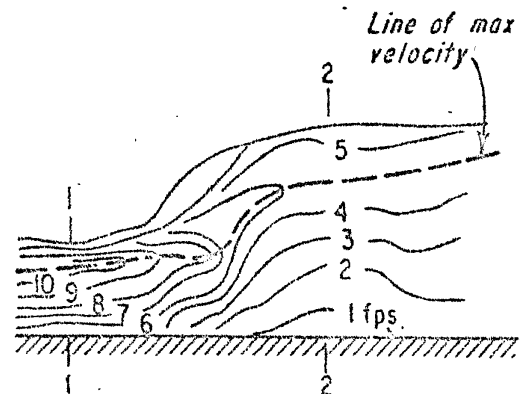


FIG. 7-6. Longitudinal section of the hydraulic jump, showing the distribution of velocities.

the hydraulic jump, as shown by Fig. 7-6 (at section 2-2, the velocities are not uniform). Also, as shown in Fig. 7-6, it will be observed that the line of maximum velocity is lifted off the bottom of the channel at the terminus of the hydraulic jump.

7-4. Friction Effects. To date, there have been few experiments conducted to determine the effect of friction upon the hydraulic jump. Experiments by Puls⁵ indicate that, when friction is included, the water surface of the hydraulic jump is somewhat depressed. For all practical purposes, friction can be neglected in computations of the hydraulic jump.

REFERENCES

1. Bureau of Reclamation, Progress Report II, Research Study on Stilling Basins, Energy Dissipators, and Associated Appurtenances, *Hydraulic Lab. Rep. Hyd.-399*, June 1, 1955.
2. Crump, E. S.: "Note on an Approximate Method of Determining the Position of a Standing Wave," Government Printing Office, Punjab, Lahore, May, 1930.
3. Miami Conservancy District, The Hydraulic Jump as a Means of Dissipating Energy, *Tech. Rep.*, part III, 1917.
4. Oosterholt, G. A.: An Investigation of the Energy Dissipated in a Surface Roller, Waterloopkundig Laboratorium, University of Delft, Netherlands, *Appl. Sci. Rev.*, vol. 1, 1947.
5. Puls, L. G.: Mechanics of the Hydraulic Jump, *Bur. Reclamation Tech. Memorandum 623*, 1941.
6. Stevens, J. C.: Determining the Energy Lost in the Hydraulic Jump, *Eng. News-Record*, p. 928, June 4, 1925.
7. Nagaratnam, S.: "The Mechanism of Energy Dissipation in the Hydraulic Jump," unpublished M.S. thesis, State University of Iowa, 1957.

8

Hydraulic-design Criteria

In order to design an energy dissipator, the designer must have knowledge of the specific hydraulic data for the proposed structure and site. Probably the most important data are the relationship between the jump-height and the tailwater-rating curves for the range of discharges contemplated. The purpose of this chapter is to familiarize the reader with the hydraulic data that are required and to indicate how they can be obtained.

8-1. Jump-height and Stage-discharge Relationships. The formation of the hydraulic jump at the base of a spillway depends upon the relationship between the tailwater depth of the stream and the conjugate depth y_2 of the hydraulic jump. Hereafter, y_2 will be referred to as the

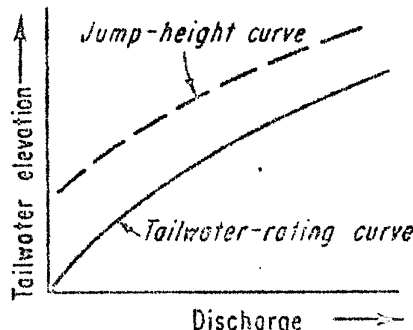
jump-height. Jump-height curves are essential in determining the most suitable method of dissipating the energy of spillway flows.

Under ideal conditions, when the tailwater depth is equal to y_2 , it is necessary only to design a horizontal apron upon which the jump will form. However, this condition is rarely achieved, and it may be necessary to design a sloping apron, which will allow the hydraulic jump to form under fluctuating tailwater conditions.

FIG. 8-1. Jump-height curve always above tailwater-rating curve.

Lane² has divided stilling basins into four classes, which are dependent upon the relationship between the tailwater depth and jump-height y_2 .

If the tailwater is always less than necessary to form the hydraulic jump, as in the case illustrated in Fig. 8-1, the flow will sweep across the apron at a high velocity and is likely to scour the streambed downstream from the apron. The stream bottom will be scoured out until sufficient



depth is provided to permit the hydraulic jump to form. Serious scour caused in this manner occurred at the Wilson Dam, located on the Tennessee River in Alabama, and also at the Waco Dam in Texas. At the Wilson Dam, the tailwater was insufficient to permit the jump to form, and high velocities passed across the horizontal apron, 200 ft in length, eroding a large hole in the solid rock located at the downstream edge of the apron. To prevent this condition, the tailwater depth can be increased by excavating a pool or by depressing the apron. The latter method was used at the Willwood Dam, illustrated in Fig. 8-2. The

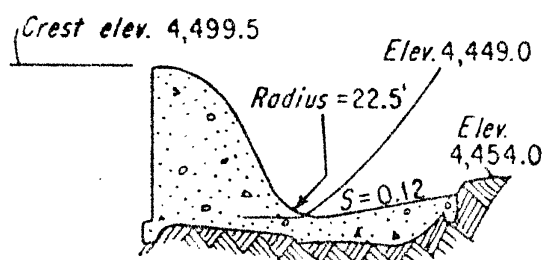


FIG. 8-2. Willwood Dam.

apron of the Willwood Dam is designed to keep the hydraulic jump close to the downstream face of the dam by lowering the surface of the apron 5 ft below the streambed and then raising the apron surface to the level of the streambed at the downstream edge of the apron. The

apron extends 54 ft downstream from the dam and terminates in a cutoff wall 8 ft deep.

When insufficient tailwater depth occurs, the apron can be lowered below the streambed level, as in the case of the Wheeler and Norris Dams, illustrated by Figs. 8-3 and 8-4, respectively. For this condition, the

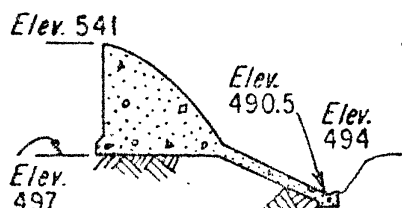


FIG. 8-3. Wheeler Dam.

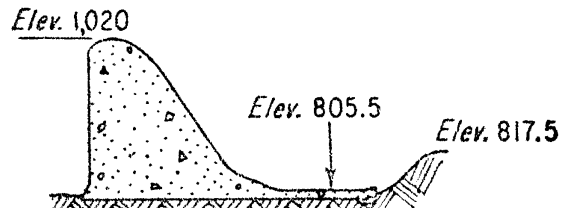


FIG. 8-4. Norris Dam.

sloping apron should be placed entirely below the streambed level. Figure 8-5 is a photograph showing the performance of the Wheeler Dam stilling basin.

Another possible solution can be had by providing the structure with an upturned bucket, which will direct the water away from the dam. The use of a trajectory bucket necessitates that the streambed be composed of firm rock, which will withstand considerable scour.

One of the earliest types of structures employing this method was the Holyoke Dam, located on the Connecticut River in Massachusetts. Other structures designed for the same condition are the Conowingo and Safe Harbor Dams, located on the Susquehanna River, in Pennsylvania, depicted by Figs. 8-6 and 8-7, respectively. At the Safe Harbor Dam, a short bucket is used to deflect the high-velocity jet away from the dam.

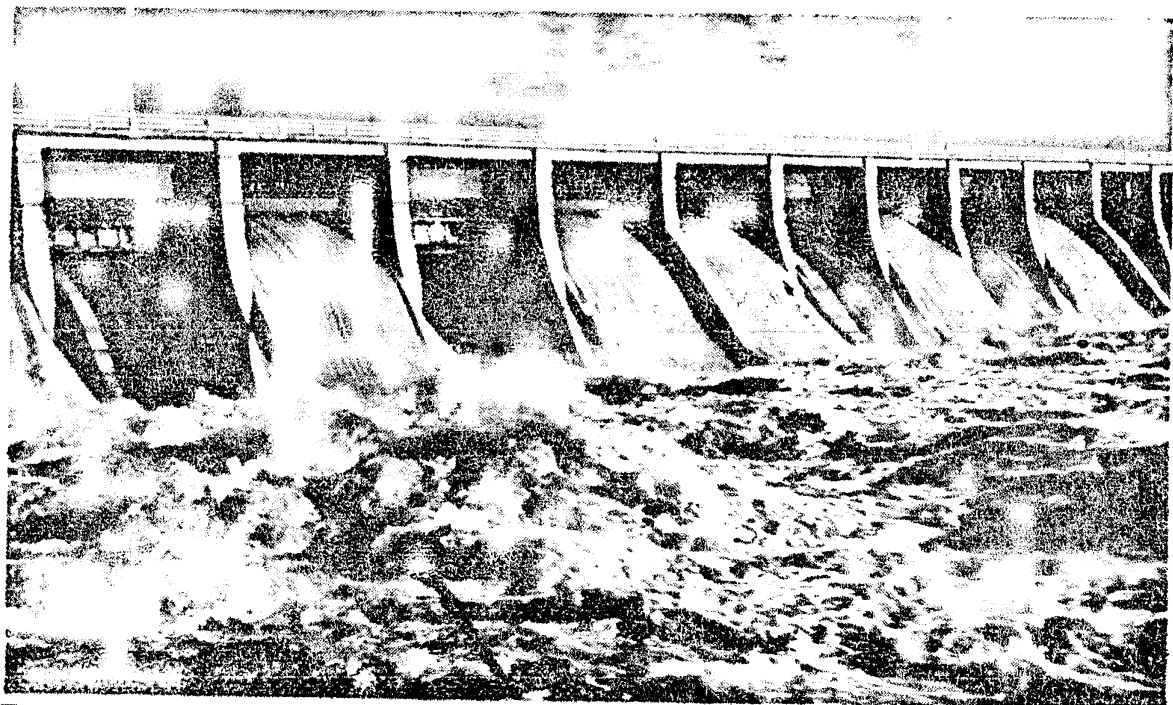


FIG. 8-5. Wheeler Dam spillway stilling basin in operation. (Courtesy of Tennessee Valley Authority.)

A fourth solution can be had by constructing a low secondary dam downstream from the main dam; this will create a pool with sufficient tailwater to permit the jump to be formed. This has been used on earth

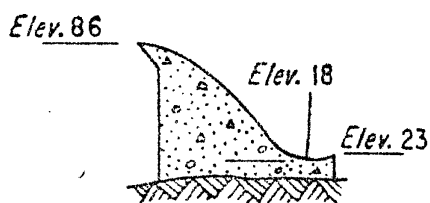


FIG. 8-6. Conowingo Dam.

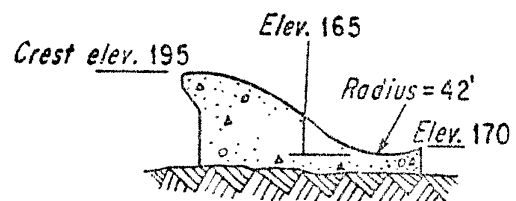


FIG. 8-7. Safe Harbor Dam.

foundations as in the case of the Junction Dam, constructed on the Manistee River in Michigan, as shown in Fig. 8-8.

When the tailwater is nearly sufficient to cause the jump to form, baffles or sills may be placed on the floor of the basin to increase the tailwater depth. Perhaps the best example of the use of baffle piers with a low tailwater depth is the Gatun Dam, built in conjunction with the Panama Canal. At the toe of the spillway, the water impinges directly upon the baffles, and much of it is thrown high into the air. During this operation, the principal effect of the baffle piers is to distribute the impact over a large area.

The case in which the jump-height curve is always below the tailwater-

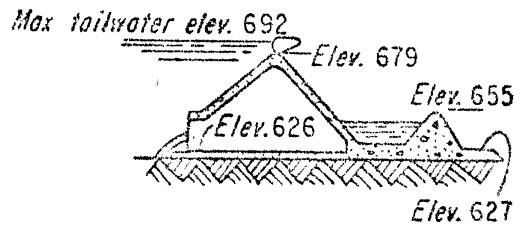


FIG. 8-8. Junction Dam.

rating curve is illustrated by Fig. 8-9. This is apt to occur when the foundation rock is at a considerable depth, and therefore the tailwater depth is higher than necessary for the jump to form. Because of the exhaustion of good dam sites, this case will be encountered more in the future than it has in the past.

In many cases, water flowing down the steep face of a dam dives under

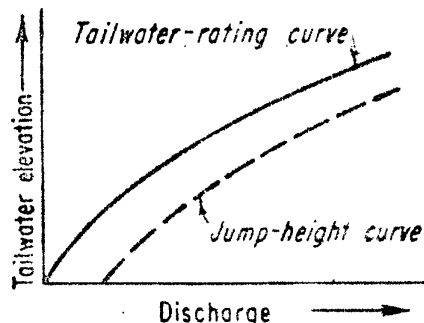
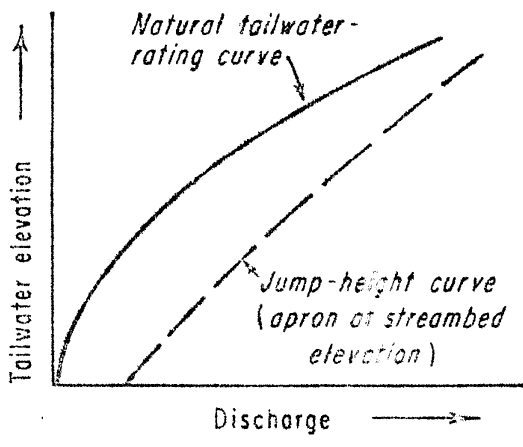


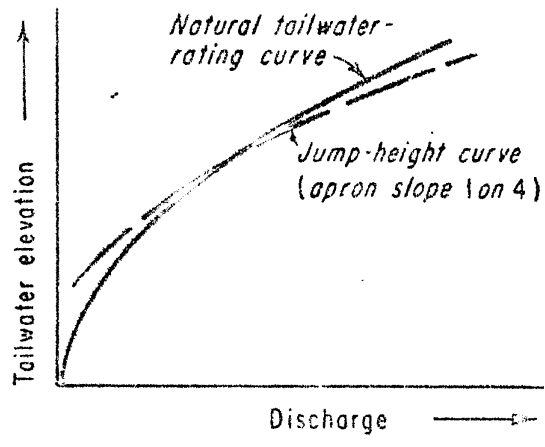
FIG. 8-9. Jump-height curve always below tailwater-rating curve.

the tailwater and travels at a high velocity a long distance along the stream bottom before being dissipated. The more nearly the tailwater depth corresponds to the conjugate depth y_2 , the shorter will be the distance the high velocities travel downstream. To alleviate this condition, a sloping apron can be utilized to help form an efficient jump at all discharges. In contrast to the first case, the sloping apron must be constructed entirely above the streambed level.

Probably the most outstanding use of this case is the Madden Dam, located on the Chagres River in Panama. The slope of the apron used for the Madden Dam spillway was developed as a result of extensive model studies. Figure 8-10a shows the relationship of the jump-height and tailwater-rating curves for the Madden Dam. The slope of the apron was determined by trial. By varying the tailwater level, it was



(a)



(b)

FIG. 8-10. Madden Dam jump-height and tailwater-rating curves.

possible to determine, for each slope of apron tested, the tailwater levels required at various discharges to permit the jump to form at the upstream edge of the apron. Figure 8-10b shows the jump-height curve that best agrees with the tailwater-rating curve. The apron which was developed had a slope of 1 vertical to 4 horizontal, with its upstream edge approximately 30 ft above the foundation level. At large discharges, high

velocities extend across the apron and are deflected away from the streambed by a small triangular end sill.

A low roller bucket is another type of device that can be used in this class. The roller bucket may be satisfactory if the jump-height curve is not too far below the tailwater curve. When the roller bucket is employed, the overflowing water flows around the bottom of the curved bucket and is thrown upward by the bucket lip, forming a surface roller in the bucket and a ground roller downstream from it. A bucket of this type was employed at the base of the spillway of the Grand Coulee Dam.

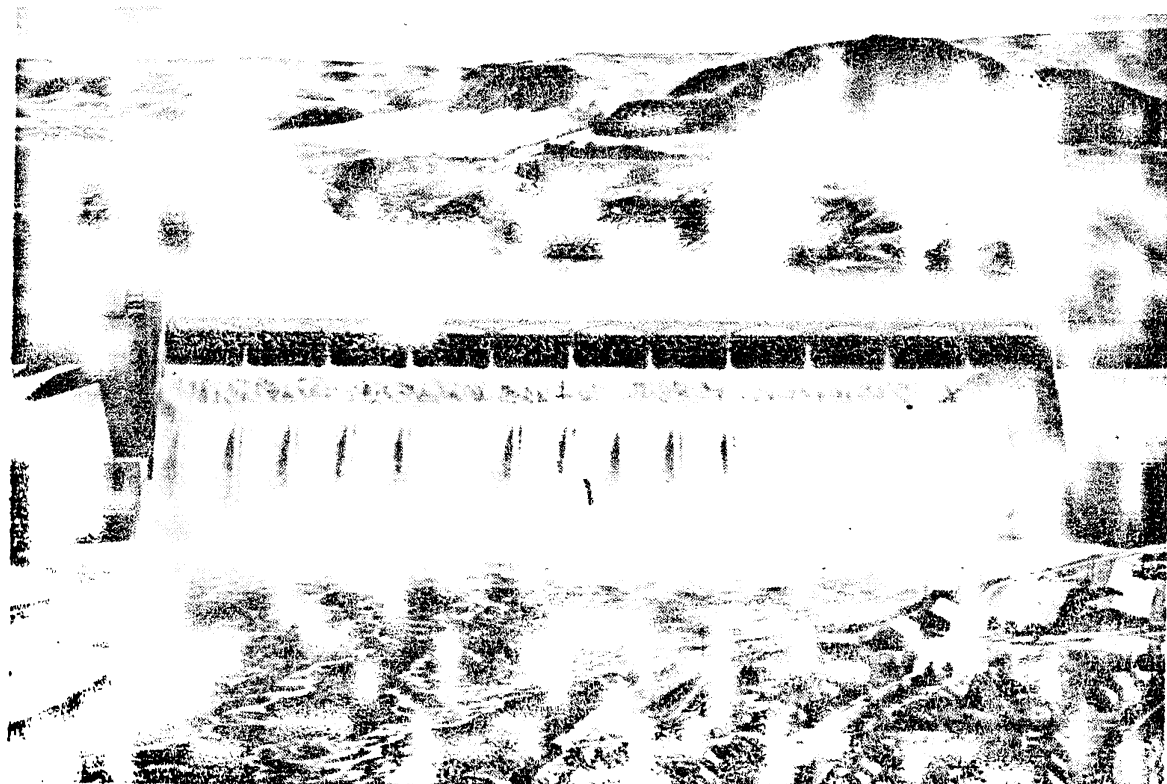


FIG. 8-11. Air entrainment on the face of Grand Coulee Dam spillway. (*Courtesy of Bureau of Reclamation.*)

At low flows, the bucket with insufficient tailwater may not remain submerged and water will be directed upward, forming a large amount of spray which may damage powerhouses and other works. A photograph of the Grand Coulee Dam is shown in Fig. 8-11.

The case in which the jump-height curve is above the tailwater-rating curve at low discharges and below it at high discharges is shown in Fig. 8-12. The solution lies in creating enough tailwater depth to permit the hydraulic jump to form on the sloping apron at low discharges. This situation can be remedied by utilizing a sloping apron positioned with its upper end above the bed level and its lower end below the bed level. In some cases, the problem can also be solved by constructing a secondary dam near the downstream end of a level apron.

Where the jump-height curve is below the tailwater-rating curve at low

discharges and above it at high discharges, illustrated by Fig. 8-13, the tailwater depth should be increased to permit a jump to form at high discharges. This can be accomplished by constructing a combination of a sloping apron and excavated pool.

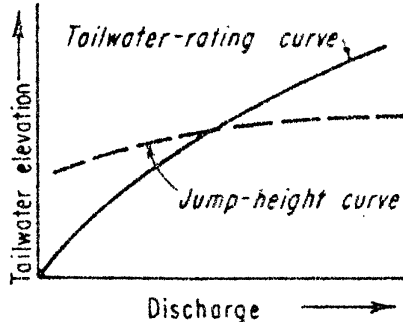


FIG. 8-12. Jump-height curve above tailwater-rating curve at low discharges and below it at high discharges.

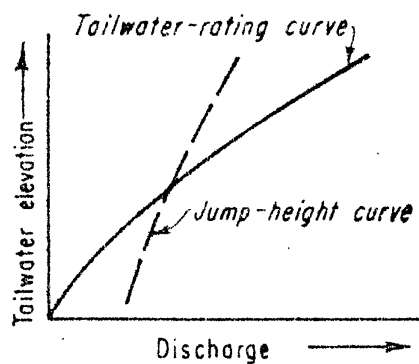


FIG. 8-13. Jump-height curve below tailwater-rating curve at low discharges and above it at high discharges.

By properly selecting the spillway crest length, it will be possible to secure a closer agreement between the tailwater and jump-height curves than would be obtained by choosing an arbitrary crest length. If an assumed length produces insufficient tailwater, the agreement between the curves will be improved by increasing the spillway crest length, which will reduce the discharge per foot of spillway width and consequently lower the jump-height curve.

8-2. Preparation of Jump-height and Tailwater-rating Curves. A jump-height curve can be obtained by assuming various discharges and computing the jump-height y_2 . In most instances it will be desirable to convert the depth into an elevation above mean sea level. When the jump-height elevation versus the discharge is plotted, the desired curve will be obtained.

A stage-discharge relation or tailwater-rating curve for a stilling basin is required to determine the most suitable method of dissipating the energy of spillway flows. The tailwater-rating curve may be determined by actual readings of a gage located near the site, which will cover a wide range of discharges, or by backwater computations. When it is necessary to determine the tailwater elevations by means of backwater computations, a profile and cross sections of the river should be obtained for a considerable distance downstream or to a known point of control. Backwater computations are then initiated for the range of discharges desired, and the stage-discharge relation is determined at the desired location, usually at the end sill of the stilling basin.

The stage-discharge relation at the stilling basin may not remain constant because of factors such as the operation of other discharge facilities of the project, possible retrogression of the outlet channel, the river

channel, downstream channel inflows, and the future construction of downstream projects. Because of these conditions, the stilling basin should be designed for optimum stilling action, with the tailwater rating expected to occur the largest portion of the time, and it should be safe for the entire range of possible tailwater ratings. The accuracy and reliability of the basic data used in developing the tailwater curves should be carefully considered in determining the adequacy of the stilling-basin design for a wide range of tailwater conditions.

For all sediment-bearing streams, channel retrogression will occur below the structure as a result of reduced sediment load. Retrogression in an 8-mile section below the Hoover Dam caused an average lowering of 6.7 ft in the bed of the river during the first 2 years following closure of the dam.¹ Channel retrogression extended farther downstream, but it gradually diminished and became negligible 50 miles downstream. It is important that an estimate be made of the ultimate tailwater-rating curve after channel retrogression has occurred.

8-3. Stilling-basin Design Discharge. Determination of the design discharge for an energy dissipator depends to a large extent upon the purpose of the project. For flood-control projects, the design discharge can be determined from hydrological studies and flood hydrographs of the natural stream. For spillway stilling basins, the design discharge of the basin will be equivalent to that of the spillway. When sluices discharge into a common spillway, the stilling-basin design discharge will be equivalent to the total sluice discharge plus the spillway design discharge. In the case of flood-control outlets, studies of the downstream capacity of the channel and a series of flood-routing studies may be required to determine the outlet capacity.

Design discharges for the outlet works of irrigation and power projects are primarily governed by the downstream flow requirements, which may include water flow determined by riparian rights, navigation, fish and wildlife releases, or irrigation demands. The requirements for river diversion during construction of the dam are often an important, if not a controlling, factor in determining the outlet capacity. Because of the many project purposes, it is not possible to standardize the method of selecting the outlet capacity. The outlet-works discharge will, of course, be limited by the downstream channel capacity.

8-4. Stilling-basin Width. The effect of increasing the stilling-basin width is to reduce the required depth of the basin. Various combinations of basin width and depth are compared to obtain the lowest-cost combination. In determining the final width of the basin, consideration should be given to assure that the uplift pressure on the floor slab, as represented by the difference in depth before and after the hydraulic jump, will not be excessive.

In some instances, the stilling-basin floor must be set high enough to avoid undercutting foundation material. Examples of this can be found at the Denison and Fort Randall Dams, where the foundation material was of limited depth. For these structures a double stilling basin consisting of a primary high basin formed by low weirs and a secondary low basin, each employing a hydraulic jump-type basin, was adopted. The stilling basin should be designed to avoid excessive channel erosion as a result of the exit velocities leaving the paved basin.

8-5. Outlet Channels. An outlet channel will be required to connect the stilling basin with the natural-stream channel. If the required channel is quite long, the excavation cost may represent a considerable expenditure. The dimensions of the outlet channel should be determined so that the water surface does not overtop the stilling-basin walls. It is important that the outlet channel be designed to avoid the creation of an excessive head differential during the diversion closure operation by unduly restricting the outlet-channel flow.

Unfortunately, there are no fixed criteria by which the designer can immediately determine a safe, noneroding channel velocity. Soil borings and geological data can be used, however, to determine the depths and types of material composing the exit channel. It is often possible to locate channel sections in the main stream where materials similar to those in the contemplated channel are exposed. Erosion resistance may be judged by observation of scour and stream velocities during periods of high water. A study of previous high-water marks may also yield valuable information.

Side-slope erosion in the outlet channel is caused by waves generated in the stilling basin as part of the energy-dissipation process. Waves spread out laterally below the stilling basin and attack the embankment below the wing walls. Erosion can be usually controlled by placing a riprap cover over the exposed slopes.

REFERENCES

1. Corfitzen, W. G.: Retrogression below Boulder Dam, *Reclamation Era*, p. 240, October, 1937.
2. Lane, E. W.: Scour, Sec. 9 in C. V. Davis (ed.), "Handbook of Applied Hydraulics," pp. 347-356, McGraw-Hill Book Company, Inc., New York, 1942.

9

Hydraulic-jump-type Stilling Basins

A stilling basin can be defined as a structure in which all or part of the hydraulic jump, or other energy-reducing action, is confined. Generally, stilling pools are installed at the lower end of chutes and drops in order to obtain the required loss of energy between the lower end of the chute and the streambed below the pool. In a stilling basin, kinetic energy is converted into turbulent energy and ultimately into heat. Recommended designs for canal, diversion, and sluiceway stilling basins are included in this chapter.

CANAL STILLING BASINS

9-1. Design Procedure. Factors involved in the design of canal stilling basins include the basin height and length, reduction in velocity, and apron elevation. The exit section of the channel should be located with respect to the lowest possible tailwater elevation for the maximum discharge contemplated. The following method will serve as a general guide in designing stilling basins, making the model serve as a check or verification of the design. Where the projects are small, the cost of model studies may not be justified, and the rational method will be of infinite value.

Consider the rectangular canal drop depicted by Fig. 9-1. In Fig. 9-1, it is assumed that y_0 , v_0 , y_3 , v_3 , elevation A , elevation C , and the discharge are known. The problem will be to determine elevation B , y_1 , v_1 , y_2 , v_2 , and H_L .

For a given discharge, the critical depth for a rectangular channel can be found by using the equation

$$y_c = \sqrt[3]{\frac{q^2}{g}}$$

The angle of the flared section between the projected outlet conduit axis and the stilling-basin side walls is usually determined by model studies. Of the many considerations in the design of a flared section, the most important is that the flow be spread uniformly over the flared section. If an abrupt enlargement occurs in an open channel, the proper flare of the side walls may be computed from Eq. (9-8).

$$\theta = \tan^{-1} \frac{1}{K} \quad (9-8)$$

In Eq. (9-8), K is termed the flare ratio, which represents the distance along the axis in the direction of flow for a unit divergence. If the flare ratio is too great, the flow will be unstable and concentrated in the center of the basin.

On the other hand, if the flare ratio is too small, the stilling-basin length becomes excessive. Laboratory tests indicate a satisfactory flare ratio will occur when $K = 2\sqrt{\lambda_1}$.

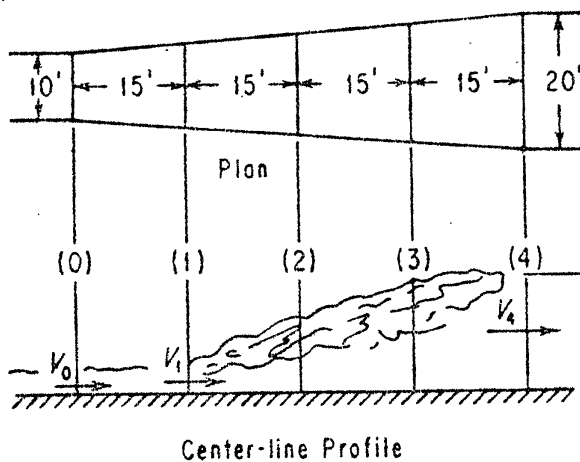


FIG. 9-4. Hydraulic-jump formation in a diverging channel.

decelerated in the direction of the flow. Equation (9-10) may be employed to determine the reduction in velocity.

$$v_x = \sqrt{v_0^2 + 2gx} \quad (9-10)$$

where v_x = longitudinal velocity

v_0 = initial velocity

x = longitudinal distance

Consider the case shown in Fig. 9-4, where the hydraulic jump is expected to form at location 1. Assume that v_0 and v_4 are 40 and 2 fps, respectively, and that the pool diverges from 10 to 20 ft in width and is 60 ft in length. The problem will be to determine v_1 . It is first necessary to determine the value of g .

$$v_4 = \sqrt{v_0^2 + 2gx}$$

$$2 = \sqrt{40^2 + 2g(60)}$$

$$g = -13.3$$

and

$$v_1 = \sqrt{40^2 + 2(-13.3)(15)} \\ = 34.6 \text{ fps}$$

Velocities at other sections can be computed in a similar manner.

DIVERSION-STRUCTURE STILLING BASINS

9-5. Design of Protective Works. Some protection against erosion at the downstream edge of an overflow diversion dam is always needed. Even for structures that are to be constructed on solid rock which extends below the dam, some sort of protective measures will be necessary. An example of this occurred at the Black Canyon Dam, a 184-ft-high structure originally constructed on solid rock without any protection. Erosion along the edge of the base during 28 years of operation finally required an apron to be added to protect the structure from possible undermining.

For low diversion dams, sufficient protection against erosion can be secured by constructing a wide downstream apron with a cutoff wall to prevent undercutting at the downstream edge. Further protection can be secured by placing riprap in the channel below the apron. Riprap or concrete blocks should be placed on a blanket of gravel to prevent the streambed material from being drawn up through the voids in the protection. In the case of fine streambed materials, it may be necessary to construct this blanket as a filter, using a layer of sand in the lower course with a layer of gravel on top.

One of the most effective means of dissipating the excess energy of water discharging over the diversion dam is a hydraulic jump formed on a concrete apron. For the formation of the hydraulic jump to occur, there must be sufficient tailwater depth equal to y_2 , which can be computed from Eq. (9-11).

$$\text{Required tailwater} = \frac{y_1}{2} (\sqrt{1 + 8\lambda_1} - 1) \quad (9-11)$$

The jump-height and tailwater-rating curves should always be plotted on the same diagram, so that their relationship may be studied. If possible, the depth of the stilling pool should be adjusted to permit the two curves to intersect at the point of maximum discharge. If it is not possible or it is impracticable to adjust the stilling-basin depth, an increase or decrease in the length of the spillway crest may be accomplished. On streams where retrogression is expected, it is very important to make an estimate of the amount of retrogression, so that the tailwater-rating curve can be adjusted to represent future conditions.

For most diversion structures, the length of the horizontal apron should be made equal to the length of the hydraulic jump. The only appurtenance needed in connection with the horizontal apron is a solid triangular end sill placed at the downstream end of the apron. It serves to lift the flow off the streambed as it leaves the apron and thereby reduces scour. The dimensions of the end sill are variable, but the most effective sill height will be between $0.05y_2$ and $0.1y_2$, with an upstream slope of 1 vertical on 3 horizontal and a vertical downstream slope.

An upturned slotted roller bucket may sometimes prove to be more economical than a concrete apron where high tailwater is available, because of the smaller amount of concrete needed for construction. A detailed discussion of slotted spillway roller buckets will be given in Chap. 18.

In general, a bucket-type energy dissipator should not be used where there is a possibility that degradation of the streambed will lower the tailwater below the design minimum.

An upstream concrete apron has been found to be advantageous for diversion dams constructed on pervious sand and gravel foundations. In addition to the increased path of percolation provided by the apron, it often prevents erosion to the dam during periods of flood flow. In place of a concrete apron, it may be more economical and desirable to use an impervious blanket, suitably protected by riprap or gravel. Upstream cutoff walls are desirable to increase the path of percolation under a diversion dam. These cutoff walls may be composed of steel, timber, or concrete piling.

Often it is necessary to furnish some protection against erosion of the downstream channel and banks. Riprap is the most commonly used material for this purpose. Since the maximum velocities upstream from the dam are lower than the original river velocities before the dam was built, the riprap usually need not be very heavy. In most cases a coarse gravel blanket will be sufficient. Adequate freeboard must be provided to prevent overtopping by wave action. The minimum recommended freeboard is 2 ft.

Wing walls are provided to join the overflow weir on the headworks to an earth dike or the banks. They prevent erosion of the banks and provide a longer path of percolation around the end of the overflow weir. Wing walls may be warped, vertical, or sloped.

The Cochiti Diversion Dam,² located on the Rio Grande, near Bernallillo, N.Mex., has successfully passed discharges up to 60,000 cfs without any noticeable erosion. Figure 9-5 shows the principal dimensions of the structure.

The following procedure is recommended to be used in determining the apron length and dimensions of the end sill. It is assumed that the data

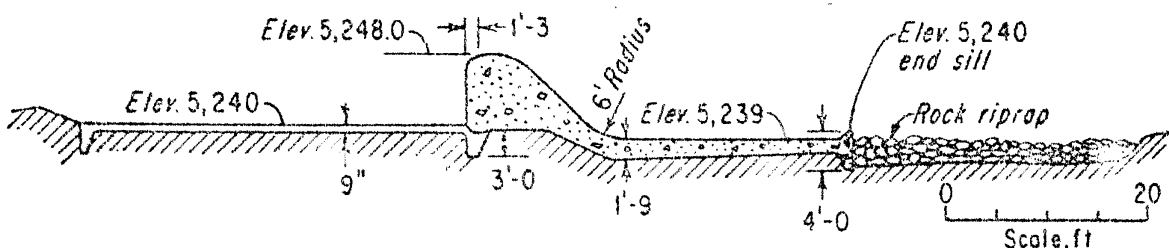


FIG. 9-5. Profile of Cochiti Diversion Dam, N.Mex.

for the example problem given below have been previously determined.

1. Design discharge $Q = 5,000 \text{ cfs}$
2. Gross spillway width = 100 ft
3. Head (from pool level to toe of dam) = 10 ft
4. Tailwater depth, at design discharge = 8.0 ft

Step 1. Compute v_1 and y_1 .

$$\begin{aligned} v_1 &= \sqrt{2gH} = \sqrt{2(32.2)(10)} \\ &= 25.4 \text{ fps} \\ y_1 &= \frac{q}{v_1} = \frac{50}{25.4} \\ &= 1.97 \text{ ft} \end{aligned}$$

Step 2. Determine λ_1 .

$$\lambda_1 = \frac{v_1^2}{gy_1} = \frac{25.4^2}{1.97(32.2)} = 10.2$$

Step 3. Compute y_2 .

$$\begin{aligned} \frac{y_2}{y_1} &= \frac{1}{2} (\sqrt{1 + 8\lambda_1} - 1) \\ &= \frac{1}{2} [\sqrt{1 + (8)(10.2)} - 1] \\ &= 4.05 \\ y_2 &= 1.97(4.05) = 8.10 \text{ ft} \end{aligned}$$

Step 4. Determine length of hydraulic jump.

$$\begin{aligned} L_j &= 6.9(y_2 - y_1) = 6.9(8.10 - 1.97) \\ &= 42 \text{ ft} \end{aligned}$$

If the bed material is loose and unstable, the length of the apron should be made equal to the length of the hydraulic jump. If, however, the bed material is composed of rock or stable material, the length of the apron can be reduced and made equal to 60 per cent of the jump length.

Step 5. Dimensions of end sill

$$\begin{aligned} \text{Height} &= 0.1y_2 = 0.1(8.10) \\ &= 0.81 \text{ ft} \end{aligned}$$

The end sill should have a 1 vertical on 3 horizontal upstream slope, with a vertical downstream face.

SLUICEWAY STILLING BASINS

9-6. Hydraulic Jump below a Sluice Gate. Frequently the designer is called upon to find the discharge of water flowing from a sluice gate. The discharge will depend upon the sluice-gate opening, the water level in the reservoir, and the tailwater depth below the sluice gate. The relationship between the tailwater depth and gate opening will indicate whether a free or submerged jump will be formed.

The three types of hydraulic jumps which may be formed below a sluice gate are dependent upon the relationship between the tailwater depth and y_2 . When the tailwater depth is equal to the conjugate depth y_2 , a free jump will be formed. Of the three types, this case produces a jump of maximum height. When the tailwater depth is greater than y_2 , a submerged jump may be formed. In this case the tailwater may back up to the sluice gate, thereby reducing the effective head and limiting the discharge through the sluice gate.

When the tailwater depth is less than y_2 , a repelled jump will be formed. In this case the jump will form downstream from the sluice gate, at a point where the tailwater depth, reduced by friction, equals y_2 .

A fourth case may occur when the flow of water through the sluice gate is under a very low head. During this time, flow through the gate will be subcritical and no jump can be formed, regardless of the tailwater elevation.

9-7. Constant-head Characteristics. The elements of flow below a sluice gate are shown in Fig. 9-6. By raising or lowering the sluice gate, the depth y_1 will be changed and with it other flow features. When y_1 equals $2H/3$, a free efflux similar to flow over a broad-crested weir will occur; y_1 then equals y_c , and the discharge will be a maximum for the

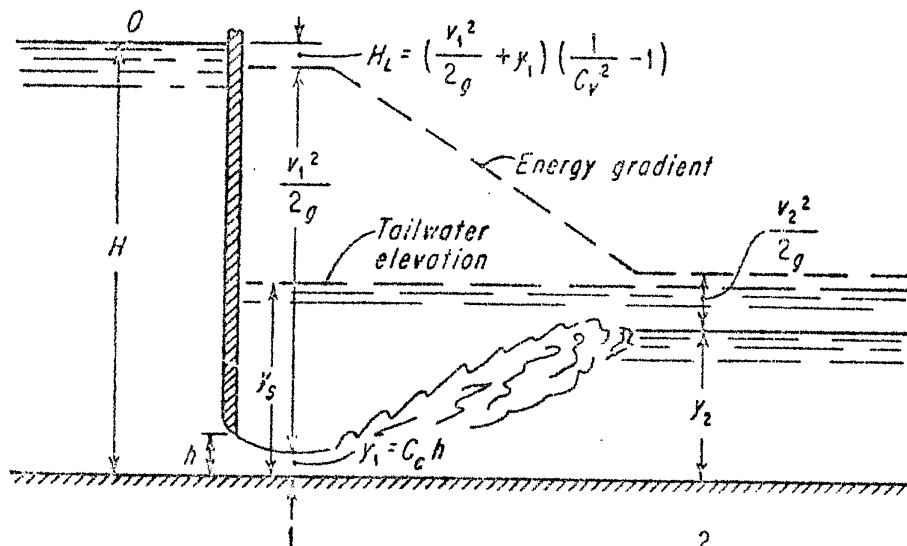


FIG. 9-6. Formation of a hydraulic jump below a sluice gate.

given gate opening and head. For all values of y_1 less than $2H/3$ the flow will be supercritical, and some type of hydraulic jump will occur if the flow is subcritical below the sluice gate.

Because of the contraction of the water flowing under the gate, the depth at section 1 will be less than the gate opening and equal to

$$y_1 = C_c h \quad (9-12)$$

where C_c = coefficient of contraction

and h = gate opening, ft

The velocity discharging from the sluice gate will be

$$v_1 = C_v \sqrt{2g(H - y_1)} \quad (9-13)$$

In Eq. (9-13), C_v , the coefficient of velocity, is defined as the ratio of the actual velocity to the theoretical velocity.

The total head producing the discharge is

$$H - y_1 = \frac{1}{C_v^2} \frac{v_1^2}{2g}$$

The quantity $H - y_1$ is called the "effective head." From point 0 to 1 the head lost will be

$$H_L = \left(\frac{v_1^2}{2g} + y_1 \right) \left(\frac{1}{C_v^2} - 1 \right) \quad (9-14)$$

For a constant head,

$$v_1 = C_v \sqrt{2g(H - y_1)} \quad (9-13)$$

Since $q = v_1 y_1$ for a rectangular channel of unit width, Eq. (9-13) becomes

$$q = y_1 C_v \sqrt{2g \frac{[1 - (y_1/H)]}{H}}$$

and

$$\lambda_1 = 2C_v^2 \frac{1 - (y_1/H)}{y_1/H}$$

For a rectangular channel of unit width,

$$\frac{y_2}{y_1} = \frac{1}{2} \left[-1 + \sqrt{1 + 16C_v^2 \left(\frac{H}{y_1} - 1 \right)} \right] \quad (9-15)$$

With a known level in the reservoir, y_2 can be computed directly by using Eq. (9-15).

The coefficient of velocity C_v will usually vary from 0.92 to 0.99. In most cases C_v can be assumed equal to unity, which will result in an error of little magnitude.

If the outlet is permitted to become submerged, the hydrostatic pressure acting opposite the direction of flow will increase beyond that for the

free jet, as the depth of submergence increases. Since the latter will in turn reduce the effective head on the outlet, it can readily be seen that the discharge will be dependent upon the degree of submergence for a given efflux depth.

If the outlet is submerged by a depth y_s , the effective head becomes $H - y_s$ and

$$v_1 = C_r \sqrt{2g(H - y_s)} \quad (9-16)$$

and, for a rectangular channel of unit width,

$$q = C_r y_1 \sqrt{2g(H - y_s)} \quad (9-17)$$

In deriving Eq. (9-17), the assumption is made that the tailwater backs all the way up to the sluice gate. This will not be true in many cases. We know, of course, that the flow of water passing under the sluice gate repels the tailwater away from the sluice gate and that the only time the tailwater will back up completely to the sluice gate is when the gate is under a high degree of submergence.

The following example is used to illustrate the usage of the theory presented.

Example. It is assumed that the outlet for a reservoir consists of a 4-ft-square gate opening that is being operated under a constant head of 40 ft. If C_r is unity and C_c is 0.75, find the following items:

1. Is a free or submerged jump formed if the tailwater depth is 22 ft?
2. What is the discharge?
3. Determine the tailwater depth necessary for the maximum discharge.

Solution.

$$\begin{aligned} 1. \quad y_1 &= C_c h \\ &= 0.75(4) = 3.0 \text{ ft} \\ y_2 &= \frac{y_1}{2} \left[-1 + \sqrt{1 + 16C_r^2 \left(\frac{H}{y_1} - 1 \right)} \right] \quad (9-15) \\ &= \frac{3}{2} [-1 + \sqrt{1 + 16(1)^2(13.33 - 1)}] \\ &= 19.6 \text{ ft} \end{aligned}$$

Since $y_2 <$ tailwater depth, a submerged hydraulic jump will be formed.

2. The effective head will be $H - y_s$, which equals 18 ft. Then

$$\begin{aligned} q &= C_r y_1 \sqrt{2g(H - y_s)} \quad (9-16) \\ &= 1.0(3.0) \sqrt{2g(40 - 22)} \\ &= 102 \text{ cfs per foot of basin width} \end{aligned}$$

3. A free jump will form when the tailwater depth is equal to y_2 . When this occurs, the discharge will then be maximum for the given set of conditions.

$$\begin{aligned} q &= C_r y_1 \sqrt{2g(H - y_1)} \\ &= (1.0)(3.0) \sqrt{2g(40 - 3)} \\ &= 146 \text{ cfs per foot of basin width} \end{aligned}$$

When a free jump is formed, an additional 44 cfs per foot of basin width can then be released from the reservoir under a constant head of 40 ft.

9-8. Submerged Hydraulic Jump. A submerged hydraulic jump will be formed when the tailwater depth exceeds the conjugate depth of the jump y_2 . In this case the tailwater level may completely back up to the sluice gate. When this occurs, the discharge through the sluice gate will be diminished because of the hydrostatic force of the tailwater opposing the head in the reservoir. The reduction in discharge is dependent upon the degree of submergence for a given efflux depth.

If a turbine is in operation, its efficiency will be materially reduced by the excess tailwater. Essentially, the problem can be relieved by constructing a basin or abrupt drop, which will cause the jump to form under a wide range of tailwater conditions.

For a submerged jump, energy dissipation is accomplished by turbulent diffusion as the high-velocity jet enters a deep body of water. High velocities may prevail, in this case, for a long distance along the floor of the channel. For low heads and large gate openings, the flow at the outlet may be subcritical, and energy dissipation will again be by diffusion.

REFERENCES

1. Bureau of Reclamation, "Design and Construction Manual," vol. X, "Canals and Related Structures," April, 1942.
2. Newcomer, A. W.: Profile for a Low Dam Determined by Models, *Civil Eng.*, pp. 623-626, October, 1942.

10

Stilling-basin Appurtenances

Appurtenances such as chute blocks, baffle piers, and end sills are often installed to help increase the performance of a stilling basin. In addition, they are helpful in stabilizing the flow, increasing the turbulence, and distributing the velocities more evenly throughout the basin. In some cases a reduction in the required tailwater depth and length of the basin may be possible by the addition of appurtenances to the basin. Figure 10-1 shows the general location of the appurtenances in a stilling basin.

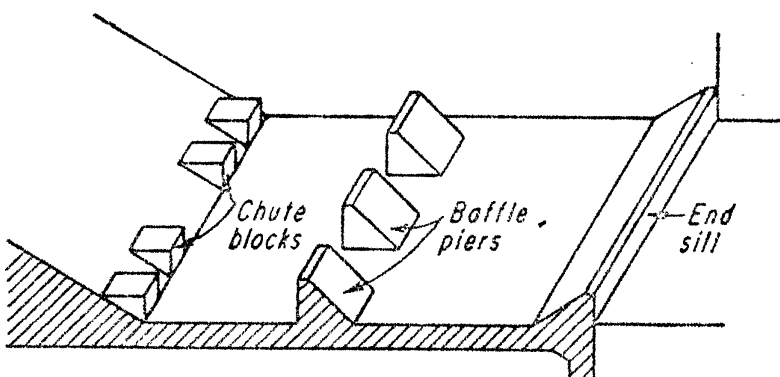


FIG. 10-1. Location of appurtenances in stilling basin.

10-1. Chute Blocks. Chute blocks are installed at the entrance of the stilling basin to increase the effective depth of the entering stream, to break up the flow into a number of jets, and to help create the turbulence required for energy dissipation. The blocks also tend to lift the jet off the floor and result in a shorter basin length than would be possible without them. The blocks should be placed parallel to the direction of flow and symmetrically about the center line of the basin. In the case of divergent side walls, blocks that are fan-shaped in plan may be utilized. Chute blocks may become objectionable when streams carry a considerable amount of debris, ice, or sediment, which may damage the blocks both by impact and abrasion.

Table 10-1 lists chute-block dimensions and relationships for 31 existing stilling basins.

TABLE 10-1.⁵ CHUTE-BLOCK DIMENSIONS OF EXISTING STILLING BASINS

Structure	Type	h_1	h_1/y_1	w_1	w_1/h_1	w_1/s_1
Rye Patch.....	Solid	4.0	1.18			
Unity.....	Teeth	3.5	1.21	1.83	0.52	1.0
Alcova.....	Solid	4.3	1.15			
Shadow Mountain.....	T	3.0	1.16	4.0	1.33	1.78
Boysen (final).....	T	4.0	1.13	4.25	1.31	1.75
Boysen (preliminary).....	T	6.0	1.05	7.5	1.25	1.8
Scofield	T	3.5	1.38	3.5	1.0	1.91
Boca.....	T	4.0	2.72	3.0	0.75	1.0
Fresno	T	4.0	1.04	4.0	1.0	1.0
Caballo.....	T	4.5	1.07	4.0	0.89	1.0
Moon Lake.....	T	2.6	1.44	1.875	0.72	1.0
Deer Creek.....	T	3.0	1.60	3.0	1.0	1.0
Alamogordo.....	T	8.0	1.51	3.5	0.44	1.0
Enders.....	T	6.0	0.95	5.0	0.83	1.0
Medicine Creek.....	T	6.75	1.07	6.0	0.89	1.0
Cedar Bluff.....	T	7.0	1.49	6.0	0.86	1.0
Falcon	T	8.0	0.91	10.0	1.25	1.0
Trenton	T	5.0	0.81	5.0	1.0	1.0
Cachuma	T	5.5	1.19	5.08	0.92	1.0
Tiber.....	T	7.0	2.51	5.0	0.71	1.0
Imperial Spillway.....	T	2.33	0.90	2.49	1.02	1.03
Imperial Sluiceway.....	T	3.33	1.33	3.0	0.90	0.95
Grassy Lake.....	T	1.0	1.05	1.67	1.67	1.0
Box Butte.....	T	3.3	2.06	3.0	0.91	1.0
Siphon Drop Turnout...	T	2.25	1.50	2.25	1.0	1.0
Pilot Knob Wasteway...	T	2.5	1.56	2.5	1.0	1.0
Big Sandy No. 2.....	T	1.75	0.97	1.75	1.0	1.0
Agency Valley.....	Solid	2.5	1.12	3.25	1.30	1.0
Davis.....	T	2.5	0.83			
Bonny.....	T	14.3	1.96	13.0	0.91	1.86
Cle Elum.....	T	7.0	1.94	5.0	0.72	1.0
Maximum.....	2.72	1.67	1.91
Minimum.....	0.81	0.44	0.95
Average.....	1.35	0.97	1.15

NOTE: h_1 = height of chute block, ft; w_1 = width of chute block, ft; s_1 = spacing between chute blocks, ft.

10-2. Baffle Piers. Baffle piers are installed in the stilling basin principally to stabilize the formation of the jump and increase the turbulence, thereby assisting in the dissipation of energy. For low flows, baffle piers help to compensate for a slight deficiency of tailwater, and for high flows, they help to deflect the flow away from the riverbed. The

employment of baffles will be helpful in reducing the tailwater depth required and also in shortening the basin length.

An analysis can be made of the hydraulic jump formed in a rectangular channel containing baffles. Referring to Fig. 10-2, the momentum equa-

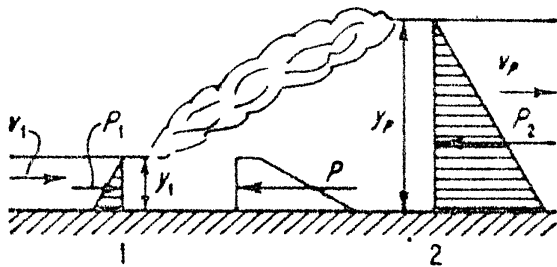


FIG. 10-2. Force exerted by baffle piers.

tion between section 1 and 2 becomes

$$\frac{\gamma y_1^2}{2} - \frac{\gamma y_p^2}{2} - \frac{P}{b} = \frac{\gamma}{g} q(v_p - v_1) \quad (10-1)$$

where \$y_p\$ = depth resulting at section 2 with baffle piers in place

\$P\$ = force exerted by piers

\$b\$ = width of channel

Since, by the equation of continuity,

$$q = v_1 y_1 = v_p y_p$$

the velocities in Eq. (10-1) can now be eliminated, and by rearranging terms, we can solve for \$P\$.

$$\frac{P}{\gamma b} = \frac{1}{2} (y_1^2 - y_p^2) - \frac{q^2}{g} \left(\frac{1}{y_p} - \frac{1}{y_1} \right) \quad (10-2)$$

If the pier force \$P = 0\$, then \$y_p = y_2\$, and the depth of the free jump without baffles is obtained.

$$\frac{1}{2} (y_1^2 - y_2^2) = \frac{q^2}{g} \left(\frac{1}{y_2} - \frac{1}{y_1} \right) \quad (10-3)$$

Subtracting Eq. (10-3) from (10-2),

$$\frac{P}{\gamma b} = \frac{q^2}{g} \left(\frac{1}{y_2} - \frac{1}{y_p} \right) + \frac{1}{2} (y_2^2 - y_p^2) \quad (10-4)$$

Dividing both sides by \$y_2^2/2\$ and rearranging the terms, we have

$$\frac{P/b}{\gamma y_2^2/2} = \frac{2q^2}{gy_2^3} \left(1 - \frac{y_2}{y_p} \right) + 1 - \frac{y_p^2}{y_2^2} \quad (10-5)$$

but

$$\frac{2q^2}{gy_2^3} = \frac{16\lambda_1}{(\sqrt[3]{8\lambda_1 + 1} - 1)^3} \quad (10-6)$$

Equation (10-5) may now be written

$$\frac{P/b}{\gamma y_2^2/2} = 1 - \left(\frac{y_p}{y_2} \right)^2 - \left(\frac{y_2}{y_p} - 1 \right) \frac{16\lambda_1}{(\sqrt{8\lambda_1 + 1} - 1)^3} \quad (10-7)$$

Equation (10-7) may now be utilized to find the permissible reduction in downstream depth due to a given force exerted by the baffle piers. The force P can be evaluated by means of the drag equation

$$P = C_b \rho \frac{v^2}{2} A \quad (10-8)$$

where C_b = drag coefficient of the baffles

v = velocity

ρ = mass density

A = area of the blocks

Some recourse to the laboratory must be made to evaluate C_b for various pier shapes and spacings.

Harleman⁷ indicates that the maximum force exerted by the baffle piers is approximately 20 per cent of the pressure force due to the downstream depth.

In some cases, baffles should be used in the stilling basin even if not required to form a good hydraulic jump. For example, in the stilling basin below the Sardis Dam outlet works, baffle piers were not required to form a good hydraulic jump. Under initial operating conditions, however, the gates were opened much faster than the tailwater could build up, so that there was a deficiency of tailwater for about 4 or 5 hours. The baffle piers prevented excessive erosion of the exit area during this period. Baffle piers also help to ensure good jump action for unbalanced spillway-gate operation or submerged conditions occurring at discharges greater than those for which the stilling basin was designed.

There are many types and shapes of baffles that have been used which have served their intended purpose. Because of the many variables, no one solution may be applicable for all conditions. The various types of baffles employed in existing structures are illustrated in Fig. 10-3a to g.

Recent experiments indicate that triangular blocks are satisfactory for most stilling basins. When two rows of baffles are used, the blocks of the second row should be staggered in such a manner that they face the spaces between the blocks of the first row. The portion of the flow striking the upstream face of the baffles is deflected upward through the otherwise horizontal flows just passing over the baffles. Also, the portions of flow passing through the spaces in the front row are immediately deflected upward when they encounter the front faces of the second row of baffles. Eddy currents produced by this impact action absorb a considerable amount of energy.

HYDRAULIC ENERGY DISSIPATORS

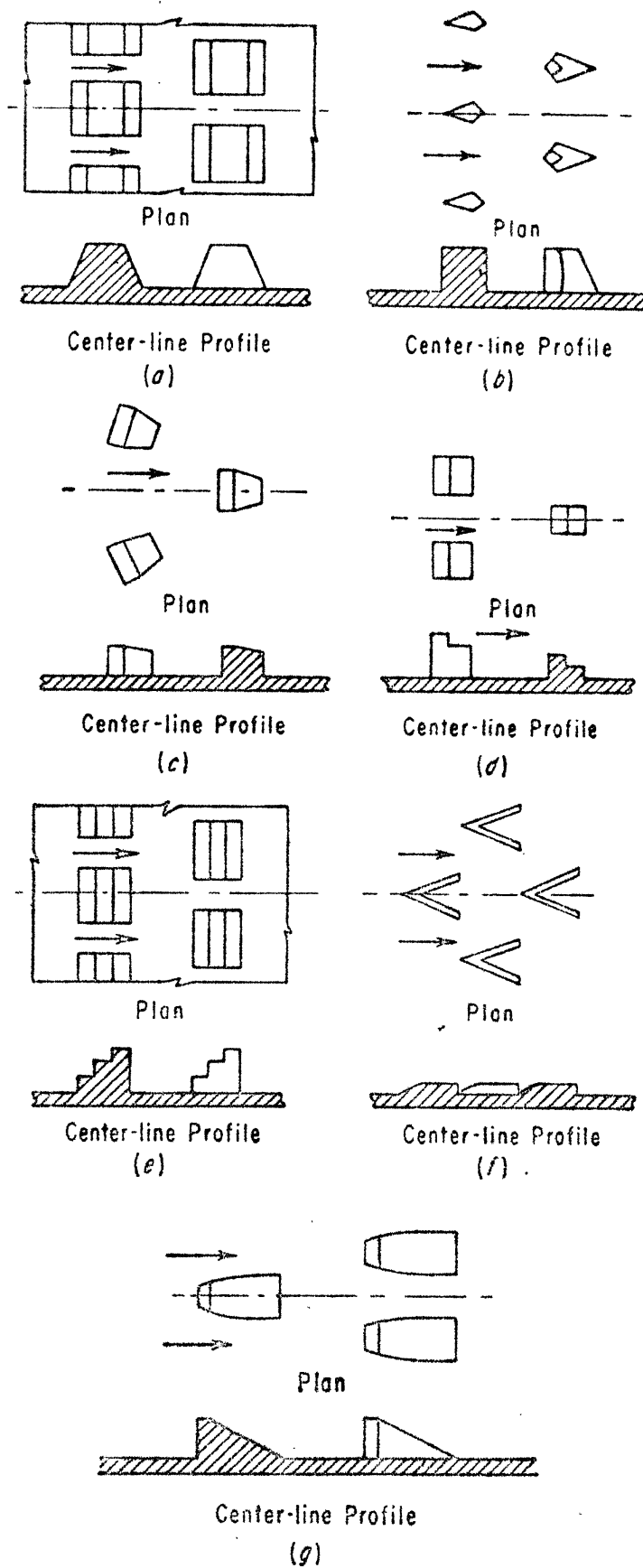


FIG. 10-3. Types of baffles: (a) Bonneville Dam; (b) Pit River No. 3 Dam; (c) Gatun Dam; (d) Texarkana Dam; (e) Mississippi River Dam No. 8; (f) Khanki Weir, India; (g) Stevenson Dam.

As with the various types of baffles, there are many arrangements that can be made with the floor blocks. It should be remembered that sufficient water will not pass between the blocks if they occupy too much of the stilling-basin-floor width. When the blocks occupy too much of the floor space, they tend to act more like a sill than individual blocks. Tests made by Blaisdell² indicate that the floor blocks should occupy between 40 and 55 per cent of the stilling-basin width. The aggregate width of all floor blocks should be held within these limits even if it is necessary to reduce the width of the floor blocks to do so. The most favorable conditions result when the baffles are placed perpendicular to the oncoming flow.

In addition to the features previously mentioned, the baffle piers should be easy to construct, maintain, and, if possible, should be nonclogging and self cleansing. In some cases, the blocks are subject to cavitation and abrasion when the velocity is high or when heavy sediment, debris, or ice is present in the flow. Cavitation is not likely to occur when the maximum basin velocities are less than 50 fps.

Cavitation can be defined as the successive formation and collapse of vapor pockets in low-pressure areas associated with the high-velocity flow which frequently causes severe damage to concrete or steel surfaces. The roughening or formation of pockets on surfaces due to cavitation is commonly called "pitting." Where cavitation pressures are present, conditions are most severe on the sides of the baffles, although the top and apron floor are also susceptible to damage.

There are three known cases where baffles have been damaged by cavitation and abrasion. At the Conchas Dam,³ located on the Canadian River in northern New Mexico, baffle piers adjacent to the side walls were damaged on the downstream face, where eddy action caused gravel and debris in the flow to grind away concrete to a depth of 12 in. At the Norfolk Dam,³ the blocks were damaged on the upstream face by gravel carried by the flow and by the impact of the high-velocity jets. In both cases, the damage was not dangerous and was easy to repair. Figure 10-4 is a photograph of the Norfolk Dam stepped baffles and end sill.

The third case deals with the erosion of the baffle piers of the Bonneville Dam¹ by cavitation. The maximum erosion of the baffles occurred on the sides, up to 22 in. in depth. Generally, damage to the upstream row of baffles was much more severe and extensive than to the downstream row. In repairing the baffles, model tests indicated that it would be desirable to convert the second row of baffles into a solid end sill. To prevent cavitation, blocks should be placed far enough downstream, where sufficient submergence exists under the tailwater, to avoid impact by the high-velocity flows. A photograph of the damaged baffle piers is shown in Fig. 10-5. Figure 10-6 shows the form of baffles recommended

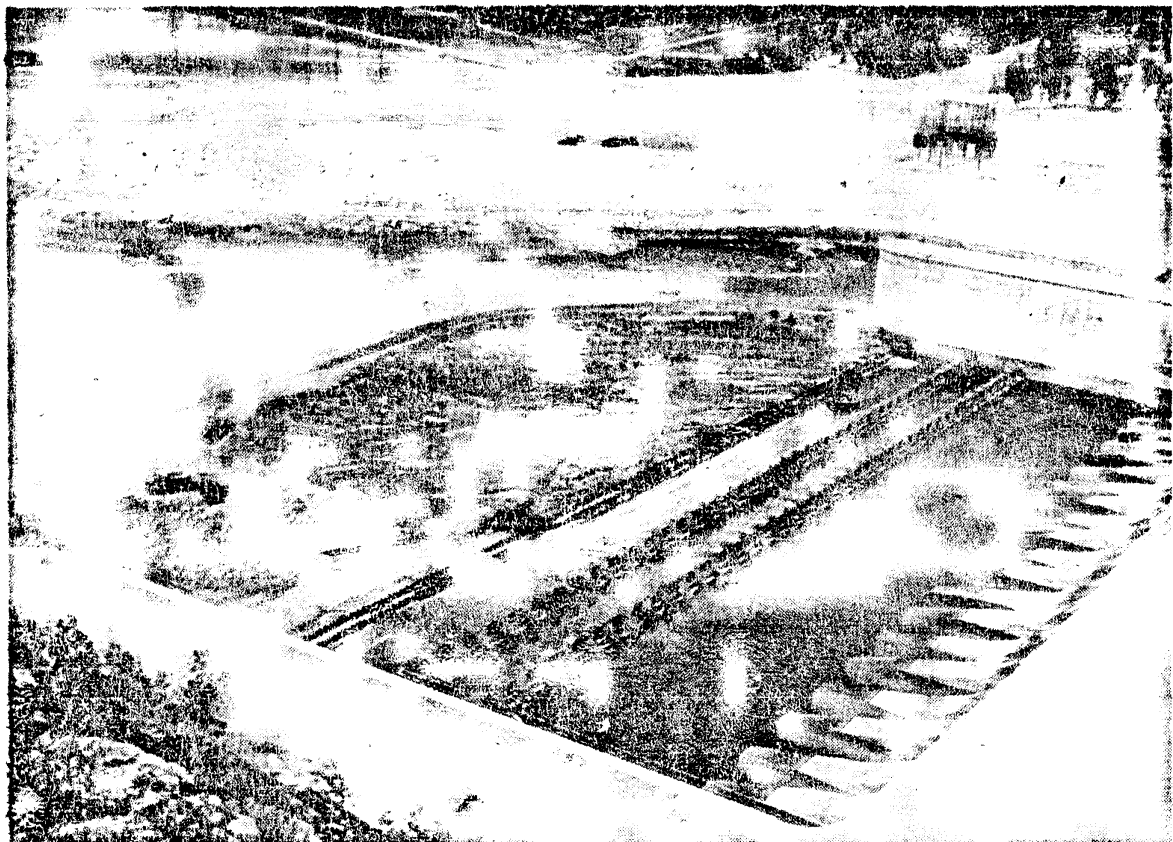


FIG. 10-4. Stilling basin of the Norfolk Dam, Ark., showing two rows of stepped baffles and an end sill. (Courtesy of Corps of Engineers, Little Rock District.)



FIG. 10-5. Damaged baffle piers in the stilling basin below the Bonneville Dam, Columbia River. (Courtesy of Corps of Engineers, Walla Walla District.).

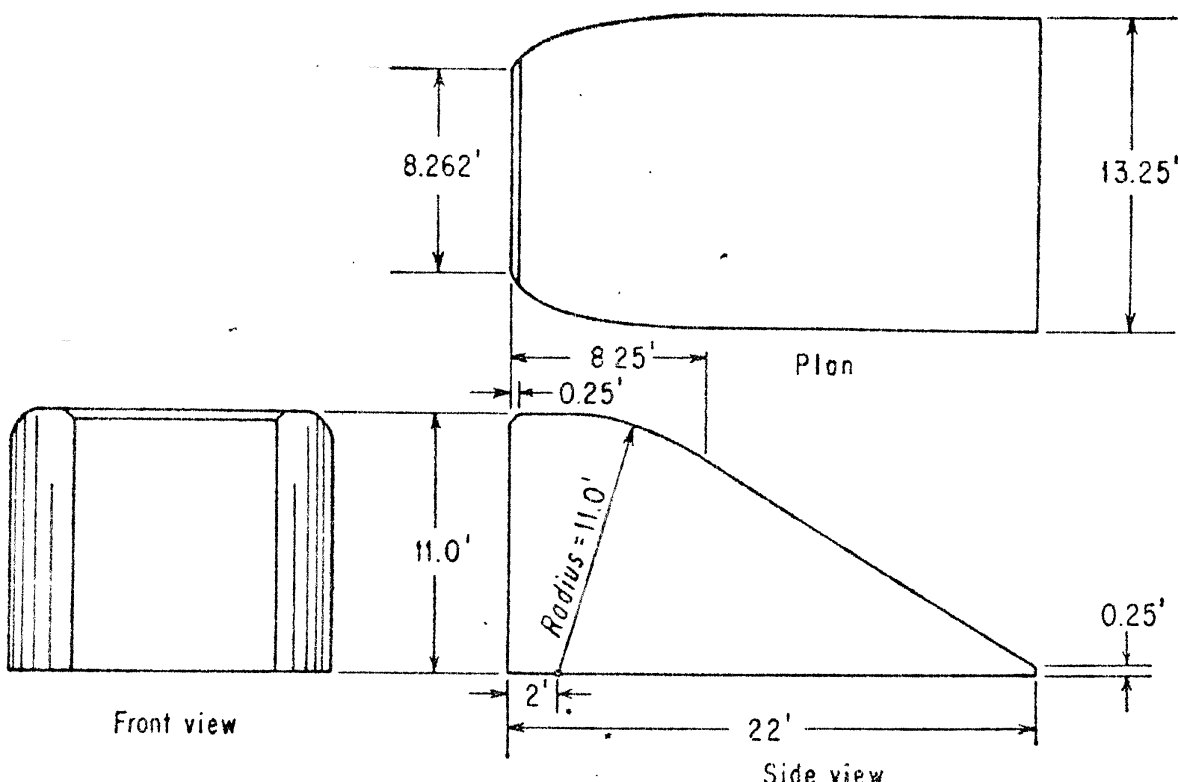


FIG. 10-6. Chief Joseph Dam—dimensions of streamlined baffles.

for the Chief Joseph Dam⁶ by the Waterways Experiment Station of the Corps of Engineers. Triangular-shaped blocks of the McNary Dam are shown in Fig. 10-7.

Although instantaneous cavitation pressures were not completely eliminated by curving the baffle sides, the duration of erosion was reduced to an extent considered safe on the basis of previous experience. Where high entrance velocities occur, only one row of baffles should be used to minimize cavitation.

In many structures there is evidence that logs and debris take their toll in damage to baffle piers. This damage can be somewhat eliminated by providing the piers with steel nose plates. Baffle piers of the Pit River Dams⁸ were provided with $12 \times 12 \times \frac{1}{2}$ in. steel nose plates to protect the piers from floating logs and debris. Figure 10-8 is a photograph of the Pit River Dam No. 3 baffles.

Laboratory investigations at the Massachusetts Institute of Technology⁷ hydrodynamics laboratory indicate that appreciable depth reductions due to baffle piers are possible only if the toe of the hydraulic jump is within 10 to 20 block heights of the piers. Under maximum discharge conditions, the piers cannot be placed close enough to the toe of the hydraulic jump to provide any useful depth reduction without making the piers liable to serious cavitation damage. It was concluded that the depth reductions due to the piers be considered only as insurance against dangerous displacements of the hydraulic jump into the basin through

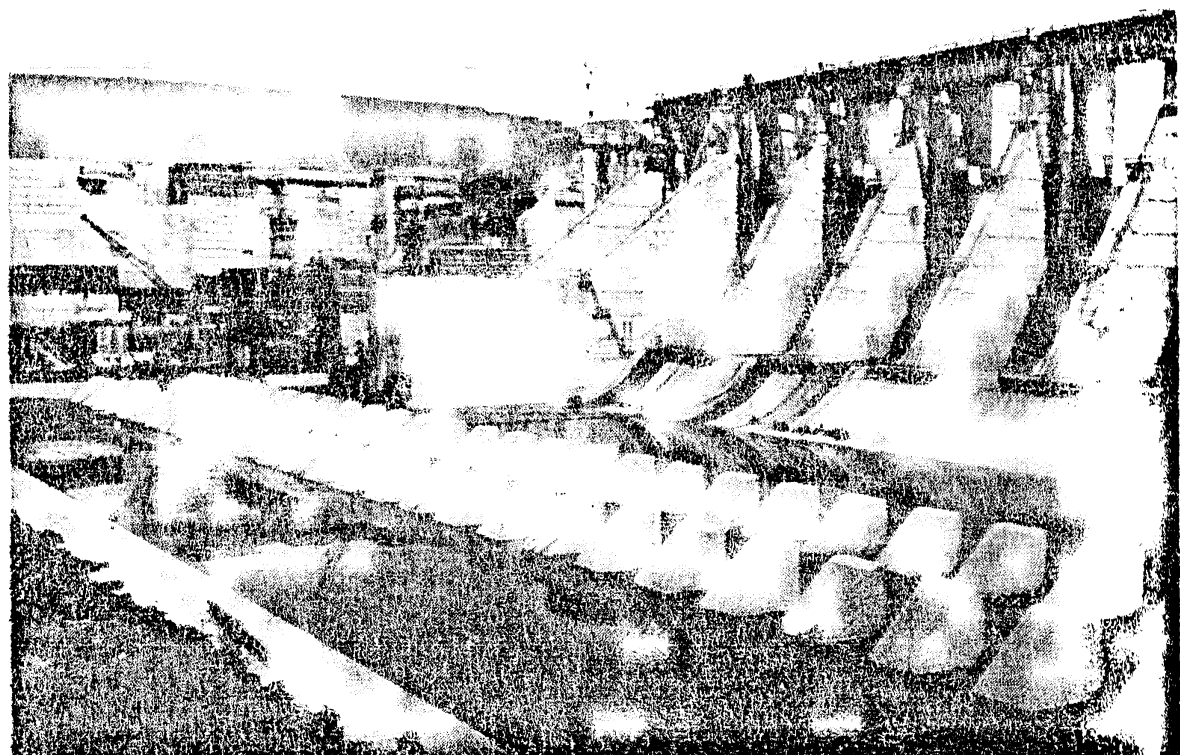


FIG. 10-7. Two rows of staggered triangular-shaped baffles of the McNary Dam stilling basin. (*Courtesy of Corps of Engineers, Walla Walla District.*)



FIG. 10-8. Water impinging upon baffles below Pit River Dam No. 3, Pit River, Calif. (*Courtesy of Pacific Gas and Electric Company.*)

fluctuations or changes in the initial Froude number or the tailwater depth.

Weide made a special study of the use of floor blocks and their effect on the control of the jump. He found that gravitational, inertial, and viscous forces affect the flow conditions and that the best performance results when there is an optimum balance between these forces. A block coefficient C_b dependent upon these forces can be determined by using Eq. (10-9).

$$C_b = \left(\frac{y_2}{y_1} \right)^2 + \frac{y_2}{y_1} - 2\lambda_1 \quad (10-9)$$

Also, Weide suggests that when baffles are used, the conjugate depth can be found by employing Eq. (10-10).

$$y_2 = \frac{y_1}{2} (\sqrt{1 + 4C_b + 8\lambda_1} - 1) \quad (10-10)$$

10-3. End Sills. An end sill is a vertical, stepped, sloped, or dentated wall constructed at the downstream end of the stilling basin. The purpose of the end sill is to lift the flow off the riverbed and create a back current, which causes bed material to be transported and heaped up against the back face of the sill. The sill also stabilizes the flow, deflects the current away from the river bottom, and may be of help in reducing the tailwater depth. Laboratory tests indicate that the sill greatly increases the efficiency of the basin.

There are seven types of end sills that have been employed in the design of stilling basins: rectangular, trapezoidal, triangular, Hornsby, Smetana, Schoklitsch, and Rehbock dentated sills. They are illustrated in Fig. 10-9a to g.

The Rehbock dentated sill has been proved by model studies to be the most efficient type of end sill. The principle of its action is that water is deflected in an upward direction by the vertical faces of the teeth, thereby producing a long, flat ground roller immediately below the sill. This movement is counteracted by the lower threads of fan-shaped jets, which are pressed through the gaps between the teeth in order to dissipate the energy without appreciable scouring of the unprotected riverbed. The upper threads of the jet repel the ground roller and prevent the main stream, deflected upward by the teeth, from dropping to the bottom, which it would normally do. The ground roller then transports bed material upstream and deposits it at the end of the basin. There is a simultaneous decrease in the bottom velocities, which leads to a normal distribution of velocities in the discharging stream. This device was invented by Professor Rehbock, who called it a "zahnschwelle," or notched sill. In place of the indented crest of the Rehbock end sill,

modern technique prefers a solid end sill with an upstream sloping face of 2 horizontal on 1 vertical, with a vertical downstream face. Trapezoidal sills have been used in some cases, since they are subject to less wear by material transported over the dam than are triangular and rectangular sills. Figure 10-10a to f illustrates several types of end sills used for existing structures.

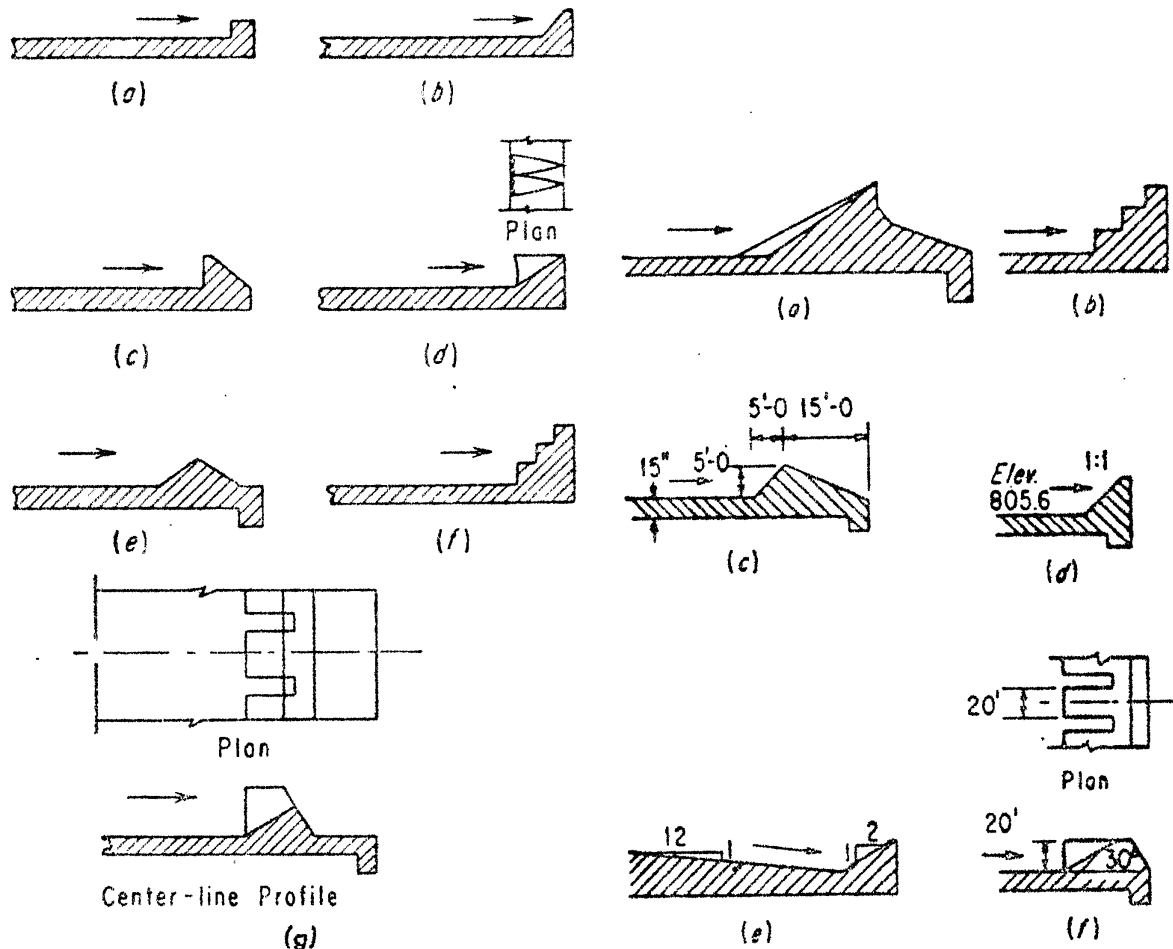


FIG. 10-9. Types of end-sill profiles: (a) rectangular, (b) triangular, (c) trapezoidal, (d) Hornsby, (e) Schölkitsch, (f) Smetana, (g) Rehbock dentated end sill.

FIG. 10-10. Constructed end-sill profiles: (a) Bull Run Dam, (b) Mississippi River Dam No. 8, (c) Pine View Dam, (d) Norris Dam, (e) Shasta Dam, (f) Hirakud Dam.

For the Hirakud Dam, illustrated by Fig. 10-10f, model studies indicated that a dentated end sill was more satisfactory than a solid end sill in directing the flow into the lower channel at a flatter angle, in spreading out the flow over the sill, and in reducing the violence of the ground roller.

The most important dimension of the sill is its height. If the sill is not high enough, the flow may simply pass over the sill as a standing wave or swell and be of little benefit. On the other hand, if the sill is too high, a violent roller will be set into motion, which will pick up the material and draw it into the basin. The sill should act only as a deflector

TABLE 10-2.⁵ END-SILL DIMENSIONS OF EXISTING STILLING BASINS

Structure	Type	x/L_b	h_2	h_2/y_2	w_2/h_2	w_2/s_2
Rye Patch.....	Solid	1.0	2.0	0.09	—	—
Unity.....	Teeth	0.93	5.5	0.22	0.39	1.0
Alcova.....	T	1.0	10.0	0.22	0.50	1.0
Shadow Mountain.....	T	1.0	3.5	0.17	1.14	1.78
Boysen (final).....	T	0.68	8.75	0.23	0.60	1.75
Boysen (preliminary).....	T	1.0	8.0	0.16	0.94	1.8
Scofield.....	T	1.0	4.0	0.17	0.88	1.91
Boca.....	T	1.0	4.0	0.19	0.75	1.0
Fresno.....	T	1.0	6.0	0.19	0.67	1.0
Bull Lake.....	T	1.0	4.0	0.22	1.25	1.0
Caballo.....	T	0.90	6.5	0.19	0.62	1.0
Moon Lake.....	T	0.85	5.0	0.21	0.75	1.0
Deer Creek.....	T	1.0	5.0	0.18	0.60	1.0
Alamogordo.....	T	1.0	9.0	0.17	0.44	1.0
Enders.....	T	1.0	12.0	0.26	0.42	1.0
Medicine Creek.....	T	1.0	8.0	0.17	0.75	1.0
Cedar Bluff.....	T	1.0	9.0	0.19	0.67	1.0
Falcon.....	T	1.0	12.0	0.20	0.83	1.0
Trenton.....	T	1.0	9.0	0.19	0.56	1.0
Cachuma.....	T	1.0	12.0	0.21	0.42	1.0
Tiber.....	T	1.0	8.0	0.21	0.62	1.0
Imperial Spillway.....	T	1.0	3.75	0.20	1.01	1.0
Imperial Sluiceway.....	T	0.65	5.0	0.36	1.13	1.1
Grassy Lake.....	T	1.0	2.0	0.14	0.66	1.0
Box Butte.....	T	1.0	3.0	0.18	1.0	1.0
Siphon Turnout.....	T	1.0	3.25	0.29	0.69	1.0
Pilot Knob Wasteway.....	T	1.0	5.0	0.28	1.0	1.0
AA Canal Drop 1.....	Solid	1.0	1.0	0.08	—	—
Wasteway No. 2.....	Solid	1.0	2.0	0.12	—	—
Big Sandy No. 2.....	T	1.0	3.0	0.12	1.08	1.0
Cherry Creek.....	Solid	1.0	5.0	0.12	—	—
Pine View.....	T	1.0	5.0	0.19	1.20	1.0
Agency Valley.....	T	0.91	10.0	0.37	0.33	1.0
Davis.....	T	1.0	14.3	0.23	0.91	1.86
Bonny.....	T	1.0	8.0	0.21	0.62	1.0
Cle Elum.....	T	1.0	10.0	0.33	1.0	1.0
Maximum.....	1.0	0.37	1.25	1.91
Minimum.....	0.65	0.08	0.33	1.00
Average.....	0.97	0.20	0.76	1.13

NOTE: x = distance from downstream edge of chute blocks to end sill, ft; L_b = length of stilling basin, ft; h_2 = height of end sill, ft; w_2 = width of sill dentates, ft; s_2 = spacing between dentates, ft.

and not as an impact device. Weide⁹ states that the shape of the sill has little effect on the formation of the jump. To have the same degree of deflection for all depths of water at the end of the basin, the height of the end sill should vary with y_2 . Recommended dimensions of the end sill will be given in subsequent chapters. Table 10-2 lists the dimensions and relationships of end sills of 36 existing stilling basins.

A Rehbock sill was employed for the stilling basin of the Pine View Dam,⁴ located on the Ogden River near Ogden, Utah. The Rehbock sill was used because of the possibility of a material lowering of the riverbed below the spillway and because of its simple construction.

REFERENCES

1. Basgen, D. H.: Bonneville Dam Spillway Erosion Repaired. *Eng. News-Record*, pp. 36-38, Apr. 21, 1955.
2. Blaisdell, F. W.: Development and Hydraulic Design of St. Anthony Falls Stilling Basin, *Proc. ASCE*, pp. 123-159, February, 1947.
3. Brown, F. R.: Hydraulic Models as an Aid to the Development of Design Criteria, *Waterways Exp. Sta. Corps Engrs. Bull.* 37, 1951.
4. Borland, W. M., and J. B. Drisko: Hydraulic Model Experiments for the Design of the Pine View Dam Spillway, *Bur. Reclamation Tech. Memorandum* 393, August, 1934.
5. Bureau of Reclamation, Progress Report II, Research Study on Stilling Basins, Energy Dissipators, and Associated Appurtenances, *Hydraulic Lab. Rep. Hyd.-399*, Denver, Colo., June 1, 1955.
6. Corps of Engineers, Hydraulic Design: Reservoir Outlet Structures. *Eng. Manual Civil Works Construction*, part CXVI, chap. 2, February, 1953.
7. Harleman, D. R.: Effect of Baffle Piers on Stilling Basin Performance, *J. Boston Soc. Civil Engrs.*, April, 1955.
8. Monroe, R. A., and I. C. Steele: Baffle Pier Experiments on Models of Pit River Dams, *Trans. ASCE*, p. 527, 1929.
9. Weide, L.: "The Effect of the Size and the Spacing of Floor Blocks in the Control of the Hydraulic Jump," unpublished M.S. thesis, Colorado A. & M., 1951.

Stilling Basins for Small Outlet Works and Low and Medium-high Spillways

The design procedure recommended in this chapter is for stilling basins that have entering velocities not exceeding 50 fps. It is not the intention of this chapter to give the impression that hydraulic laboratory tests are unnecessary in determining the best form of scour protection below dams. Such tests should be made of all important structures and will usually pay for themselves in the improvements they bring to the design. The purpose of this chapter is only to indicate a solution that has proven to yield satisfactory results for many existing structures. A typical structure of this class is the Nimrod Dam stilling basin, shown in Fig. 11-1.

11-1. Design Procedure. The most effective way to shorten the length of a stilling basin is by the addition of appurtenances such as chute blocks, baffle piers, and an end sill. It is the purpose of this section to present a design procedure with respect to the height, width, spacing, and position of the appurtenances in the stilling basin. The following steps are recommended for the design of this type of stilling basin.

Step 1. Jump-height and Tailwater-rating Curves. It is assumed that for each structure, the design discharge and width of basin have already been determined. The first step will be to develop a jump-height curve and find its relationship to the natural tailwater curve. After this relationship has been determined, the next step will be to find the elevation of the stilling-basin apron. The apron-floor elevation can be determined by applying the procedure as outlined in Chap. 9.

With the addition of appurtenances in the stilling basin, laboratory tests have shown that a satisfactory hydraulic jump will occur if the tailwater depth is made equal to $0.9y_2$, thereby providing a reduction in the required tailwater depth. In cases where retrogression will occur in the downstream channel after the dam is constructed, estimates should be made of the ultimate tailwater curve. The ultimate tailwater curve

should be used in designing the stilling basin. No particular advantage is attained by using a depth greater than the tailwater depth, since little improvement in the basin will be obtained. A condition of excess tailwater does not justify the shortening of the basin length.

Step 2. Stilling-basin Length. With the addition of appurtenances in the stilling basin, it will be possible to reduce the length of the basin to $4.5(y_2 - y_1)$. The required length of the basin is to some extent dependent upon the scour resistance of the downstream channel.

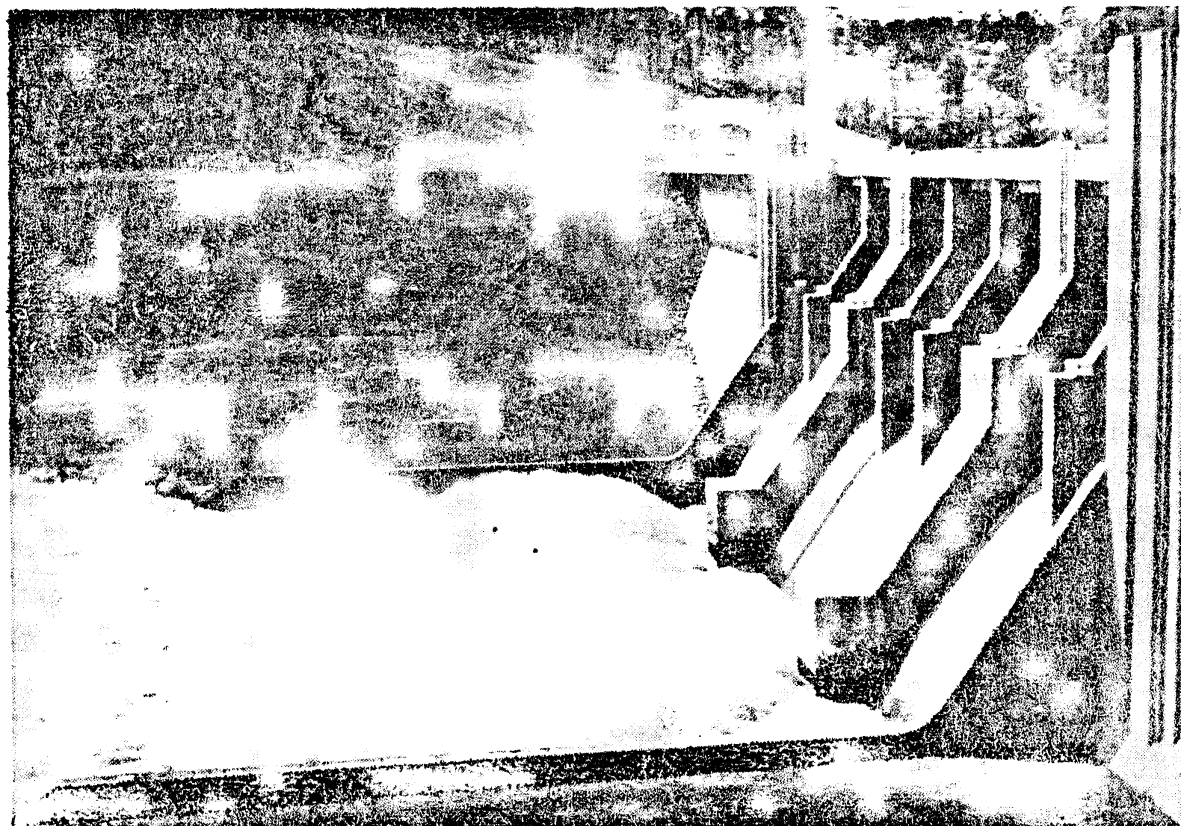


FIG. 11-1. Small hydraulic-jump-type stilling basin of Nimrod Dam, Fourche la Fave River, Arkansas. Approximate discharge: 19,000 cfs. (Courtesy of Corps of Engineers, Little Rock District.)

Step 3. Chute Blocks. Chute blocks are placed at the entrance of the stilling basin to stabilize the formation of the hydraulic jump. It is recommended that the height of the chute blocks be made equal to y_1 , and the width and spacing of the blocks be made equal to $\frac{3}{4}y_1$.

Step 4. Baffle Piers. The principal function of baffles is to increase the turbulence in the basin and help stabilize the formation of the hydraulic jump. When the entering velocities exceed 50 fps, baffle piers are not recommended, since it is possible that they may be damaged by cavitation. To minimize the tendencies of cavitation, the blocks, when used, should be placed far enough downstream, where sufficient submergence exists under the tailwater. It is important that the upstream face of the

baffle piers be placed at a minimum distance of $0.9y_2$ from the downstream face of the chute blocks.

The height of the baffle is the most important dimension. If the baffles are too high, they will produce a cascade, and if they are too low, a rough water surface will result. The upstream faces of the blocks should be in a vertical plane; with the baffle height made equal to $2.5y_1$. The width and spacing of the blocks should both be made equal to $2.0y_1$, with the downstream face having a slope of 1 on 1. Under no circumstances should the blocks be placed with less than a spacing equal to y_1 between the block and the side wall.

To minimize cavitation, the corners of the blocks should be rounded. It is advisable to place reinforcing steel at least 6 in. from the block surface, when possible, to avoid spalling of the concrete.

In some instances, model studies may indicate the desirability of installing two rows of baffles. If two rows of baffles are used, they should be staggered so that the second row intercepts and breaks up the flow through the spaces of the first row. Blaisdell¹ recommends that the floor blocks should occupy between 40 and 55 per cent of the stilling-basin width. When appurtenances are added, the basin length can be made equal to $4.5(y_2 - y_1)$.

Step 5. End Sills. End sills are used primarily for scour control. A solid end sill is recommended, with a height of $0.20y_2$ and top width of $0.04y_2$.

Step 6. Recommended Dimensions for Stilling-basin Appurtenances. The preceding rules can be used in proportioning the dimensions of chute blocks, baffles, and an end sill. If the proportioning is changed, model studies are advisable. Limitation of this design procedure occurs when the discharge exceeds 200 cfs per foot of basin width. Figure 11-2 shows

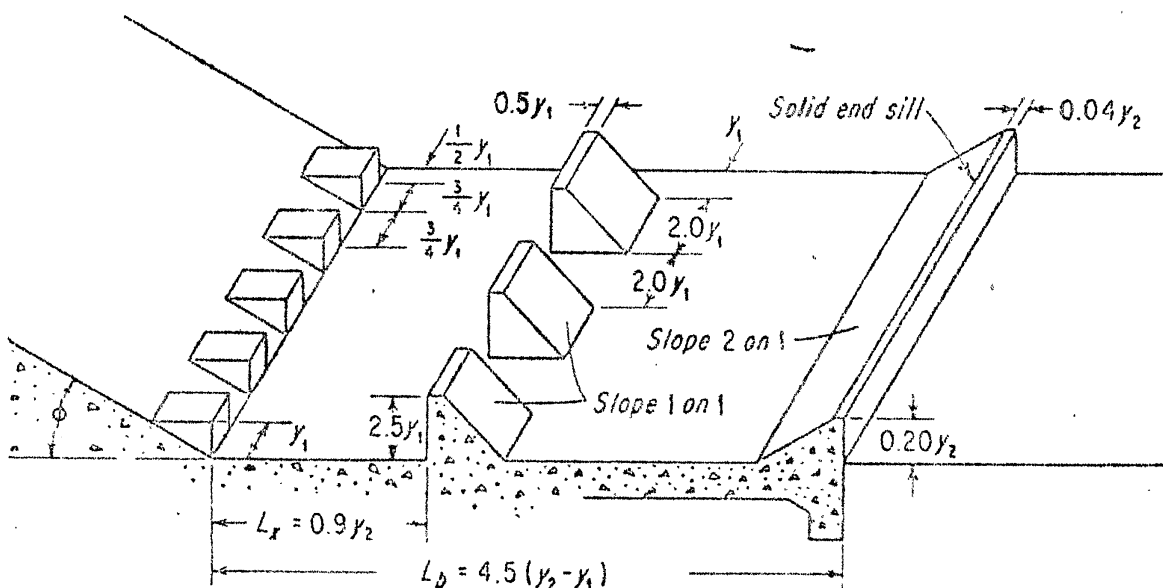


FIG. 11-2. Recommended dimensions for stilling-basin appurtenances.

the recommended dimensions and locations of chute blocks, baffles, and an end sill in the stilling basin.

An example problem will be given to show how the aforementioned procedure may be applied. The problem will be to determine the necessary dimensions of the chute blocks, baffles, and end sill for a stilling basin of a small spillway with the following data known:

1. Design discharge = 10,000 cfs
2. Spillway width = 100 ft
3. $q = 100$ cfs per foot of spillway width
4. Drop in water surface = 25 ft

Step 1. Jump-height and Tailwater-rating Curves. Assuming no losses due to friction, the velocity entering the hydraulic jump will be equal to

$$\begin{aligned} v_1 &= \sqrt{2gH} \\ &= \sqrt{2g(25)} \\ &= 40.1 \text{ fps} \end{aligned}$$

For a rectangular channel,

$$\begin{aligned} y_1 &= \frac{g}{v_1} \\ &= \frac{100}{40.1} \\ &= 2.5 \text{ ft} \end{aligned}$$

and the kinetic-flow factor will be equal to

$$\begin{aligned} \lambda_1 &= \frac{v_1^2}{gy_1} \\ &= \frac{40.1^2}{32.2(2.5)} \\ &= 20 \end{aligned}$$

Then y_2 can be determined.

$$\begin{aligned} y_2 &= \frac{y_1}{2} (\sqrt{1 + 8\lambda_1} - 1) \\ &= \frac{2.5}{2} [\sqrt{1 + (8)(20)} - 1] \\ &= 14.8 \text{ ft} \end{aligned}$$

The required tailwater depth should be made equal to $0.9y_2$.

$$\text{Required tailwater} = 0.9(14.8) = 13.3 \text{ ft}$$

Figure 11-3 indicates the relationship between the tailwater-rating curve and the jump-height curve. From these relationships, we observe

that there is a deficiency of tailwater and that the elevation of the stilling-basin apron will have to be lowered to compensate for this deficiency.

For the design discharge, Fig. 11-3 shows that the apron will have to be lowered by 2 ft in order for the jump-height and tailwater-rating curves to coincide at the design discharge. However, because of the reduction in tailwater provided by the addition of appurtenances in the basin, the apron floor will have to be lowered only by 0.5 ft, as shown in Fig. 11-4.

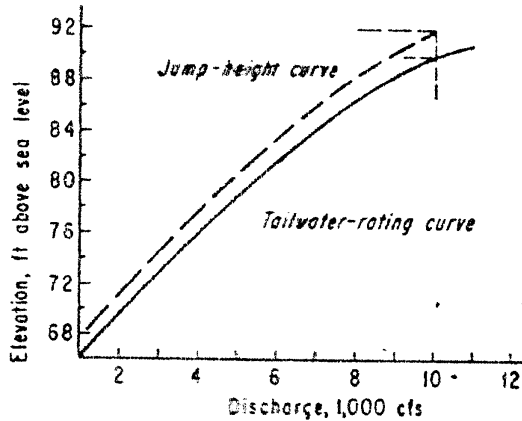


FIG. 11-3. Jump-height and tailwater-rating curves.

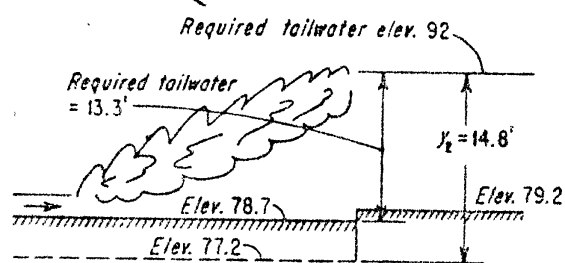


FIG. 11-4. Elevation of stilling-basin apron.

Step 2. Length of Stilling Basin

$$\begin{aligned} L_b &= 4.5(y_2 - y_1) \\ &= 4.5(14.8 - 2.5) \\ &= 55.3 \text{ ft} \end{aligned}$$

L_b , the length of the stilling basin, is defined as being the distance from the downstream edge of the chute blocks to the downstream edge of the end sill.

Step 3. Chute Blocks

Height: $y_1 = 2.5$ ft

Width and spacing: $\frac{3}{4}y_1 = 1.88$ ft

Step 4. Baffles

Height: $2.5y_1 = 6.25$ ft

Width and spacing: $2.0y_1 = 5.0$ ft

Ten baffle piers will be required, each having a width and spacing of 5.0 ft and a distance of 2.5 ft between the end baffles and the side walls.

The blocks will occupy 50 per cent of the stilling-basin width and will be located at a distance equal to $0.9y_2$ from the downstream face of the chute blocks.

$$\begin{aligned} L_x &= 0.9y_2 = 0.9(14.8) \\ &= 13.3 \text{ ft} \end{aligned}$$

Step 5. End Sill

Height: $0.20y_2 = 2.96$ ft

Horizontal top width: $0.04y_2 = 0.59$ ft

The end sill should have a 2 on 1 upstream slope and vertical downstream face.

Step 6. Recommended Dimensions for Appurtenances in the Example Problem. The recommended dimensions for the example problem are shown in Fig. 11-5. It should be noted that this procedure is only a general solution, based upon the design of existing stilling basins and may not be applicable for all cases.

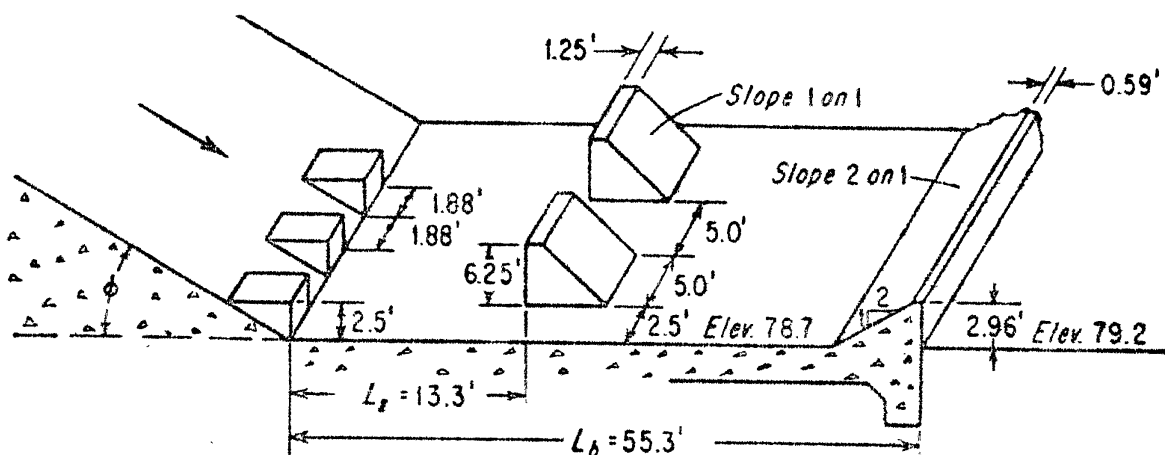


FIG. 11-5

For streams heavily laden with debris, baffles and chute blocks may be objectionable from the standpoint of maintenance. If the chute blocks are omitted from the basin, the other dimensions will still be applicable. If, however, both the baffle piers and chute blocks are omitted from the basin, it will be necessary to increase the length of the basin, and no reduction in the tailwater depth should be permitted.

11-2. Uplift Forces. In designing an apron, attention must be given to the force of uplift consequent on the percolation of water in the permeable foundation beneath the apron. Without the hydraulic jump, the apron remains stable, since it is heavier than water. When the jump is formed, the downstream head acts upward upon the underside of the apron. If this uplift force exceeds the downward forces, the apron may be torn loose from its foundation. Figure 11-6 illustrates the unbalanced head on the Merala Weir apron.

When the floor of a dam or weir is between piers, the distributed load under the surface of the concrete remains the same. Hence the weight of the hydraulic jump does not need to be included when calculating the required weight between the piers of the masonry or concrete for aprons.

To calculate the weight of the hydraulic jump on an apron and to

apply it to the uplift force, we must know the profile of the water surface between y_1 and y_2 . The water surface can usually be found by model studies or, for small structures, a line can be drawn between y_2 and y_1 , thus giving an approximate water surface. This profile may change when appurtenances are added to the basin. The volume of water on the apron will be equal to the product of the longitudinal area times apron width.

Weep holes are often provided in the apron to reduce the uplift pressure. The weep holes should be placed over the pockets of gravel so that the fine materials are not washed out of the foundations by drainage. Inverted

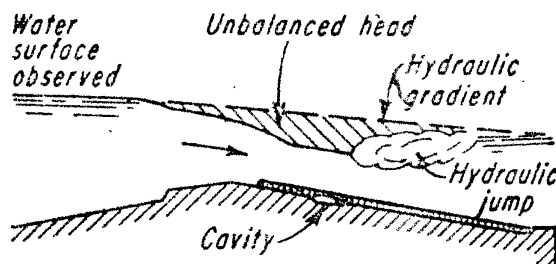


FIG. 11-6. Diagram showing unbalanced head on Merala Weir, India, August, 1929.

filters are ordinary filters built upside down, so that percolating waters move first through the fine materials at the bottom of the filter, then upward through the layer of gradually increased porosity.

Excessive water pressure caused the failure of the Narora Weir on the Ganges River, India. This pressure caused the floor of the weir to be blown upward, because the weight of the apron floor was insufficient to balance the upward pressure of water percolating under the weir. The weight of the hydraulic jump should be included in uplift calculations.

REFERENCE

1. Blaisdell, F. W.: Development and Hydraulic Design of St. Anthony Falls Stilling Basin, *Proc. ASCE*, pp. 123-159, February, 1947.

12

Stilling Basins for Large Outlet Works and High Spillways

The purpose of this chapter is to provide a design procedure for stilling basins of large outlet works and high spillways, where the entering velocities exceed 50 fps. It is recommended that the design be verified by model studies for all structures of this class. A typical structure of this type is the Fort Peck Dam, shown in Fig. 12-1.

12-1. Design Procedure. For this type of basin, chute blocks and a dentated end sill are used to shorten the length of the stilling basin, assist in the energy dissipation, and enhance the performance of the basin. Baffles are omitted from the basin, since at high velocities they will probably be subject to damage by cavitation. The following steps are recommended for the design of basins that have entering velocities which exceed 50 fps.

Step 1. Basic Data. For high spillways, the effect of air entrainment upon the depth of flow and the actual velocity at the base of the spillway should be considered. After the velocity and unit discharge have been found, the corresponding depth, including water and entrained air, can be found by using Fig. 12-2, which was developed by Gumensky.²

Step 2. Required Tailwater Depth. For this type of stilling basin, without baffles, the tailwater-rating and jump-height curves should coincide at the design discharge and should be fairly close at intermediate discharges. A minimum tailwater safety factor of 5 per cent should be included in the design of this type of stilling basin. Also, a careful evaluation of all factors that may affect the tailwater depth at a later date should be made.

Step 3. Flow Conditions. The slope of the spillway section preceding the basin is unimportant except that the velocity distribution of the high-velocity jet must be uniform.

Long, flat spillway sections should be avoided, because frictional resistance on the bottom and side walls is sufficient to produce a center velocity

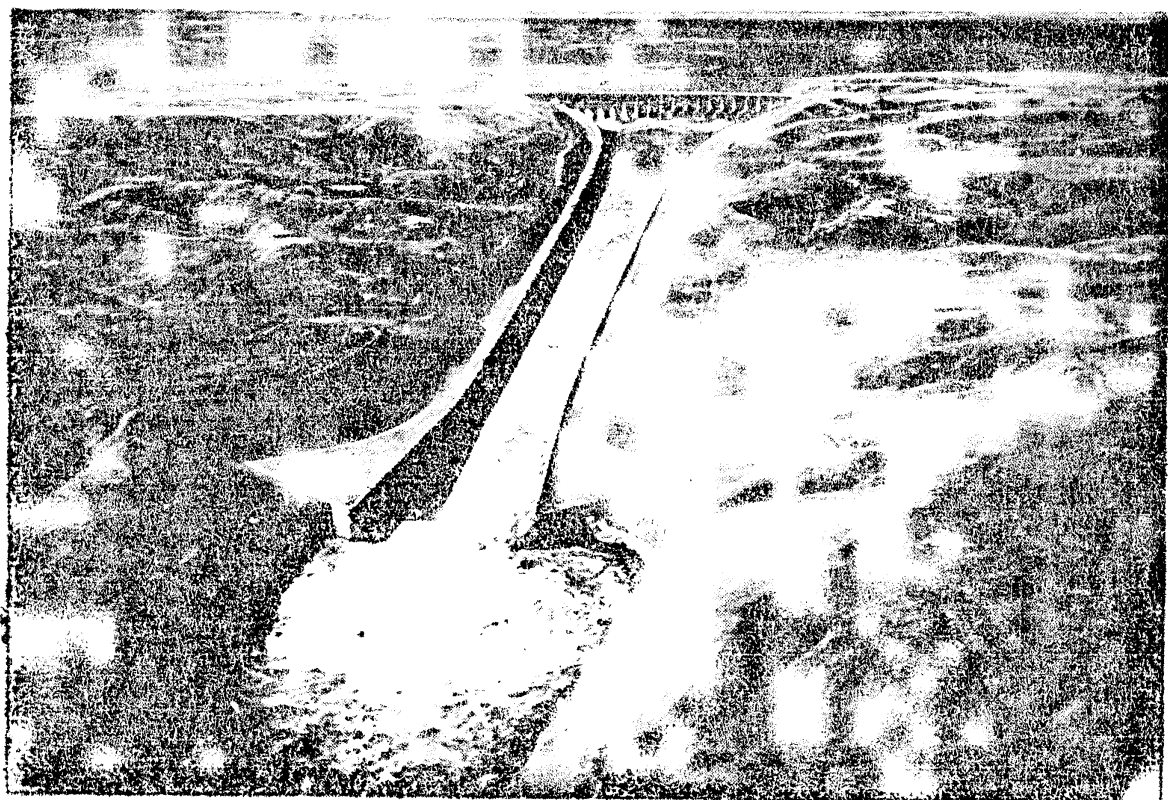


FIG. 12-1. Aerial view of the mile-long chute stilling basin of the Fort Peck Dam, Missouri River, Montana. Spillway capacity: 250,000 cfs. (Courtesy of Corps of Engineers, Fort Peck Area Office, Fort Peck, Montana.)

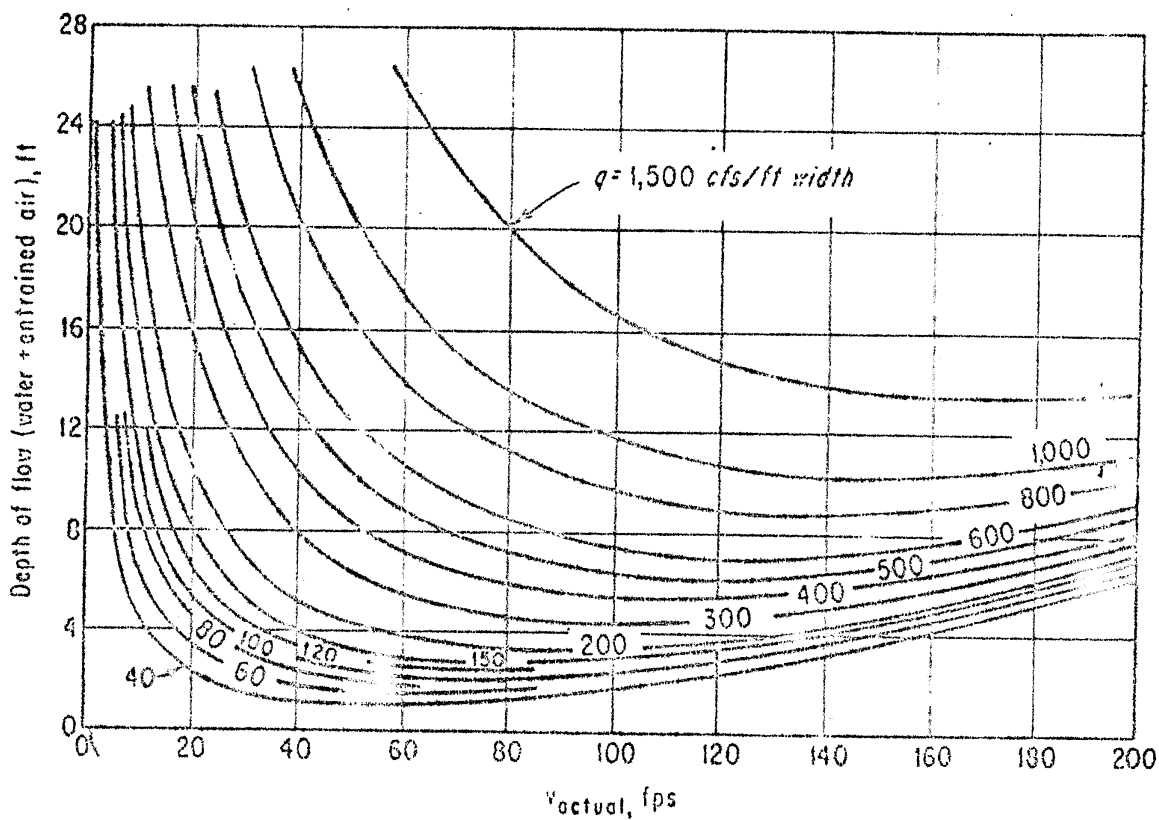


FIG. 12-2. Air-entrainment data for high spillways.

greatly exceeding that on the sides and bottom of the basin. When this happens, greater activity results in the center of the basin than on the sides, producing an unsymmetrical jump with violent side eddies.

The same effect will be witnessed when the angle of divergence of the spillway section is too great for the water to follow, resulting in a non-uniform distribution of velocities. Unbalanced velocity distribution in the entering jet and excessive divergence may result in the formation of a rough jump.

It is also important that the outlet entrance and bridge piers be streamlined to eliminate undesirable flow conditions. In the case of the Dos Bocas Dam, a square entrance caused water to spray from the spillway sides and to concentrate the flow in the center of the stilling pool. This unbalanced condition produced a severe whirl on each side of the pool, which disrupted the formation of the hydraulic jump. The problem was solved by introducing a curved entrance at each outlet and streamlining the bridge piers, thereby eliminating the undesirable flow conditions.

Step 4. Stilling-basin Length. When chute blocks and a dentated end sill are installed in the basin, a reduction can be made in the length required for the stilling basin. It is recommended that the length of the basin be made equal to $5.0(y_2 - y_1)$.

Step 5. Chute Blocks. Chute blocks are placed at the entrance of the basin to corrugate the jet, lifting a portion of it off the floor and thereby providing a shorter length of basin than would be possible without them. These blocks also tend to improve the action of the jump. Recommended dimensions for the chute blocks are: height = y_1 , width and spacing = $\frac{3}{4}y_1$. A space of $\frac{1}{2}y_1$ from the end block to the side wall is preferable to reduce spray and maintain desirable pressures.

Step 6. Dentated Sill. A dentated sill should be placed at the downstream end of the apron to reduce scour and improve the action of the hydraulic jump. It is recommended that the height of the sill be made equal to $0.25y_2$, and the width and spacing be made equal to $0.15y_2$. The continuous portion of the sill should have a slope of 2 horizontal on 1 vertical. For narrow basins, the width and spacing of the blocks should be reduced proportionately, since minimum width and spacing will be governed by structural considerations. It is not necessary to stagger the chute blocks and the sill dentates, since this practice is undesirable from a construction standpoint.

Step 7. Recommended Dimensions for Stilling Basins for High Spillways and Large Outlet Works. Figure 12-3 shows the recommended dimensions for stilling pools of high spillways and large outlet works having entering velocities which exceed 50 fps.

When the slope of the chute or spillway is 1 on 1 or greater, it is recom-

mended that the sharp intersection between the chute and apron be replaced with a smooth curve having a radius equal to or greater than $4y_1$. Chute blocks can be installed on the curved face as readily as on plane surfaces.

By reducing or increasing the discharge per foot of spillway length, the jump-height curve can be lowered or raised. These changes may result in increases of the cost of the crest gates, spillway crest length, or other features of dams, but this might be much more than offset by a reduction in stilling-basin costs. Where circumstances permit, a careful choice of the spillway length may result in large savings in stilling-basin costs.

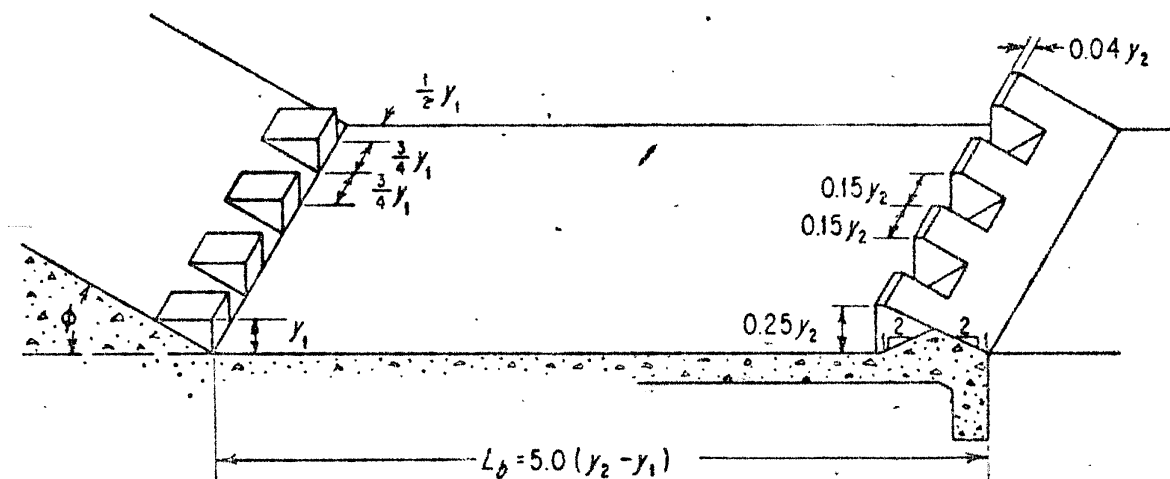


FIG. 12-3. Recommended dimensions for stilling-basin appurtenances for high spillways and large outlet works.

An example problem is given to show how the design procedure may be applied. The problem is to find the dimensions of the necessary stilling-basin appurtenances for a spillway 90 ft high with a crest length of 200 ft. At the design discharge of 40,000 cfs. 10 ft of water passes over the spillway crest.

Step 1. Basic Data. The theoretical velocity will be equal to

$$\begin{aligned} v_t &= \sqrt{2gH} \\ &= \sqrt{2g(95)} \\ &= 78.2 \text{ fps} \end{aligned}$$

To compensate for friction losses it is assumed that the actual velocity will be 90 per cent of the theoretical velocity.

$$\begin{aligned} v_a &= 0.9(v_t) \\ &= 0.9(78.2) \\ &= 70.4 \text{ fps} \end{aligned}$$

From Fig. 12-2, with the actual velocity and the discharge per foot of spillway crest known, we can find the depth of flow, including entrained air. Using Fig. 12-2, y_1 is found to be 3.5 ft.

Step 2. Required Tailwater Depth. First, compute the kinetic-flow factor. With λ_1 and y_1 known, we can then find y_2 .

$$\begin{aligned}\lambda_1 &= \frac{v_1^2}{gy_1} \\ &= \frac{70.4^2}{32.2(3.5)} \\ &= 44.1\end{aligned}$$

Then

$$\begin{aligned}y_2 &= \frac{y_1}{2} (\sqrt{1 + 8\lambda_1} - 1) \\ &= 1.75[\sqrt{1 + (8)(44.1)} - 1] \\ &= 31.2 \text{ ft}\end{aligned}$$

The tailwater depth required, including a safety factor of 5 per cent, will be equal to

$$\begin{aligned}\text{Required tailwater} &= 1.05y_2 \\ &= 1.05(31.2) \\ &= 32.8 \text{ ft}\end{aligned}$$

Step 3. Flow Conditions. Not applicable.

Step 4. Stilling-basin Length

$$\begin{aligned}L_b &= 5.0(y_2 - y_1) \\ \text{Therefore} \quad L_b &= 5.0(31.2 - 3.5) \\ &= 138.5 \text{ ft}\end{aligned}$$

Step 5. Chute Blocks

Height: $y_1 = 3.5 \text{ ft}$

Width and spacing: $\frac{3}{4}y_1 = 2.6 \text{ ft}$

Thirty-eight chute blocks will be required, with a spacing between the end blocks and walls of 2.5 ft.

Step 6. Dentated End Sill

Height: $0.25y_2 = 0.25(31.2) = 7.8 \text{ ft}$

Width and spacing of dentals: $0.15y_2 = 4.78 \text{ ft}$

The continuous portion of the end sill should have a slope of 2 on 1, with a top horizontal width of $0.04y_2 = 0.04(31.2) = 1.25 \text{ ft}$.

Step 7. Recommended Dimensions for Stilling-Basin Appurtenances of Example Problem. The recommended dimensions for the basin and the

TABLE 12-1. MODEL RESULTS OF EXISTING STILLING BASINS

Structure	q	L_b	ϕ	Type of basin	Wing walls
Rye Patch.....	182	46	33	Rectangular	45° warped
Unity.....	180	59	26.7	R	Normal
Aleova.....	367	125	25	R	None
Shadow Mountain.....	143	56	28	R	Normal
Boysen (final).....	303	151	34	R	None
Boysen (preliminary).....	496	140	33.7	R	None
Scofield.....	155	60	33.7	R	Normal
Boca.....	107	58.6	26.7	R	Normal
Fresno.....	268	85	33.7	R	45° warped
Bull Lake.....	100	75	14	R	Normal
Caballo.....	306	78.2	26.7	R	Normal
Moon Lake.....	133	60	26.7	R	Normal
Deer Creek.....	160	75	26.7	R	Normal
Alamogordo.....	509	125	26.7	R	Normal
Enders.....	500	115	26.7	R	Normal
Medicine Creek.....	373	125	26.7	R	Normal
Cedar Bluff.....	437	140	18.5	R	Normal
Falcon.....	760	180	26.7	R	45° vertical
Trenton.....	500	125	18.5	R	Normal
Cachuma.....	500	153	26.7	R	Normal
Tiber.....	271	117	18	R	Normal
Imperial Spillway.....	125	41	14	R	20° warped
Imperial Sluiceway.....	97	69	14	R	20° warped
Grassy Lake.....	60	45	26.7	R	Normal
Box Butte.....	62	50	22	R	Normal
Siphon Drop Turnout.....	60	36	22	R	45° warped
Pilot Knob Wasteway.....	94	60	18.5	R	45° warped
AA Canal Drop 1.....	74	27	22	R	30° warped
Wasteway No. 2.....	52	45	24.7	R	30° warped
Big Sandy No. 2.....	150	75	33.7	Trapezoidal	Normal
Cherry Creek.....	388	120	25	R	None
Pine View.....	225	96	33.7	T	Warped curve
Agency Valley.....	200	110	33.7	T	50° warped
Davis.....	711	100	14	R	Normal
Bonny.....	301	102	20	R	Normal
Cle Elum.....	200	103	33.7	R	None
Maximum.....	760	180	34		
Minimum.....	52	27	14		
Average.....	265				

NOTE: q = discharge per foot of basin width, cfs per foot; L_b = stilling-basin length, ft; ϕ = slope entering stilling basin, °.

necessary appurtenances are shown in Fig. 12-4. A tabulation of the model results of 36 stilling-basin tests conducted by the Bureau of Reclamation is shown in Table 12-1.

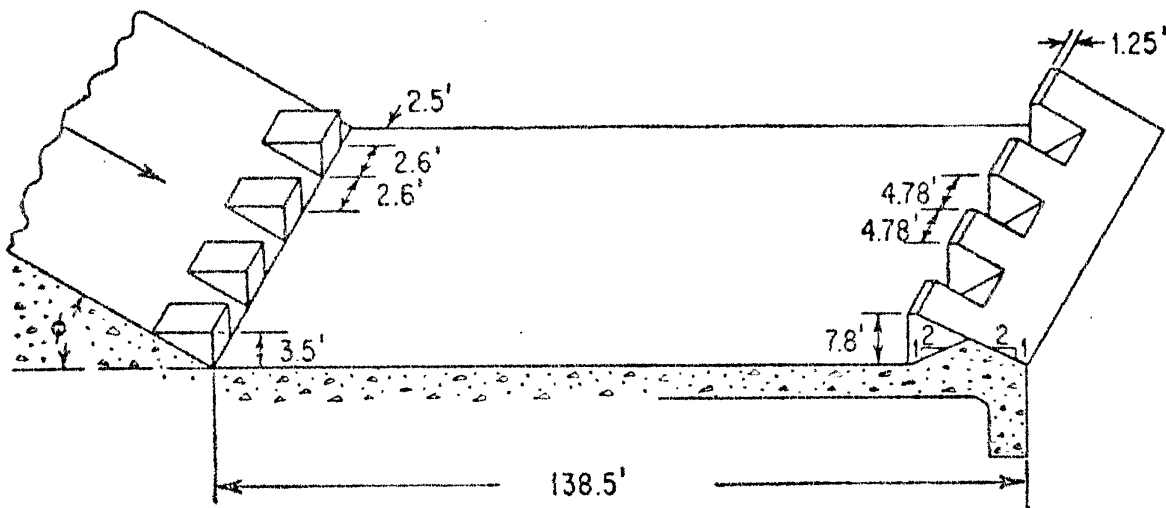


FIG. 12-4

DIRECT SOLUTION FOR APRON ELEVATION

The standard solution for the apron elevation has been a trial-and-error process requiring considerable amounts of time. It is possible, however, to relate the pertinent variables, shown in Fig. 12-5, in dimensionless form and secure a direct solution.

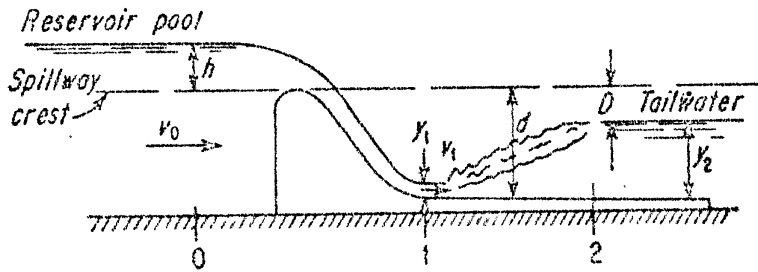


FIG. 12-5

By writing the energy equations between sections 0 and 1, neglecting v_0 , the velocity of approach, and the frictional loss between the sections, the velocity at the base of the spillway is

$$v_1 = \sqrt{2g(d + h)} \quad (12-1)$$

Since $y_1 = \frac{q}{v_1}$, where q is the discharge per foot of spillway width, Eq. (12-1) becomes

$$y_1 = \frac{q}{\sqrt{2g(d + h)}} \quad (12-2)$$

or

$$y_1 = \frac{q}{\sqrt{2} g^{1/2} \left(\frac{d}{h} + 1\right)^{1/2} h^{1/2}} \quad (12-3)$$

The downstream depth y_2 necessary for the hydraulic jump to form is given by Eq. (12-4).

$$\frac{y_2}{y_1} = \frac{1}{2} \left(\sqrt{1 + \frac{8q^2}{gy_1^3}} - 1 \right) \quad (12-4)$$

Referring to Fig. 12-5,

$$\frac{y_2}{y_1} = \frac{d - D}{y_1} \quad (12-5)$$

Substituting Eqs. (12-3) and (12-5) into Eq. (12-4), we have

$$\frac{2d - 2D}{y_1} + 1 = \sqrt{1 + \frac{16 \sqrt{2} g^{3/2} [(d/h) + 1]^{3/2} h^{3/2}}{q}} \quad (12-6)$$

or, in dimensionless form,

$$\begin{aligned} \left(\frac{g^{1/2} h^{3/2}}{q} \right) \left(\frac{d}{h} + 1 \right)^{3/2} \left(\frac{d}{h} - \frac{D}{h} \right) + 0.353 \\ = \left\{ 0.125 + \frac{2.828 g^{1/2} h^{3/2} [(d/h) + 1]^{3/2}}{q} \right\}^{1/2} \end{aligned} \quad (12-7)$$

If we let

$$\pi_1 = \frac{g^{1/2} h^{3/2}}{q} \quad \pi_2 = \frac{D}{h} \quad \pi_3 = \frac{d}{h}$$

then

$$\pi_1(\pi_3 + 1)^{1/2}(\pi_3 - \pi_2) + 0.353 = [0.125 + 2.828\pi_1(\pi_3 + 1)^{3/2}]^{1/2} \quad (12-8)$$

Values of π_3 for the corresponding values of π_1 and π_2 have been computed from Eq. (12-8) and are plotted in Fig. 12-6. The range of the π_1 curves represents the values normally encountered by the designer. The curves use $g = 32.2$ ft per sec², and are applicable therefore only in the foot-pound-second system. Equation (12-8) is applicable for all systems, provided consistent units are employed. The following example applies the solution to a specific problem:

Example. Find the apron elevation required for a hydraulic-jump-type stilling basin below the spillway portion of a dam with the following items known:

Unit discharge: $q = 100$ cfs per foot

Reservoir pool elevation = 100 ft

Spillway crest elevation = 90 ft

Tailwater elevation = 31 ft

Solution. Compute π_1 and π_2 .

$$\pi_1 = \frac{5.67 h^{3/2}}{q} = \frac{5.67(10)^{3/2}}{100} = 1.79 \quad \pi_2 = \frac{D}{h} = \frac{90 - 31}{10} = 5.9$$

Entering Fig. 12-6 with the computed values, we find $\pi_3 = 8.0$. Then

$$d = 8.0(10) = 80 \text{ ft}$$

Therefore, the required elevation of the stilling-basin apron would be $90 - 80$, or 10 ft.

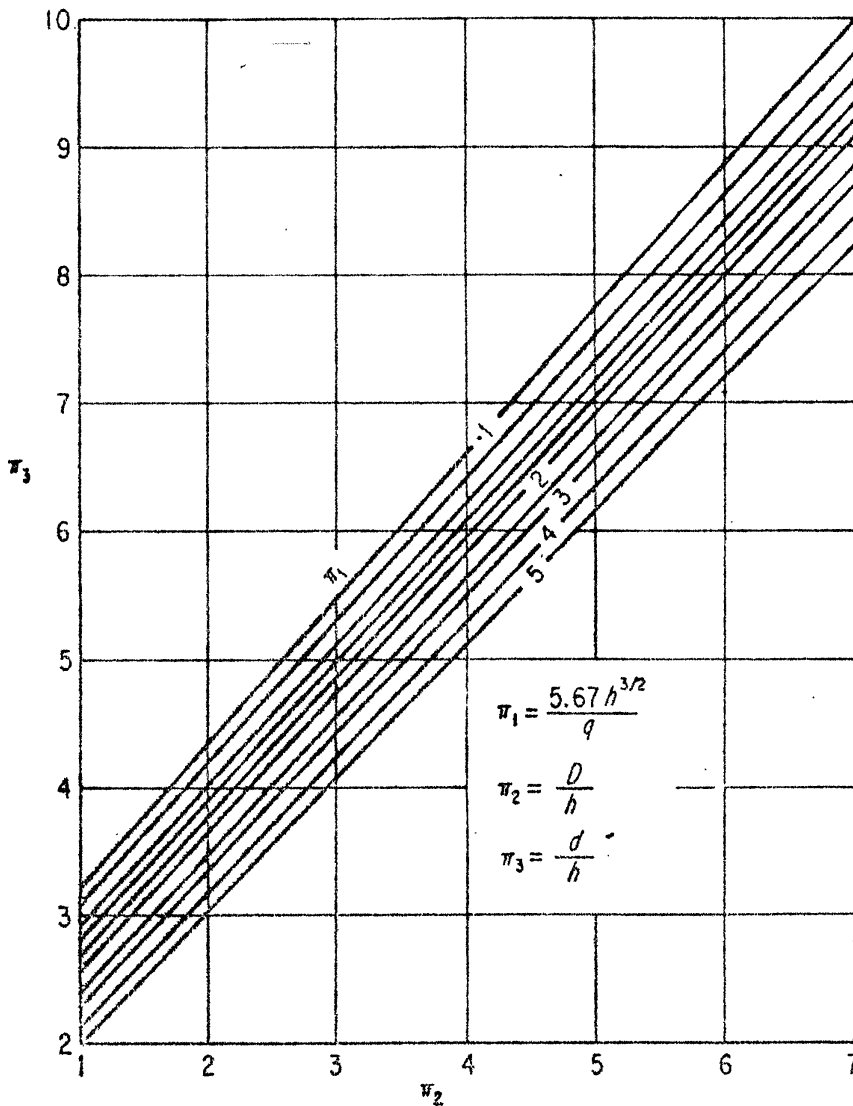


FIG. 12-6. Diagram for determining stilling-basin elevation.

The energy loss on the spillway face has been neglected in the analysis. For high spillways, the influence of boundary resistance may be appreciable. By neglecting the loss due to friction, however, a slight excess of tailwater will be provided in the basin. It has been observed that a slightly drowned jump produces a better all-round energy dissipator compared to one designed for the y_2 depth. A slight excess of tailwater also moves the toe of the jump against the sloping face of the spillway, stabilizing the jump and producing a smoother over-all operation.

STILLING-BASIN WALLS

Although a few trapezoidal basins have been constructed, practically all existing stilling basins are rectangular in shape. Of the two types, the rectangular basin is preferable, since there is less difficulty in producing a satisfactory jump of reasonable length. Model tests of the Enid Dam⁵ have shown that vertical or near vertical training walls provide better flow conditions in the stilling basin than do sloping walls.

There is one distinct advantage to using trapezoidal basins. The construction of sloping walls will provide an economy in materials. The poor formation of a jump, however, will offset the economic advantage. The main weakness of ordinary trapezoidal pools is the tendency toward too great a proportion of the momentum forces in the central portion of the pool. This requires a y_* value high enough to resist the momentum force over the width in which the momentum force acts. As a result, the outside edges are filled with more or less dead water at lower elevations, and the tendency is for the main stream to flow down the center of the canal below the pool and for the water to flow upstream on the sides back to the pool. If sufficient y_* is not obtained to oppose the momentum forces, the jump may sweep through the pool. For this reason it will seldom be possible to design an ordinary trapezoidal pool with the bottom width increasing, unless much of the outside pressure force at y_* is ignored. In general, it is not considered good practice to use trapezoidal basins for discharges exceeding 25 cfs, unless model studies indicate that satisfactory results can be obtained in larger basins.

A model study conducted at the Case Institute of Technology for the Mount Morris Dam¹ eliminated this difficulty by constructing steps 6 to 7 ft high in the side walls. The Bureau of Reclamation has constructed three trapezoidal basins which have operated satisfactorily: the Big Sandy No. 2, Pine View, and Agency Valley Dams.

The initial design of the Fort Randall spillway is another example illustrating the importance of training walls. The original design called for training walls with a slope of 1 horizontal to 4 vertical. Because, however, the flow was deeper in the basin area, side eddies developed which caused the jump action to be confined to the center of the basin. This situation was alleviated by making the top alignment of the training walls parallel to the spillway, thereby causing the toe of the walls in the basin area to protrude into the flow. Figures 12-7 and 12-8 are photographs of the primary and secondary stilling basins of the Fort Randall Dam.

12-2. Stilling-basin Training Walls. Stilling-basin side walls serve also as embankment retaining walls. The tops of the walls are usually set so that the maximum tailwater for the design discharge will be con-

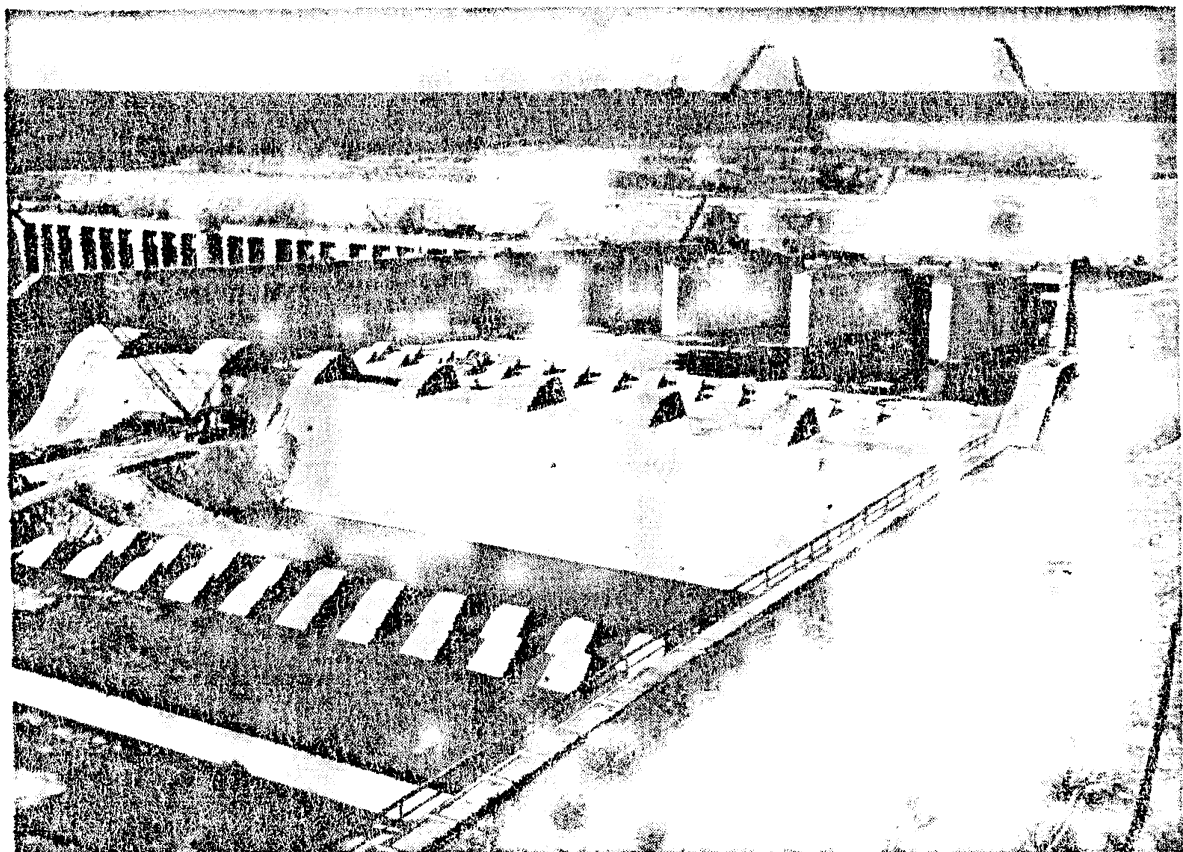


FIG. 12-7. General view of the primary and secondary stilling basins of the Fort Randall Dam, under construction. (*Courtesy of Corps of Engineers, Omaha District.*)



FIG. 12-8. Center bay of Fort Randall Dam, South Dakota, discharging approximately 130,000 cfs. (*Courtesy of Corps of Engineers, Omaha District.*)

tained within the stilling basin with sufficient freeboard. Sufficient freeboard will be necessary to allow for spray and air entrainment of the turbulent water which might overtop the walls if the freeboard were omitted. It is recommended that the amount of freeboard for rectangular stilling basins be chosen from Table 12-2.

TABLE 12-2. FREEBOARD FOR RECTANGULAR STILLING-BASIN SIDE WALLS

<i>Design discharge, cfs</i>	<i>Freeboard, ft</i>
0-100	2
100-500	3
500-1,000	4
1,000-5,000	5
5,000-10,000	6
10,000-50,000	8
50,000-100,000	10
More than 100,000	$\frac{1}{3}y_2$

Two typical stilling-basin training-wall profiles are shown in Fig. 12-9a and b. Studies to determine the effect of side-wall submergence conducted by Nicolaou³ indicate that when the tailwater depth was less than

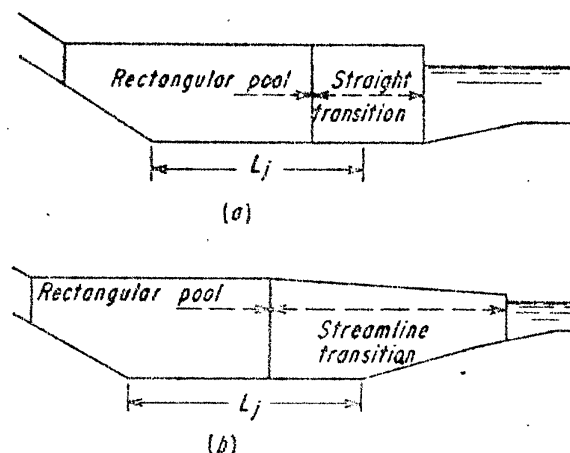


FIG. 12-9. Typical stilling-basin side-wall profiles.

y_2 , a portion of the flow overtopped the side walls. Outside of the stilling-basin side walls, a region was formed where the flow divided, part of it flowing upstream and the remainder downstream. For certain cases, the side walls may be designed to be overtopped, but until additional research has been performed, this procedure is not recommended. Side walls may be reduced in height when the basin is confined by high-quality rock.

12-3. Wing Walls. Wing walls are required at the end of the side walls of the basin to prevent the side walls from being undermined. They are also of use in calming the water in back of the wall and in preventing eddies from extending as far upstream as they would if the wing walls were absent. Straight wing walls set at an angle of 45° to the direction of flow provide an economical wall for small projects or where foundation

conditions are not subject to scour. Sharp corners, angles, or abrupt changes lead to the formation of eddies which will scour the material close to the foot of the wall. It is important that a gradual, smooth transition be provided from the stilling pool to the outlet channel. It is suggested that the minimum length of the wing walls be made equal to one-half the side-wall length. Lengths larger than this do not increase the hydraulic performance of the basin. The height of the wing walls should be made equal to that of the side walls.

In general, the type of wing wall used will be dictated by local conditions, such as the width of the downstream channel, the depth to foundation rock, and the degree of protection required. Figure 12-10 is a photograph of the wing walls of the Stevenson Dam stilling basin, located on Sinnemahoning Creek in Pennsylvania. In this case, 45° , rounded wing walls were adopted.

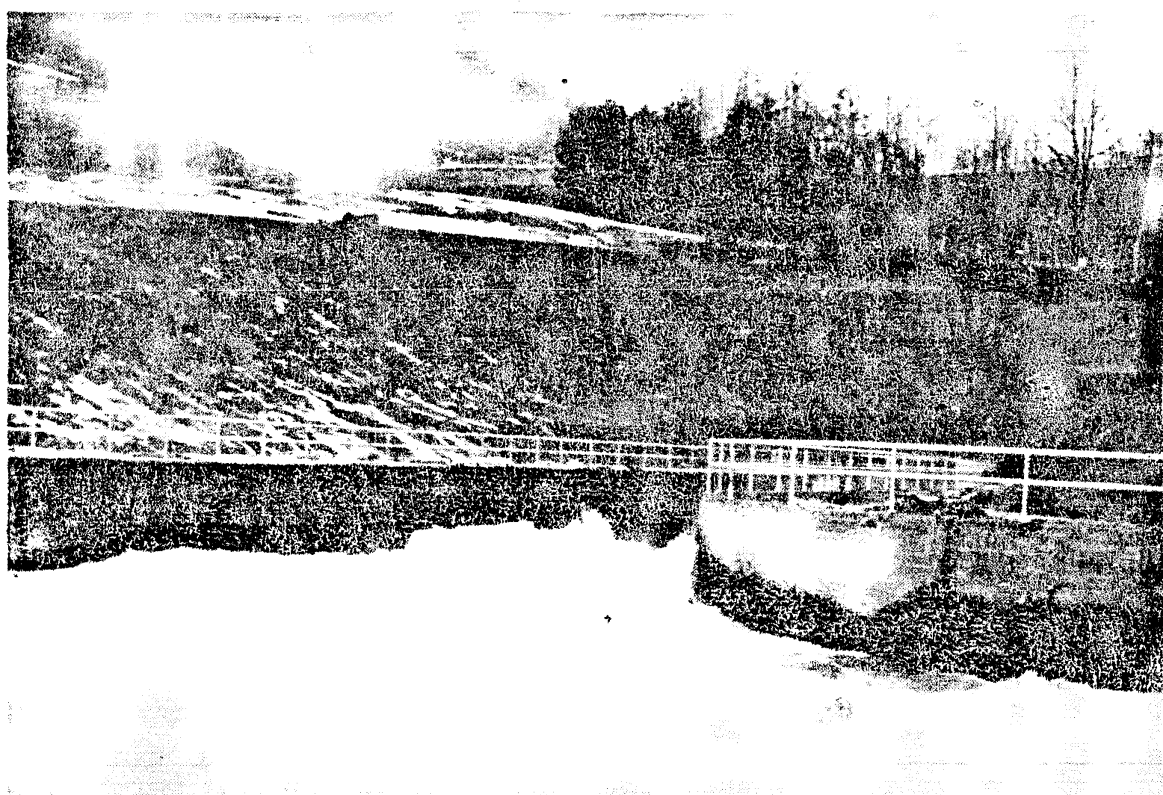


Fig. 12-10. View of the turbulence occurring at the exit of the stilling basin of the Stevenson Dam, Pennsylvania. Approximate discharge: 9,000 cfs.

12-4. Splitter Walls. When two or more conduits discharge into a hydraulic-jump-type stilling basin, it is necessary for the basin to be separated by divider, or splitter, walls. The splitter wall is necessary to prevent return eddies and the flow from "spreading" in the basin when each conduit is operating separately. Such a design would provide two separate basins, one for high-velocity flow and the second for low-velocity flow. Each half will act as a separate basin, and efforts will be directed

toward securing a smoother water surface and uniform downstream velocities.

As a result of model studies, the Hoosic River⁴ junction stilling basin was designed in this manner. The Hoosic River stilling basin was divided into two separate basins by a splitter wall. Each half of the basin was designed as a separate unit, with the width and elevation of the apron on each side of the dividing wall varied to secure good jump action. An end view of the recommended design of the Hoosic River junction stilling basin is shown in Fig. 12-11. Tests indicated the desirability of

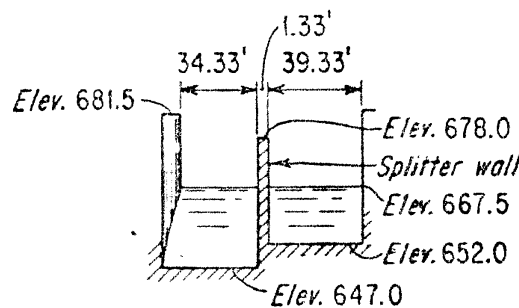


FIG. 12-11. End view of Hoosic River stilling basin, North Adams, Massachusetts.

using a series of steps on the basin floor in preference to a single high end sill. The height and length of the steps were varied until optimum basin performance was achieved in the model.

REFERENCES

1. Corps of Engineers, Buffalo District, Model Studies for Spillway and Outlet Works of Mount Morris Dam, Genessee River, New York, March, 1946.
2. Gumenksy, D. B.: Air Entrainment in Fast Water Affects Design of Training Walls and Stilling Basin, *Civil Eng.*, vol. 19, pp. 831-833, 889, 1949.
3. Nicolaou, S.: "Effect of the Submergence of the Stilling Basin Sidewalls on the Hydraulic Jump," unpublished M.S. thesis, State University of Iowa, August, 1951.
4. Waterways Experiment Station, Model Investigation of Stilling Basin and Channel Junctions, Hoosic River, North Adams, Massachusetts, *Tech. Memorandum 2-638*, 1955.
5. Waterways Experiment Station, Model Study of Enid Dam Spillway, Yacona River, Mississippi, *Tech. Memorandum 2-223*, 1947.

13

Outlet-works Control Mechanisms

The relative importance of outlet-works control mechanisms and their design varies according to the manner in which the discharge is conducted from the reservoir to the downstream side of the dam. In concrete dams, the most economical location for the outlet works is generally through the dam, while for earth dams, the only feasible locations are usually through a tunnel in the abutment or through a cut-and-cover conduit under the dam.

In concrete dams it is possible to place outlets at different levels that terminate in the downstream face of the overflow portion of the dam. These outlets may be placed in tiers and operated alternately under low heads for any reservoir level. Figure 13-1 is a photograph of four sluices discharging into the Chief Joseph Dam stilling basin.

For earth dams, all discharges must often be taken through one tunnel or conduit which must ordinarily be made large enough to accommodate temporary diversion flows during the construction of the dam.

Regulation of discharge through an outlet is normally made by means of gates or valves which, because of the accurate regulation required, must be capable of being operated at any degree of opening. For controlling and regulating outflow from a reservoir, low-pressure slide gates or commercial gate valves are commonly used for heads up to about 50 ft. high-pressure slide gates are used for heads up to about 75 ft, and needle, tube, hollow-jet valves, or radial gates are used for higher heads. High-pressure slide gates may be used for heads in excess of 75 ft, if they are operated in either the fully open or fully closed positions. Most valves are designed so that they may be operated at partial openings for all required heads, thereby permitting close regulation of the discharge.

Regulating gates or valves may be placed at the intake end, at some point inside, or at the outlet end of the conduit, depending upon the particular arrangement of the structure. For conduits placed through con-

crete dams, the position of the control device will depend upon whether the conduits terminate in the overflow or nonoverflow portions of the dam. In a nonoverflow section, valves placed on the downstream end of the conduit may be the most desirable, since they provide easy access to the mechanism, permit the dissipation of the high-velocity flow outside the conduit, and render better flow conditions.

When outlets are located in the spillway portion of the dam, the control must be located at the upstream end, usually inside the conduit, where



FIG. 13-1. Four sluices discharging into the Chief Joseph Dam stilling basin. (*Courtesy of Corps of Engineers, Seattle District.*)

operation and servicing can be accomplished from the galleries. To prevent cavitation, this type of installation should be operated only at certain ranges for partial openings and should not be used for higher-head installations.

To make it possible to dewater the control gates or valves for repairs without emptying the reservoir or to shut off the flow should the control devices become inoperative, the usual practice is to install emergency gates farther upstream in the outlet conduit. For concrete dams the emergency gates may be placed either at the entrance to the conduit or inside the conduit and operated from the galleries. Vertical-leaf or fixed-wheel gates are ordinarily used at the entrance to the conduit, while high-pressure, ring-follower, or butterfly valves are used inside the con-

duit. For tunnel or conduit outlets, low-pressure or high-pressure slide gates may be used as emergency gates for the lower-head installations.

The purpose of this chapter is to describe the types of outlet gates and valves and where they may be used in connection with energy dissipators. The design of gates and valves, however, is beyond the scope of this text.

GATES

13-1. High-pressure Gates. High-pressure gates are of the slide type, in which the rectangular leaf is encased in a body and bonnet equipped with a hydraulic hoist for moving the gate. The sliding, load-carrying surfaces of the gate also act as the seals and are rigidly attached to the leaf and housing.

Since sliding friction has to be overcome in moving the gate, operating forces are very large even for nominal heads, and an oil-operated, double-acting-piston cylinder hoist is required to move the gate leaf. By moving the leaf slowly, the horsepower requirements for the gate hoist are reduced.

High-pressure gates are normally used as control gates for lower-head installations. They are often placed in tandem, the upper gate being used as the emergency gate and the lower gate as the regulating gate. These gates may also be used as emergency gates in connection with other types of regulating valves or gates.

When a high-pressure gate is used for regulating or throttling, a large supply of air is required in the conduit downstream from the gate leaf to minimize pressure fluctuations and to inhibit cavitation below the gates.

13-2. Radial Gates. Radial gates are used in closed conduits under moderate head conditions and are generally employed when relatively large discharges are required.

Early radial gates were often made of wood, but modern gates are made wholly of steel. Basically, the gate consists of a section of a cylinder connected to and supported by the two side beams which are connected by hinge pins to the supporting structure. High-head radial gates are usually operated by means of a screw lift, which permits opening the gate and holding it at any desired opening, thereby allowing variable discharges. They are advantageous where large, unobstructed passages are desired, since no guides or seals protrude into the waterway.

Radial gates are similar to spillway-tainter gates, except that the structural members are much heavier, in order to resist increased water load, and seals across the top are required in addition to those on the sides and bottom. The tunnel downstream from the gates must be designed to flow always partly full when the gates are fully opened, and ample air passages must be provided to the downstream side of the gates.

13-3. Jet-flow Gates. The jet-flow gate consists of a wheel-mounted leaf moved vertically by a water-driven screw hoist. An upstream entrance to the gate is provided with a conical, converging transition ring, so that a contracted, circular jet that does not subject the housing to high pressures under any condition of discharge is formed in the vicinity of the leaf opening. The jet springs free of the wheel slots at the side of the gate leaf and decreases the impingement of the high-velocity water on the bottom portion of the conduit. Large air vents must be provided for supplying air to the conduit downstream from the gate so that, when the gate is discharging at partial openings, the effects of cavitation resulting from subatmospheric pressures are minimized.

Jet-flow gates are normally used in circular conduits for operation at medium heads and are usually operated only in a fully open position. Experience indicates that these gates may be satisfactorily operated at partial gate openings under moderate heads. Gates have been designed and placed in operation in conduits as large as 8 ft in diameter and have operated in the fully open position under heads up to 200 ft.

Flow releases for the Canyon Ferry Dam are made through the spillway section and are controlled by four 77-in. jet-flow gates. These outlets discharge into the stilling pool and are used primarily to regulate the river below the dam by controlling the releases that supplement the flow passing through the power plant. Under a maximum head of 150 ft, the four outlets are designed to discharge a total of 9,500 cfs.

13-4. Vertical-leaf Gates. Vertical-leaf gates are used in connection with outlet works primarily as emergency gates and are of the slide type, equipped with roller trains or wheels. Such gates are usually located at the face of the dam and are generally used for the maintenance and servicing of the conduits and the control gates or valves. Normally, these gates are lowered into position on their guides by means of hoists or cranes and, because of frictional resistance, must be lowered into place when heads are balanced on each side of the gate.

Ring-follower gates are similar to high-pressure gates, except that a follower, having a circular opening the same diameter as the conduit, is attached to the bottom of the leaf, so that it fills the gate slot when the gate leaf is in the fully open position. The entrance and exit passages of the housing are circular instead of rectangular. Gates of this type have been installed for conduit diameters up to $8\frac{1}{2}$ ft, with heads up to 330 ft. Flows through the Hungry Horse Dam outlet works are controlled by three 96-in. ring-follower gates.

For relatively high heads, vertical-leaf gates are equipped with roller trains and may be suitable for use as emergency gates. This type of gate may be installed on the face of the dam or at intermediate points in the conduit. The roller devices consist of one or more caterpillar-type roller

trains located on each side of the leaf and arranged so that they carry the entire water load. Because of their construction, the frictional resistance for roller-train gates is comparatively small.

Roller-train gates for use on the face of the dam have been installed in sizes up to 15 ft wide by 35 ft high to close off flow against unbalanced heads up to 260 ft. For use at intermediate points in conduits, roller-train gates have been designed for conduit diameters up to 126 in. to close off flow against unbalanced heads up to 230 ft.

Fixed-wheel gates are used in applications similar to those discussed for roller-train gates. The major difference in construction is that the loads are carried by wheels rather than by caterpillar-type roller trains. The greater simplicity of construction is an advantage of this type of gate over the roller-train type. The fixed-wheel gate, however, cannot be operated under very high heads. Fixed-wheel gates for use on the face of a dam have been installed with sizes up to 13 ft wide by 19 ft high, to effect closure against unbalanced heads up to 250 ft.

VALVES

13-5. Needle Valves. Needle valves are used at the outlet end of a conduit to control discharges under extremely high heads and are designed to discharge into the air, thereby eliminating the opportunity for cavitation within the conduit. Such valves have operated successfully under heads in excess of 550 ft.

The needle valve consists primarily of an outer globular casting housing a cylindrical inner mechanism, so that an annular water passage is formed between the casting and the cylinders. The inner mechanism is so arranged that the discharge end of the annular passage is closed when hydrostatic pressure is supplied to the proper chamber inside the cylinders. Needle points are placed at the upstream and downstream faces of the cylindrical mechanism to guide the water flow into and out of the annular passage.

In opening and closing the valve, the movement of the needle is actuated and controlled by pressures within the cylinder chamber, supplied by a compensating valve located directly beneath the body of the main valve. The compensating valve is so constructed that it controls the pressures within the valve chamber and holds the needle stationary at any desired position. Water issuing from the valve is always in the form of a jet, regardless of the valve opening, and control is easy to achieve. Usually needle valves are protected by emergency gates located in the conduit upstream from the valve.

At the Hoover Dam, six 84-in.-diameter needle valves are installed on each side of the river and discharge into the atmosphere approximately

175 ft above the normal elevation of the riverbed. The valves are directed at an angle of 60° downstream to give the issuing water a downstream component and are located so that jets issuing from the two sides of the river meet approximately in the center of the stream. Upstream from the needle valves, 96-in.-diameter paradox emergency gates are installed.

13-6. Tube Valves. The construction of tube valves is similar to that of needle valves, except that the movable needle is eliminated. It was designed to minimize the cavitation which developed at the downstream end of needle valves. Modifying the needle valve in this manner also resulted in a large saving on weight and permitted its use in a conduit with less danger of damage from cavitation. The tube is normally moved by means of a motor-driven, screw-type actuator.

Tube valves are ordinarily better adapted to submerged discharges or for use inside a conduit, since an insufficient air supply does not appear to produce all the cavitation effects inherent in other types of valves. When located in the center portion of the conduit, tube valves have long bodies with a 30° nozzle and are provided with air inlets to aerate the jet immediately downstream from the valve seat. Tube valves at the downstream ends of the conduits have relatively short bodies with a 45° nozzle. The jet issuing from a tube valve has an opening of about 30 per cent and is rough and unstable; it may not be satisfactory for this reason.

13-7. Hollow-jet Valves. The hollow-jet valve is the most recent development in control valves. Essentially, it consists of one-half the needle valve, with the needle turned so that it moves in the upstream direction in closing. The downstream nozzle is eliminated by allowing water to discharge from the bell-shaped body in a tubular or hollow jet, the outside diameter of which remains unchanged regardless of the valve opening. The hollow-jet valve derives its name from the shape of its discharge—a hollow or annular jet dispersed over a wide area.

For a given size, the valve will discharge 25 per cent more water than a needle valve. The body of the hollow-jet valve is not subject to the pressure of water in the reservoir and can therefore be of lighter construction than other control devices. The water passageways are proportioned to prevent subatmospheric pressures and consequent cavitation. Splitters in the water-passage area are necessary to support the interior parts of the valve, providing a means for introducing air inside the issuing jet.

Figure 13-2 is a photograph of 96-in.-diameter hollow-jet valves in use at the Hungry Horse Dam in Montana. Hollow-jet valves are usually operated by mechanically moving the needle with a motor-driven, screw-type actuator, although small valves are often operated by hand.

Hollow-jet valves as large as 96 in. in diameter have operated satis-

factorily under heads up to 250 ft. Four 96-in. hollow-jet valves were installed at the downstream end of the river-outlet conduits of the Friant Dam to provide regulated releases of stored water directly to the river. Each valve is designed to discharge 4,100 cfs under a head of 247 ft at full opening. The canal outlets of the Friant Dam also utilize four 96-in. hollow-jet valves similar to those in the river outlets. Each valve is designed to discharge a maximum of 2,900 cfs.



FIG. 13-2. Discharge of two of three 96-in.-diameter hollow-jet valves at Hungry Horse Dam, Montana. (*Courtesy of Bureau of Reclamation.*)

13-8. Butterfly Valves. Butterfly valves are most generally used as emergency valves located immediately upstream from hydroelectric generating units, where the penstocks are long, or as emergency closure valves for outlet works. Essentially, butterfly valves consist of a circular leaf slightly convex in form, mounted on diametrically opposed pivot shafts. One of the shafts is extended and fitted with a crank which is attached to a hydraulic cylinder hoist providing the motivating force for rotating the valve leaf from an open to a closed position.

When used for emergency closure, the butterfly valve operates in either a fully open or fully closed position and never remains at intermediate positions. Although butterfly valves can be used as control gates for low heads, they can only be used as emergency closure gates for higher-head installations. Butterfly valves with leaf diameters of 168 in., capable of closure against unbalanced heads of over 360 ft, have been installed in the 13 main penstocks of the Hoover Dam.

14

Jet-diffusion and Impact Stilling Basins

The discharge from an outlet—whether from gates, valves, free-flow tunnels, or conduits—usually emerges at a high velocity in a nearly horizontal direction at the toe of the dam. To prevent or minimize erosion of the outlet channel and structures, it will be necessary to provide some means of dissipating a large part of the high-velocity flow as quickly as possible upon its emergence from the outlet.

In some instances, where the outlet is located at some distance from the dam and the material in the riverbed is composed of firm rock, the jets may be allowed to discharge directly into the stream with no artificial means of dissipating their energy. If scour is permissible, a jet may be left to excavate its own stilling pool. After sufficient depth is reached and the bed becomes covered with large boulders as a result of the sorting action, scour will practically cease. This type of action occurred at the Tieton Dam.

More commonly, when high-velocity jets emerge from the outlet—jet-diffusion, free-jet, hump, or impact basins will be required. In most cases, energy dissipation of the flow from gates or valves usually presents difficult problems because of the wide variation in the quantity of water discharged and in the number of jets operating at any one time. An odd number of jets will provide more efficient operation and better performance than an even number of jets. Symmetrical discharge from the outlet works under all conditions is possible when an odd number of jets are employed.

14-1. Jet-diffusion Basins. Flow from a valve is usually concentrated into a narrow width as it enters the stilling basin. Before a hydraulic jump can be formed, the flow must be spread laterally. Consequently, a large percentage of the basin length is utilized in preparing the flow to enter the hydraulic jump. Engineers of the Bureau of Reclamation^s have developed a jet-diffusion basin which can be utilized to reduce the length

of the basin normally required by the hydraulic jump. For a structure with two outlets, it was found necessary to provide two hydraulic-jump stilling basins, one for each outlet, in order to perform satisfactorily when only one outlet was operating. By using a jet-diffusion stilling basin, it was found possible to eliminate, or considerably reduce, the length of the dividing wall.

Experiments indicated that satisfactory results could be obtained by directing the jets sharply toward the bottom, rather than over the tailwater surface. It was found necessary to protect the inflowing water with a hood, or some other device, until it was considerably beneath the tailwater surface. A deflector hood prevented the jet from being torn apart by induced eddies until it was well submerged, thereby accomplishing energy dissipation in a less violent and more efficient manner.

It is believed that the effectiveness of this method is due to the small-grain turbulence which is created in the basin. Because the outflow is well protected until submerged, the flow still contains sufficient energy to produce many small, efficient, energy-dissipating eddies at the bottom of the basin. From a theoretical standpoint, it has been proved that a large number of small eddies are more efficient in dissipating the energy than a few large eddies.

Jet-diffusion stilling basins were designed for both the Enders and Boysen Dams. The outlet works of each consist of two hollow-jet valves placed at the ends of the conduits. As discussed in Chap. 13, hollow-jet valves discharge a jet which is annular in cross section. The limits of the jet are very definite in form, with little or no flying spray, and the center core, composed of air, is adequately ventilated. From a performance standpoint, the annular jet differs from a solid jet mainly in the fact that it has less penetrating power when directed into the pool of water. High-velocity currents quickly rise to the surface of the pool. This is probably because of the relatively great amount of air in the jet. A solid jet will provide more penetrating power into the pool of relatively great width, but will be difficult to diffuse over a wide area.

A jet-diffusion stilling basin was employed for the Enders Dam,⁸ illustrated by Fig. 14-1a and b. The structure consists of two 60-in. hollow-jet valves which discharge horizontally into a stilling basin. The maximum discharge of the two valves, 1,360 cfs, occurred under a head of 52.5 ft. The preliminary hydraulic-jump-type stilling basin was 175 ft long and had a center dividing wall 22 ft high that extended nearly the entire basin length. The purpose of the center wall was to provide a separate stilling basin for each valve when only one was operating.

The adopted jet-diffusion basin reduced the stilling-basin length to 75 ft and elevated the bottom half of the downstream end of the shortened basin, which was not being utilized in the dissipation of energy. Conse-

quently, the amount of excavation and the height of the basin side walls could be reduced. The best operation consisted of a raised floor, crenelated in plan. A deflector hood was used to direct the flow downward without submerging the valves.

The Boysen Dam⁸ outlet works also employs a jet-diffusion stilling basin. The discharge control of the outlet works consists of two 84-in. hollow-jet valves which together discharge a total of 1,200 cfs, with a corresponding outlet velocity of 68 fps.

Figure 14-2 illustrates the adopted Boysen Dam stilling basin. In this case, a deflector hood was not satisfactory because of the center dividing wall, which prevented mixing of the two jets under the hood. The center dividing wall was not necessary from a hydraulic standpoint, but was required as a structural support. Experiments indicated that satisfactory performance could be attained by depressing the valves 24° downward. When this was accomplished, the water-surface profile in the stilling basin became almost level, and practically the entire volume of the basin became useful in dissipating the energy.

A submerged jet-diffusion stilling basin was employed for the Soldier Canyon Dam⁸ outlet works, illustrated by Fig. 14-3. An 18-in. pivot valve was used to discharge a maximum of 99 cfs with a maximum velocity of 115 fps. Side rails were installed in the basin to reduce wave heights and high-velocity surface currents at the basin exit.

It is strongly recommended that model tests be conducted for all proposed jet-diffusion stilling basins. The general principles enumerated herein, however, will be of assistance to the design engineer.

14-2. Free-jet Stilling Basins. For cases where the jet discharges into the air and plunges into the pool, it may be desirable to construct a trapezoidal riprap-lined stilling basin. In order for this type of basin to operate satisfactorily, the jets should plunge into the water pool from a point above the maximum tailwater elevation. When the jets are too near the tailwater elevation, high velocities will travel along the surface

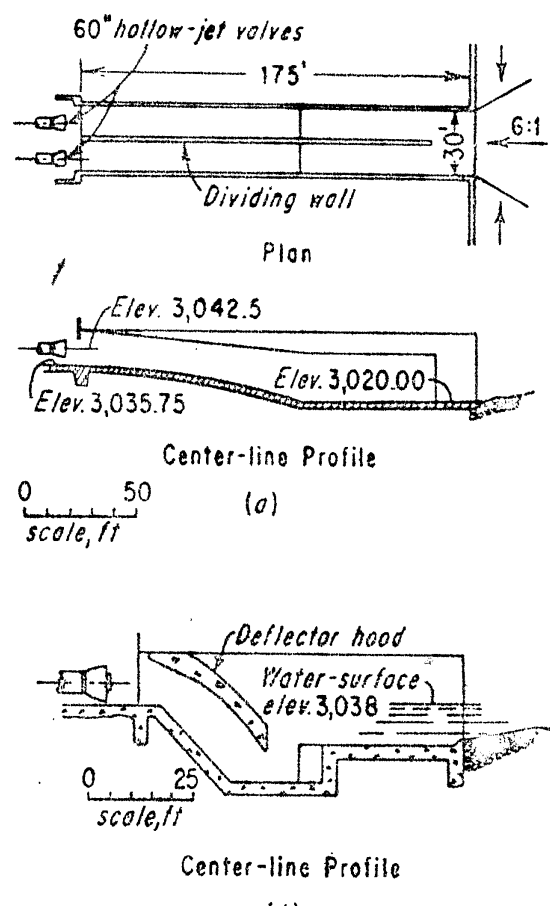


FIG. 14-1. Enders Dam outlet-works stilling basin: (a) preliminary design, (b) final design.

directly downstream from the jets, with stagnation or backflow resulting along the sides of the basin. If the jets are below the tailwater elevation, but not far enough to be submerged, a very unstable hydraulic jump forms downstream from the jets.

A trapezoidal free-jet stilling basin consists of an excavated pool with its side slopes surfaced with concrete or covered with large-size derrick rock to prevent scour and erosion. The actual shape or dimensions of the pool should be determined by model tests or by using proportions similar to those of a basin which is known to have operated satisfactorily. In order to minimize backflow and eddy currents along the sides, the basin should be relatively narrow. The length and width should be such that the jet trajectory for maximum discharge will strike well within the pool, and energy dissipation will occur before the jets strike the bottom.

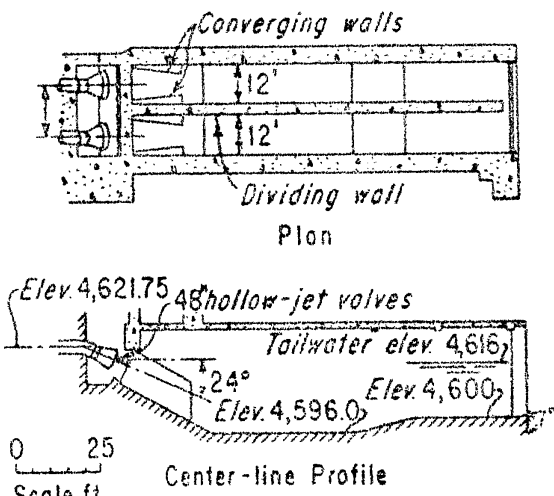


FIG. 14-2. Boysen Dam outlet-works stilling basin.

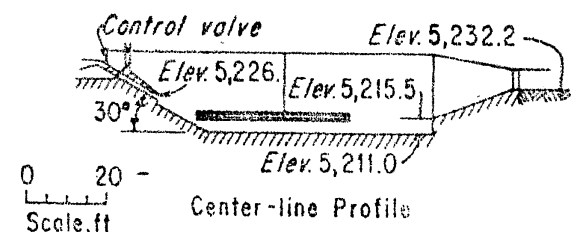
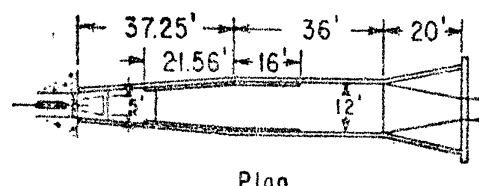


FIG. 14-3. Soldier Canyon Dam outlet-works stilling basin.

Laboratory tests by the Bureau of Reclamation indicate that a free-jet basin with the dimensions shown in Fig. 14-4 will render satisfactory operation for a pair of jets. Minimum dimensions are shown, and these can be increased to fit the river channel, if desirable, and still give good basin performance, provided that the basin is symmetrical with respect to the jets. If the basin is unsymmetrical, heavy riprap should be placed along the wider side as protection against eddy currents. If possible, the alignment of the jets should be such that their center lines will intersect at the downstream end of the basin.

Flow is released from the Deer Creek Dam¹ through two 48-in.-diameter tube valves, which discharge into a trapezoidal riprap-lined basin, as shown in Fig. 14-5. Under a hydrostatic head of 137 ft, the valves are designed to discharge a total of approximately 1,500 cfs.

Hydraulic model tests of the Deer Creek outlet works have demonstrated the practicability of permitting the tube valves to discharge

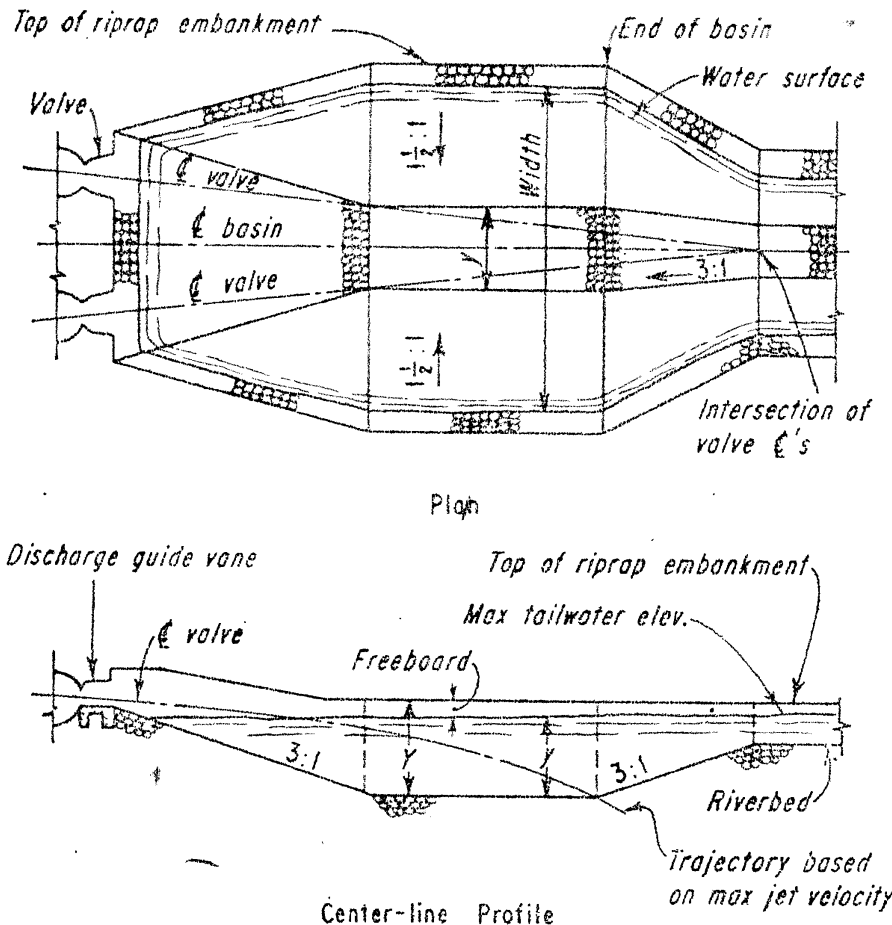


FIG. 14-4. Recommended dimensions for free-jet stilling basin.



FIG. 14-5. Two 48-in.-diameter tube valves discharging into riprap-lined stilling basin below Deer Creek Dam, Utah.

directly into a riprap-lined pool without providing a concrete-lined basin. Experiments indicated that by turning each valve inward the operation was improved and upstream currents were reduced. The recommended design consisted of a total valve convergence of 25° with the horizontal.

14-3. Free-jet Chutes. When the center line of the jets is above the streambed elevation, a free-jet, concrete-lined chute extending from the outlet to the stilling basin may be utilized. In order to prevent sub-atmospheric pressures and cavitation, the floor of the chute should be parabolic in shape, made equal to the jet trajectory for the maximum anticipated velocity.

To prevent the water from leaving the floor of the drop, the invert curve must not be sharper than the trajectory that would be followed by the high-velocity flow under the action of gravity. The floor profile should be based upon the theoretical Eq. (14-1) of the jet trajectory.

$$y = - \left[x \tan \phi + \frac{gx^2}{2v_{\max}^2} (1 + \tan^2 \phi) \right] \quad (14-1)$$

where y = vertical coordinate measured from the beginning of the curve in feet

x = horizontal coordinate measured from the beginning of the curve in feet

ϕ = angle between the drop and the horizontal beginning of the curve in degrees. This will be equivalent to the slope of the outlet conduit

v_{\max} = maximum velocity taken to be equal to 1.5 times the average velocity at the beginning of the trajectory

To illustrate the use of Eq. (14-1), we can find the equation of the parabolic drop required for the example problem in Chap. 9. For the example problem, the drop invert is horizontal and $\phi = 0^\circ$. Equation (14-1) is reduced to

$$y = - \frac{gx^2}{2v_{\max}^2}$$

The maximum velocity will be

$$\begin{aligned} v_{\max} &= 1.5v_{\text{avg}} = 1.5(30) \\ &= 45.0 \text{ fps} \end{aligned}$$

Then

$$y = - \frac{32.2x^2}{2(45)^2}$$

and

$$y = - 0.00795x^2$$

For the problem

$$\begin{aligned} y &= 45.00 - 13.23 \\ &= 31.77 \text{ ft} \end{aligned}$$

y is negative since it is downward.

$$x^2 = \frac{31.77}{0.00795}$$

and

$$x = 63.23 \text{ ft}$$

The beginning and end coordinates of the parabolic drop are shown in Fig. 14-6.

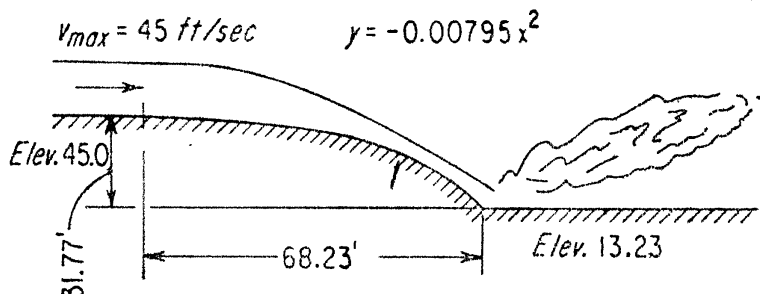


FIG. 14-6. Free-jet parabolic drop.

As the supercritical flow enters the pool, which has a slope less than that required to sustain shooting flow, a hydraulic jump may be formed. Chute blocks, baffle piers, and an end sill may be desirable. Recommended dimensions for the appurtenances are given in Chap. 11.

The above rules will also be applicable for a two-jet-chute basin, if the following additional rules are observed:

1. A dividing wall should be provided along the center line of the basin to permit satisfactory jump action with only one jet operating. The wall should extend through the chute and two-thirds of the basin length, with the top of the wall set at maximum tailwater elevation when only one jet is operating.

2. The width of the basin should be twice the jet spacing, with each half of the basin symmetrical about the center line of the jet.

A parabolic drop was adopted for the outlet works of the Heart Butte Dam,⁶ located on the Heart River in North Dakota. The main problem was to spread the high-velocity flow of about 60 fps into a uniformly distributed sheet suitable for the formation of a hydraulic jump. The problem was solved by constructing a parabolic drop which discharges the flow onto a horizontal floor. A plan and profile of the Heart Butte Dam outlet works are shown in Fig. 14-7. Two low walls divide the basin into thirds, producing excellent flow distribution and an efficient jump in the basin. Chute blocks and an end sill were placed in the basin to produce fine-grain turbulence and reduce the length of the basin.

14-4. Hump Stilling Basins. When the center line of the jets is below the streambed elevation, but not too far to be completely submerged by the tailwater, a hump in the stilling-basin floor may be pro-

HYDRAULIC ENERGY DISSIPATORS

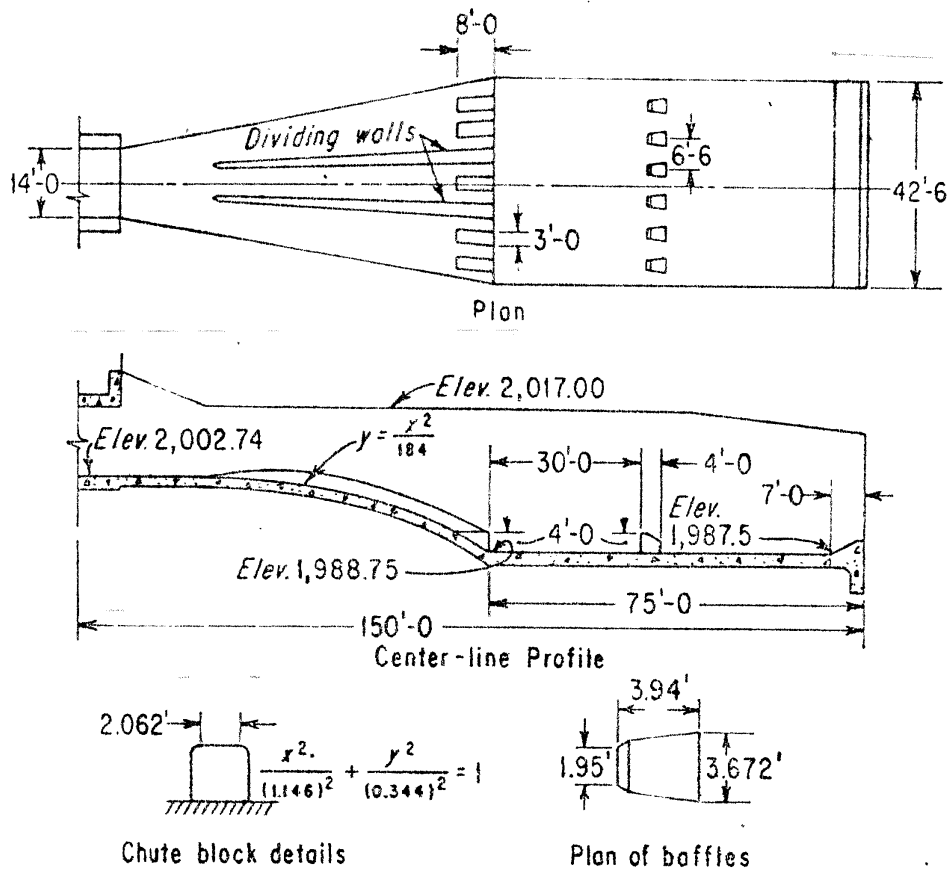


FIG. 14-7. Heart Butte Dam outlet works and stilling basin.

vided to spread the jets and permit the formation of a stable hydraulic jump. This type of basin, depicted in Fig. 14-8, is commonly known as a "hump basin." The two most important considerations in the design of a hump basin are the size and shape of the hump.

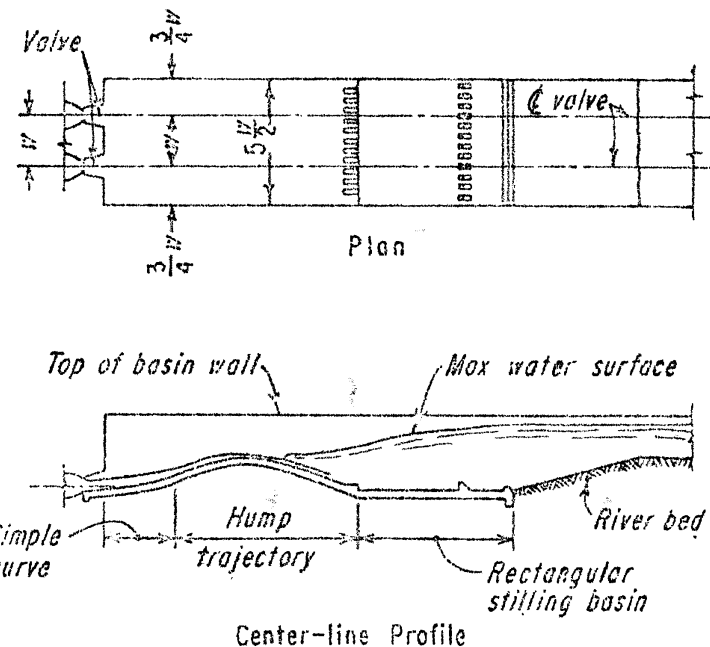


FIG. 14-8. Hump stilling basin.

In designing a hump basin, the chute floor should be shaped in the form of a circular arc at the upstream end and as a parabola at the downstream end. In actual practice, the floor of the chute upstream from the hump is usually shaped by providing one circular curve at the downstream end and another immediately upstream from the hump, with a tangent connecting the two. The portion of the hydraulic-jump basin downstream from the hump should be designed as outlined in Chap. 9.

Laboratory tests have established the fact that when the hump is too high, the jets will not spread out effectively. When the hump is too low, the tailwater for smaller flows will submerge the hydraulic jump. It is recommended that the crest of the hump be as high as the ~~riverbed~~ elevation, in order to permit the jump to form for smaller ~~discharges~~. Extreme caution should be taken in assuring that the jets are spread evenly across the hump crest for all discharges.

In the case of a free-flow tunnel or conduit discharging into a hump basin, the crest of the hump is sometimes placed slightly higher than the crown of the outlet, in order to prevent freezing within the outlet during the winter. A small volume of water exposed to the air between the outlet portal and the hump may be kept from freezing by permitting a small, constant release from the control gates.

A basin of this type was designed for the outlet works of the Horsetooth Dam,² located near Loveland, Colo. Satisfactory operation of the stilling basin was required for a total discharge of 1,500 cfs through two 72-in. hollow-jet valves under a head of 135 ft. The design finally adopted for the Horsetooth Dam is shown in Fig. 14-9. The sill below the valves, the flat portion of the upturned apron, and the head were designed to reduce excessive splash from the jets which discharged onto the apron. A crown

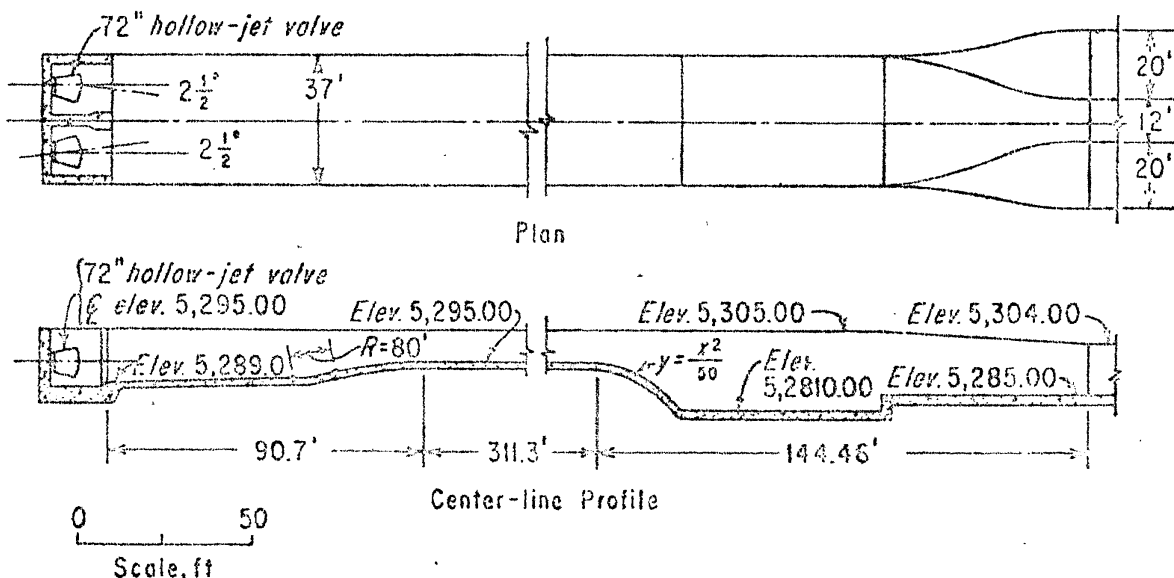


FIG. 14-9. Adopted design for Horsetooth Dam stilling basin.

was placed on the hump to direct the distribution of flow toward the side walls, and this in turn stabilized the formation of the hydraulic jump. Because of the difficulty in predicting the splash in the prototype from model studies, it was decided to defer construction of the hood until data for the operation of the prototype were obtained. An inward valve convergence of $2\frac{1}{2}^{\circ}$ assisted in the performance of the basin.

A hump basin was also designed for the Bull Lake Dam outlet works, shown in Fig. 14-10. Hump basins were also employed at the Tappan,

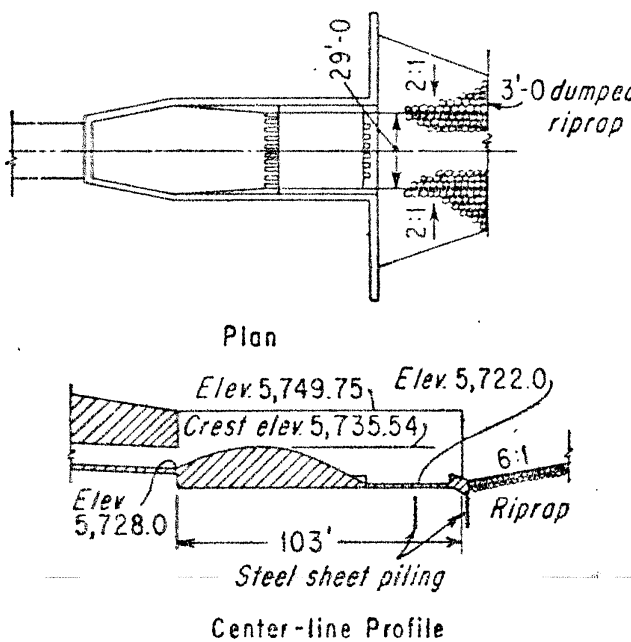


FIG. 14-10. Hump stilling basin for Bull Lake Dam.

Clendering, and Piedmont Dams, operated by the Muskingum Conservancy District in Ohio. This type of basin was preferred when difficulty arose in raising the tunnel located below the streambed level. Performance in the prototype closely agreed with the model.

14-5. Impact Stilling Basins. The least desirable condition in a stilling basin occurs when the jets are completely submerged by the tailwater, since the control gates or valves will be underwater and thus inaccessible. Discharges from the jets may vary from horizontal to vertical, and energy dissipation is accomplished by permitting the jet to impinge upon a pool of water of relatively great depth.

In effect, the horizontal submerged-jet basin is similar to the free-jet chute basin with the chute omitted. For most structures, it will be desirable to depress the jet slightly downward into the pool. Model studies are advisable to determine the optimum dimensions of the basin and the degree to which the valves should be depressed or converged.

Impact basins that require no tailwater for their performance have been designed by the Bureau of Reclamation. These basins are recommended only for entering velocities of less than 30 fps. The efficiency of the

impact basin as an energy-dissipating device is greater than that of the hydraulic jump by the same Froude number, as shown in Fig. 14-11.

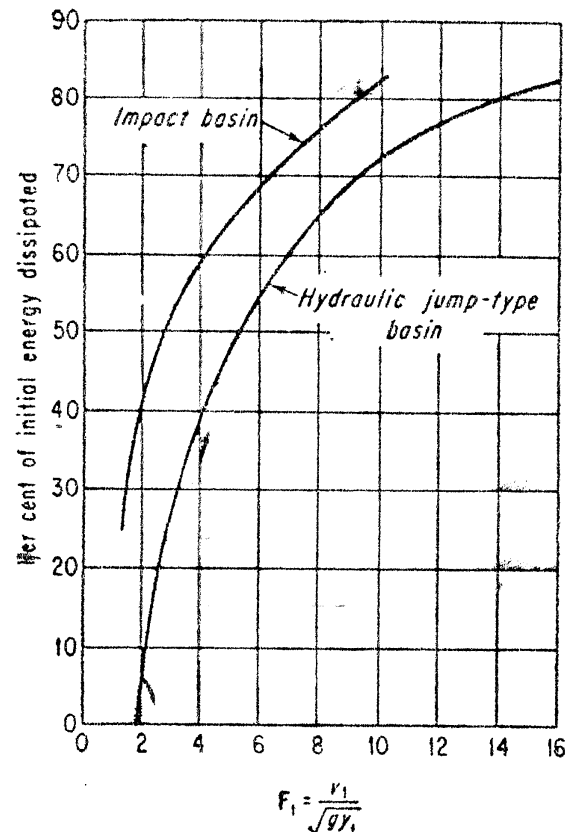


FIG. 14-11. Comparison of energy dissipation by impact and hydraulic-jump-type stilling basins.

The development of the impact basin was initiated by the need for relatively small basins to provide energy dissipation independent of tailwater variations or any tailwater at all.

As shown in Fig. 14-12, a vertical hanging baffle can be used to convert many possible flow patterns into one common pattern. Energy dissipation is initiated when the flow strikes the vertical hanging baffles and is turned upstream and when the floor causes vertical eddies to form. This structure requires no tailwater for energy dissipation, although the addition of tailwater will improve the performance of the basin by reducing the outlet velocities.

For the best operation of an impact basin, an alternate end sill and 45° wall design is recommended, as shown in Fig. 14-13. The entrance conduit may be tilted downward without adversely affecting the performance of the basin. A limit of 10° is a suggested maximum slope, although the loss in efficiency of energy dissipation may not cause excessive erosion.

This type of basin should not be confused with the early impact basins which deflected water high into the air and caused it to form a spray and

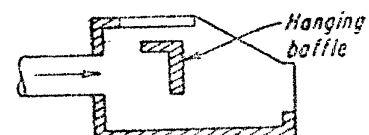


FIG. 14-12. Impact basin.

fall back into the pool below. In this manner, there is a direct impingement of the flow on some obstruction placed in the basin. The chief objections to the early impact basin were the relatively small amount of energy dissipated and the damage caused to piers or other obstructions.

An impact basin was successfully employed in the design of the Pole Hill and Flatiron Power Plants⁷ constructed in Colorado. The problem

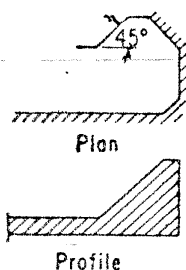


FIG. 14-13.
End-sill design
for impact
basins.

was to develop a suitable stilling basin in the power-plant afterbays, to distribute and quiet the discharge from the turbine-bypass energy absorber, and to prevent erosion damage to the afterbay channels. The Pole Hill and the Flatiron plants are designed to operate under maximum heads of 838 and 1,055 ft, respectively. Dimensions in the model of the impact stilling basin of the Pole Hill plant are shown in Fig. 14-14. Principal features of the basin include a short channel 9 ft wide and 8 ft deep, with a sloping downstream end and two large transverse baffles inclined downstream at an angle

of 75° to the horizontal. A small 45° deflector was installed in the afterbay of the Pole Hill plant to reduce the water velocities along the left afterbay channel.

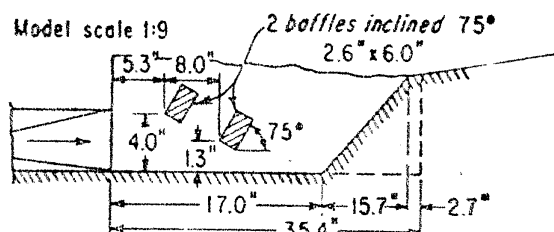


FIG. 14-14. Dimensions of model impact stilling basin, Pole Hill Power Plant, Colorado.

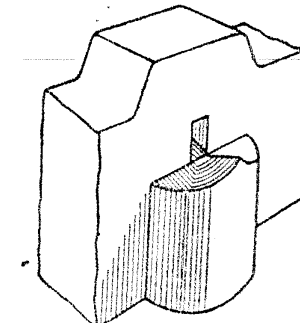


FIG. 14-15. Jet deflector for Tygart Dam conduit exits.

Jet deflectors were used for the outlet conduits of the Tygart Dam,⁵ constructed on the Tygart River near Grafton, W.Va. The jets issuing from each of the eight outlet conduits have a cross-sectional area of 57.5 sq ft and, under a head of 178 ft, the efflux velocity reaches 88 fps. The reduction of velocity of each jet requires that energy be dissipated at the rate of 37,400,000 ft-lb per sec, or 67,900 hp. It is evident that if the high-velocity flow is to be prevented from eroding deep holes in the riverbed below the dam, the energy must be dissipated by impact against a pool of water. For the Tygart Dam, a cushion pool was created by constructing an auxillary dam 250 ft downstream from the main structure.

A sketch of the final design of the jet deflectors for the Tygart Dam is shown in Fig. 14-15. Each deflector proper consists of two conical sur-

faces intersecting each other in the vertical plane. The purpose of the deflector is to flare the jet into a horizontal, fan-shaped sheet.

When a jet is discharged horizontally into a stilling pool, its impact on the water in the pool and its effect of scour on the bottom of the pool will be considerably reduced if the jet is flared out laterally by a jet deflector before striking the pool. Energy-dissipating action in the model was found to be best when the tailwater elevation in the cushion pool was near the mid-point of the conduit exit. It was then found that when the conduits were submerged 50 per cent under average conditions, good energy-dissipating action resulted.

With varying tailwater, it may be desirable to construct an upturned apron with high floor blocks of special design. An example of the use of high-diffusion floor blocks for the All-American Canal stilling basin is shown in Fig. 14-16. This design is characterized by a lip containing notches with sides sloping outward and upward in the direction of flow. Water entering the relatively narrow upstream openings of the notches is forced to diffuse over a much larger area at the top and downstream exit, thereby reducing the velocity.

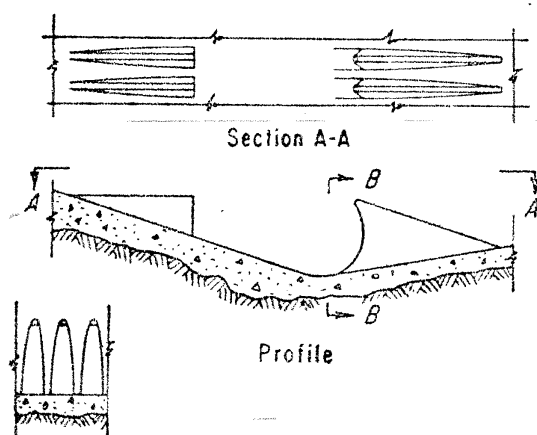


FIG. 14-16. All-American Canal stilling-basin blocks.

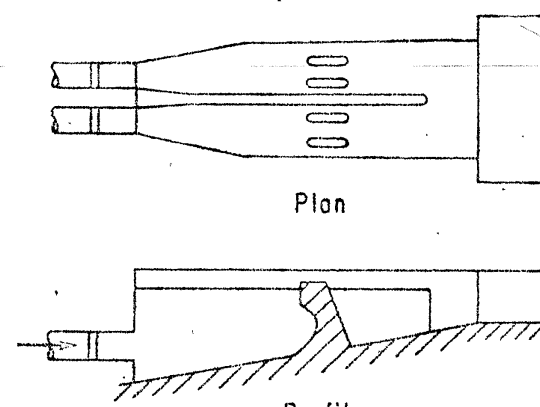


FIG. 14-17. Angostura Canal Outlet Works stilling basin.

Diffusion blocks were also employed on the upturned apron of the Angostura Canal³ Outlet Works, illustrated by Fig. 14-17. The floor blocks on this apron were of a special shape, designed to project above the maximum tailwater elevation, and were undercut in the middle to improve the flow conditions at low tailwater.

REFERENCES

1. Bureau of Reclamation, Hydraulic Model Studies of Deer Creek Dam Spillway and Outlet Works and a Report on the Operation of the Prototype Tube Valves and Stilling Basin, *Hydraulic Lab. Rep.* 215, November, 1946.

2. Bureau of Reclamation, Hydraulic Model Studies of the Outlet Works—Horse-tooth Dam, Colorado Big-Thompson Project, Colorado, *Rep. Hyd.*-263, 1949.
3. Bureau of Reclamation, Hydraulic Model Studies for the Design of the Angostura Canal Outlet Works, Missouri River Basin, South Dakota, *Hydraulic Lab. Rep.* 235, 1947.
4. Bureau of Reclamation, Progress Report II, Research Study on Stilling Basins, Energy Dissipators, and Associated Appurtenances, *Hydraulic Lab. Rep. Hyd.*-399, June 1, 1955.
5. Hamilton, W. S., and H. A. Thomas: Jet Deflectors for High Dam Outlet Conduits, *Civil Engineering*, pp. 297-300, May, 1939.
6. Peterka, A. J.: Spillway Tests Confirm Model-Prototype Conformance, *Bur. Reclamation Eng. Monograph* 16, 1954.
7. Simmons, W. P.: Hydraulic Model Studies of the Stilling Basin for Energy Absorber Discharges at Pole Hill and Flatiron Power Plants, *Bur. Reclamation Hydraulic Lab. Rep.* 353, March, 1953.
8. Tabor, H. W., and A. J. Peterka: Progress in New Designs for Outlet Works Stilling Basin, *Bur. Reclamation Hydraulic Lab. Rep.* 302, 1950.

15

Special Stilling Basins

Several special stilling basins have been developed which have performed very satisfactorily for their intended purpose. The purpose of this chapter is to discuss the unusual, unconventional designs of the SAF, Bhavani, and roller stilling basins. Each of these basins was developed after extensive model tests.

It is recommended that the adoption of the designs of the Bhavani and roller stilling basins be made only after extensive model tests have been conducted. Further tests may indicate the desirability and merits of adopting and standardizing the design. Use of the SAF basin should be limited to drainage structures which discharge relatively small quantities of flow. A photograph of the SAF drop-structure stilling basin at the Milton Air Station, Fla., is shown in Fig. 15-1.

15-1. SAF Basin. The SAF¹ stilling basin, an abbreviation for the Saint Anthony Falls Hydraulic Laboratory, is a term coined to differentiate this design from other types of stilling basins. Principally, the SAF basin has been used for drainage structures where relatively small quantities of flow are released. Although the SAF basin serves the needs for which it was intended, it does not provide a sufficient safety factor for larger basins. Through the addition of stilling-basin appurtenances, the SAF basin has considerably reduced the length of a conventional hydraulic-jump-type stilling basin.

As a result of experimentation, the length of the stilling basin for entering Froude numbers between 3 and 300 was found to be

$$L_b = y_2 \left(\frac{4.5}{F_1^{0.38}} \right) \quad (15-1)$$

Chute blocks are added to the basin to increase the effective depth of the stream and to break it up into a number of jets. The recommended optimum height of the chute blocks is equivalent to y_1 , with a width and spacing of approximately $\frac{3}{4}y_1$.

Floor blocks similar to the baffle piers commonly used in other types of energy dissipators are recommended. In conducting the model tests, particular attention was given to finding the best hydraulic position for these blocks, so that they would not impede the zone of action upstream of the floor blocks and, at the same time, would allow full action of the floor blocks before the flow reaches the end sill. It was discovered that placing the floor blocks at a distance equal to one-third the basin length

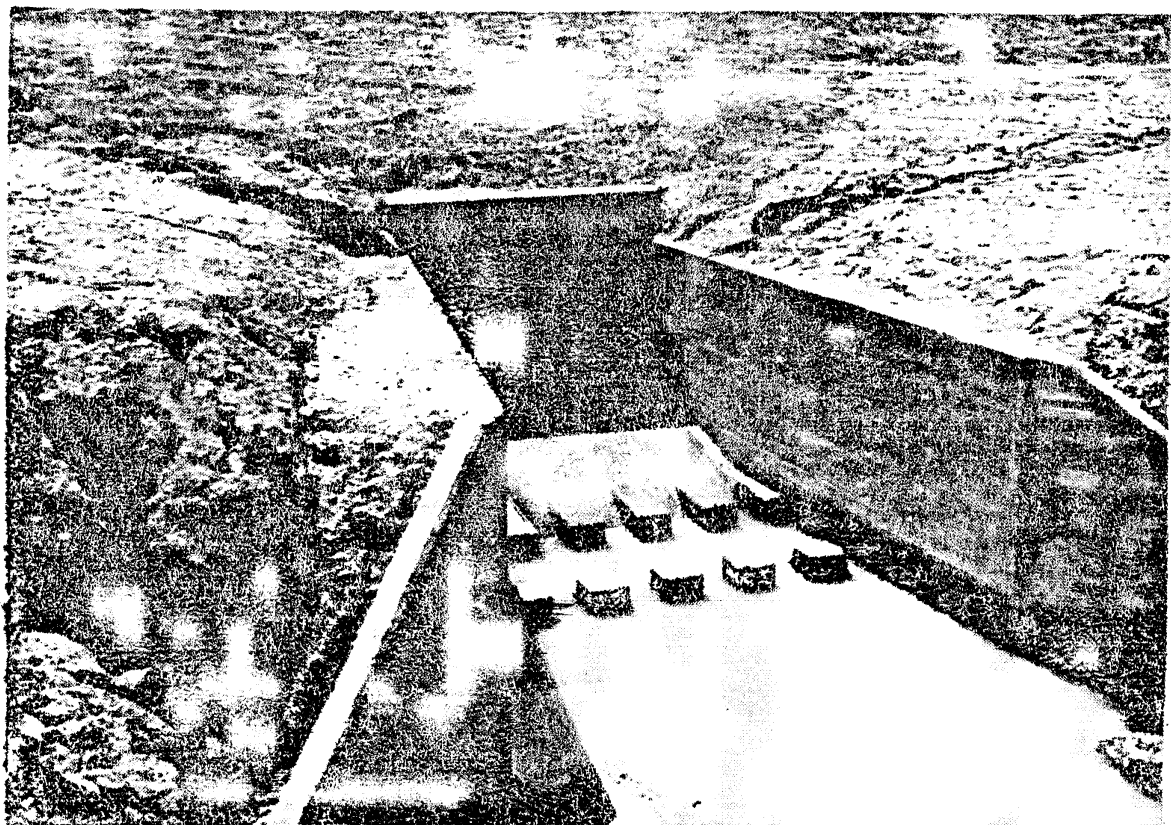


FIG. 15-1. SAF drop-structure stilling basin at the Milton Air Station, Florida. (*Courtesy of St. Anthony Falls Hydraulic Laboratory and Department of the Navy.*)

from the chute blocks produced the best results, both in regard to the minimum erosion behind the basin and lowest height of "boil" above it.

The size and spacing previously chosen for the chute blocks were later found to be applicable also to the floor blocks, provided that the floor blocks were located opposite the empty spaces between the chute blocks. The aggregate width of all the floor blocks should not be less than 40 per cent nor greater than 55 per cent of the total basin width in the section where they are located. No floor block should be placed less than a distance equal to $\frac{3}{8}y_1$ from the side wall.

Investigations showed that an end sill with a height equal to $0.07y_2$ would improve the performance of the basin and reduce scour at its downstream edge. Recommended dimensions for the SAF stilling basin are shown in Fig. 15-2.

The depth of tailwater above the stilling-basin floor is given by the following equations: When F_1 varies from 3 to 30,

$$\text{Tailwater depth} = y_2 \left(1.10 - \frac{F_1}{120} \right) \quad (15-2)$$

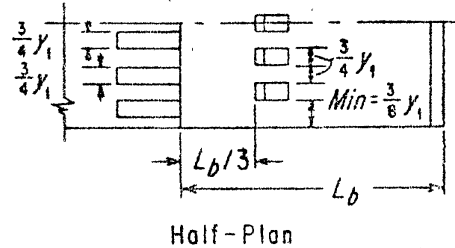
When F_1 varies from 30 to 120.

$$\text{Tailwater depth} = 0.85y_2 \quad (15-3)$$

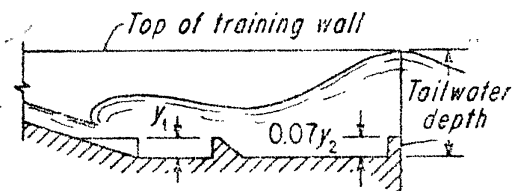
When F_1 varies from 120 to 300.

$$\text{Tailwater depth} = y_2 \left(1.00 - \frac{F_1}{800} \right) \quad (15-4)$$

In estimating the cost of a stilling basin, the height of the side walls will be an important consideration. To prevent the "boil" from splashing over the wall, a certain amount of freeboard must be allowed between the maximum water surface and the top of the wall. Experiments indicate that the freeboard should be made equal to $\frac{1}{3}y_2$. The side walls may be placed parallel to the main axis of flow or they may be divergent in plan. Wing walls should preferably be placed at an angle of 45° to the outlet center line, and their tops should have a slope of 1 on 1 from the top of the side walls. In all cases, a cutoff wall of nominal depth should be placed at the end of the stilling basin.



Half-Plan



Center-line Section

FIG. 15-2. SAF stilling-basin dimensions.

15-2. Bhavani-type Stilling Basin. A relatively new type of stilling basin was designed for the Lower Bhavani Dam,³ constructed in Madras, India. The stilling basin was developed as a result of nearly 300 experiments. The final design has been termed "Bhavani" stilling basin.

The design consists of a depressed apron provided with T-shaped floor blocks that allow the length of the apron to be materially reduced. Energy dissipation is accomplished by the formation of the hydraulic jump and by impact of the high-velocity flow on the T-shaped blocks.

Dimensions of the Bhavani-type stilling basin are materially reduced over those used in a conventional hydraulic-jump-type basin. Flow over the 108-ft-high Lower Bhavani Dam spillway is discharged into a short stilling basin 30 ft long and 10 ft deep. As shown in Fig. 15-3, a single row of the T-shaped blocks 16 ft apart (center to center) was installed in

the basin. Each of the blocks is buttressed against the vertical end wall of the basin by a long wall 4 ft wide and 5 ft deep. This design, developed by the Poondi Irrigation Research Station of the Madras Public Works Department, makes it possible for a hydraulic jump to be formed over a wide range of tailwater fluctuations in a short distance. Cavitation of the blocks in the Bhavani basin seems unlikely, since they are under a high degree of submergence.

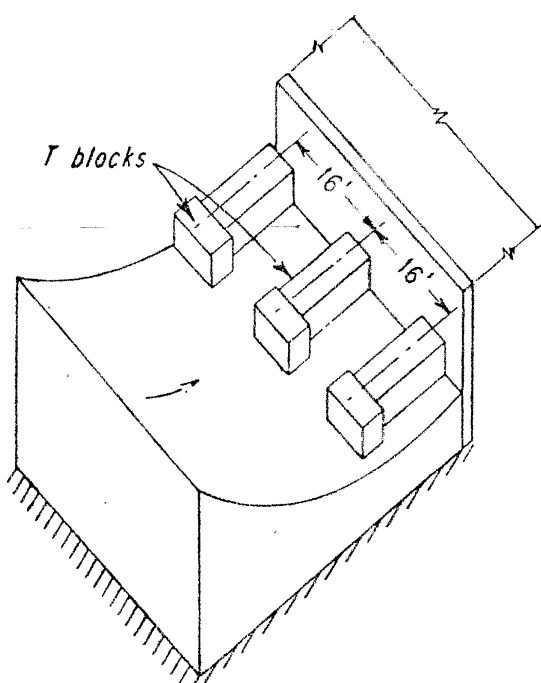


FIG. 15-3. Bhavani-type stilling basin.

stilling basin, depicted in Fig. 15-4, may be utilized. For this type of basin, a characteristic flow pattern results within the range of tailwater depths, at which roller stilling action occurs, if a short basin and end sill are used. This pattern consists of the formation of a standing wave in the vicinity of the end sill together with a surface roller upstream therefrom and of a downstream ground roller in which the bottom velocities continually move in an upstream direction.

Roller-type stilling basins may in some cases make it considerably more economical to use relatively short basins than to use a sloping apron or a horizontal apron specifically designed for submerged-hydraulic-jump conditions. Considerable energy is dissipated in the standing wave and surface roller. The high-velocity vein emerges from the standing wave near the surface of the tailwater, and considerable dispersion occurs before the vein reaches the bottom of the channel downstream from the end sill. Along the channel bottom beneath the vein, a ground roller with relatively mild velocities in an upstream direction continually forms. This tends to deposit material toward the dam rather than away from it.

To date, standard design criteria for roller-type stilling basins have not been developed. Existing designs have, in large measure, been devel-

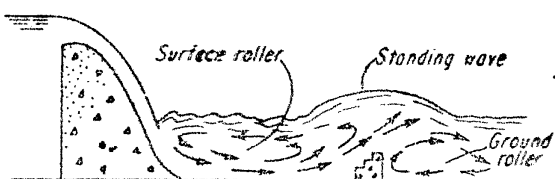


FIG. 15-4. Roller-type stilling basin.

oped as a result of individual hydraulic model studies. The most extensive experiments on roller-type stilling basins were conducted by Feldt,² while attending the State University of Iowa. Design curves were obtained from a small-scale, fixed-bed model with a horizontal apron and stepped end sill.

A serious disadvantage in the use of roller-type stilling basins has been that the high upstream bottom velocities in the ground roller downstream from the end sill may move bed material into the basin, where it may be trapped and become a continual source of scouring action. The use of dentated sills to suppress this action has met with only mediocre success.

Two examples of the roller-type stilling basin can be found at the Fort Gibson and Demopolis dams. The Demopolis Lock and Dam, a navigation project in Alabama, utilizes a roller-type stilling basin composed of two sections. One section is 585 ft long and has a 27.5-ft level apron at elevation 19.0, surmounted by a 4.4-ft-high sloping end sill. The other section is 895 ft long and has a 29-ft level apron set at elevation 45.0 with a 3-ft-high sloping end sill. A flood occurred during April, 1955, when the dam was essentially complete except for several cofferdam cells, which were still in place. The maximum discharge was 85,000 cfs, with a net head of 5.6 ft. In the model, the most critical stilling-basin conditions were obtained with a flow of 80,000 cfs and a net head of 5.9 ft. Observed performance of the prototype appeared the same as that of the model, with no erosion reported.

In 1950, the Fort Gibson Dam, having a concrete gravity spillway controlled by 30 tainter gates 40 ft wide by 35 ft high, separated by 10-ft-wide piers, and totaling 1,490 ft in width, was completed. Ten sluices, each 5.67 ft high by 7 ft wide, are located in the base of the spillway, along the center line of 10 successive spillway monoliths. The inverts of the sluices are horizontal at their outlets and are located about 10 ft above the stilling-basin apron. The sluice outlets are of the "jet-deflector" type, with a tetrahedral concrete block 3 ft high located within the exit portal. Energy dissipation is accomplished within a roller-type stilling basin composed of a 60-ft-long apron and a 6-ft-high stepped end sill. Below the sluices, the model indicated that a somewhat longer apron would be desirable to obtain stilling action and uniform spreading of the sluice flow before passing over the end sill. Accordingly, the basin was made 20 ft longer in the section downstream from the sluices, with dividing walls separating this portion of the basin from the remainder.

In 1953, the stilling basin was dewatered and found to be in good condition, except in the area occupied by the 10 sluices. The apron and end-sill steps below several of the sluices were eroded to a depth of 3 to 4 in. In sections below the left end sill, eroded depths up to 8 in. were found, with the reinforcing steel exposed in some spots. In addition, the steps

on the end sill directly in line with the sluices were eroded to a maximum depth of 6 in. Most of the erosion is believed to have been started by the action of eddies transporting gravel and boulders during the diversion stage. Subsequently, sluice flows helped to deepen the eroded areas.

15-4. Spillway Splitters. A unique method was used to dissipate the energy of flood waters flowing over the Loskop and Vaalbank Dams⁴ in South Africa. Energy dissipation is accomplished by a row of bucketlike projections along the downstream face of the spillway just below the crest. This device, known as a "splitter," spreads and aerates the flow over a large area, thereby reducing erosive damage.

Loskop Dam is an overflow structure with a spillway 800 ft long, located 110 ft above the riverbed. The extra thickness of the spillway crest, as illustrated in Fig. 15-5, was carried up to a point near the crest and then reduced by a horizontal step 6 ft high. Flood flows over the

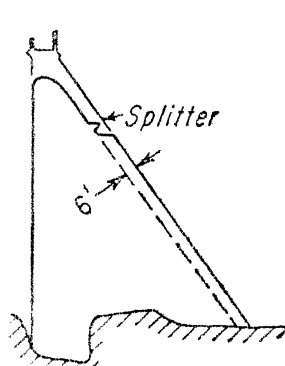


FIG. 15-5. Spillway splitters, Loskop Dam, South Africa.

crest are thrown clear of the dam by the step and strike the apron, located 80 to 90 ft below, in an almost vertical direction. With a design discharge of 100,000 cfs, the energy generated at the toe of the dam would total 1,000,000 hp, or 1,250 hp per foot of spillway width. The length, width, and spacing of the splitters were determined from model tests. At the Loskop Dam, about 100 splitters were used for a spillway length of 800 ft, with a center to center spacing of about 8 ft. The originators of the splitter design have recommended that the device deflect the stream clear of the base of the dam, but not too far downstream to necessitate a long, costly apron.

REFERENCES

1. Blaisdell, F. W.: Development and Hydraulic Design, St. Anthony Falls Basin, *Trans. ASCE*, vol. 113, 1948.
2. Feklt, H. W.: "Roller-type Stilling Action," unpublished M.S. thesis, State University of Iowa, 1945.
3. Kuttiammu, T. P.; and J. V. Rao: Bhavani Type Stilling Basin for Spillways of Large Dams, *Fourth Congr. Large Dams Rep.* 44, New Delhi, India, 1951.
4. Eng. News-Record, Spillway Energy Dissipated on the Face of Dam, p. 99, Dec. 12, 1946.

16

Ski-jump and Arch-dam Energy Dissipators

There are several engineering examples of the use of air to absorb the energy of high-velocity flow. One particularly pertinent example is the use of a ski-jump-type energy dissipator. At the point where the overflow leaves the ski-jump spillway, the concrete is purposely shaped to spread the flow so that the surrounding air can attack the largest possible area. This device has performed very well in France, Portugal, and other countries. Design details of the ski-jump spillways are primarily the work of the French designer, André Coyne.

The remainder of this chapter is devoted to designs and examples of energy dissipators of free-overfall spillways located at or near the center of high-arch dams. Few high-arch dams have been constructed in the United States and, consequently, very little data are available on the design, operation, and maintenance of their energy dissipators.

16-1. Ski-jump Energy Dissipators. Ski-jump energy dissipators are purposely designed to spread the high-velocity flow leaving the spillway so that surrounding air can attack the largest possible area and move the erosive impact of the water away from the toe of the dam. The erosion is usually moved downstream to a less critical location in the riverbed.

As the jet leaves the spillway, it is affected by internal turbulence, by shearing action of the air surrounding it, and by surface tension. If either the internal turbulence or shearing action is large enough, the jet may be partially disintegrated before it strikes the riverbed. It is possible for the jet to disintegrate so completely that it will be composed essentially of a heavy spray formed of various-sized water droplets.

Ski-jump spillways were first constructed in France and used at the 100-m-high Mareges Dam.⁵ Flow from the spillway is thrown high into the air and a hundred feet or more downstream. The resemblance of this falling cascade to a ski-jump is readily apparent. After 15 years of operation, with flood flows ranging from 500 to 1,500 cu m per sec, water had

dug a large pit in alluvium and granite rock. No tendency toward regressive erosion has been found. The pit formed by the impact of the jet on the riverbed is 20 m deep, located 60 m from the spillway lip, and has a movable bottom that takes a new equilibrium shape after each flood. Downstream from the pit, a bar 6 m high was formed as a result of bed material expelled from the pit.

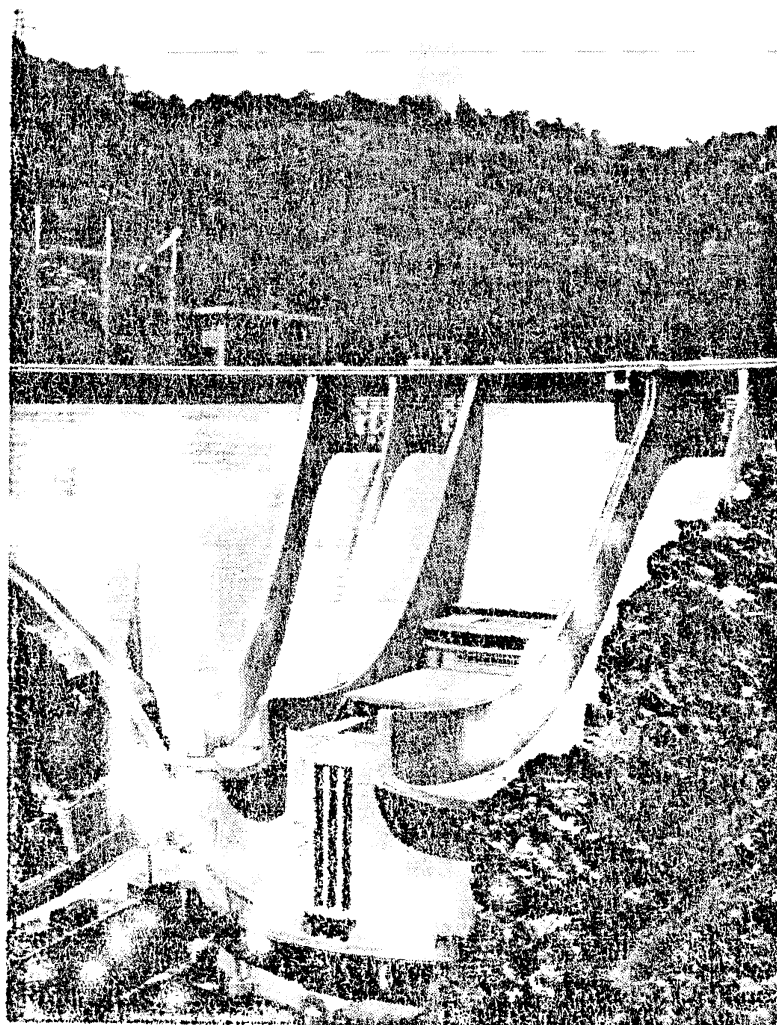


FIG. 16-1. L'Aigle ski-jump spillways, France. (*Courtesy of Constructions Mécaniques et Hydrauliques, Grenoble, France.*)

Three additional dams employing ski-jump-spillway energy dissipators have been constructed on the Dordogne River in central France. They are the L'Aigle, Chastang, and Bort-les-Orgues Dams, having respective heights of 295, 233, and 377 ft.

The two L'Aigle Dam⁶ spillways are placed symmetrically about the dam center line and are designed for a maximum discharge of 2,000 cu m per sec, under a fall of 90 m. Because of the lack of room in the narrow gorge, the spillways were shaped to direct the jets of water into the center of the stream and away from the gorge walls. This was accomplished by tilting the discharge ends of the slab until the inside edges were 10 ft

higher than the outside edges, giving the spillway something of a spoon shape. Flow down the spillway rotates or twists, thereby increasing the height while decreasing the width of the discharge jet. Such rotation also increases air entrainment. With a discharge of 1,000 cu m per sec, the flow was directed 165 ft downstream. For reasons of economy, the spillway also served as the powerhouse roof. The front of the powerhouse is always accessible during spillway discharges, which lower the tailwater level by a water blast effect. Huge waves with violent sprays occur in the impact area, while the water is smooth at the foot of the powerhouse. Erosion of the hard gneiss rock of the Dordogne riverbed is negligible. A photograph of the L'Aigle ski-jump spillways is shown in Fig. 16-1.

The Chastang Dam¹ is also equipped with two ski-jump spillways capable of discharging a total of 140,000 cfs. The spillways also serve as the powerhouse roof and are positioned in such a manner that the jets will intersect. Spillway gates are synchronized by electric controls. A photograph of the Chastang Dam spillways is shown in Fig. 16-2.

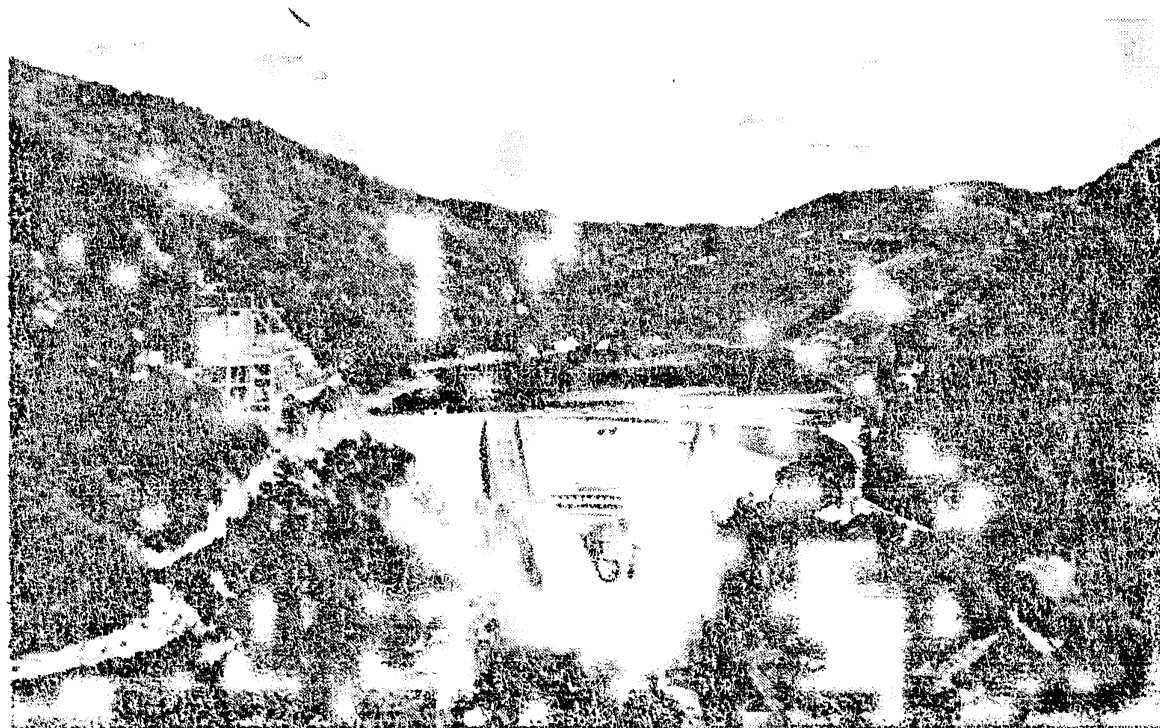


FIG. 16-2. Chastang Dam ski-jump spillways in operation, France. (*Courtesy of Constructions Mécaniques et Hydrauliques, Grenoble, France.*)

St. Étienne-Cantales Dam, constructed on the Cere River in France, has a single ski-jump spillway which carries the flow over the powerhouse and deflects it far away from the dam. The total drop from spillway crest to tailwater elevation is almost 200 ft, with a design discharge of 1,200 cu m per sec.

In Portugal, ski-jump spillways of the Castelo do Bode and Picote

Dams, illustrated by Figs. 16-3 and 16-4, respectively, have operated satisfactorily. The two ski-jumps of the Castelo do Bode Dam are designed to discharge a total of 141,000 cfs.

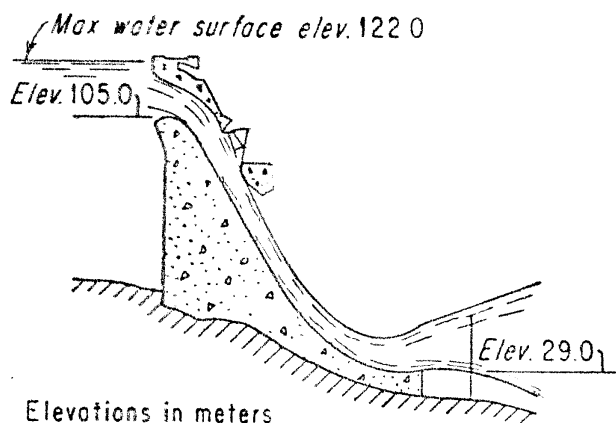


FIG. 16-3. Castelo do Bode Dam spillway, Portugal.

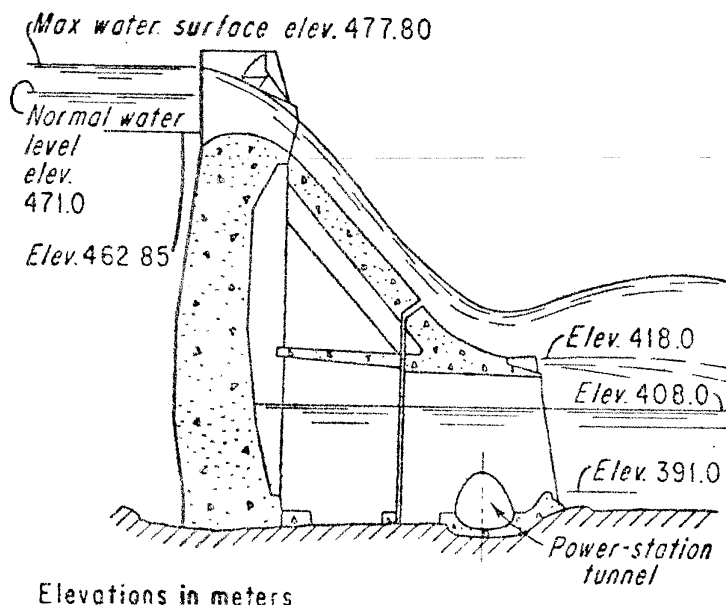


FIG. 16-4. Picote Dam spillway, Portugal.

The 110-m Kamishiiba Arch Dam,² located on the Mimi River near Kamishiiba, Japan, employs twin ski-jump spillways capable of discharging 2,160 cu m per sec. Model tests were conducted to assure that the jets impinge upon each other. During October, 1955, the spillways were subjected to flood flows of approximately 1,000 and 680 cu m per sec, and model-prototype conformance was found to be fairly good.

A ski-jump spillway was also employed for the Cleveland Dam,⁴ constructed near Vancouver, British Columbia. In order to reduce the cost of the structure, a ski-jump spillway was adopted in preference to a hydraulic-jump-type basin. The end of the ski-jump spillway, illustrated by Fig. 16-5, was slotted to form splitters, which spread the flow and deflected it high into the air for all discharges. Subatmospheric pressures sufficient to cause cavitation occurred on the concrete surface just

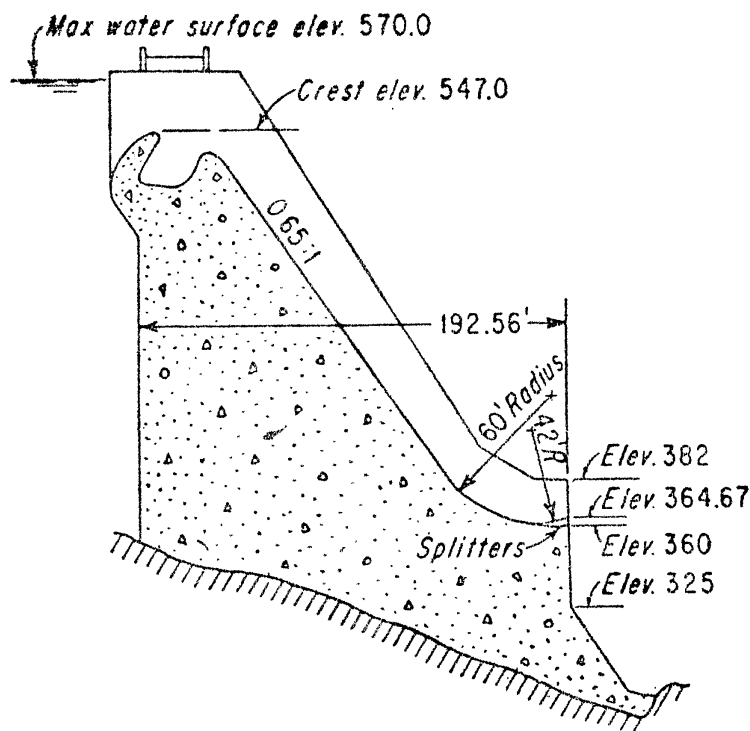


FIG. 16-5. Cleveland Dam spillway, British Columbia.

below the sharp edges of the flow splitters. Cavitation can be eliminated by rounding or chamfering the edges of the splitters. With a maximum design discharge of 43,000 cfs, erosion took place far enough downstream to preclude any damage to the structure.

Table 16-1 lists the design characteristics of existing ski-jump spillways.

TABLE 16-1. SKI-JUMP SPILLWAY CHARACTERISTICS

Structure	Location	Number of spillways	H	h/H	Q	q
Bort.....	France	One	377	0.64	42,200	977
Castelo do Bode.....	Portugal	Two	370	0.82*	70,600	2,690
Chastang.....	France	Two	233	0.59	70,400	1,580
Cleveland.....	British Columbia	One	300	0.62	43,000	540
Genissiat.....	France	210	0.75	95,000	1,935
Kamishiiba.....	Japan	Two	361	0.30†	38,000	600
L'Aigle.....	France	Two	295	0.60	70,400	1,342
Mareges.....	France	One	253	0.48	24,600	290
Picote.....	Portugal	One	298	0.66		
St. Étienne-Cantales.....	France	Two	230	0.53	17,600	753

NOTE: H = vertical distance between maximum pool elevation and riverbed, ft; h = vertical distance between maximum pool elevation and spillway exit, ft; Q = discharge for single spillway, cfs; q = discharge per foot of spillway width at exit, cfs.

* Right spillway only.

† Average.

In general, ski-jump-spillway energy dissipators may prove satisfactory when the downstream channel is composed of exceptionally high-quality rock. Considerable spray will occur, which may be undesirable if other structures are located immediately downstream from the dam. In all cases, it is strongly recommended that the design of ski-jump energy dissipators be verified by model studies. Some of the considerations in plan include convergence of the side walls, the angle of the lip, and the shape of the dentated sill that provides the best possible aeration of the jet.

16-2. Free-overfall Spillways of Arch Dams. Energy dissipation below an overflow spillway located at or near the center of a high-arch dam is similar to the problem of determining the hydraulic behavior below a free overfall. Operation and maintenance experience on free-overfall spillways has proved this type of spillway to be a satisfactory means of discharging flood waters over arch dams. Flow from the outlets of the Arrowrock Arch Dam is shown in the photograph of Fig. 16-6.

Erosion below a free overfall will be affected by the following features:

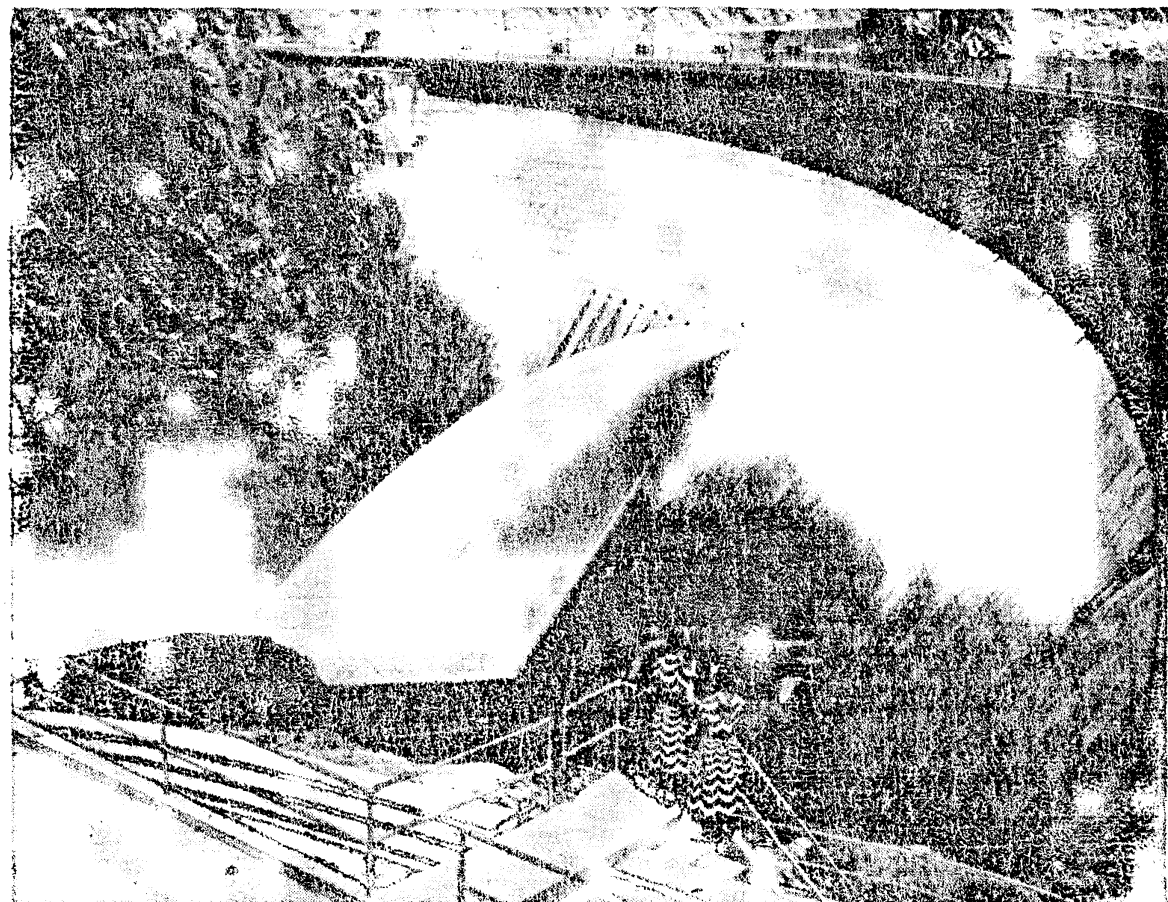


FIG. 16-6. Discharges from outlets of Arrowrock Dam, Idaho. (Courtesy of Bureau of Reclamation.)

energy, thickness and angle of inclination of the jet, depth of pool, and characteristics of material being scoured. The last factor is by far the dominant one. It is sometimes thought that the most rapid erosion occurs at places where the velocities are the highest. It is more probable, however, that erosion is caused by differential pressures which cause particles to be lifted into the stream and then carried away. If the second thesis is accepted, the problem of rock erosion by a falling jet can be avoided by protecting the rock with a concrete mat at those points where damage might occur. Drains should be constructed beneath the mat. This will limit the development of differential pressures should dynamic pressures penetrate along the cracks and joints.

Other factors, while playing a part in erosion, also influence the differential pressures acting on the material being eroded. This is certainly true of the energy content of the jet. In the case of jet size, the thicker the jet, the deeper will be the penetration into the pool. The angle of inclination of the jet and depth of pool also contribute to the effectiveness of energy dissipation. The narrower the valley, the greater will be the depth of water in the riverbed for higher discharges, which facilitates energy dissipation. Therefore, it can be seen that all these factors influence the jet-energy content, which in turn affects the differential pressures acting on the material being eroded.

A horizontal concrete mat constructed on solid rock at the base of an arch dam will usually provide the desired protection. Some designers may be concerned over the ability of concrete to resist erosion due to high velocities. In the cases of the Walters and Kerr Dams, high-velocity jets struck the concrete mat in a nearly vertical direction with no resultant erosion. One of the severest exposures of concrete to the direct action of high-velocity flow occurred in tests made by the Bureau of Reclamation.³ In the course of these tests, jets of water with a velocity of 175 fps were directed against concrete blocks for periods of from 2 to 39 days. This resulted in a remarkably small amount of erosion. It can be safely concluded that if the concrete mat is properly designed and constructed, it should be able to resist the direct action of high velocities of any free-overfall spillway within economic dam heights, irrespective of the depth of water cushion over the mat.

The solid stream of water on the mat imposes a steady dynamic force on the concrete, which must furnish the reaction developed in turning the jet into a horizontal direction. Once the jet is turned, the water thrashes about, developing vibrations. The impact of the water particles is random, so there is little danger of a synchronous period of vibration being developed.

In many hydraulic problems, it is impractical to obtain prototype data

on hydraulic behavior. For this reason, resort is frequently made to laboratory studies to analyze particular actions and evaluate their effects, at least qualitatively, if not quantitatively. The destruction of energy contained by a free-falling jet entering a pool of water is an example of this type of problem. The lack of uniformity in presenting these data makes comparison difficult.

Laboratory experiments indicate that the following factors influence the depth of scour: discharge per unit spillway crest length, height of overfall, tailwater depth, and characteristics of bed material. Studies have revealed that the discharge per unit spillway crest length is by far the predominant factor in the scour of an erodible bed material. For example, doubling the unit discharge while keeping the height of fall constant will increase the depth of scour about 50 per cent, but in order to develop the same increase in scour with the discharge remaining constant, the height of fall would have to be increased six or seven times.

Factors affecting the dissipation of energy are, in the order of their importance, discharge per unit spillway ~~crest length~~, depth of pool, and height of fall. The kinetic energy due to ~~the height of~~ fall increases only to the point at which the effect of an increasing amount of air is compensating. Beyond this point, the energy content may be reduced by diffusion of the jet in air.

Table 16-2, prepared by Ebasco Services Incorporated, lists prototype data for free-overfall spillways and arch dams.

TABLE 16-2.* FREE-OVERFALL ARCH-DAM SPILLWAYS

Structure	Maximum spillway height, m	Maximum design Q		Theoretical velocity,* m per sec	Dynamic forces	
		Q , m^3 per sec	Tailwater depth, m		Total force, million kg	Maximum pressure, kg per cm^2
Cabinet Gorge†..	57	7,100	30.5	20.3	14.7	5.7
Deadwood†.....	42	320	29.0	0.9	4.2
Kamishiiba.....	110	1,800	12.8	43.3	8.0	11.0
Kerr†.....	55	3,400	31.0	11.1	5.5
Lumieit†.....	134	250	48.9	1.2	13.4
Parker†§.....	98	11,300	80.0	19.3	22.3	9.8
Santa Anita† ..	69	35.7	6.9
Val Gallina†.....	92	200	40.8	0.8	9.2
Walters†.....	60	1,700	7.6	31.6	5.5	6.0

* At base of dam.

† Downstream rock protected by concrete.

‡ Downstream rock not protected by concrete.

§ Unusually deep tailwater.

At the Parker Dam, where the overflow nappe is very thick, reliance was apparently placed on deep tailwater, whereas at the Kerr Dam, which also has a thick nappe, tailwater depth was considered to be insignificant. There appears to be little if any consistency among engineers in their approach to the relationship between height of fall and tailwater depth.

REFERENCES

1. Auroy, F.: "Les Évacuateurs de crues du barrage de Chastang," paper delivered before the Fourth Congress on Large Dams, New Delhi, India, 1951.
2. Bonin, C. C., H. W. Stuber, K. M. Mathisen, and H. Kimishima: Kamishiiba Arch Dam, Design and Construction Measurements and Studies, Ebasco Services, Inc., June, 1956.
3. Bureau of Reclamation, Boulder Dam Studies, part VI, *Bull.* 1, 1938.
4. Bureau of Reclamation, Hydraulic Model Studies of the Ski-jump Spillway for Cleveland Dam, Greater Vancouver Water District, British Columbia, *Hydraulic Lab. Rep.* 369, May, 1953.
5. Coyne, A.: "Observation sur les déversoirs en saut de ski," paper delivered before the Fourth Congress on Large Dams, New Delhi, India, 1951.
6. Free Overfall Spillways, Mountain Sheep and Pleasant Valley Arch Dams, Ebasco Services, Inc., January, 1955.

Drop-structure Stilling Basins

A drop structure can be defined as a combination of an inclined drop and a stilling basin. Primarily, drop structures are utilized to control the water-surface elevation or stream gradient. When placed at intervals along a gully, these structures can also be used to change the profile from a steep gradient to a series of gently sloping reaches separated by artificial drops.

Drop structures can be classified as being vertical or inclined and may be of rectangular or trapezoidal shape. Design data will be presented only for the vertical drop structure, since the inclined drop is analogous to the canal drops discussed in Chap. 9.

17-1. Rectangular Drop Structures. For satisfactory performance, the structure must drop the water within its own confines and discharge it downstream in such a manner as to cause a minimum of locally intensified erosion. The action produced by this structure laterally constricts the flow and often creates an objectionable deposition of silt material at the end of the drop structure. Although the performance of the drop structure does not require any tailwater, the addition of tailwater will improve flow conditions within the basin.

A typical vertical drop structure is illustrated by Fig. 17-1, which shows the variable elements of the basin. For each problem, it is

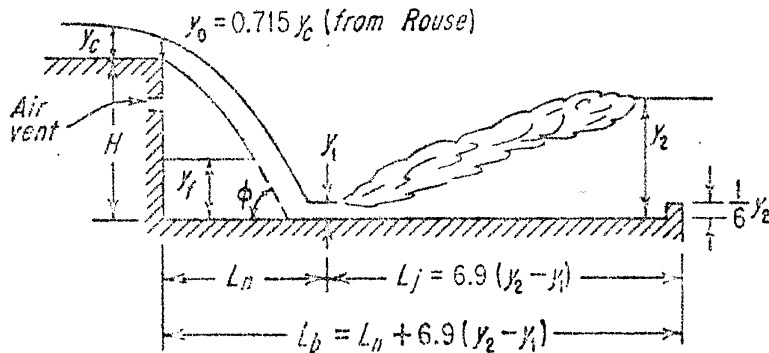


FIG. 17-1. Typical vertical drop structure.

assumed that the design discharge and height of fall have already been determined. The first step will be to determine the critical depth y_c and the ratio y_c/H .

Recent experiments by Rand⁶ indicate that for vertical rectangular drop structures

$$\left(\frac{y_1}{H} = 0.54 \left(\frac{y_c}{H} \right)^{1.275} \right) \quad (17-1)$$

and

$$\frac{y_2}{y_1} = \frac{3.07}{(y_c/H)^{0.465}} \quad (17-2)$$

Both y_1 and y_2 can be found by using Eqs. (17-1) and (17-2), after y_c/H has been determined. These equations were developed from experimental data and therefore include energy losses.

The flow geometry within the basin will depend upon the discharge, height of drop, and depth of uniform flow in the channel both upstream and downstream from the drop structure.

The drop distance L_n can be determined from the experimental data collected by Rand. A plot of L_n/H versus q^2/gH^3 is shown in Fig. 17-2.

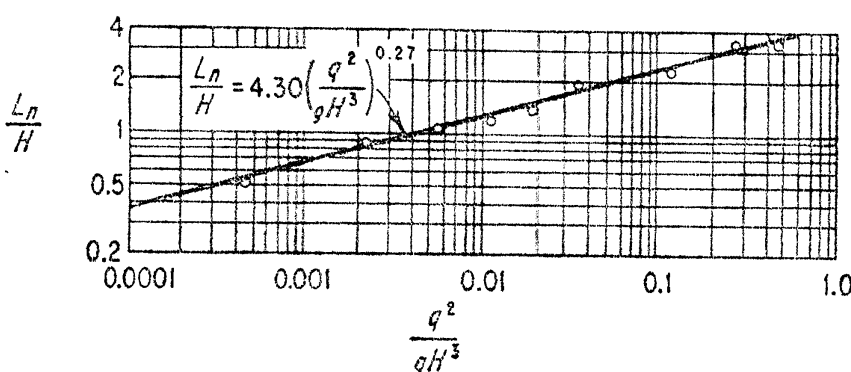


FIG. 17-2. Determination of vertical drop length.

The length of the basin should be made equal to L_n plus the length of the jump, as shown in Eq. (17-3).

$$L_b = L_n + 6.9(y_2 - y_1) \quad (17-3)$$

For erodable channels it may be necessary to extend the apron somewhat farther downstream beyond the length of the basin given by Eq. (17-3), and for stable channels the converse will be true. A great deal of energy is dissipated by the transfer of energy from the falling nappe to the circulating flow in the pool. Figure 17-3 shows the values of H/y_c versus E_1/y_c developed by Moore⁵ for both experimental data and theoretical values (no energy loss).

In Fig. 17-3, a horizontal line drawn between the initial head and experimental curve represents the head loss of the stream due to the existence of a pool upstream from the impingement of the jet. The

magnitude of this dissipation shows the effectiveness of such a pool in reducing the head. An increase in energy dissipation can be had by increasing the width of the overfall section and thereby reducing y_c . It should be remembered that the loss at the base of a fall is neither negligible nor constant, but varies over a considerable range as a function of the relative fall height. Maximum energy dissipation will occur in the transition zone between the pool and the jet, where the energy gradient has its maximum slope.

$$\frac{E_1}{y_c} = \frac{\sqrt{2}}{1.06 + \sqrt{\frac{H}{y_c} + \frac{3}{2}}} + \frac{\left(1.06 + \sqrt{\frac{H}{y_c} + \frac{3}{2}}\right)^2}{4}$$

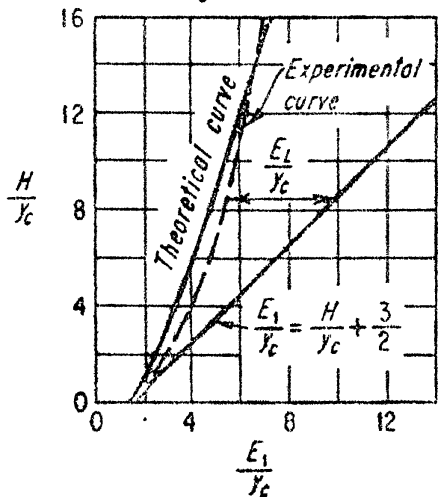


FIG. 17-3. Energy dissipation at the base of a free overfall.

The angle of impingement ϕ , shown in Fig. 17-1, was developed by Ippen⁴ and can be computed by using Eq. (17-4).

$$\cos \phi = \frac{1.06}{\sqrt{(H/y_c) + \frac{3}{2}}} \quad (17-4)$$

In Fig. 17-1, y_f , representing the depth of water standing behind the fall, is used to make stability calculations for drop structures. Moore⁵ suggests the following equation for determining y_f :

$$y_f = y_c \left[\left(\frac{y_1}{y_c} \right)^2 + 2 \left(\frac{y_c}{y_1} \right) - 3 \right]^{\frac{1}{2}} \quad (17-5)$$

An end sill should be placed at the end of the basin to assist the formation of a ground roller below the basin and thereby cause material to be deposited in an upstream direction. Experiments have indicated that the optimum dimension for the height of the end sill is approximately one-sixth y_2 .

Tests by Blaisdell and Donnelly¹ indicate that the side walls should be vertical or placed on a slope of 1 on 1. If the side walls are flatter than 1 on 1, the flow does not spread out rapidly enough to follow the side walls. Consequently, the main stream will be concentrated at the center of the stilling basin, and whirls will develop between the main stream and the side walls.

If the stilling-basin side walls are flared, longitudinal sills should start at the exit of the box inlet and extend to the end sill. The height and width of the longitudinal sills should be equal to the height of the end sill. For most conditions, only two longitudinal sills will be necessary. Each sill should be placed at a distance from the center line of the basin and be equal to approximately one-fourth to one-sixth the basin width.

Wing walls should be constructed at the end of the basin to protect the side walls from scour, caused principally by eddies. The wing walls should be placed at an angle of 6°, and the center line and the slope of the top of the wing walls should be 1 to 1. Flare angles of 45° are permissible, but wing walls parallel to the outlet center line should be avoided.

Based on two previous designs, the Soil Conservation Service and St. Anthony Falls hydraulic laboratory designed the Whiting straight drop spillway² outlet for the Whiting Field Naval Air Station at Milton, Fla. This structure, depicted by Fig. 17-4, has an end sill and only one row of baffles. These appurtenances proved to be satisfactory, although some scour still occurred along the center line of the basin.

An air vent in a drop structure will be necessary, since without it a low-pressure area will be formed under the fall when air bubbles are trapped and carried downstream, thereby causing water to rise behind the vertical drop.

It should be remembered that a hydraulic jump will not readily form in the stilling basin of a drop structure, because of the lack or variability of the tailwater.

17-2. Trapezoidal Drop Structures. Drop structures with trapezoidal cross sections that have been built in the past have exhibited various undesirable characteristics. This is partly attributed to the fact that an inefficient hydraulic jump was formed and only a relatively small amount of the total energy contained in the flow was dissipated in the stilling pool.

It was observed that in some cases a single current appeared to shoot through the basin in an unstable fashion and failed to spread out across the entire cross-sectional area. As a result of this instability, waves were formed on the surface of the canal section below the drop and caused serious erosion of the canal banks. At higher flows, strong side rollers formed just below the structure and water swept back along the sides of the pool, causing erosion of the canal banks and transition lining. For some flows, an unstable whirlpool formed in the stilling basin, instead of the intended hydraulic jump. Again, in other ranges of flow, the jump swept completely out of the stilling basin and formed in the canal section below the drop.

Poor operation is caused by the inherent tendency of the trapezoidal drop to concentrate the flow of water entering the pool into a relatively

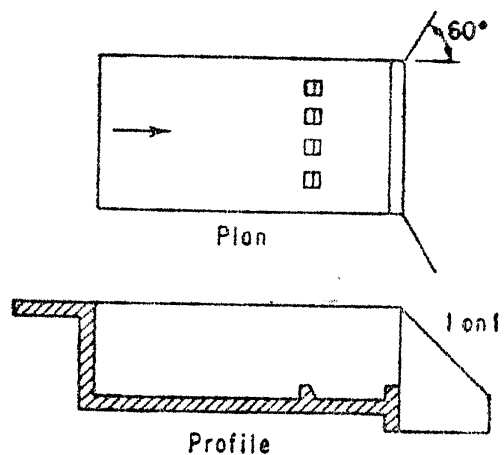


FIG. 17-4. Whiting straight drop spillway, Florida.

narrow jet, which shoots along the bottom of the pool and fails to spread out across the entire cross-sectional area of the stilling pool, particularly in the triangular areas bounded by the basin sides and the water surfaces. Trapezoidal drop structures have been developed by the Bureau of Reclamation which have resulted in a major saving through the elimination of the form work for placing the concrete and through a sizable reduction in the quantity of reinforcing steel required by the conventional rectangular drop structure.

Based upon hydraulic model studies, the trapezoidal drop structure depicted by Fig. 17-5 is recommended for discharges less than 200 cfs. The recommended structure consists of two V-shaped channels, to divide the flow evenly and baffle piers installed near the upstream end of

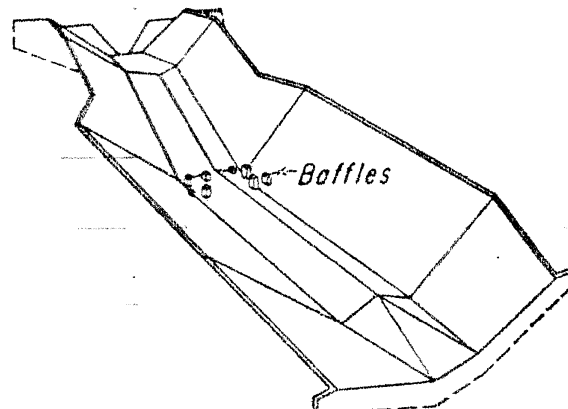


FIG. 17-5. A typical trapezoidal drop structure for flows up to 200 cfs.

the basin to reduce wave heights in the canal and distribute the flow. The two jets deflected by the basin sides intersect at the bottom of the pool near the lower end of the basin. Baffle piers should be staggered and arranged so that they do not become obstructed with floating trash and debris. Trapezoidal drop structures of this design were used for the Sand Hollow Wasteway,³ constructed near Caldwell, Idaho.

REFERENCES

1. Blaisdell, F. W., and C. A. Donnelly: Straight Drop Spillway Stilling Basins, *St. Anthony Falls Hydraulic Lab. Paper 15*, ser. B, October, 1954.
2. Blaisdell, F. W., and C. A. Donnelly: Hydraulic Model Studies for Whiting Field Naval Air Station, Milton, Florida, *Soil Conservation Service and St. Anthony Falls Hydraulic Lab. Rep. 23*, 1950.
3. Bureau of Reclamation, Hydraulic Model Study of Trapezoidal Drop Structures for Sand Hollow Wasteway (East Branch), *Hydraulic Lab. Rep. 250*, May, 1949.
4. Ippen, A. T.: "Engineering Hydraulics" (H. Rouse, ed.), p. 575, John Wiley & Sons, Inc., New York, 1950.
5. Moore, W. L.: Energy Loss at the Base of a Free Overfall, *Proc. ASCE*, pp. 1697-1714, November, 1941.
6. Rand, W.: Flow Geometry at Straight Drop Spillways, *Proc. ASCE*, paper 791, September, 1955.

18

Bucket-type Energy Dissipators

When the streambed is composed of rock, a bucket-type energy dissipator may allow the use of a relatively short structure, with marked economy over a sloping-apron or hydraulic-jump-type stilling basin. In the case of roller buckets, a considerable portion of the energy is dissipated in the bucket, while other types of buckets are used to deflect the flow as far away from the dam as possible.

Slotted buckets have been adopted for low and medium-high dams and have operated satisfactorily in preventing bed material from becoming trapped in the bucket. Trajectory and tunnel-deflector buckets are employed to direct the flow away from the outlet or dam during infrequent or emergency use of the spillway.

This chapter discusses the principal features of bucket-type energy dissipators and gives examples of their use. Until design criteria are fully developed, all bucket-type energy-dissipator designs should be verified by model tests.

18-1. Solid Roller Buckets. A solid roller bucket may be suitable when the tailwater depth is moderately in excess of that required for the formation of a hydraulic jump. The solid roller bucket depicted in

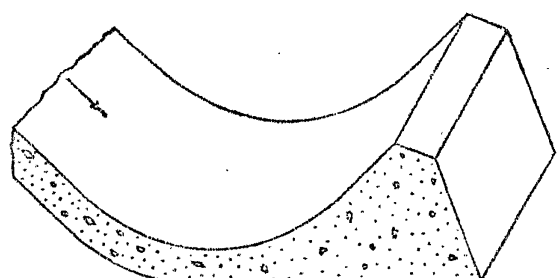


FIG. 18-1. A typical solid roller bucket.

Fig. 18-1 consists simply of a bucketlike apron with a concave, circular profile of considerable radius, and a lip which will deflect the high-velocity flow away from the streambed. The sheet of water is deflected upward by the bucket lip, forming two elliptical rollers: a surface roller, or high boil, on the water surface and a ground roller below the bucket. Energy dissipation is accomplished by interaction of the submerged roller in the bucket and the high boil created on the water surface above and below the

bucket. Reverse flow in an upstream direction along the streambed is provided by the ground roller. Typical action of a solid roller bucket is shown in Fig. 18-2. As a result of this action, the high-velocity vein emerges from the standing wave near the surface of the tailwater, and considerable energy dissipation occurs before it reaches the channel bottom. Beneath the remaining high-velocity vein, a ground roller continually forms, with relatively mild bottom velocities in an upstream direction. This action tends to deposit material against the bucket lip rather than transport it away.

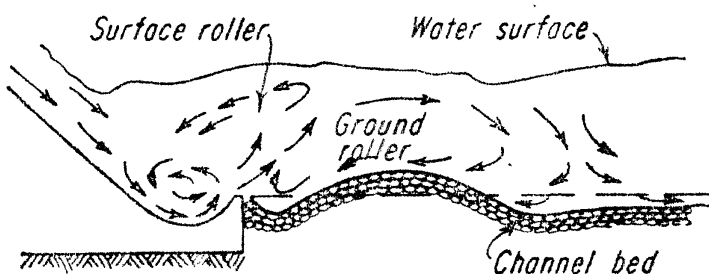


FIG. 18-2. Typical action below a solid roller bucket.

Existing designs have, in large measure, been based on the results of individual model tests. One disadvantage of this type of energy dissipator is that the upstream velocities in the ground roller downstream from the bucket may move bed materials into the bucket. When this occurs, the material may be trapped and become a continual source of scouring action. To some extent this action can be suppressed by the use of a dentated bucket lip. When large quantities of bed material are drawn into the bucket, the dentated lip may be damaged by abrasion.

The bucket radius should be selected by trial, with consideration given to the ability of the exit area to withstand high velocities in the exit channel. Cost estimates should be made for several trial widths and bucket radii, along with corresponding bucket depths. The optimum bucket will be the one which costs the least and which still functions satisfactorily. Model tests conducted at the Waterways Experiment Station¹³ have indicated that the volume of water in the bucket has little effect upon bucket action.

The height and slope of the bucket lip are of particular importance in deflecting the flow upward and maintaining a sizable ground roller below the bucket. The smaller the roller, the less effective it will be in deflecting the jet away from the channel bottom. It has been determined from model tests that a 45° lip slope is necessary to secure the best results. If the lip slope is made steeper, the impact of the flow on the lip wall will disrupt the roller action. For flatter lip slopes, the high-velocity flow becomes submerged downstream from the lip. If possible, the height of the bucket lip should be made approximately equal to one-sixth the

maximum tailwater depth. To prevent material from being drawn into the bucket, the channel-bed elevation should be set slightly below the bucket lip elevation. Figure 18-3 shows the recommended dimensions of the bucket lip height and slope.

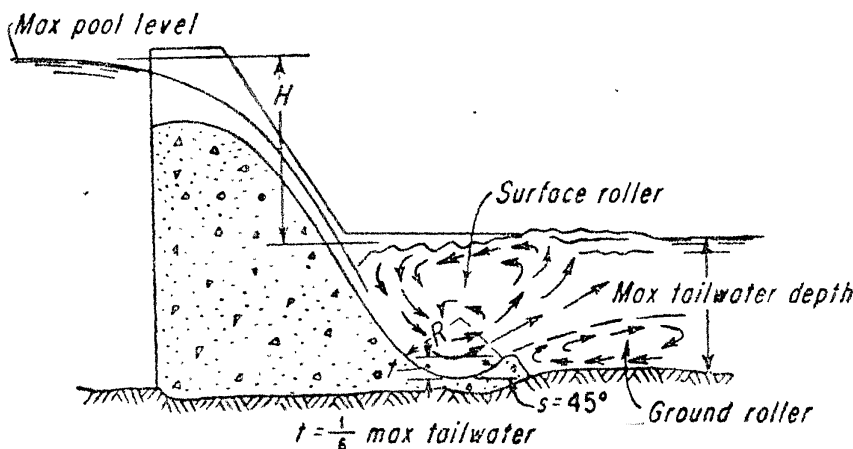


FIG. 18-3. Solid-roller-bucket dimensions.

Model tests should be made to assure that satisfactory bucket action occurs for the expected tailwater conditions and discharges. In general, the minimum tailwater depth should be made equivalent to approximately 110 per cent of the depth necessary for the hydraulic jump to form. When the tailwater depth is lowered materially, the high-velocity jet may have sufficient momentum to break through the supernatant water blanket and result in flip-bucket action. For excessive tailwater depths, the entering sheet will dive toward the bottom, and only a small amount of energy will be dissipated. Trial settings of the bucket-invert elevation should be made so that satisfactory bucket action will exist for both the maximum and minimum tailwater conditions.

When sluices discharge into the bucket, their ends should be curved downward to avoid causing the jets to impinge on the bucket lip, thereby subjecting it to great impact. At tailwater depths above the bucket lip, flow from the sluices is cushioned by water in the bucket. For tailwater depths below the bucket lip, sluice flows follow the curvature of the bucket and are spread over a large area by the lip. A large amount of spray will result in bucket action, and spray walls must be designed to guide the flow down the spillway.

There are very few spillway buckets which have undergone large flow releases. This is brought about primarily by the fact that the flood-control storage provided in the reservoir often contains the flood of record, and only rare floods produce major spillway discharges. Consequently, a number of years may elapse before a spillway bucket is exposed to large spillway flows. For this reason, the bucket training walls are frequently

designed to be overtopped. When overtopped, side flows over the walls tend to submerge the flow from the spillway instead of permitting the bucket to deflect the flow upward. Unsymmetrical gate operation may cause eddies to sweep material into the bucket and make this type of bucket undesirable. Once the material is in the bucket, it becomes trapped and may cause considerable erosion to the concrete surfaces as it moves about laterally and longitudinally inside the bucket arc. For gate-controlled dams, low dividing walls between outlets in the bucket are

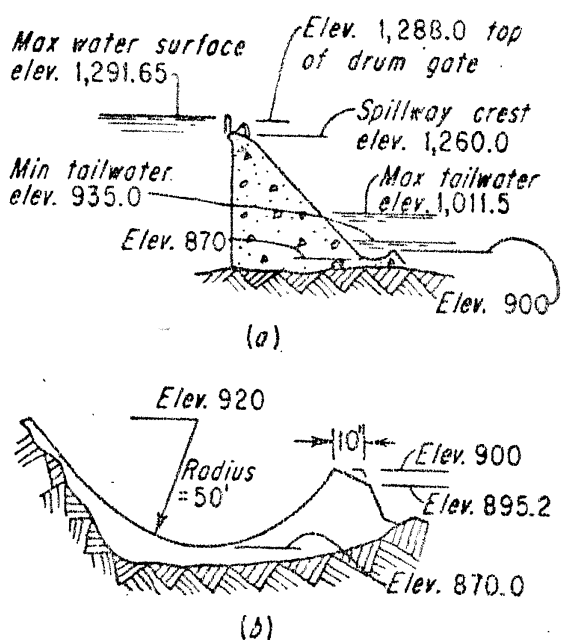


FIG. 18-4. Grand Coulee spillway bucket dimensions.

the energy to be dissipated at the base of the dam totals 31,800,000 hp, or 193,000 hp per foot of spillway crest length.

As a result of model studies, the final design shown in Fig. 18-4a and b was adopted. In the course of these studies, model buckets with radii of 30, 50, 75, and 100 ft were tested. The circular roller produced by the 30-ft bucket was much less effective than the elliptical roller of the 50-ft bucket. Use of a 75- or 100-ft radius resulted in an improvement too slight to justify the additional costs. A photograph of the Grand Coulee spillway bucket is shown in Fig. 18-5.

For the Grand Coulee Dam, a hydraulic-jump basin was first designed which required a parabolic apron of enormous thickness, as shown in Fig. 18-6. This comparative figure shows clearly how much more economical the roller bucket is than the hydraulic-jump-type basin. It was observed during model studies that, as the discharge was increased to capacity, the riverbed material was carried back against the bucket, completely filling the trench and forming a deposit approximately parallel to the bucket lip and roughly parabolic in section.

recommended to prevent the formation of side rollers when the outlets are not operated symmetrically. Although the use of a bucket may result in large savings of construction costs, high maintenance costs may offset these.

It is strongly recommended that unsymmetrical gate operation be avoided. All construction debris should be removed both from and below the bucket prior to initial flow releases.

The solid-roller-type bucket was probably first used in the design of the spillway for the Grand Coulee Dam.¹² With a design discharge of 1,000,000 cfs and a head of 280 ft,

In 1943, divers examined the Grand Coulee bucket and found that up to 18 in. of erosion occurred at certain locations, because of boulders and gravel drawn into the bucket and debris from construction. Irregular

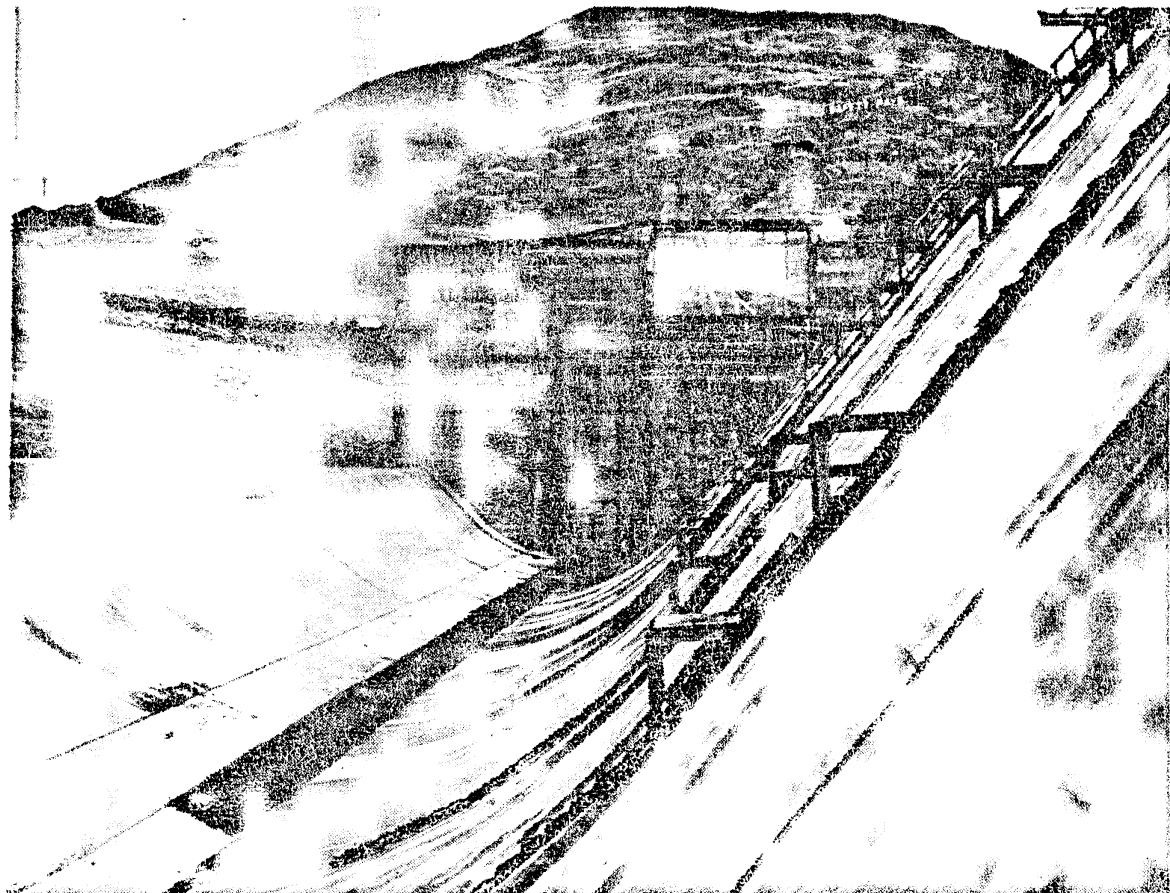


FIG. 18-5. Grand Coulee spillway bucket, near completion. (*Courtesy of Bureau of Reclamation.*)

flow during construction accelerated the erosive action. A study of riverbed topography indicated that the sand, gravel, and boulders picked up by strong reverse currents were carried into the bucket. This entrapped material was subject to swift, direct crosscurrents, producing a volume of erosion equal to an average depth of 2 in. throughout the bucket length between the spillway training walls. The removal of this material has created a difficult and costly maintenance problem. Table 18-1 lists solid-roller-bucket characteristics for 12 existing structures.

At the Sakuma Dam,¹⁰ located on the Tenryu River in Japan, a secondary dam was constructed to increase the tailwater depth necessary

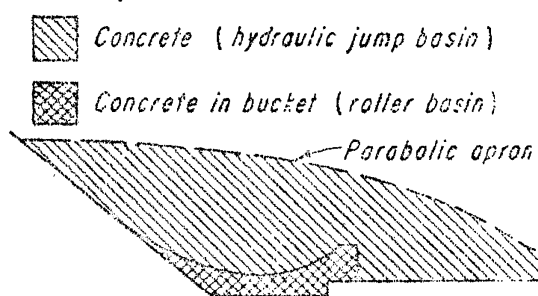


FIG. 18-6. Hydraulic-jump versus roller-bucket basin, Grand Coulee Dam, Washington.

TABLE 18-1. SLOID-BUCKET Prototype Characteristics

Structure	Location	Bucket radius, ft	Maximum Q , cfs	Maximum q , cfs per foot of bucket width	Lead, * ft	Bucket lip slope, °	Bucket lip height, ft	Tail-water depth, † ft	Remarks
Baggs Island.....	Virginia-No. Carolina	40	770,000	705	167	45	7.0	70	Bucket invert varies
Center Hill.....	Tennessee	50	457,000	973	226‡	45	14.6	86.4	
Clark Hill.....	Georgia-So. Carolina	50	1,058,000	964	185	45	14.6	69.2	
Davis.....	Arizona-California	75	1,192,000	781	177	45	20	70.§	
Grand Coulee.....	Washington	50	1,000,000	606	421.6	45	30.1	161.5	
Greensboro.....	No. Carolina	17	32,000	540	72	45	...	33.0	
Headgate Rock.....	Arizona-California	40	290,000	500	83	45	10	55.6	
Murdock.....	Utah	5	5,000	500	21	37	3.1		
Penn Forest.....	Pennsylvania	17	12,000	300	132.5	45	5.0		
Sakuma.....	Japan	63.1	3,46,000	1,315	389†	45	22.1	90	
Stewart's Ferry.....	Tennessee	40	190,250	607	422§	45	11.7	60.5	Bucket invert varies
Wolf Creek.....	Kentucky	50	535,000	907	227	45	15.0	102.6	

* From maximum pool level to bucket invert.

§ Approximate.

† At maximum discharge.

¶ Varies.

‡ From spillway crest to bucket invert.

for satisfactory roller-bucket action. The secondary dam shown in Fig. 18-7 was preferred over excavation of a deep stilling pool. With a spillway design discharge of 346,000 cfs, the maximum discharge per foot of bucket width is 1,315 cfs per foot of spillway width, or twice that of the Grand Coulee Dam. In determining the spillway crest elevation for the secondary dam, consideration should be given to the desired water depths in the subdam pool and the apron requirements for a secondary stilling basin below the subdam.

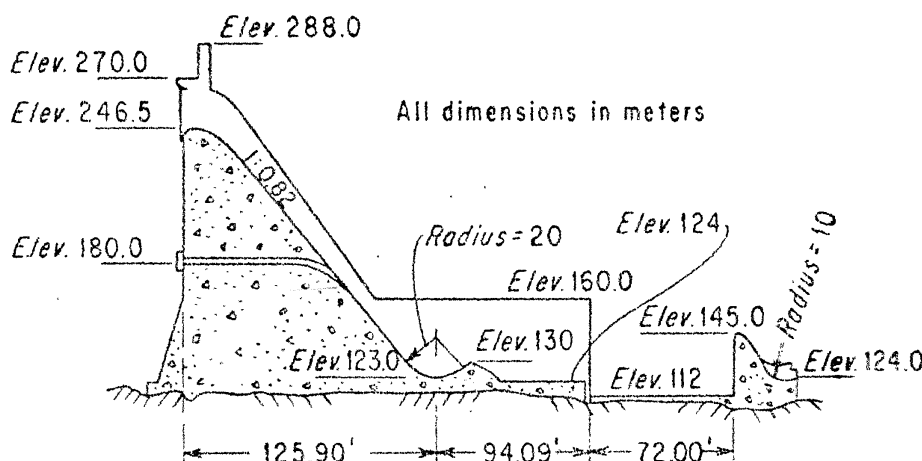


FIG. 18-7. Sakuma Dam roller-bucket basin, Japan.

Prototype data were obtained for the operation of the Center Hill¹⁵ Dam spillway bucket when discharges of approximately 40,000 cfs were made continuously for 8 days. Observations indicated that the flow was satisfactorily spread, and no trouble from spray resulted. A large quantity of stone and rock was accidentally spilled into the bucket during its construction. As a result, several large cavities, probably caused by the abrasive action of the rock during sluice discharges, were found in the bucket. Since this damage was repaired, several inspections have been made; no additional bed material, however, was found in the bucket.

18-2. Slotted Roller Buckets. As described in the previous section, the solid roller bucket creates a high boil on the water surface and a violent ground roller that deposits loose bed material toward the bucket lip. Unsymmetrical gate operation may cause eddies to sweep material into the bucket and, together with the constant motion of the loose bed material against the bucket lip, may make this type of bucket undesirable for some installations.

In the operation of the slotted bucket, both the high boil and violent ground roller are materially reduced. A comparison of the flow characteristics below slotted and solid roller buckets is depicted in Fig. 18-8a and b. As noted in Fig. 18-8b, only part of the flow is directed away by the slotted bucket, and the boil is less pronounced. The part of the flow directed downstream through the slots is spread laterally and is lifted

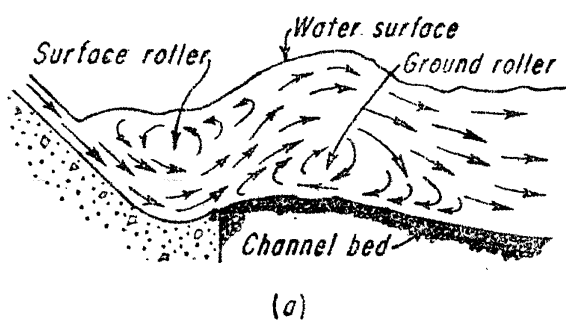
away from the channel bottom by the apron extending downward from the slots. Consequently, the flow is dispersed and distributed over a greater area, providing less flow concentration than occurs with a solid roller bucket.

The slotted bucket will provide a self-cleansing action to reduce abrasion in the bucket arc. For low tailwater elevations, the water surface may be rougher than desirable, making it necessary to consider the effects of possible riverbank erosion. Figure 18-9 is an illustration of a typical slotted bucket.

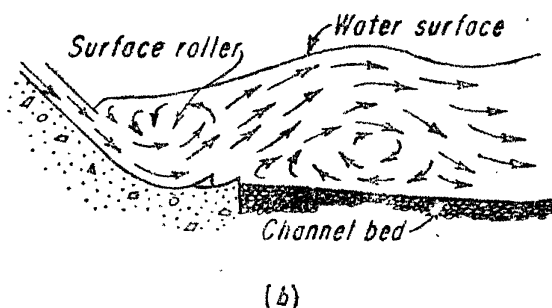
Experiments by the Bureau of Reclamation⁵ have indicated that the tailwater range over which the slotted bucket operates satisfactorily will be less than that for a solid bucket.

If the tailwater is too high, the flow may dive beneath the apron lip and scour the streambed. In general, the slotted bucket was found to be an improvement over the solid-roller type.

Bucket slots are installed to keep the bucket lip free of loose bed



(a)



(b)

FIG. 18-8. Spillway-bucket flow characteristics: (a) solid-roller-bucket action, (b) slotted-roller-bucket action.

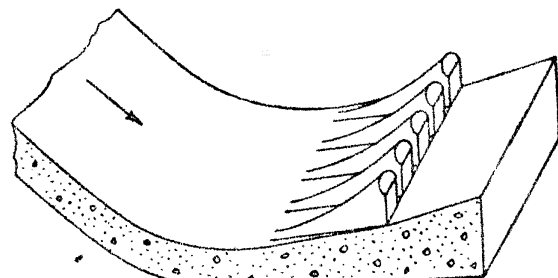


FIG. 18-9. Typical slotted roller bucket.

material and provide exits for material that may become trapped in the bucket. In order to maintain the effectiveness of the buckets in dissipating the energy of spillway flows, the slots should be made no larger than is necessary to prevent deposition at the bucket lip.

To reduce the water-surface fluctuations and stabilize the flow downstream, teeth were added to the basin. Small eddies in the jets leaving the slots lifted the loose bed material, thus reducing abrasive action on the face of the teeth. In order to help spread the jets and to keep loose material away from the teeth, a sloping apron should be installed downstream from the teeth. The upward slope of the apron should be steeper than the slope of slots, to provide for better contact with the jets and to avoid subatmospheric pressures.

Although definite design criteria for slotted buckets have not been established, the following rules may be helpful in obtaining the desired energy dissipation, a smooth water surface, and a minimum amount of river-channel erosion:

1. The bucket should be designed for the full range of tailwater and discharge conditions.
2. Trial settings of bucket-invert elevations should be made to satisfy the design for minimum and maximum tailwater elevations.
3. The minimum allowable bucket radius will be dependent upon the discharge and hydrostatic head, measured from the pool elevation to the bucket invert.
4. To prevent material from entering the bucket, the elevation of the apron lip should be located slightly below the channel bed.
5. The shape and spacing of the teeth, slope, and length of apron downstream from the teeth should be determined from model studies.

It should be remembered that the teeth will probably be subject to cavitation when entering velocities exceed 50 fps. Consequently, the slotted bucket is not recommended for use when the entering velocities exceed 50 fps. Individual model studies should be conducted to determine optimum dimensions for the bucket teeth, slots, and apron.

Figure 18-10 shows the dimensions of the slotted bucket adopted for the Angostura Dam⁴ spillway. A saving of approximately \$500,000 was realized by constructing a slotted bucket rather than a sloping apron,

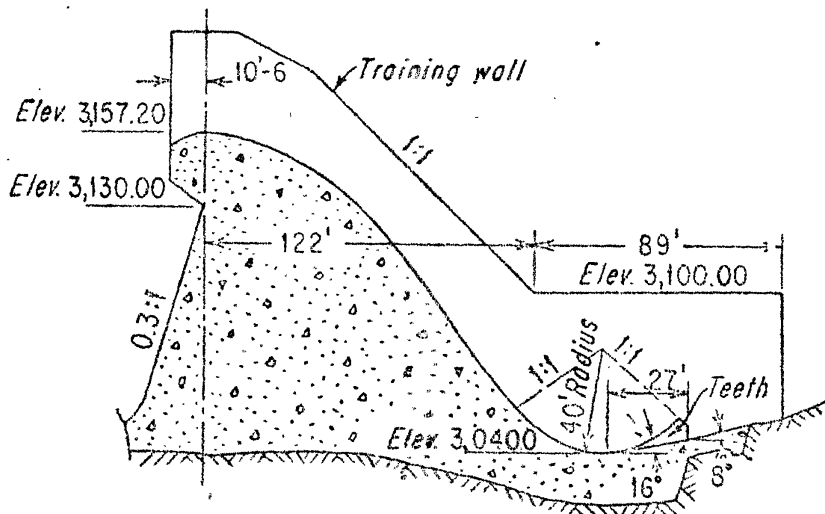


FIG. 18-10. Angostura Dam slotted-roller spillway bucket.

which would have been necessary were it not for the development of this type of bucket. The spillway is designed to discharge a total of 277,000 cfs, or 1,028 cfs per foot of bucket width. Energy dissipation by the slotted bucket occurred principally as a spreading rather than a roller action. The Superior-Courtland⁵ and Cambridge diversion dams also

employ slotted buckets, having design discharges of 100 and 257 cfs per foot of bucket width, respectively.

18-3. Trajectory Buckets. When the tailwater depth is less than required for the formation of the hydraulic jump, satisfactory scour protection can sometimes be obtained by deflecting the flow as far as possible from the toe of the dam. Devices employed for this purpose are commonly called trajectory or flip buckets.

Use of this type of design should be restricted to structures where the streambed is composed of firm rock. It is important to make certain

that the scour will not progress upstream to the extent that the safety of the structure might be endangered. High-velocity flow leaving the trajectory bucket will form a large amount of spray as it is dis-

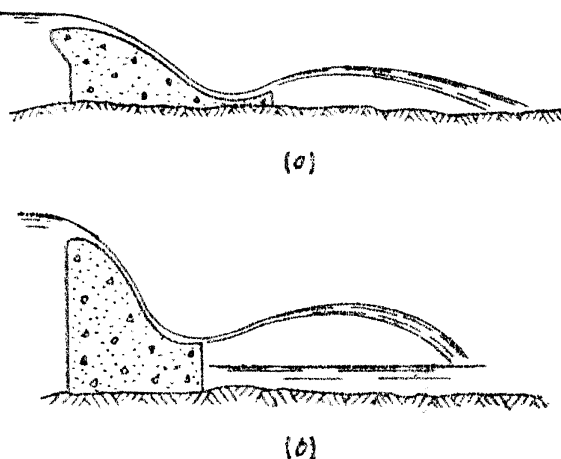


FIG. 18-11. Trajectory buckets: (a) low bucket, (b) high bucket.

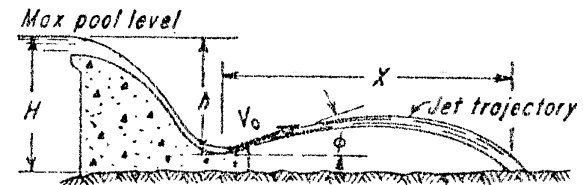


FIG. 18-12. Trajectory-bucket variables.

persed into the air. For some installations, where buildings may be damaged by heavy spray, employment of the trajectory bucket may be objectionable.

In general, buckets may be high or low, depending upon their location with respect to the riverbed. Figure 18-11a and b depict typical low and high trajectory buckets, respectively.

Probably the most important consideration in the design of trajectory buckets is to determine how far the jet will be deflected downstream. Theoretically, if we neglect friction, retardation of air, and disruption of the jet, Eq. (18-1) can be used to compute the horizontal component of the jet trajectory:

$$x = \frac{v_0^2 \sin 2\phi}{g} \quad (18-1)$$

The variables of Eq. (18-1) are depicted in Fig. 18-12. Equation (18-1) can be transformed into dimensionless form by dividing each side of the equation by H , the vertical distance between the maximum pool and the riverbed.

$$\frac{x}{H} = 2 \frac{h}{H} \sin 2\phi \quad (18-2)$$

Measurements made by Maitre and Obolensky¹⁷ at the St. Etienne-Cantales and Chastang Dams in France for flows less than one-half the maximum discharge show that approximately 19 to 20 per cent of the total energy is dissipated by interaction of the jet with air. To compensate for the velocity reduction and loss of energy of the jet during its flight, it is suggested that the following equation be used:

$$\frac{x}{H} = 1.9 \frac{h}{H} \sin 2\phi \quad (18-3)$$

Obviously, the maximum value of $\sin 2\phi$ in Eq. (18-3) is unity. Consequently, the maximum jet-trajectory length will occur at a 45° lip angle.

Figure 18-13 presents theoretical curves of x/H versus h/H for bucket angles ranging from 10° to 45° . Experimental data collected by Pana-senkov¹⁸ are also plotted in Fig. 18-13. Note that these data agree very well with the theoretical curves. Data compiled from model and prototype tests for the Pine Flat Dam are also plotted. Additional experimental data collected by De Vito¹⁹ closely approximate the relationship of Eq. (18-3). Trajectory lengths observed in model tests for exit

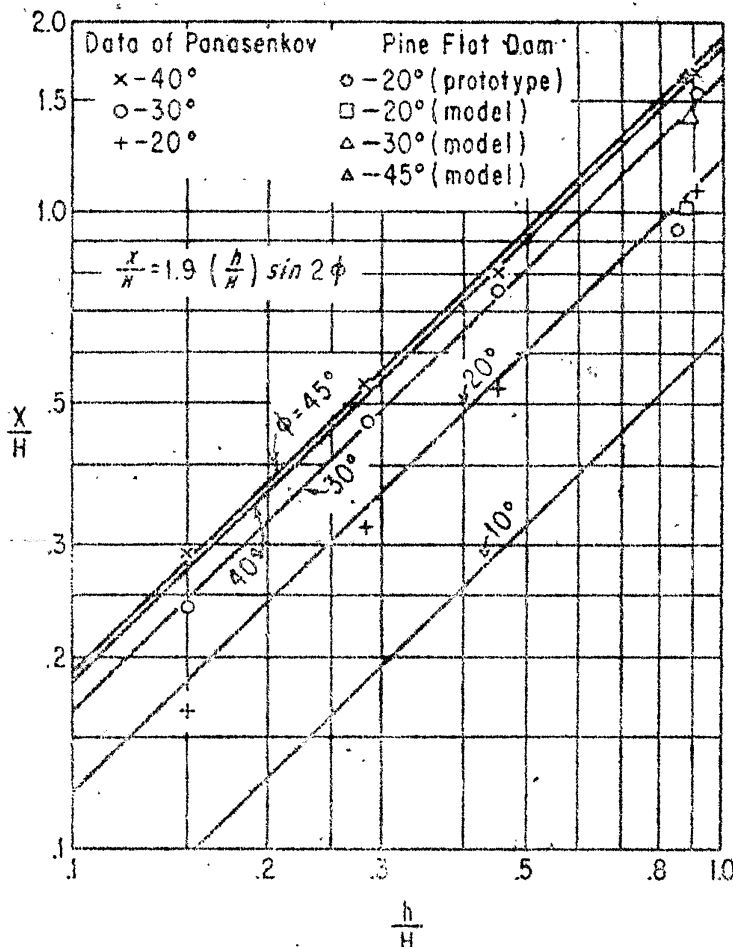


FIG. 18-13. Jet-trajectory lengths.

angles ranging from $25^\circ 45'$ to $45^\circ 45'$ were slightly greater than those yielded by Eq. (18-3).

The designer may also wish to determine the vertical component, or height, of the jet trajectory. If air resistance and disruption of the jet are neglected, Eq. (18-4) can be used to compute the jet-trajectory height.

$$y = v_0^2 \sin^2 \phi / 2g \quad (18-4)$$

Since $v_0^2 / 2g = h$, Eq. (18-4) becomes

$$\frac{y}{h} = \sin^2 \phi \quad (18-5)$$

Neither Eq. (18-3) nor Eq. (18-5) accounts for changes in the bucket radii, which affect both the height and length of the jet trajectory. Experiments conducted for the Hartwell Dam²⁰ indicate that a larger bucket radius caused the flow to be deflected slightly higher and farther downstream than did a small bucket radius.

Several factors to be considered in the design of a trajectory bucket include the bucket radius, lip elevation, lip angle, and trajectory of the jet. For most structures, a bucket radius of between 30 and 50 ft will be adequate. On the basis of model studies for the Pine Flat Dam,¹⁴ it is recommended that the bucket lip elevation be approximately the same as the maximum tailwater elevation. Adequate deflection can be provided with a bucket lip angle of 20 or 30° . Although a greater lip angle will deflect the jet farther downstream, it will also produce more spray, require more concrete, and therefore be more costly.

Table 18-2 lists prototype characteristics of existing trajectory buckets. Examples of low trajectory buckets can be found at the Chilhowee, Safe Harbor, and Conowingo Dams. A low trajectory bucket was employed for the Conowingo Dam,¹⁶ illustrated by Fig. 8-6. The final design incorporated a 12.5° deflector 20 ft long, which maintained a smooth, continuous surface with the bucket radius of 40 ft and terminated in a vertical downstream face. After over 20 years of operation, no abrasion or erosion of the bucket has occurred.

The Safe Harbor Dam also employs a low trajectory bucket, located at the streambed elevation. Figure 18-14 is a photograph showing the bucket of the Safe Harbor Dam in operation.

Pine Flat Dam,¹⁴ located on the Kings River in northern California, is an example of the use of a high trajectory bucket. Model studies indicated that with a maximum discharge of 395,000 cfs, the flow would be deflected approximately 400 ft downstream from the toe of the dam.

TABLE 18-2. TRAJECTORY-BUCKET PROTOTYPE CHARACTERISTICS

Structure	Location	Maxi- mum Q , cfs	Maxi- mum q , cfs per foot of bucket width	Head,* ft	Bucket radius, ft	Bucket lip slope, °	$X\ddagger$, ft
Anchor	Wyoming	13,500	193	101.5	parabolic	57
Arkport	New York	29,100	341	10.2	45	10.5
Chilhowee	Tennessee	230,000	865	71	32	20	0
Conowingo	Pennsylvania	880,000	391	91.5	40	12.5	22
Dnieprostroy	Russia	835,000	334	37.9		
Hartwell	Georgia	565,000	975	161	30	30	69
Hirakud	India	1,187,000	697	130	50	40	12
Pine Flat	California	395,000	1,350	372	50	20	40
Safe Harbor	Pennsylvania	970,000	365	58.5	42	27	10

* From maximum pool level to bucket invert.

† Vertical distance from bucket lip to streambed below.



FIG. 18-14. Performance of trajectory buckets of Safe Harbor Dam, Susquehanna River, Pennsylvania. (Safe Harbor Water Power Corporation.)

Figure 18-15 is a photograph of the Pine Flat Dam flip buckets in operation. Two levels of sluices were provided through the overflow spillway and they have operated satisfactorily under a maximum head of 280 ft.

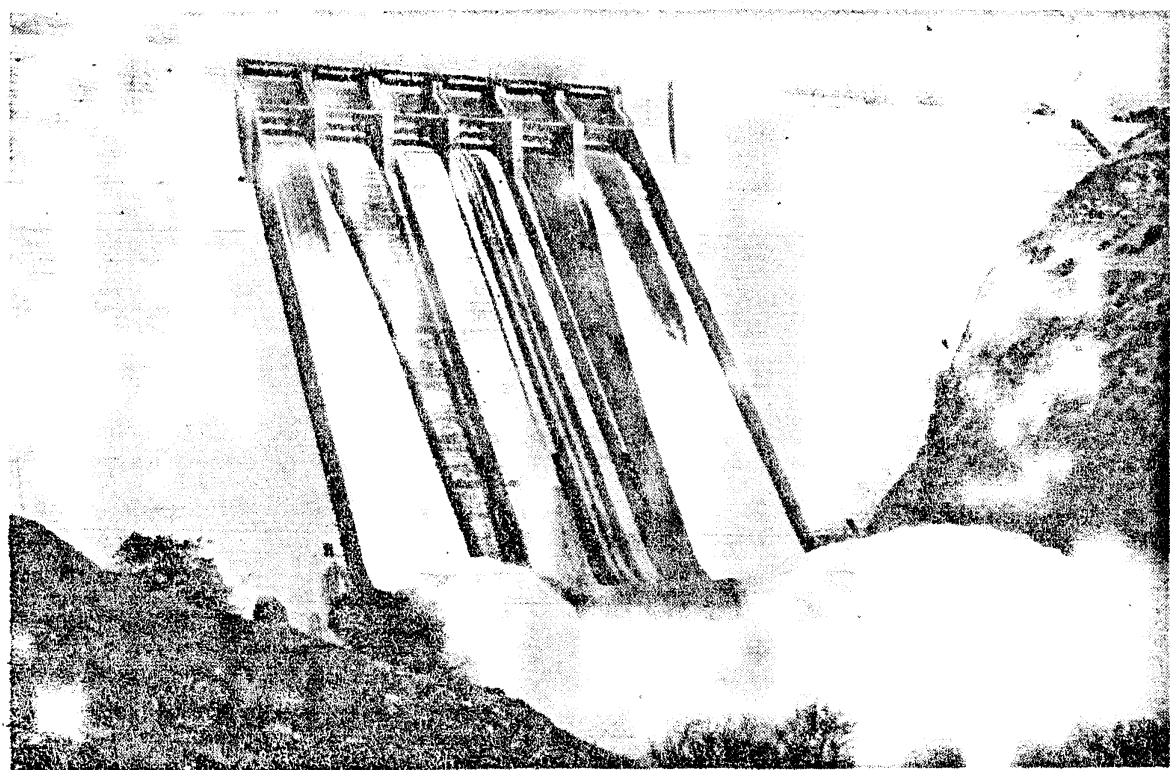


FIG. 18-15. Performance of trajectory buckets at Pine Flat Dam, California. (*Courtesy of Corps of Engineers, Sacramento District.*)

A trajectory bucket was also employed in the design of the Arkport Dam,⁷ a 110-ft-high dam located on the Canisteo River in New York. The use of a deep stilling basin, necessary because of insufficient tailwater, was found to be too expensive. Flows were directed and spread by the bucket in such a manner that scour did not endanger the safety of the structure.

An elevated trajectory bucket was designed for the proposed Anchor Dam² to be constructed on the South Fork of Owl Creek in Wyoming. The bucket was first designed circular in shape, but was later changed to parabolic in order to provide a smooth water surface without increasing the size of the structure. Model studies had shown that splashing and vibration occurred when a circular arc was used. Alternate 40-in. slots were provided to drain the bucket. It was found that a dentated lip provided good directional control and doubled the length of the jet-impact area on the streambed, thereby reducing the depth of scour. The design adopted for the Anchor Dam bucket is shown in Fig. 18-16. It will be noted that the bucket is situated about 50 ft above the riverbed. Water flows over the spillway crest and then passes 91 ft down the face of the trajectory bucket. Model tests indi-

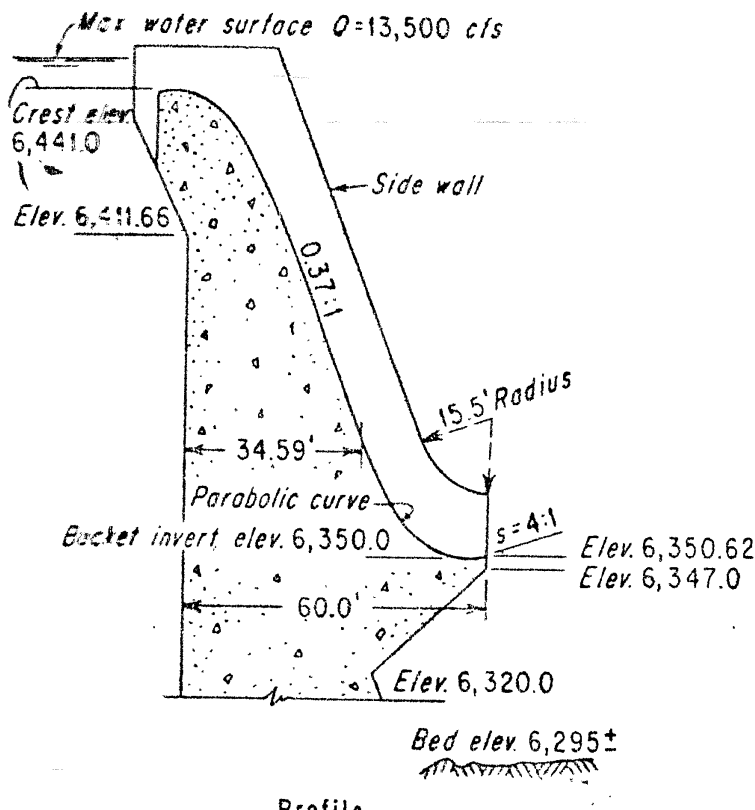


FIG. 18-16. Profile of Anchor Dam spillway trajectory bucket.

cated that scour for the adopted bucket design will be centered about 165 ft downstream from the dam, extending to within 20 ft of the downstream face for smaller flows. No damage will be incurred at the toe of the dam, and operation of the structure will be independent of the tail-water depth or scour of the river channel. Converging side walls were used for the spillway with a 70-ft-wide bucket. The curved side walls improved flow conditions and provided a more economical structure.

Model studies should be conducted for all proposed trajectory buckets to evaluate the merits of alternate buckets and to develop refinements in the design.

18-4. Tunnel Deflectors. Tunnel deflectors are utilized to deflect the high-velocity flow as far as possible away from the tunnel outlet. For successful operation of this device, it is essential that the streambed below the tunnel be composed of firm rock not subject to severe scouring. In some cases, scour may be permitted below a tunnel spillway that is detached and separated from the main dam. Generally, operation of tunnel-spillway deflectors should be confined to emergency or infrequent use. Examples of the use of tunnel-spillway deflectors can be found at the Lucky Peak, Bhakra, Fontana, and Hungry Horse Dams.

Flows from the tunnel spillway of the Lucky Peak Dam,⁶ located on the Boise River near Boise, Idaho, are controlled by six vertical-slide valves in a six-branch manifold. Releases from the tunnel are directed by

six individual deflector buckets into an unlined stilling basin excavated in the bedrock and the overburden of the river channel. Use of the deflector buckets was dictated by a desire to avoid an expensive, lined stilling basin.

Flow from the Lucky Peak buckets is deflected high into the air, forming a spectacular plume of water, as shown in the photograph of Fig. 18-17. With hydrostatic heads up to 233 ft, velocities up to 122 fps were attained with small gate openings.



FIG. 18-17. Lucky Peak Dam, Boise River, near Boise, Idaho, showing dam up to left, tunnel manifold to the right, with trajectory bucket discharging approximately 6,000 cfs. (*Courtesy of Corps of Engineers, Walla Walla District.*)

During 1955, releases up to 5,000 cfs were made through five gates at openings of 2 ft for a period of 13 days. Although observed flow conditions indicated satisfactory dispersal and stilling action of the jets, it was noted that erosion of the concrete invert and the walls downstream from the gates resulted. Apparently cavitation pressures were produced as a result of the high-velocity jets issuing from small gate openings. The depth of erosion of the bucket invert varied because of the cement-water mixture in the concrete; it reached a maximum of approximately 40 in.

Figure 18-18 illustrates the left spillway tunnel adopted for the Bhakra Dam¹ to be constructed in India. For the left tunnel, a deflector having a length of 137 ft and rise of 25 ft, capable of discharging a maximum of 166,000 cfs, was designed.

At the Fontana Dam,¹¹ two unique tunnel-spillway buckets were designed to deflect and spread the high-velocity flow high into the air and permit the dissipation of energy at a safe distance downstream from the outlet structure. Tailwater depths at the tunnel outlet were found to be

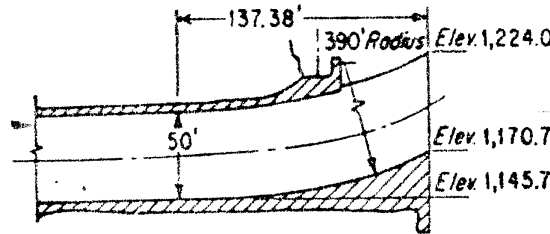


FIG. 18-18. Left spillway tunnel deflector of Bhakra Dam, India.

insufficient to form a hydraulic jump. A deflector bucket was preferred over a deep, expensive, concrete-lined stilling basin. At the design discharge of 40,000 cfs per tunnel, a velocity of 146 fps was attained. With this velocity, the energy concentration at the bucket exit totaled 44,000 hp per foot of width.

The location of the tunnel buckets with respect to the dam is shown in Fig. 18-19. After extensive experimentation, two buckets composed of cylindrical sill surfaces were adopted. In order to perform properly, each bucket was designed with varying horizontal and vertical deflections, and a toe wall was constructed in the rock on the downstream side. This protection is necessary because, for water releases of 2,000 cfs or less, a hydraulic jump will form along the horizontal leg of the tunnel. When

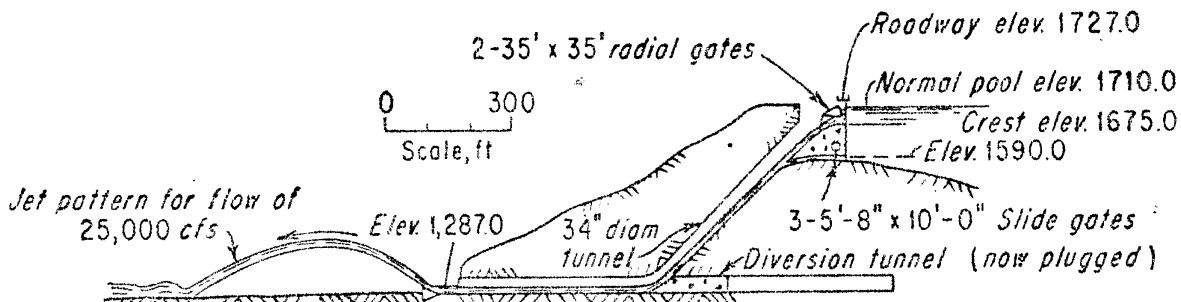


FIG. 18-19. Location of Fontana Dam spillway tunnel.

this condition exists, the lip of the bucket will act as an overflow weir, producing substantial scouring at the foot of the bucket. Where the jets strike the riverbed, stones weighing 6 tons or more were placed as part of the riprap blanket. About 2,000 linear feet of bank slopes had to be protected along each side of the river, with a concrete toe wall constructed to protect the base of the slopes.

During 1945, conditions were favorable for making tunnel-spillway tests. A discharge of 10,000 cfs was released through each tunnel, and the performance was observed with the tunnels discharging together. With a discharge of 10,000 cfs, the corresponding exit velocity was 120 fps. Figure 18-20 shows the flow as it leaves the Fontana bucket. As the water left the bucket, it appeared to break completely into spray and was directed about 150 ft vertically into the air. In general, model-prototype operation was similar, except that considerably more spray



FIG. 18-20. High-velocity flow as it leaves Fontana spillway tunnel. (Courtesy of Tennessee Valley Authority.)

existed in the prototype. This difference was probably due to surface tension in the small-scale model. Cross sections of the riverbed were made before and after the prototype tests. About 14,400 cu yd of bed material was removed from the riverbed and deposited farther downstream. Substantial scour will have to occur before a stable river bottom will be obtained. This will in no way affect the safety of the structure. Observations also indicated that prototype erosion was not as great as indicated by the model.

REFERENCES

1. Bureau of Reclamation, Hydraulic Model Studies for the Design of Bhakra Dam, India, *Hydraulic Lab. Rep.* 210, October, 1946.
2. Bureau of Reclamation, Hydraulic Model Studies of the Spillway and Outlet Works of Anchor Dam, Owl Creek Unit, Missouri River Basin, *Hydraulic Lab. Rep.* 289, February, 1951.
3. Bureau of Reclamation, Hydraulic Model Studies of Superior-Courtland Diversion Dam, Headworks, and Sluiceway Structures, *Hydraulic Lab. Rep.* 275, March, 1950.
4. Bureau of Reclamation, Hydraulic Model Studies on the Spillway for the Angostura Dam, Missouri River Basin, South Dakota, *Hydraulic Lab. Rep.* 192, January, 1946.
5. Bureau of Reclamation, Progress Report II, Research Study on Stilling Basins, Energy Dissipators, and Associated Appurtenances, sec. 7, Slotted and Solid Buckets for High, Medium, and Low Dam Spillways, *Hydraulic Lab. Rep.* 415, July, 1956.

6. Corps of Engineers, Outlet Works and Stilling Basin for Lucky Peak Dam, Boise River, Idaho, *Bonneville Hydraulic Lab. Rep.* 43-1, July, 1956.
7. Corps of Engineers, Hydraulic Model Tests of the Arkport Side Channel Spillway and Outlet Structures, Report of Binghampton District, June, 1939.
8. Davis, L. M.: Model Tests on Structures for Hydro-electric Developments, *Trans. ASCE*, vol. 108, pp. 803-830, 1943.
9. Keener, K. B.: Spillway Erosion at Grand Coulee. *Eng. News-Record*, vol. 113, pp. 41-47, 1944.
10. Okada, A., and T. Ishibashi: Hydraulic Model Tests of Sakuma Dam, *Central Research Industry of Electric Power*. Japan, June, 1956.
11. Tennessee Valley Authority, Fontana Project, Hydraulic Model Studies, *Tech. Memorandum* 68, 1953.
12. Warnock, J. E.: Experiments Aid in Designing Grand Coulee Dam, *Civil Eng.*, vol. 6, p. 737, 1936.
13. Tiffany, J. B.: Laboratory Research Applied to the Hydraulic Design of Large Dams, *Waterways Experiment Station Bull.* 32, 1948.
14. Waterways Experiment Station, Spillway and Conduits for Pine Flat Dam, *Tech. Memorandum* 2-375, December, 1953.
15. Waterways Experiment Station, Model Study of Spillway and Bucket for Center Hill Dam, Caney Fork River, Tennessee, *Tech. Memorandum* 202-1, August, 1946.
16. Erosion below Conowingo Dam Proves Value of Model Studies, *Eng. News-Record*, pp. 127-130, Jan. 28, 1932.
17. Maitre, R., and S. Obolensky: Étude de quelques caractéristiques de l'écoulement dans la partie aval des évacuateurs de surface, *La Houille blanche*, no. 4, July-August, 1954.
18. Panasenkov, N. S.: Vlijanije turbulentnost zidkoj strui na jeje raspylenije, *Zurnal Techniceskoj Fisiki*, vol. 21, pp. 161-166, 1951.
19. De Vito, L.: "Ricerca Sperimentale si Scaricatori a Scivolo con Deviatore a Getto," paper delivered before the Primo Congress di Construzioni Idrauliche, Rome, 1954.
20. Waterways Experiment Station, Sluice Outlet Portal and Spillway Flip Bucket, Hartwell Dam, Savannah River, Georgia, *Tech. Memorandum* 2-393, August, 1954.

Model Tests and Hydraulic Similitude

Mathematical theory and experimental data have helped to develop solutions to many hydraulic problems. Important hydraulic structures are now designed and constructed only after extensive model studies have been performed. The application of dimensional analysis and hydraulic similitude has enabled engineers to organize and simplify the experiments and to analyze the results therefrom.

In this chapter, we shall describe several model-prototype conformances and the conclusions which may be drawn from prototype performances. There is a great need for data which can be used to compare the performance of models and prototypes and to extend the range of usefulness of hydraulic models as an aid to the designer. Ordinarily, prototype data are difficult to obtain and usually the data obtained from model tests are not in the same range of heads or discharges, making direct comparison difficult. Figure 19-1 shows the Gavins Point Dam stilling-basin model in operation, with a discharge of 626,000 cfs.

19-1. Hydraulic Model Studies. For many cases, hydraulic model studies have resulted in more economical stilling basins or outlet works. Hydraulic model studies of the proposed Mt. Morris Dam² resulted in a stilling-basin design that was constructed for nearly \$700,000 less than any equally effective alternate design. A stepped transition between the downstream face of the dam and the training walls was developed with the aid of models, which corrected a serious velocity-distribution problem and made the use of sloped training walls possible.

Models of hydraulic structures are usually geometrically undistorted and are operated in accordance with the Froudian relationship, which usually means that the model must be constructed with the smoothest possible surface. For instance, a 1:50 scale model of a spillway having a surface roughness (Manning) of 0.016 would require a model roughness of about 0.0083. Consequently the roughness scale frequently serves to place a lower limit on the linear scale of the model.

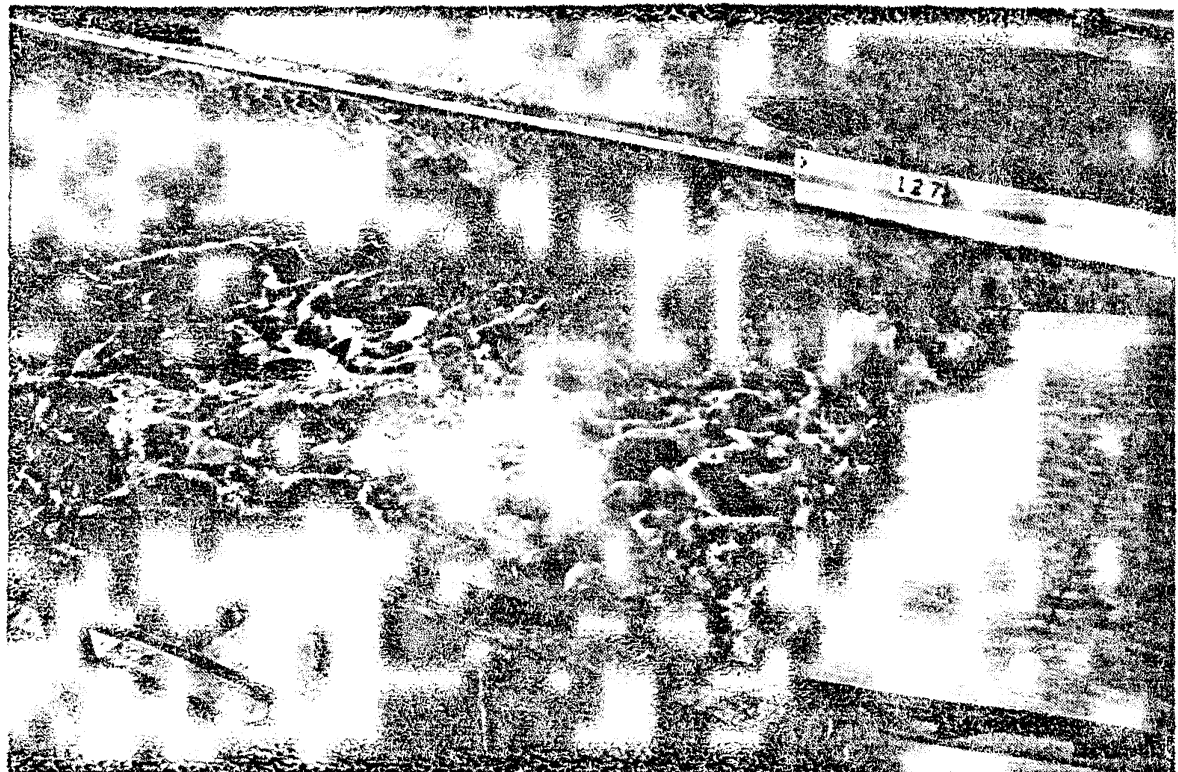


FIG. 19-1. Model of hydraulic-jump-type stilling basin of the Gavins Point Dam with approximate discharge of 626,000 cfs. (*Courtesy of Corps of Engineers, Waterways Experiment Station.*)

The lower limit on scales for models of hydraulic structures is probably between 1:70 and 1:10 because, at smaller scales, models cannot be made smooth enough to obtain similitude and because the size of the elements being studied (baffle piers, gates, etc.) becomes so small that changes in their shape, size, and location fail to show changes in hydraulic behavior.

Hydraulic models, in general, may be either true or distorted. True models have all the significant characteristics of the prototype reproduced to scale (geometric similitude) to satisfy design restrictions (kinematic and dynamic similitude). Model-prototype comparisons have clearly shown that the correspondence of behavior is often well beyond expectations; this has been attested to by the successful operation of many structures designed from model tests. A photograph of the model of the Garrison Dam spillway stilling basin is shown in Fig. 19-2.

19-2. Hydraulic Similitude. A thorough knowledge of the mechanics of similitude is indispensable in the hydraulic laboratory, regardless of whether the laboratory research involves fundamental studies of fluid flow on the experimental design or the analysis of hydraulic structures by means of models. Perfect similarity of motion occurrences from a strictly mathematical viewpoint is very seldom obtainable, but results are frequently compatible within the desired accuracy.

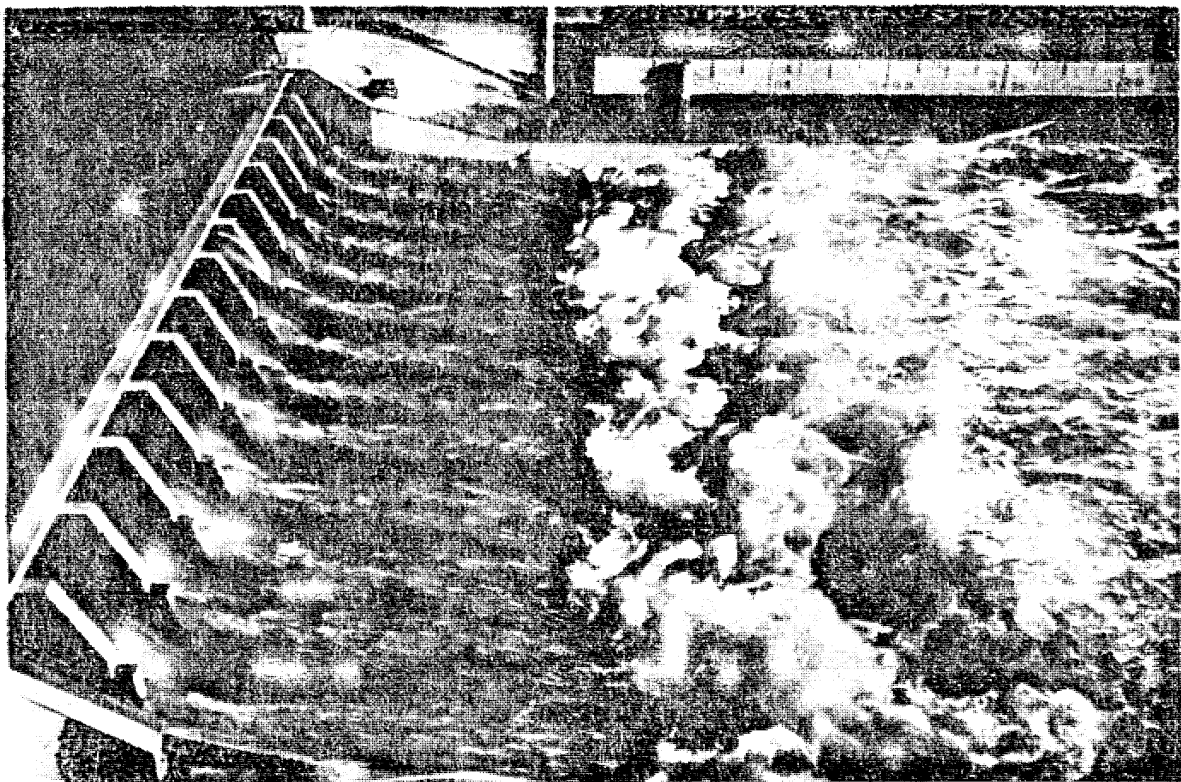


FIG. 19-2. Model of Garrison Dam spillway stilling basin with approximate discharge of 827,000 cfs. (Courtesy of Corps of Engineers, Waterways Experiment Station.)

Dimensional analysis is the mathematics of dimensions of quantities and is a useful tool in fluid mechanics. In an equation expressing a physical relationship between quantities, dimensional as well as numerical equality must exist. In general, all such physical characteristics can be reduced to the fundamental quantities of force (F), length (L), and time (T), or mass (m), length, and time. Applications include converting one system of units to another, developing equations, reducing the number of variables required in an experimental program, and establishing principles of model design.

Geometric Similarity. Two objects are said to be geometrically similar if the ratios of all homologous dimensions are equal. In the form of an equation,

$$L_r = \frac{L_m}{L_p} \quad (19-1)$$

where L_r = linear model-scale ratio

m = linear dimensions of the model

p = linear dimensions of the prototype

Homologous areas vary directly as L_r^2 , and homologous volumes vary directly as L_r^3 .

Kinematic Similarity. Two motion occurrences are kinematically similar if the patterns or paths of motion are equal and if the ratios of the

velocities of the various homologous particles involved in the motion are equal. Or, in the form of an equation,

$$v_r = \frac{v_m}{v_p} \quad (19-2)$$

Equation (19-2), in accordance with the Froudian relationship, where gravity forces predominate, becomes

$$v_r = \frac{L_m^{1/2}}{L_p^{1/2}} \quad (19-3)$$

or

$$v_r = L_r^{1/2} \quad (19-4)$$

As represented by Eq. (19-4), homologous velocities will vary directly as the square root of the linear model-scale ratio.

Dynamic Similarity. In practically all energy dissipators, gravity forces predominate, and dynamic similarity is attained by designing the model in accordance with the Froudian relationship. Two motion occurrences are dynamically similar if they are kinematically similar, i.e., if the ratios of the masses of the objects involved in the motion occurrences are equal and if the homologous forces which may affect the motion of the homologous objects are equal. Complete dynamic similarity is an ideal seldom attained in model testing. Since

$$v_r = L_r^{1/2}$$

and

$$A_r = L_r^2$$

then the discharge scale becomes

$$Q_r = A_r v_r$$

and

$$Q_r = L_r^{5/2} \quad (19-5)$$

As represented by Eq. (19-5), the discharge will vary directly as the five-halves power of the linear model-scale ratio.

Similarity of Power and Energy Dissipated. In accordance with the Froudian relationship, the homologous power will vary directly as the seven-halves power of the linear model-scale ratio, represented by Eq. (19-6).

$$P_r = L_r^{7/2} \quad (19-6)$$

The homologous energy will vary directly as the fourth power of the linear model scale, or, in the form of an equation,

$$E_r = L_r^4 \quad (19-7)$$

Certain factors such as the atmospheric pressure, viscosity, and density of the fluid remain the same, both in the model and in the prototype.

Roughness Similarity. Expressed in terms of the Froudian relationship, the roughness scale n_r will vary directly as the linear model-scale

ratio to the one-sixth power. The roughness-scale requirements usually fix the lower limit of the linear scale of an outlet works model; thus the flow in the model conduit must be large enough to produce turbulent flow in the prototype. The roughness coefficient is difficult to simulate in models of large size because there is a physical limit to the smoothest possible surface that can be obtained. Models of stilling basins usually vary from a lower limit of 1:60 to a scale as large as 1:10.

Table 19-1 lists the scale ratios for characteristics that will be encountered in model studies of spillways, stilling basins, and outlet works.

TABLE 19-1. SCALE RATIOS

Characteristic	Unit	Symbol	Scale ratio, F-L-T system
Area.....	ft ²	A	L_r^2
Volume.....	ft ³	V	L_r^3
Velocity.....	fps	v	$L_r T_r^{-1}$
Acceleration.....	ft per sec ²	g	$L_r T_r^{-2}$
Force.....	lb	F	F_r
Mass.....	lb-sec ² per ft	m	$F_r T_r^2 L_r^{-1}$
Specific weight.....	lb per ft ³	γ	$F_r L_r^{-3}$
Density.....	lb-sec ² per ft ⁴	ρ	$F_r T_r^2 L_r^{-4}$
Pressure.....	lb per ft ²	p	$F_r L_r^{-2}$
Absolute viscosity.....	lb-sec per ft ²	μ	$F_r T_r L_r^{-2}$
Kinematic viscosity.....	ft ² per sec	ν	$L_r^2 T_r^{-1}$
Power.....	ft-lb per sec	P	$F_r L_r T_r^{-1}$
Discharge.....	ft ³ per sec	Q	$L_r^3 T_r^{-1}$
Surface tension.....	lb per ft	σ	$F_r L_r^{-1}$
Roughness (Manning).....	n	$L_r^{1/6}$

NOTE: When gravity forces predominate and $g_r = 1$, $T_r = L_r^{1/2}$; when viscous forces predominate and $g_r = 1$, $T_r = L_r^{2/3}/\nu_r$.

Example. It is observed that a hydraulic jump is formed in a 1:10 scale model of a stilling basin. The following dimensions were measured in the model:

$$q_m = 5 \text{ cfs per foot of basin width}$$

$$y_{1m} = 0.25 \text{ ft}$$

$$v_{1m} = 20 \text{ fps}$$

$$P_m = 0.5 \text{ hp}$$

What are the corresponding dimensions in the prototype?

Solution. First, we shall investigate the geometric quantities, with

$$L_r = 0.1 \text{ ft} \quad \text{and} \quad y_{1m} = 0.25 \text{ ft}$$

Then

$$y_{1p} = \frac{y_{1m}}{L_r} = \frac{0.25}{0.1} \\ = 2.5 \text{ ft}$$

Since $q_m = 5$ cfs per ft, then

$$\begin{aligned} q_p &= \frac{q_m}{L_r^{5/2}} = \frac{5}{0.00317} \\ &= 1,581 \text{ cfs per foot of basin width} \end{aligned}$$

Next we shall find the kinematic elements when $v_{1m} = 20$ fps. Then

$$\begin{aligned} v_{1p} &= \frac{20}{L_r^{1/2}} = \frac{20}{0.317} \\ &= 62.5 \text{ fps} \end{aligned}$$

If the energy dissipated in the model of the hydraulic jump is 0.5 hp, the energy dissipated in the prototype by the hydraulic jump will be equal to

$$\begin{aligned} P_r &= L_r^{7/2} = 0.1^{7/2} \\ &= 0.000317 \end{aligned}$$

then $P_p = \frac{P_m}{P_r} = \frac{0.5}{0.000317}$
 $= 1,581 \text{ hp dissipated in the prototype}$
 $\text{by the hydraulic jump}$

19-3. Erosion Tests. The most important criterion with which to judge stilling-basin action is that of comparative erosion. To make qualitative erosion studies, a readily erodable sand or other material is used to represent the channel bed downstream from the stilling basin. The measured depth and extent of erosion indicate the effectiveness of the basin under test when compared to erosive patterns from other designs with the same bed material. It will be necessary that the model be operated for a time interval sufficient to develop considerable erosion.

The presence of extreme turbulence, waves, high exit velocities, and eddies or pulsating flow in the downstream portion of the structure indicates the need for refinement of the design or abandonment of the original scheme.

Each design should be tested over the complete range of discharge and tailwater conditions. Stilling basins that do not have a fairly wide range of permissible tailwater conditions are ordinarily not practical. Refinement in the design of stilling basins may be evaluated by comparing measured velocities, wave heights, pressures, and erosion patterns.

19-4. Model-Prototype Conformances. Prototype data are usually difficult to obtain, and model data are frequently not in the prototype range of heads or discharges, making direct comparisons difficult. There are few spillways which have sustained large flow releases. Consequently, a number of years may elapse before a project undergoes large spillway releases.

Discharges from the outlet works at reservoirs are, of course, frequent.

At several projects where the stilling basin is common to both the spillway and outlet works, flows released from the outlet works have been more critical for the design of stilling basins than have flows from the spillway. Prototype data for a number of structures compiled by Berryhill¹ will be discussed subsequently.

Arkabutla Dam. The Arkabutla Dam has a 300-ft-long, uncontrolled, concrete-chute spillway, which has a 3 to 1 slope and is capable of discharging 89,000 cfs. A stilling basin with a 95-ft-long level floor containing two rows of baffles and an end sill was developed from model studies.

In 1953, the spillway went into operation for the first time. With a maximum discharge of 7,100 cfs, the stilling action was observed to be satisfactory. It was noted that the tailwater during the 1953 flow was 16 ft higher than that used for model tests. An investigation revealed that the outlet channel was not constructed to the bottom grade and width used in the model study. The channel had been excavated to a bottom grade varying from 5 ft higher at the lower end to 13 ft higher at the upper end.

Baldhill Dam. Baldhill Dam employs a 140-ft-long ogee spillway section, which is joined to a chute on a 15 per cent slope. The stilling basin consists of a level apron 70 ft long, with a flare, in plan, of 1 in 6, averaging about 155 ft in width, complete with two rows of baffle piers and an end sill. The maximum head available from reservoir pool to apron is 51 ft with a discharge of 43,100 cfs.

Comparisons between model and prototype indicated a good agreement during the 1950 flood, with a maximum release of 3,150 cfs. In both the model and the prototype, the hydraulic jump began and ended in the chute section, and flow was distributed uniformly across the basin width. For discharges above 10,000 cfs, the model indicated that the hydraulic jump would begin in the chute and end on the level stilling-basin floor.

Bonneville Dam. Bonneville Dam, a power and navigation project constructed on the Columbia River, was completed in 1937. In the ensuing 20 years, the large daily and annual flood flows have subjected the stilling-basin baffle piers to extremely heavy pounding for prolonged periods of time, resulting in gradual erosion of the concrete over large areas of the baffle piers and apron. Damage to the baffle piers was discussed in Chap. 10. During the Columbia River flood of 1948, the stilling basin was subjected to a severe test. For 1 day's duration, the peak river flow was 1,300,000 cfs, whereas the design discharge is 1,600,000 cfs. Stilling action was very turbulent, and eye witnesses reported almost instantaneous surges about 25 to 30 ft vertical in height near the spillway abutments. Flow remained over 900,000 cfs for 18 days' duration.

Recent observations of flow in the south half of the stilling basin, where

the downstream row of baffle piers has been filled in solid to form a sill, indicate more turbulent water-surface conditions than in the original basin. Model studies indicated that the new basin design, with a solid end sill on the apron, would deflect the flow upward, producing more turbulence on the surface, but providing a large, slow-moving eddy in an upstream direction on the bottom of the riverbed.

Bull Shoals Dam. Flow over the 284-ft-high Bull Shoals Dam spillway is controlled by 17 tainter gates 40 ft wide and 28 ft high. Release of floodwaters when the reservoir pool elevation is below the spillway crest is accomplished by 16 sluices 4 ft wide by 9 ft high, controlled by hydraulic slide gates. The stilling basin was constructed with a stepped apron 808 ft wide and 203.3 ft long, with elevations varying from 437.2 to 446.5 and a 4-ft-high end sill. The apron has a 1.0-ft-high step located 35.3 ft downstream from the toe of the dam, a 1.5-ft-high step located 47.3 ft downstream from the toe, and 2.5-ft-high steps located 71.8 and 98.8 ft downstream from the toe. Figure 19-3 is a photograph of the 1:50 scale model of the Bull Shoals stilling basin.



FIG. 19-3. Scale model, 1:50, of Bull Shoals Dam stilling basin, White River, Arkansas, Missouri. (Courtesy of Corps of Engineers, Little Rock District.)

Extensive damage was noticed near several of the outlet portals in 1952, after one year of operation. Erosion, varying from a depth of less than 2 ft to a maximum of 3.5 ft, had occurred in the 5-ft-thick concrete slab below the outlet portals of 12 of the 16 sluices. Severe erosion on the top of the first step appeared to be the result of cavitation. It seemed probable that, once started, the erosive process may have been accelerated by dislodged concrete and broken reinforcing steel.

In order to increase the effective tailwater depth for sluice flows, the final design for the stilling basin incorporated a 12-ft-high end sill. The upstream face of the end sill was provided with a 1 on 2 slope, in order to increase the lateral spread of individual conduit flows over the sill. Since a relatively large drop occurs over the high end sill, a 24-ft-long secondary basin with a 2-ft-high end sill was added. One row of 8-ft-high baffles 7.5 ft wide and spaced 8.5 ft apart was added to the main basin to improve stilling action for large spillway flows.

Soundings of the exit channel in the first 100 ft downstream from the end sill in 1948 and again in 1953 indicated that erosion of 2 to 5 ft had occurred at a number of locations in the moderately hard limestone.

Conchas Dam. The Conchas Dam spillway consists of a concrete gravity ogee weir 340 ft wide and 178 ft high from the spillway crest to the toe, capable of discharging a maximum of 182,000 cfs. The stilling basin consists of a 134-ft-long horizontal apron with one row of 8-ft-high baffle piers and a 12-ft-high end sill. The basin length is unusually short, equivalent to $2.3y_2$ for the maximum discharge. In addition, the ends of the training walls are tapered back from the end sill on a slope of 1.1 to 1.

An inspection of the basin in 1944 revealed that most of the basin was in good condition. However, the apron floor was eroded to a depth of 9 to 12 in. in the area bounded by the baffle pier attached to the side wall. Erosion up to 6 in. in depth extended into the training wall and the downstream faces of the baffles. This wear was caused by eddies which formed in the "stagnation" spots behind the baffle piers. In addition, erosion on the level apron downstream from two of the regulating sluices varied from a depth of 3 in. near the baffle piers to virtually none at the spillway toe. Repairs consisted of replacing the concrete behind each of the end baffles.

Observation of prototype spillway flows up to 38,000 cfs indicated that the hydraulic jump was completely submerged, whereas model tests had indicated that a free jump should occur for all anticipated tailwater conditions for flows less than 75,000 cfs. Channel retrogression occurred downstream for a distance of more than 40 miles. The streambed near the dam has been lowered nearly 10 ft.

Denison Dam. The outlet works of the Denison Dam consist of three 20-ft-diameter circular conduits which discharge into an upper stilling basin that is terminated by an ogee weir and thence into a lower stilling basin. The two-level stilling basin was adopted because of unusual foundation conditions.

The upper basin is 235 ft long and has a maximum width of 172 ft, with two rows of 10-ft-high baffle piers located 209 ft downstream from the output portal. At the end of the basin, the weir crest rises 19.5 ft above the floor. The lower basin is approximately 20 ft below the upper weir and extends 140 ft downstream from the 172-ft-wide ogee weir. Two rows of 8-ft-high baffle piers and a 7-ft-high end sill are provided.

In 1947, the maximum release was 60,000 cfs, which produced satisfactory hydraulic-jump action. Observation of the high-velocity flow, approximately 65 fps, from the outlet portals indicated that the upstream row of baffles was absorbing large impact forces, since the hydraulic jump began forming quite near the baffle piers. Occasional surges overtopped the 44-ft-high walls of the upper basin. Flows over the intermediate weir, although rough, were surprisingly uniform, considering the turbulence of the hydraulic jump in the upper basin.

Within reasonable limits, the model tests predicted the prototype performance of the stilling basin in every respect. Model studies indicated that flow in the exit channel beyond the end sill would have relatively high bottom velocities, ranging from 13 to 16 fps for both small and large discharges. The ability of limestone to withstand these sustained velocities was questioned, and about 50 ft of concrete paving was provided below the prototype end sill to protect against this condition.

In 1948, after 4 years of operation, the upper basin was found to be in excellent condition, with no evidence of pitting or cavitation. The lower basin was not dewatered, but was inspected by a diver and an engineer using diving equipment. The basin was found to be in good condition, and the only notable evidence of wear was found on the floor at the downstream edges of the end baffle piers, where a small amount of pitting was noted. A considerable number of large rocks were found between the baffle piers and end sill. One rock was reported to be 8 to 10 ft long and 3 to 4 ft thick. The limestone exit channel was carefully inspected, but no signs of erosion were noted from the sustained velocities.

In the Red River channel, downstream from the limestone ledge at the outlet works, degradation of the alluvial bed has been progressive since 1939. The effect on tailwater elevations at the outlet works in a 15-year period (1939 to 1954) has been a lowering of 1.5 ft at 40,000 cfs, 4.5 ft at 20,000 cfs, and 6.5 ft at 5,000 cfs. Little degradation is expected in the future, since the channel bed is now near equilibrium.

Folsom Dam. The spillway for the Folsom Dam consists of a high concrete gravity ogee weir topped with five 42-ft-wide by 50-ft-high "operating" tainter gates and three 42-ft-wide by 55-ft-high "emergency" tainter gates. The spillway stilling basin below the five operating gates consists of an 8 on 1 slope 175 ft long, joined to a level apron 147 ft long, with a 15-ft-high vertical end sill. With a spillway design flood of 200,000 cfs and a basin width of 242 ft, the design discharge will be 826 cfs per foot of spillway width.

During the flood of December, 1955, a total flow of 64,000 cfs was released from the five service gates, providing a unit discharge of 264 cfs per foot of spillway width. With a discharge of 64,000 cfs, the reservoir pool level was 36.7 ft above the spillway crest and 340 ft above the level apron, and the tailwater was 63 ft above the apron. As predicted by the model, stilling action was not complete, and moderately high velocities continued downstream from the end sill for a considerable distance. In the model, a simulated discharge of 110,000 cfs resulted in bottom velocities of 16 fps immediately downstream from the end sill.

Heart Butte Dam. Heart Butte Dam³ was constructed on the Heart River west of Bismarck, N.Dak. The spillway is of the morning-glory type, which discharges into a spillway tunnel and thence into a hydraulic-jump-type stilling basin. In order to provide good energy dissipation and a smooth water surface in the downstream channel, flow is discharged onto a horizontal floor after it passes through a transition section at the end of the tunnel. The flat floor induces more spreading before the flow drops downward on the trajectory curve. Two low walls divide the basin into thirds, producing excellent distribution of flow and an efficient hydraulic jump. Chute blocks and baffle piers were used to increase the fine-grain turbulence in the basin and thereby reduce the required length of the stilling basin.

During the 1950 flood, many prototype observations were made both in the spillway and in the stilling basin. The performance of the stilling basin with an outflow of about 3,700 cfs, about 60 per cent of capacity, was satisfactory in every respect and performed according to the predictions made from model tests. Although the entire basin contained extremely turbulent water, the full length of the hydraulic jump was contained in the basin. At times, considerable amounts of spray shot into the air at a point where the outflow from the tunnel plunged beneath the tailwater. The amount of spray which fell adjacent to the basin caused no difficulty. Flow leaving the basin had a relatively smooth water surface with few measurable waves. Water-surface profiles were measured in the prototype for discharges of 1,050, 2,350, 3,300, and 3,700 cfs. Although no exact comparisons could be made, the prototype profile seemed to be in good agreement with the model profile. The prototype

profiles were slightly higher than those in the model for the same discharge because of greater air entrainment in the prototype.

No significant erosion occurred in the channel bottom below the stilling basin, but despite riprap cover, the channel banks were eroded to a greater degree. It was observed that the actual tailwater curve was approximately 3 ft lower than the computed tailwater curve. Should the tailwater continue to recede, the jump may sweep completely out of the basin.

Kanopolis Dam. The Kanopolis Dam employs a hydraulic-jump-type stilling basin with two rows of baffles 5 ft high and a 4-ft-high end sill. From the tunnel portal, the side walls flare in plan, with a slope of 3 on 1, until a basin width of 52 ft is reached at the location of the downstream row of baffles. The walls then extend parallel for the remaining distance to the end of the basin. At the location of the upstream row of baffle piers, the stilling basin is 40 ft wide. The length of the sloping portion extends 42 ft from the outlet portal, whereas the horizontal portion of the apron extends for a distance of 78 ft. Capacity of the outlet works at full reservoir pool is 5,700 cfs, but maximum releases are limited to about 3,000 cfs.

A progressive scour problem existed in the outlet channel below the basin. In 4 years (1948 to 1952), a small channel was eroded through the 18-in. rock paving. In order to stabilize the outlet channel, the 18-in. depth of grouted rock paving was repaired for a distance of 200 ft downstream from the basin, and a concrete cutoff wall 8 ft deep by 3 ft wide was constructed 100 ft downstream from the basin.

Field observations indicate that a hydraulic jump occurs for discharges up to the normal maximum of 3,000 cfs, but for a flow of 5,500 cfs, considerable spray action results from the impact of tunnel discharges on the upstream row of baffle piers. Considerable turbulence in the outlet channel and incomplete stilling action also result. A later inspection revealed that the sides of the upstream row of baffles, as well as the floor immediately adjacent, are pitted to a depth of 1 to 2 in. as a result of cavitation. A preliminary study indicated that the tailwater depth is equivalent to $0.7y_2$ at a discharge of 5,500 cfs.

Mississippi Lock and Dam No. 1. Lock and Dam No. 1, located on the Mississippi River in Minnesota, is 574 ft long and consists of a level concrete apron approximately 80 ft long, 30 ft below the spillway crest. The elevation of the concrete apron is too high to allow the hydraulic jump to form, except for high discharges. In 1952, the maximum flood of record occurred, and a discharge of 69,200 cfs passed over the spillway. With a tailwater depth of 21 ft, the hydraulic jump formed at the downstream edge of the apron. A hydraulic model study was made to determine the most feasible method of modifying the apron. As a result of the model

tests, a baffle wall was placed about 30 ft downstream from the toe of the dam, constructed with 2-ft-square openings, making it possible for the hydraulic jump to move well up on the apron.

There are 26 navigation projects constructed on the upper Mississippi River. At many of these, the spillway structures are founded on piles driven into the sand bed of the river. In most cases, a low concrete sill is followed by a concrete stilling basin about 50 ft long containing two rows of baffles, an end sill, and approximately 50 ft of derrick stone below the end sill. In a few instances, this stone has been undermined by erosion of sand and gravel. Remedial works usually require that a timber mattress be constructed, floated into position, sunk, and the entire mattress covered with a 1-ft layer of stone. This work has been relatively permanent. Gate operation on a number of these projects founded on piling is so arranged that the maximum velocity over the end sill does not exceed 5.5 fps, as determined from model tests.

McNary Dam. Flood flows of the Columbia River, at this navigation and power project, are passed through a 1,310-ft-long concrete gravity ogee spillway containing twenty-two 50-ft-high by 50-ft-wide gates, separated by 10-ft-wide spillway piers. The stilling basin is of the hydraulic-jump type, designed to discharge 2,220,000 cfs at a reservoir pool elevation of 356.5. The stilling-basin apron elevation is set at 228.0 and contains two rows of baffle piers and an end sill. The structure is unusual in that the maximum head on the spillway crest is 65.5 ft, resulting in a discharge into the stilling basin of 1,680 cfs per foot of basin width, or 100,000 cfs for each gate bay.

A spillway model was constructed with a scale of 1:36, and the apron length made equal to $3.2y_2$. The apron elevation was located so that the maximum tailwater depth of 75.5 ft was equal to $0.90y_2$, because of the anticipated effects of the baffle piers with a low entering Froude number of 3.3 at the design discharge. A photograph of the McNary stilling-basin model is shown in Fig. 19-4.

Prototype tests were made in June and July, 1955, at reservoir pool elevations of 335 and 340, with spillway bays 15, 16, and 17 discharging together and with bay 16 discharging alone. The observed stilling-basin action was satisfactory, although the large flow concentrations in the test bay created extremely rough and turbulent flow conditions. With a pool elevation of 340 ft and free flow in bay 16, the hydraulic jump remained in the stilling basin, with the tailwater 16 ft lower than the tailwater depth required for the jump, as determined in the 1:36 scale model. Apparently, the side inflow, which could not be duplicated in the model, was sufficient to stabilize the hydraulic jump partially in the prototype test bay.

It should be noted that the basin length at McNary Dam was made

somewhat shorter and the maximum end-sill velocities allowed were somewhat higher than would be desirable at some locations. This was permitted because of the very hard, durable basaltic rock which lies below the McNary Dam. During the flood of June, 1956, with flows ranging from 735,000 to 787,000 cfs, it was observed that the prototype stilling action closely followed that predicted by the model studies.



FIG. 19-4. Model of the McNary Dam stilling basin. (*Courtesy of Corps of Engineers, Walla Walla District.*)

Muskingum Reservoirs. During the 1940 flood in the Muskingum River basin, observations and tests were made at the outlet tunnels and conduits for the Atwood, Bolivar, Leesville, Mohawk, and Wills Creek Dams. These projects, with the exception of Wills Creek Dam, have conventional hydraulic-jump-type stilling basins, with horizontal aprons, two rows of baffle piers, and an end sill. Because of the limitations on the channel capacities downstream, it was not feasible to open all the gates of these structures so that hydraulic action under conditions approaching maximum capacity of the outlet works could be observed. For flows ranging from 16 to 71 per cent of the maximum capacity, the hydraulic jump remains well within the basin, with good energy dissipation and well-distributed, low velocities over the end sill. In each case, the prototype performance is equal to or better than that anticipated in the model tests.

Nimrod Dam. The Nimrod Dam employs a conventional hydraulic-jump-type stilling basin consisting of a level apron 88 ft wide and 198 ft long, surmounted by a single row of 6-ft-high stepped baffle piers and a 4-ft-high stepped end sill. Seven rectangular sluices 6 ft wide by 7.5 ft high are provided in the base of the spillway that intersects the level apron at a slope of 4 to 1. In plan, the flaring side walls of the sluice outlets intersect the spillway bucket. The sluices are separated (into groups of two, three, and two) by two longitudinal dividing walls 14 ft high, extending through the basin to the end sill. The walls prevent the formation of large eddies within the basin, thereby allowing maximum spreading of the sluice flows. In addition, the amount of gravel carried into the basin is held to a minimum.

The basin was dewatered and inspected in 1952, after 10 years of operation. Rough concrete was found at the outlet of the third sluice, with a maximum erosion depth of 5 in. There was practically no erosion at the end sluices. The baffle piers were found to be in good condition, with only slight erosion on the upstream face of the baffle piers located in the center of the basin. No repairs were made to the stilling basin, but another inspection will be made in a few years.

Norfolk Dam. The Norfolk Dam has a concrete gravity ogee spillway with a conventional hydraulic-jump-type stilling basin 568 ft wide and 185 ft long. Two rows of 8-ft-high baffles and a 6-ft-high end sill were provided. Eleven sluices, each 4 ft wide and 6 ft high, operate under an average head of 170 ft.

When the stilling basin was dewatered in 1945, it was discovered that some of the baffle piers had been damaged quite severely. The damage was attributed to erosion by recirculated debris which had not been cleaned out of the basin when it was completed in 1944. A later inspection in 1953 indicated that only a very small amount of additional wear had occurred in the 8-year period. The additional wear was noticed in a slight rounding of the upstream edges of the baffle piers. Several rough, shallow, cup-shaped, eroded spots were found on the apron upstream from the baffles near the right side of the basin. No repairs to the baffles or the apron were considered necessary.

Shadehill Dam. The Shadehill Dam³ is located on the Grand River near Lemmon, S.Dak. The spillway is of the morning-glory type and discharges into a tunnel spillway terminating in a hydraulic-jump-type stilling basin. The stilling basin contains one row each of chute blocks, baffle piers, and an end sill. The maximum vertical fall from headwater to the stilling-basin floor is about 130 ft.

During the 1952 flood, a discharge of 33,250 cfs occurred, which represented 88 per cent of maximum spillway capacity. The maximum fall from headwater to tailwater was 94.0 ft, and the energy entering the

stilling basin totaled 40,000 hp. A comparison of the water-surface profiles with eight discharges ranging from 1,300 to 4,700 cfs indicated little difference between the model and prototype basins. Flow throughout the expanding transition of the stilling basin was well distributed laterally and appeared to be of the same general pattern as that observed in the model. It was observed that the tailwater curve was about 2 ft lower than the computed curve. Despite the low tailwater conditions, there was no significant bottom erosion, although the channel banks were eroded to a large extent. To repair the bank damage, a band of riprap 50 ft long was placed across the channel bottom and up the channel bank.

The performance record of many of the stilling basins has been good. Stilling action has been equal to or better than anticipated during the design- and model-testing range, except in a few instances. Some erosion of the energy-dissipating structures has been experienced at several structures, and these instances have been discussed because of their interest and the possibility that the findings may be applied to the prevention of similar erosion of future structures. In order to improve the basin performance of future structures, it is important that we continue to observe the performance of prototype structures over a wide range of discharges and tailwater conditions.

REFERENCES

1. Berryhill, R. H.: "Stilling Basin Experiences of the Corps of Engineers," paper presented before the ASCE convention, Oct. 18, 1956.
2. Corps of Engineers, Buffalo District, "Final Report on Hydraulic Model Studies for the Outlet Works of Mount Morris Dam, Genessee River, Mount Morris, New York," October, 1947.
3. Peterka, A. J.: Spillway Tests Confirm Model-Prototype Conformance, *Bur. Reclamation Eng. Monograph* 16, October, 1954.

20

Erosion below Dams

Several modern dams of relatively low height have failed as a result of erosion at the toe of the structure, and it is a significant fact that there are no survivals among the great dams of antiquity. Some of these were more than a hundred feet high, far more massive than ancient bridges and walls, many of which still exist today. The almost complete disappearance of these ancient dams after centuries of use seems, in most cases, to be due to failure caused by long-continued erosive action. Since several modern dams have failed for this reason and considerable sums of money have been expended to correct the effect of erosion, this subject presents itself as one of much importance.

20-1. Prevention of Scour. Scour below weirs and dams results from the erosive power the water acquires in flowing over spillways. Protection against scour is afforded by ensuring that the high-velocity flows do not come into contact with the channel bottom or by directing the flow as far away from the structure as possible. Usually a combination of these methods is used.

When a high-velocity jet or sheet of water flows over the unprotected riverbed downstream from the structure, it may erode the bed material and carry it either in suspension or as bed load farther downstream. Serious scour immediately below the structure may endanger its foundation. Figure 20-1 is a photograph showing the degradation below the Fort Sumner Dam. A certain amount of scour may be permissible farther downstream if the bed material is not highly erodable. The larger the bed load normally transported by the stream, the more rapidly retrogression will take place. Under favorable circumstances the river may be induced to excavate its own channel by constructing a reservoir upstream to remove the sediment load.

The subject of channel retrogression below dams is not a recent discovery but was frequently discussed by irrigation engineers in India during the early nineteenth century. One costly failure due to channel

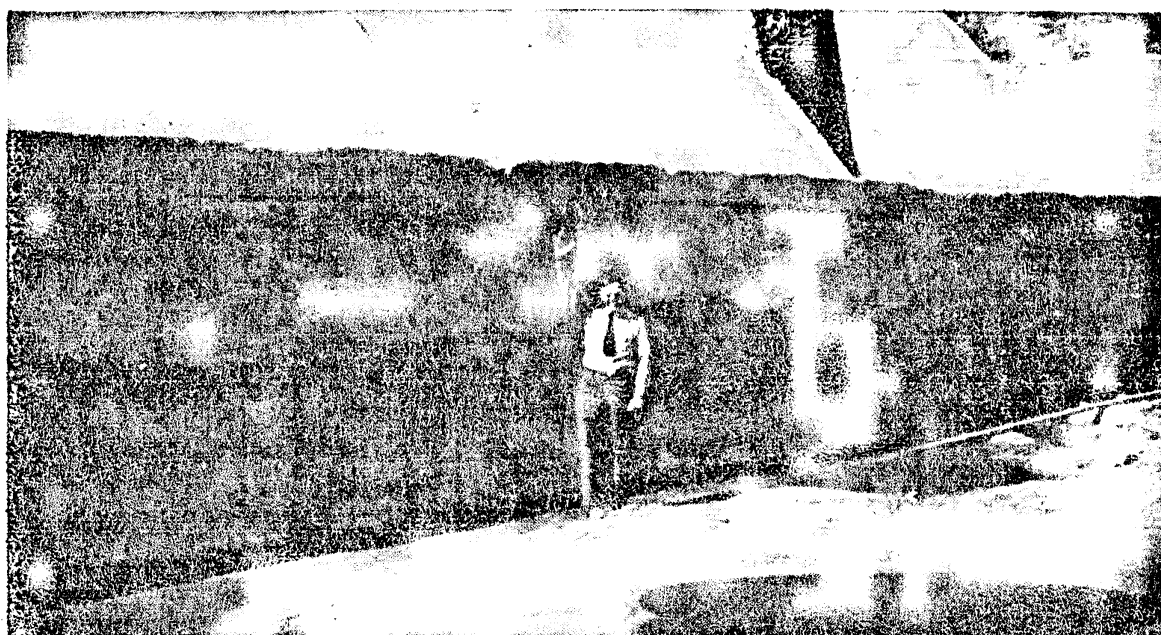


FIG. 20-1. Degradation of 9 ft at left end of Fort Sumner Dam, New Mexico. (*Courtesy of E. W. Lane.*)

retrogression was the Islam Weir,² located in the Sutlej Valley of India, where the scour resulting from the high-velocity flow destroyed a large portion of the downstream apron and finally collapsed six bays of the structure.

Although the problem of scour falls into the field of sedimentation, which is beyond the scope of this text, a short summary of the main characteristics of scour will be presented here.

Gilbert⁵ found that the scouring capacity of a stream increases with an increase in discharge, with a decrease of bed-material size, and with an increase in velocity. Scouring of the bed material will continue until a condition of equilibrium is reached. The flow pattern of erosive action below a hydraulic structure can be predicted by model studies. There is, however, a difficulty in obtaining precise similitude between the bed material used in the model and that in the prototype. Erosion tests can be used only to secure relative scouring potentialities for the various designs tested. Below dams, both negative and positive vortices may be formed. Positive vortices are in a clockwise direction, while negative vortices are counterclockwise. The positive vortices are helpful in depositing material against the end sill of the stilling basin, whereas negative vortices should be avoided.

The present tendency is to dissipate the surplus energy of the flow in some form of energy dissipator or to direct the high-velocity flow away from the structure, so that it does not come into contact with the riverbed. The most important factor in determining what form of protection will be used is the tailwater depth and its relation to the depth required to form a hydraulic jump.

20-2. Erosion below Existing Structures. Early attempts were made to reduce the velocity of water flowing over a dam by having the water fall on a series of steps on the face of the dam, thereby dissipating the energy by contact with the successive steps and reaching the bottom with insufficient energy to erode the streambed. An example of this type of structure is the Gilboa Dam,⁴ illustrated by Fig. 20-2. Modern design does not favor this type of structure, since only a very small portion of the energy is dissipated by impact with the steps.

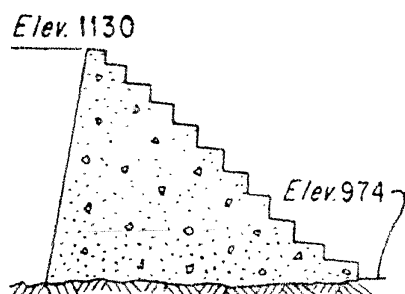


FIG. 20-2. Profile of Gilboa Dam spillway, New York.

During 1947, extensive erosion of the shale foundation underlying the apron of the Waco Dam¹ in Texas caused not only the destruction of the entire apron but carried away large quantities of the foundation. The damaged section, illustrated by Fig. 20-3, was quickly refilled to preclude any downstream movement of the dam. Twenty-two feet of shale below the apron was removed, and a total of 50,000 cu yd of concrete and

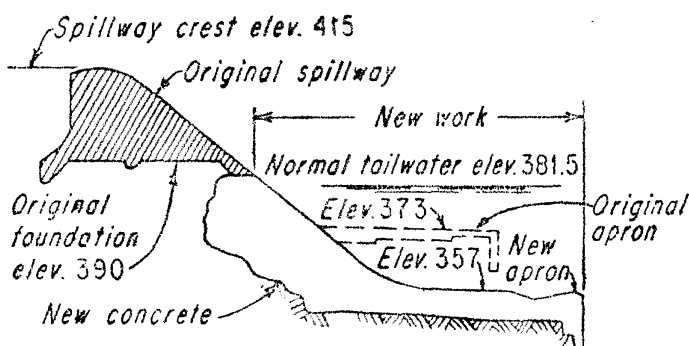


FIG. 20-3. Erosion below Waco Dam spillway, Texas.

shale was lost in the erosive process. Furthermore, disintegration of the foundation had proceeded to the extent where failure of the spillway structure was imminent. As a corrective measure, the apron was lowered to provide adequate tailwater for the hydraulic jump to form. A photograph of the serious damage to the Waco Dam spillway is shown in Fig. 20-4.

On August 3, 1933, the Calderwood Dam,⁸ located 35 miles north of Denver, Colo., on Cherry Creek, failed. Failure of the dam was attributed to water topping the dam to a depth of 1 ft and causing erosion of the lower toe of the spillway. Erosion displaced some of the rubble masonry in the spillway section, causing the collapse of the loose fill composing the main body of the dam.

Concentrated flow eroded a considerable volume of rock below the Wilson Dam,⁷ located on the Tennessee River. When dewatered in June, 1926, it was observed that extensive erosion occurred at the end of

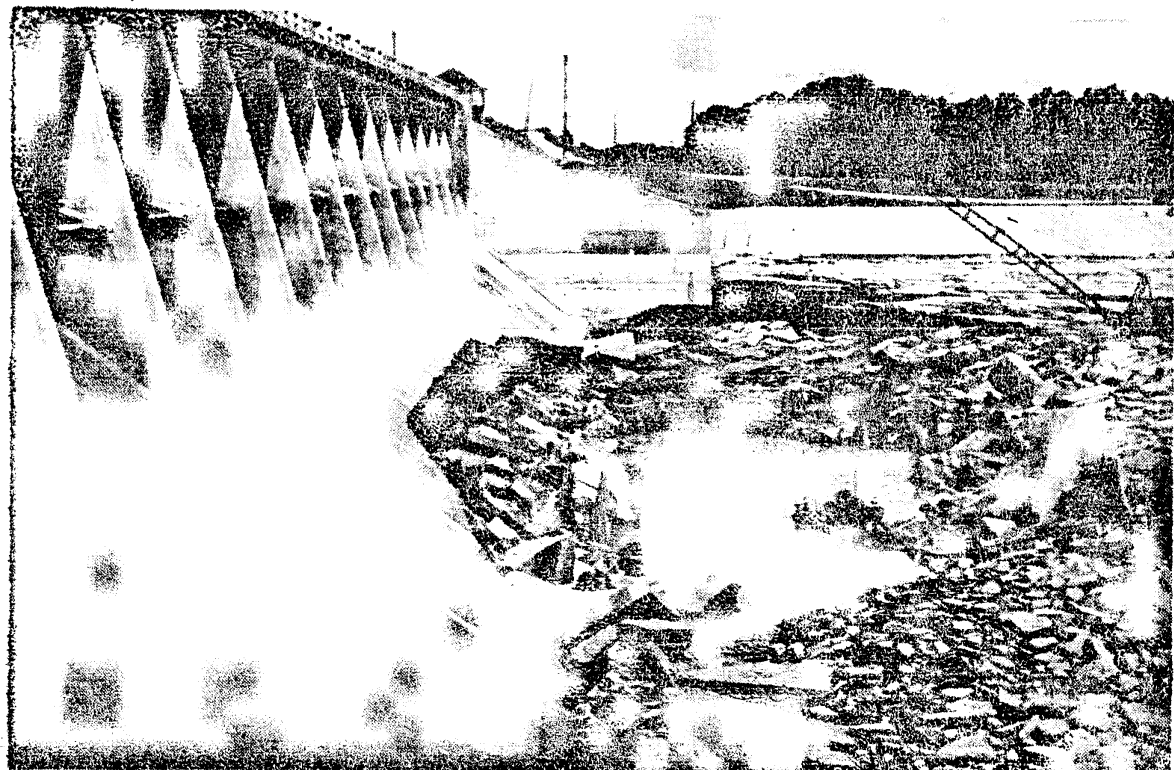


FIG. 20-4. Damage due to scour and uplift pressure at Waco Dam, Texas. (Courtesy of Waco City Water Department.)

the 252-ft horizontal apron. Large slabs of rock were torn loose from the riverbed underneath the toe of the apron, extending downstream from the apron several hundred feet, as depicted in Fig. 20-5. A photograph of the erosion at the toe of the Wilson Dam, Tennessee River, is shown in Fig. 20-6. Many slabs weighed 200 tons or more. The erosion was greatest at the toe of the apron, which was undermined to a depth of 13 ft. In the case of the Wilson Dam, the jump did not form on the apron because of a deficiency of tailwater. This difficulty was alleviated by the construction of a toe wall, which minimized the erosion by lifting the flow away from the riverbed.

The hydroelectric power plant at the Prairie du Sac Dam⁶ on the Wisconsin River was placed in operation during 1914. A few years later it was noticed that a general lowering of the tailwater and river bottom occurred downstream from the dam. The average rate of recession over a 17-year period (1913 to 1931, inclusive) was 0.43 ft per year. The most serious erosion of the riverbed occurred about 220 ft downstream from the end of the apron. The deepest erosion extended 54 ft below the top

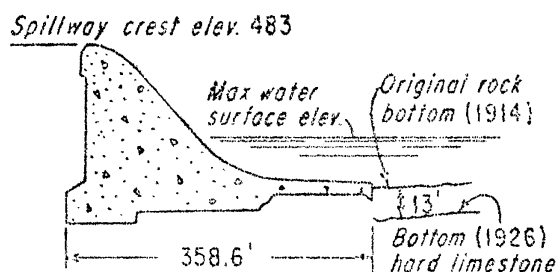


FIG. 20-5. Erosion below Wilson Dam spillway, Tennessee River.

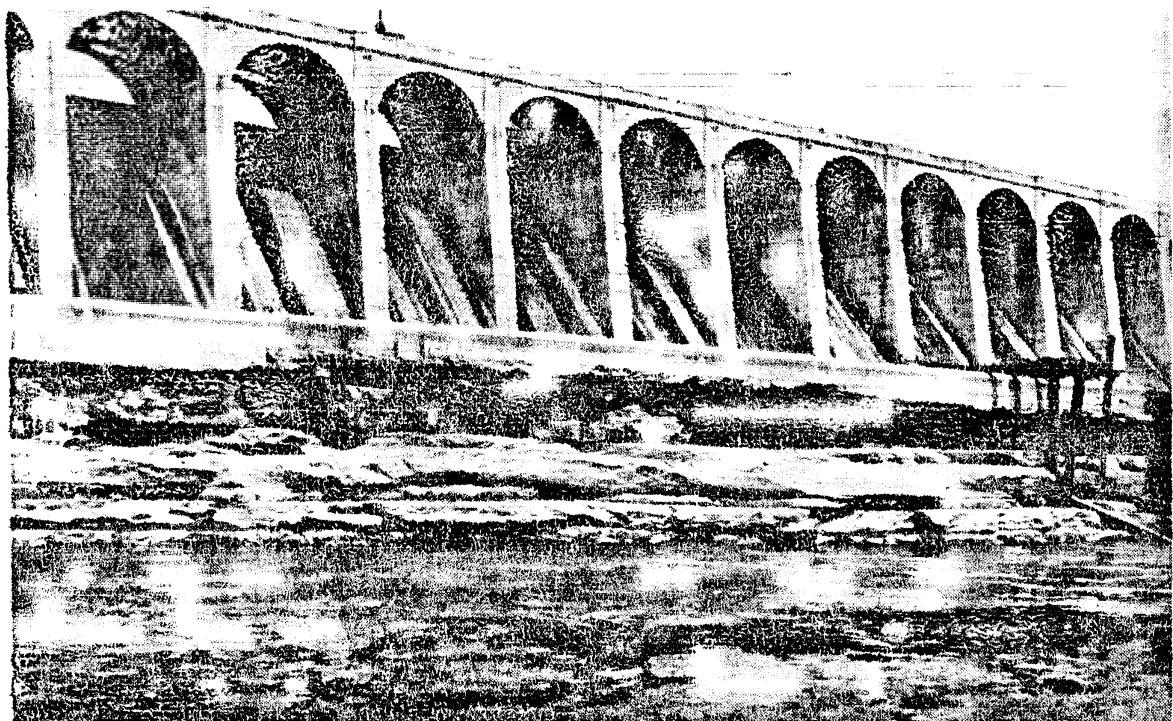


FIG. 20-6. Erosion at the toe of Wilson Dam spillway, Tennessee River. Degradation of 13 ft occurred during 1926. (Courtesy of Tennessee Valley Authority.)

of the apron. Erosion was reduced by constructing a new apron with baffles added to reduce bottom velocities.

Another case of severe scouring occurred at the Beznau Dam, located on the Aare River in Germany. In 1926, a remarkable depth of scour in the limestone of 41.3 ft was observed.

As a result of the erosion below many hydraulic structures, the subject of the prevention of scour has become one of increasing importance.

REFERENCES

1. Adams, C. S.: Speedy Repairs Save Waco Dam Spillway, *Eng. News-Record*, p. 87, Mar. 20, 1947.
2. Darley, B., et al.: Report dated Dec. 10, 1929, by Islam Enquiry Committee on failure of the Islam Weir, Public Works Department, Lahore, India, 1930.
3. Ewald, R. F.: Preventing Erosion below Overflow Dams, *Civil Eng.*, pp. 527-531, March, 1951.
4. Gausmann, R. W., and C. E. Madden: Experiments with Models of Gilboa Spillway, *Trans. ASCE*, paper 14, p. 280, 1923.
5. Gilbert, G. K.: The Transportation of Debris by Running Water, *Geol. Survey Professional Paper* 86, 1914.
6. Hunt, H. J., and C. N. Ward: Correction of Tailwater Erosion at Prairie Du Sac Dam, *Trans. ASCE*, 1947.
7. Oram, H. P.: Concentrated Flow Erodes Rock below Wilson Dam, *Eng. News-Record*, p. 126, Jan. 20, 1927.
8. Flood Overflow on Calderwood Dam Scours Deep into Rock, *Eng. News-Record*, June 26, 1930.

NAME INDEX

- Adams, C. S., 208*n.**
Aravin, W. I., 31
Argyropoulos, P. A., 51
Ashley, W. H., 49
Auroy, F., 163*n.*
Bakhmeteff, B. A., 26, 30, 31, 55
Barnes, D. P., 31
Basgen, D. H., 106*n.*
Bazin, H. E., 26
Beebe, J. C., 26, 31, 55
Behera, B., 30
Belanger, J. M., 25
Berryhill, R. H., 194
Bidone, G., 25
Blaisdell, F. W., 99, 109, 154*n.*, 166
Bonin, C. C., 163*n.*
Borland, W. M., 106*n.*
Bresse, J. A., 25
Brown, F. R., 106*n.*
Chertousov, M. D., 31
Corfitzen, W. G., 80*n.*
Coyne, A., 155, 163*n.*
Crump, E. S., 27, 69
Darcy, H. P. G., 26
Darley, B., 208*n.*
Da Vinci, L., 19
Davis, L. M., 187*n.*
De Vito, L., 179
Donnelly, C. A., 166
Douma, J. H., 31
Drisko, J. B., 106*n.*
Dubrow, M. D., 35
Dutta, D. N., 56, 59
Einwachter, J., 31
Ellms, E. W., 21, 55
Ewald, R. F., 208*n.*
Feldt, H. W., 153
Ferriday, R., 26
Forster, J. W., 35
Gausmann, R. W., 208*n.*
Gibson, A. H., 26
Gilbert, G. K., 205
Goodrum, J. C., 35
Gumensky, D. B., 114
Hamilton, W. S., 148*n.*
Harleman, D. R., 97
Hickox, G. H., 56, 59
Houk, I. E., 15*n.*
Howell, D. D., 51
Hsing, P. S., 43
Hunt, H. J., 208*n.*
Inglis, C. C., 25
Ippen, A. T., 166
Ishibashi, T., 187*n.*
Ivanchenko, A., 31
Joglekar, D. V., 25
Johnson, J. W., 9
Jourdan, J. W., 49
Keener, K. B., 187*n.*
Kennison, K. R., 24
Kimishima, H., 163*n.*
Kindsvater, C. E., 48, 56
King, H., 52*n.*
Kinney, C. W., 26, 31
Knapp, F., 31
Kuttiammu, T. P., 154*n.*
Lane, E. W., 48, 73
Levy, A. G., 21
Ludin, A., 31

* *n* means noted in References.

- Madden, C. E., 208*n.*
Maitre, R., 179
Mathisen, K. M., 163*n.*
Matzke, A. E., 26, 30, 31, 55
Merriman, M., 25
Monroe, R. A., 106*n.*
Moore, W. L., 35, 165, 166
Morgan, C. W., 35

Nagaratnam, S., 71
Newcomer, A. W., 93*n.*
Nicolaeu, S., 125

Obolensky, S., 179
O'Brien, M. P., 9
Okada, A., 187*n.*
Oosterholt, G. A., 70
Oram, H. P., 208*n.*

Page, N., 31
Panasenkov, N. S., 179
Peterka, A. J., 148*n.*, 203*n.*
Posey, C. J., 31
Puls, L. G., 55, 72

Qureshy, A. A., 30

Ramser, C. E., 15*n.*
Rand, W., 165
- Rao, J. V., 154*n.*
Reed, O., 49
Riegel, R. M., 26, 31, 55
Rindlaub, B. D., 55

Safranez, K., 26, 30, 31
Simmons, W. P., 148*n.*
Skrinde, R. A., 35
Smetana, J., 31
Steele, I. C., 106*n.*
Stevens, J. C., 32, 47, 68
Stuber, H. W., 163*n.*

Tabor, H. W., 148*n.*
Thomas, H. A., 148*n.*
Tiffany, J. B., 187*n.*
Trahern, J. W., 32

Unwin, W. E., 25

Ward, C. N., 208*n.*
Warnock, J. E., 187*n.*
Weide, L., 103
Willes, W. H., 32
Woodward, S. M., 38*n.*
Woyciecki, K., 31
Wu, C. K., 31

Yarnell, D. L., 55

S U B J E C T I N D E X

- Air demand for outlet conduits, 50
Air-entrainment data for high spillways, 114-115
All-American Canal, stilling-basin blocks for, 147
Anchor Dam, spillway bucket for, 183
Angostura Canal, stilling basin for, 147
Angostura Dam, roller bucket for, 177
Apron elevation, diagram for, 122
direct solution for, 120-122
Aprons, design considerations, 63-64
sloping, 53-55, 58
stepped, 60-62
Arch dams, energy dissipation below, 160-163
Arkabutla Dam, model-prototype conformance, 194
stilling-basin profile, 62
- Baffle piers, 95-103
arrangement of, 99
block coefficient for, 103
force exerted by, 96-97
recommended dimensions for, 103-109
types of, 98
uses of, 95-96
Baldhill Dam, model-prototype conformance, 194
Bernoulli's theorem, 7-8
Bhakra Dam, spillway tunnel for, 184-185
Bhavani-type stilling basin, 151-152
Bonneville Dam, erosion of baffles, 99-101
stilling-basin performance, 194-195
Boysen Dam, stilling basin for, 137-138
Bucket-type energy dissipators, 169-186
slotted-roller, 175-178
design criteria for, 177
performance of, 175-176
- Bucket-type energy dissipators, solid-roller, 169-175
dimensions for, 170-171
prototype characteristics, 174
typical action below, 169-170
trajectory, 178-185
design criteria, 180
prototype characteristics, 181
types of, 178
variables of, 178
Bull Lake Dam, stilling basin for, 144
Bull Shoals Dam, stilling-basin performance, 195-196
- Canal structures, stilling basins for, 81-85
Castelo do Bode Dam, ski-jump spillway for, 158
Cavitation, 99
Channel retrogression (*see* Erosion)
Chief Joseph Dam, baffles for, 101
Chute blocks, uses of, 94
recommended dimensions for, 108, 116
Chutes, parabolic, 140-141
trapezoidal, 45-46
Circular conduits, 46-50
critical depth in, 46-47
elements of, 46
formation of jump in, 47-50
hydrostatic pressure in, 48
with sloping floors, 48-49
Cleveland Dam, ski-jump spillway for, 159
Cochiti Diversion Dam, profile of, 88
Conchas Dam, damaged baffles at, 99
stilling-basin performance, 196
Conowingo Dam, spillway bucket for, 75
Contraction, coefficient of, 91
Critical depth, in circular channels, 46-47
definition of, 10
in parabolic channels, 12

- Critical depth, in rectangular channels, 11
 - in trapezoidal channels, 41-42
 - in triangular channels, 12
- Critical flow, 10-11
- Critical slope, definition of, 12
 - formula for, 13
- Demopolis Lock and Dam, stilling basin for, 153
- Denison Dam, model-prototype conformance, 197
- Diverging channels, hydraulic-jump formation in, 86
- Diversion structures, definition of, 5
 - stilling basins for, 87-89
- Drop structures, 5, 164-168
 - energy dissipation below, 165-166
 - rectangular, 164-167
 - stilling basins for, 164-168
 - trapezoidal, 167-168
 - vertical drop length, 165
- End sills, 103-106
 - profiles of, 104
 - recommended dimensions for, 109, 116
- Rehbock dentated, 103-104
 - types of, 104
 - uses of, 103
- Enders Dam, stilling basin for, 136-137
- Energy, specific, 9-10, 69-70
 - types of, 8
- Energy dissipation, equations for, 67-68
 - by hydraulic jump, 66-69
 - influences on, 162
- Englewood Dam, outlet works for, 61
- Erosion, below existing structures, 206-208
 - factors influencing, 161-162
 - model tests for, 193
- Exponential conduits, 50-52
 - graphical solutions for, 51-52
- Flow, classification of, 6, 13
 - critical, 10-11
- Folsom Dam, model-prototype conformance, 198
- Fontana Dam, spillway tunnel for, 184-186
- Fort Gibson Dam, stilling basin for, 153-154
- Freeboard, 125
- Free-jet stilling basins, design of, 137-140
 - recommended dimensions for, 139
- Friction effects on hydraulic jump, 72
- Froude number, definition of, 13
- Gates, 130-132
 - high-pressure, 130
 - jet-flow, 131
 - radial, 130
 - vertical-leaf, 131-132
- Germantown Dam, outlet works for, 61
- Gilboa Dam, spillway profile for, 206
- Grand Coulee Dam, spillway bucket for, 172-173
- Heart Butte Dam, model-prototype conformance, 198-199
 - stilling basin for, 141-142
- Hoosic River junction, stilling basin for, 127
- Hoover Dam, needle valves for, 132-133
 - retrogression below, 79
- Horsetooth Dam, stilling basin for, 143-144
- Howell's graphical solution, 51-52
- Hump stilling basins, design of, 141-143
 - recommended dimensions for, 142
- Hydraulic jump, at abrupt drop, 35-36
 - at abrupt rise, 36-37
 - basic requirements for, 16
 - energy dissipation by, 66-72
 - forms of, 17-19
 - friction, effect of, 72
 - height of, 29
 - length of, 29-32, 43-44
 - location of, 17, 32-34
 - in sloping channels, 56-60
 - below a sluice gate, 90-93
 - submerged, 91-93
 - theory of, 22-24
 - uses of, 19-21
- Hydraulic similitude, 189-193
- Hydrostatic pressure over circular segments, 47-48
- Impact stilling basins, 144-147
 - end-sill design for, 146
 - energy dissipation by, 145
 - hanging baffle for, 145
 - uses of, 144
- Jet-diffusion stilling basins, 135-137
- Jump-height curves, definition of, 78
 - preparation of, 78-79
 - relationships, 73-78
- Junction Dam, spillway profile of, 75
- Kanopolis Dam, stilling-basin performance, 199
- Kinetic-flow factor, definition of, 13
 - relationships, 28-29

- L'Aigle Dam, ski-jump spillway for, 156-157
- Length, of hydraulic jump, 29-33
definition of, 30
in rectangular channels, 31, 33
on sloping aprons, 60
in trapezoidal channels, 43-45
- of stilling basins, for canal structures, 85
for existing dams, 119
for large outlet works, 116
for small outlet works, 108
- Loskop Dam, spillway splitters for, 154
- Lucky Peak Dam, trajectory bucket for, 184
- McNary Dam, stilling-basin performance of, 200-201
- Madden Dam, sloping apron for, 62
tailwater-jump-height relationships, 76-77
- Manning formula, 14
for critical slope, 13
n values for, 15
- Mareges Dam, ski-jump spillway for, 155-156
- Merala Weir, unbalanced head on, 113
- Mississippi Lock and Dam No. 1, stilling basin for, 199-200
- Model-prototype conformances, 194-203
- Model tests, 188-193
- Mohawk Dam, stilling basin for, 62
- Momentum, conservation of, 8-9
corrective factors, 9
- Momentum formula, 22-24
for rectangular channels, 24
for trapezoidal channels, 42-43
verification of, 25-26
- n* values for Manning formula, 15
- Nimrod Dam, stilling basin for, 202
- Nonrectangular channels, 39-52
circular, 46-50
exponential, 50-52
trapezoidal, 39-46
- Norfolk Dam, stilling basin for, 202
- Normal depth, 13
- Norris Dam, spillway apron for, 74
- Open channels, Bernoulli's theorem for, 7-8
diverging, 83
elements of, 6-7
flare ratio for, 83
flow classification in, 6
formulas for, 14-15
slopes of, 13-14
- Outlet channels, 80
- Outlet-works structures, control mechanisms for, 128-130
large, recommended dimensions for, 116-117
stilling-basin design for, 114-120
small, recommended dimensions for, 112
stilling-basin design for, 107-112
- Parabolic channels, critical depth in, 12
hydraulic jump in, 51
- Parabolic drop, 140-141
- Picote Dam, ski-jump spillway for, 158
- Pine Flat Dam, trajectory bucket for, 180, 182
- Pole Hill power plant, stilling-basin model for, 146
- Prairie du Sac Dam, channel retrogression below, 207-208
- Pressure-momentum relationships, for circular channels, 48-49
diagram of, 40
for exponential channels, 51
for rectangular channels, 33-34
for trapezoidal channels, 39-41
- Rectangular channels, abrupt drop in, 35-36
abrupt rise in, 36-37
critical depth in, 11
dimensionless equations for, 27-28
discharge diagram for, 12
hydraulic jump in, 22-28
kinetic-flow factor relationships in, 28-29
length of jump in, 29-33
momentum formula, 24
- Rehbock dentated sill, 103-104
- Roller-type stilling basins, 152-154
- SAF stilling basin, 149-151
- Safe Harbor Dam, spillway bucket for, 75
- Sakuma Dam, roller bucket for, 175
- Scale ratios for models, 192
- Scour, factors influencing, 162, 205
prevention of, 204-205
- Shadehill Dam, model-prototype conformance, 202-203
- Side walls (*see* Training walls)
- Ski-jump energy dissipators, 155-160
characteristics of, 159
purpose of, 155
- Sluice gate, hydraulic jump below, 90-93
- Soldier Canyon Dam, stilling basin for, 137-138
- Specific energy (*see* Energy)

- Specific head diagram, 70
 Spillway buckets (*see* Bucket-type energy dissipators)
 Spillways, elements of, 1-3
 high, recommended dimensions for, 116-117
 stilling-basin design for, 114-120
 low and medium-high, recommended dimensions for, 112
 stilling-basin design for, 107-112
 splitters, 154
 tunnel deflectors, 183-186
 Splitter walls, 126-127
 Stage-discharge curves, 78-79
 Stilling basins, appurtenances for, 94
 Bhavani-type, 151-152
 for canal structures, 81-85
 design discharge for, 79
 for diversion structures, 87-89
 for drop structures, 164-168
 free-jet, 137-140
 hump-type, 141-144
 jet-diffusion, 135-137
 length of, 85, 108, 116, 119
 roller-type, 153-154
 SAF, 149-151
 for sluiceways, 90-93
 transitions for, 85-86
 walls for, 123-127
 width for, 79-80, 85
 (*See also* Outlet-works structures; Spillways)
 Submerged hydraulic jump, 90-93
 Surface tension effects on hydraulic jump, 35
 Tailwater curves, preparation of, 78-79
 Tappan Dam, stilling basin for, 62
 Training walls, design of, 123-125
 profiles of, 125
 Trajectory length, 179
 Trapezoidal channels, critical depth in, 41-42
 hydraulic jump in, 39-45
 Trapezoidal stilling basins, disadvantages of, 123
 for free jets, 138-139
 Tygart Dam, jet deflectors for conduits, 146-147
 Uplift forces, 112-113
 Valves, 132-134
 butterfly, 134
 hollow-jet, 133-134
 needle, 132-133
 tube, 133
 Velocity, coefficient of, 91
 Velocity-head correction factor, 9
 Viscosity effects on hydraulic jump, 35
 Waco Dam spillway, erosion below, 206
 Wheeler Dam, spillway apron for, 74
 Whiting drop structure spillway, 167
 Willwood Dam, spillway apron for, 74
 Wilson Dam spillway, erosion below, 207-208
 Wing walls, 119, 125-126
 design of, 125-126
 of existing structures, 119